Identification of Epstein-Barr virus transcription factor Zta interactome during lytic cycle reactivation

By Yaqi Zhou

A Thesis submitted for the degree of

Doctor of Philosophy

School of Life Science

University of Sussex

May 2019

I hereby declare that this thesis has not been and will not be, submitted in whole or in part to another university for the award of any other degree.

Signature:……

Acknowledgements

First, I would like to thank my main supervisor, Professor Alison Sinclair. She is always kind, patient, and her enthusiasm in science inspired me. Thank her for the guidance and supervision during my PhD study. The way she helps me to think scientifically allowed me to find where my interest lies.

I also want to thank my co-supervisor Dr Steve Sweet, although he has left the university. He always answered my questions and shared latest scientific information, which was useful for my project. I thank him for providing all the guidance and help during my PhD.

I would like to thank my co-supervisor Professor Michelle West for her useful advices for my project.

I thank all the previous lab members, Dr Kay Osborn, Dr Chris Traylen, Dr Rajaei Almohammed, Dr Ijiel Barak Naranjo Perez-Fernan, and current lab members Dr Anja Godfrey, Manal Hussain M Moalwi and Faisal Alzahrani, for all the help and support. I would like to extend my gratitude to Dr David Wood, Dr Rajesh Ponnusamy, Helen Webb, Hildegonda Veenstra, and Jacob Evans for their immense support.

I would like to thank Dr Sarika Khasnis especially for the amazing time we had in the lab. I am glad I could find a best friend in lab who enjoyed doing science together. I would also like to thank her for all the advice she gave me in the lab and during my thesis writing. I thank my friends Dr Xiangrong Chen, Di Yang, Dr Lina Chen, Xuan Du, Miao Zhang and Ying Chen for all the support and company during my hard times.

I want to thank China Scholarship Council (CSC) and University of Sussex for funding my PhD and giving me a chance to study in the UK.

Last, I would like to thank my parents and all the family members, who were always there to support my decision and help me when I felt homesick. I could not have finished my PhD without them.

UNIVERSITY OF SUSSEX

YAQI ZHOU

PhD in BIOCHEMISTRY

Identification of Epstein-Barr virus transcription factor Zta interactome during lytic cycle reactivation

SUMMARY

Epstein-Barr virus reactivation from latency promotes lytic replication, the production of infectious virions and exposes infected cells to recognition by the immune system. The key activator of EBV lytic cycle is Zta (BZLF1), a bZIP protein that binds to the host and viral genome and acts as a transcriptional regulator and origin binding protein. Zta is a homodimer with reported interactions with several of the conserved and essential herpes virus replication proteins and with several cellular transcription factors and signal transduction molecules. However, a full Zta interacting protein map is still missing.

We used an unbiased approach to identify the viral and cellular Zta interactome during lytic reactivation of epithelial cells using chromatin immunoprecipitation combined with a label-free quantitative mass spectrometry. 55 proteins were found as Zta interacting proteins. Then the method was revised to identify the Zta interactome during lytic reactivation of Burkitt's lymphoma cells. The Zta interacting proteins were isolated by immunoprecipitation, followed by Tandem Mass Tag (TMT) labelling and mass spectrometry. 267 associated proteins were identified (FDR<0.05). This included previously identified viral (BMRF1, BALF5 and BGLF4) proteins. Cellular proteins were clustered by Gene ontology and several functional groups identified.

HSC70 is central to one group. Its interaction with Zta was validated, demonstrated to occur independently of other viral proteins, and furthermore it was shown that HSC70 contributes to EBV lytic cycle. HSC70 is also targeted by other gamma herpes viruses during the viral lytic cycle, suggesting a conserved function.

A second cluster contained NFAT proteins; these are calcium-signaling transcription factors. We validated that NFATc2 interacts with Zta. We present data that Zta attenuates calcium signalling regulated transcription activation through NFATs. As calcium signalling directly activates Zta expression during EBV reactivation, this establishes a negative feedback loop that dampens cellular activation.

Table of Contents

List of Tables

List of Figures

List of Abbreviations

ACV	Acyclovir
AID	Activation-induced cytidine deaminase
AIDS	Acquired immune deficiency syndrome
AP-1	Activator protein 1
bZIP	Basic leucine zipper
BARTs	BamHI-A rightward transcripts
BCR	B cell receptor
BHV4	Bovine herpesvirus 4
BL	Burkitt's lymphoma
bp	Base pairs
BS3	Bis(sulfosuccinimidyl)suberate
CBP	CREB binding protein
C/EBPα	CCAAT/enhancer binding protein α
CD21, CR2	Complement receptor type 2
CDK1	Cyclin-dependent kinase 1
ChIP	Chromatin immunoprecipitation
CsA	Cyclosporin A
CSF-1	colony stimulating factor 1
CTCR2	CREB-regulated transcription coactivator 2
DLBCL	Diffuse large B cell lymphoma
DMP	Dimethyl pimelimidate dihydrochloride
DMSO	Dimethyl Sulfoxide
DS	Dyad symmetry
DSP	Dithiobis(succinimidyl propionate)
DTT	Dithiothreitol
EA-D	Early antigen-diffuse
EBERs	EBV encoded RNAs
EBNAs	EBV nuclear antigens
EBV	Epstein–Barr virus
EMSA	Electrophoretic mobility shift assay

EphA2	Ephrin receptor tyrosine kinase A2
FACS	Fluorescence-activated cell sorting
FAM96B	Cytosolic iron-sulfur assembly component 2B
FBS	Fetal Bovine Serum
FK506	Tacrolimus
FR	Family of repeats
GCV	Ganciclovir
HCD	High energy collision dissociation
HCMV	Human cytomegalovirus
HDACi	Histone deacetylase inhibitor
HL	Hodgkin's lymphoma
HRS	Hodgkin/Reed-Sternberg
HSPA8 / HSC70	Heat shock cognate 71 kDa protein
HSV	Herpes simplex virus
IL	Interleukin
IM	Infectious mononucleosis
IRF7	Interferon regulatory factor 7
KSHV	Kaposi's sarcoma-associated herpesvirus
LCL	Lymphoblastoid cell line
LC-MS	Liquid Chromatography-Mass Spectrometry
LCV	Lymphocryptovirus
MCAF1	MBD1-containing chromatin-associated factor 1
MEF2B	Myocyte-specific enhancer factor 2B
MEF2D	Myocyte-specific enhancer factor 2D
MHV-68	Murine herpesvirus
miRNA	Micro RNA
MMS19	Nucleotide excision repair protein homolog
MS	Multiple Sclerosis
NBD	Nucleotide-binding domain
NFATC1	Nuclear factor of activated T-cells, cytoplasmic 1
NFATC2	Nuclear factor of activated T-cells, cytoplasmic 2
NKTL	NK/T-cell lymphoma

NLP	nodular lymphocyte predominant
NPC	Nasopharyngeal Carcinoma
ORC	Origin recognition complex
PARP-1	Poly [ADP-ribose] polymerase 1
PES	2-phenylethynesulfonamide
PI3K	Phospatidylinositol-3-kinase
PKC	Protein kinase C
PMA / TPA	12-O-Tetradecanoylphorbol 13-acetate
PMSF	Phenylmethanesulfonyl fluoride
PTLD	Posttransplant lymphoproliferative disorder
p53	Cellular tumor antigen
qPCR	Real-time quantitative PCR
RACK1	Receptor for activated C kinase 1
RREs	Rta response elements
RRV	Rhesus rhadinovirus
RUNX3	Runt-related transcription factor 3
RXRα	Retnoid X receptor α
SAHA	Suberoylanilide hydroxamic acid
SBD	Substrate binding domain
SBEs	SMAD-binding elements
SDS-PAGE	sodium dodecyl sulfate polyacrylamide gel electrophoresis
Sp1	Specificity protein 1
STAT	Signal transducers and activators of transcription
TAD	Transcriptional activation domain
TAF6	Transcription initiation factor TFIID subunit 6
TBP	TATA box binding protein
TFA	Trifluoroacetic acid
TMT	Tandem mass tags
TR	terminal repeat
TSA	Trichostatin A
VCA	Viral capsid antigen
VLP	Virus-like particle

vPIC	Viral preinitiation complex
VZV	Varicella zoster virus
Zp	BZLF1 promoter
ZREs	Zta responsive elements

1 Introduction

1.1 Herpesviruses

Herpesviridae is a family of viruses that has a large size of double-stranded DNA genome and a similar structure of their particles (Gibson, 1996; Chiu and Rixon, 2002). The herpesviruses have been classified into three subfamilies including alpha, beta and gamma. Eight different human herpesviruses are divided into different subfamilies. The alpha subfamily includes neurotropic viruses, the herpes simplex virus (HSV) 1 and 2, and the varicella zoster virus (VZV). The beta subfamily includes human cytomegalovirus (HCMV), and human herpesvirus 6 and 7. The members of the gamma subfamily include Epstein–Barr virus (EBV) and Kaposi's sarcoma-associated herpesvirus (KSHV) (McGeoch et al., 2000).

The gammaherpesviruses are currently divided into two genera, Lymphocryptoviridae and rhadinoviridae. Lymphocryptoviridae only includes human and primate viruses, including Epstein–Barr virus (EBV), marmoset lymphocryptovirus (marmoset LCV) and rhesus lymphocryptovirus (Rhesus LCV). Rhadinoviridae includes virus from different mammals, including human Kaposi's sarcoma-associated herpesvirus (KSHV) and gamma herpesvirus from other species such as murine herpesvirus 68 (MHV-68), bovine herpesvirus 4 (BHV4) and rhesus rhadinoviridae (RRV) (Longnecker and Neipel, 2007; Davison, 2007).

1.2 History and epidemiology of EBV

The Epstein-Barr virus infects around 90% of human adults worldwide. It was first found by electron microscopy in a cultured lymphoma cell line and it is the first definitive human cancer relevant virus (Epstein et al., 1964). Although it was first found in a Burkitt's lymphoma cell line by the Epstein group, it has been reported to be relevant to many diseases now, including other B and T lymphomas, epithelial carcinomas and immune deficient related diseases. After 50 years, we

still have not understood this virus completely, however, a lot of work has been done and we are slowly unfolding its secrets.

The primary infection of EBV to children often happens before 5 years old or the infection delays until adolescence (Lai et al., 1975). Lower socioeconomic conditions have been reported to be associated with asymptomatic primary infection in young kids (Hesse et al., 1983; Ozkan et al., 2003). The primary infection in adolescence or adults causes infectious mononucleosis, which is an acute EBV infection with clinical symptoms (Gratama and Ernberg, 1995).

Although EBV is detected in most of the populations all over the world, it has geographical variation depends on its genome types, and this might be relevant to different EBV associated diseases (Hjalgrim et al., 2007).

The most common transmission route for EBV is through oropharyngeal secretion. Shedding of EBV in saliva varies between 27%-90% among all age ranges (Ikuta et al., 2000; Apolloni and Sculley, 1994). The main transmission route for primary infection in young kids is through saliva on toys or fingers, whereas kissing is the main transmission route for infectious mononucleosis in adolescents and adults (Crawford et al., 2002). Besides, the detection of EBV in cervical secretions in women and penile sulcus of men suggests a possibility of transmission through sexual contact. Studies about the relationship between sexual history and EBV infection also suggests this route (Crawford et al., 2002; Israele et al., 1991; Naher et al., 1992). In addition, EBV can spread through organ transplantation and it is the main risk factor for the post-transplant lymphoproliferative disease (PTLD) (Scheenstra et al., 2004).

1.3 EBV viral particles

The first EBV mass spectrometry analysis determined EBV proteins in the mature enveloped virus (Johannsen et al., 2004), and then all the proteins were mapped to the functions and common structure of herpesviruses.

The full-enveloped EBV has a capsid, which is assembled by viral capsid proteins, including major capsid proteins and mini capsid proteins, such as BVRF2, BcLF1, enclosing its double-stranded DNA genome. The capsid is surrounded by tegument, which is a layer filled with tegument proteins, and it is enclosed within the envelope. Most tegument proteins are encoded by EBV late genes, such as BPLF1, BOLF1, BNRF1 and BSRF1. A polymorphic lipid bilayer forms the envelope surrounding the capsid, which contains multiple copies of different viral glycoproteins, such as BLLF1 (gp350), BDLF3 (gp150), BXLF2 (gH), BALF4 (gB) and BKRF2 (gL), which are responsible for viral attachment and entry to host cells (Liu and Zhou, 2007; Johannsen et al., 2004). The structure of the EBV particle is shown in **Figure 1.1**.

1.4 EBV genome and strains

1.4.1 EBV genome

EBV is a double-stranded DNA virus, and its genome is about 172kb in length, which expresses around 80 viral latent and lytic genes in total (**Figure 1.2**) (Young et al., 2007). In addition, EBV encodes different non-coding RNAs, including EBV encoded RNAs (EBERs), BamHI-A rightward transcripts (BARTs), and miRNAs (Young et al., 2007).

Because EBV has two distinct life cycles, latency and lytic cycle, the genome shows different features in each life cycle. EBV has 4 different latency types, latency 0-III, and each type has different gene expression features. During latency, only restricted genes expressed, and the Epstein-Barr nuclear antigens (EBNAs) including EBNA1, EBNA2, EBNA-LP, EBNA3A, 3B and 3C are the main genes that regulate latency. EBNA1 expressed in latency I, II and III, while EBNA-LP, EBNA 2 and EBNA 3s were only expressed in latency III. While in lytic cycle, all the EBV genes are switched on, some to help replicate genome and some to assemble the viral particles (Young and Rickinson, 2004; Young et al., 2007).

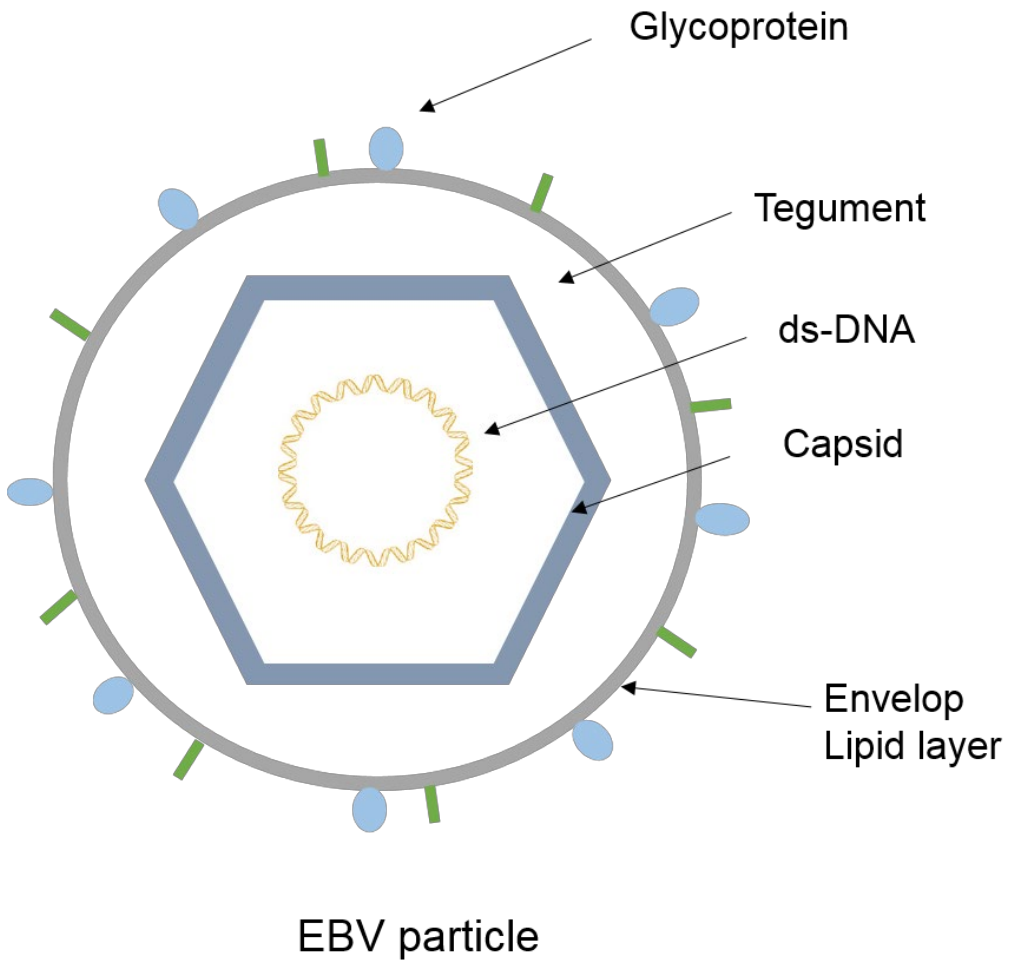

Figure 1.1 Schematic diagram illustrating the multilayer organization of EBV particle. A virion contains a double-stranded DNA. A capsid, tegument, envelop lipid layer and glycoproteins surround the viral DNA. Adapted from (Liu and Zhou, 2007)

The EBV genome has a single origin of replication during latency, called oriP. Two functional elements located in oriP, the dyad symmetry (DS) element and the family of repeats (FR). EBNA1 binds directly to the 30 base pairs (bp) repeat elements in FR and DS of oriP region in order to initiate latent DNA replication and recruit cellular DNA replication machinery (Lieberman et al., 2007).

Normally, the latency genes are transcribed from two promoters located close on the genome named Cp and Wp. During the initial infection, EBNA-LP and EBNA2 are transcribed from the Wp, as the first expressed EBV genes. Then the promoter is switched to Cp, which can transcribe the rest of EBNAs, EBNA3s and EBNA1. All the EBNA genes are transcribed from the Cp or Wp in latency III. EBNA1 can also be transcribed from Qp in Latency I and II alternatively, which only results in EBNA1 expression, but no other EBNAs (Speck and Ganem, 2010).

The Lytic replication is through two identical regions on the genome, which are about 100kbps apart and located opposite to each other, called oriLyt L and R. oriLyt region is about 7700bp, includes 1055bp duplicated long core element, two gene promoters (BHLF1 and BHRF1) and BHLF1 gene. Within the core element, there are two essential components (upstream and downstream) containing binding sites for early transcription factor BZLF1 and for cellular proteins, SP1 and ZBP-89 (Hammerschmidt and Sugden, 2013; Price and Luftig, 2014). BZLF1 can bind to the promoter region of BHRF1 and BHLF1 to enhance and support the function of oriLyt (Schepers et al., 1993). Some EBV strains with deletion of one copy of either oriLyt, such as B95-8 strain with the deletion of oriLyt R, are still able to initiate lytic cycle and produce virions (Raabtraub et al., 1980). The EBV genome scheme is shown in **Figure 1.2**.

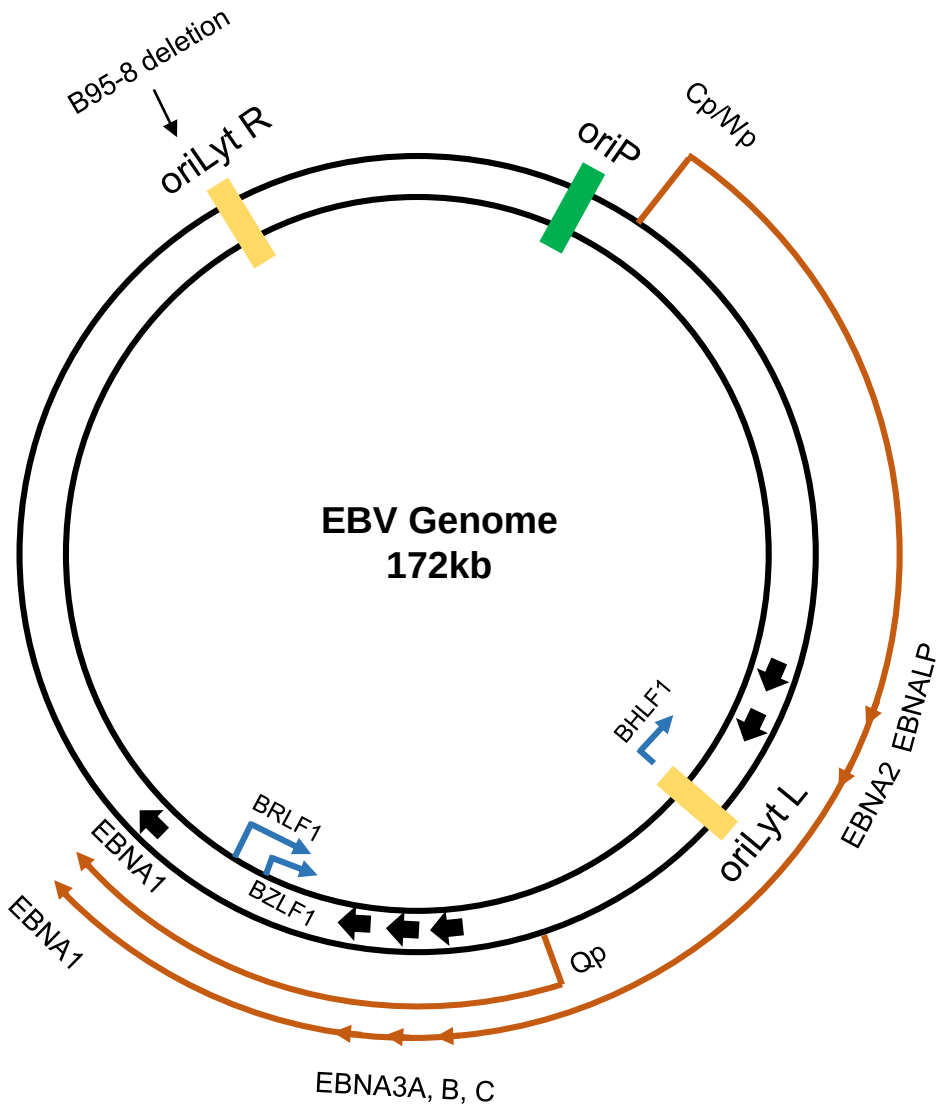

Figure 1.2 EBV genome with key genes. EBV genome is around 172kb double-stranded DNA. oriP(green) is the origin of replication in latency, where EBNA1 can bind. oriLyt L and R (yellow) are two origins of replication in the lytic cycle. oriLyt R is deleted in B95-8 strain. The EBNAs were transcribed from Cp or Wp, EBNA1 can also be transcribed from Qp. Two transcription factors BZLF1, BRLF1 and BHLF1 gene ORFs were shown in the genome with blue arrows. (Adapted from Price and Luftig, 2014)

1.4.2 EBV strains and variation

The first fully sequenced EBV strain is B95-8, although people found there is a 13.6kb deletion compare to other strains (Raabtraub et al., 1980; Baer et al., 1984). The open reading frames predicted from this sequence have been used as the basis for most EBV research. The deleted sequence was later resolved from cloned restriction enzyme digest fragments of EBV from Raji BL cell line (Parker et al. 1990). Then some errors were found and corrected (de Jesus et al., 2003), (Fruscalzo et al. 2001; Kanda et al.2011). Later on, AJ Davison and PJ Farrell released a more standard EBV sequence as the RefSeq HHV4 (EBV) NC_007605.

With the development of sequencing methods, many EBV strains have been sequenced from different regions of the whole world. AG876 strain from African BL cell line is a type 2 EBV strain (accession number DQ279927) (Dolan et al., 2006). EBV from the African Mutu BL cell line and the Japanese Akata BL cell line are also sequenced (Lin et al., 2013). The Chinese GD1 strain is from a Lymphoblastoid cell line (LCL) in Guangzhou (Zeng et al., 2005). Further EBV sequences from Hong Kong Nasopharyngeal Carcinomas (NPCs) are reported, including HKNPC1-9 from biopsy samples of nine Hong Kong NPC patients (Kwok et al., 2014; Kwok et al., 2012). The M81 strain isolated from a Chinese NPC patient shows more enhanced lytic replication than B95.8 strain and enhanced tropism for epithelial cells than other strains (Tsai et al., 2013). Sequencing of nine EBV strains (EBVaGC1-9) from EBV positive gastric cancer biopsy specimens was performed, compared with other strains, they were mostly close to the GD1 strain (Liu et al., 2016a).

Recently, A EBV sequence study has revealed new 138 EBV genome sequences data, together with 116 previously published EBV genomes, provided a chance to study the different variations linked to geographical distribution and EBV associated diseases (Correia et al., 2018).

EBV is classified as type 1 and type 2 strain based on the major sequence variation in EBNA2. EBNA3 genes also have variations, but less than that observed in EBNA2 (Dambaugh et al., 1984; Rowe et al., 1989). It is found that the biggest biological difference between the type 1 and 2 EBV is that type 1 EBV can immortalise B cells more efficiently *in vitro* than type 2 EBV (Rickinson et al., 1987). The large scale of 241 genome sequencing data also confirmed that the type 1 and type 2 classifications are the main features of EBV genome variation which defines mostly by EBNA2 and EBNA3 (Correia et al., 2018).

There are variations in other EBV latent genes, LMP1, LMP2A and EBNA1. In addition, a few lytic gene variations are found in coding and regulation regions, such as EBV early transcription factor BZLF1 and BRLF1. Chinese EBV strains such as M81 strain show polymorphisms in BZLF1, which cause more spontaneous lytic replication in the cells. However, further functional analysis is required to confirm this (Lorenzetti et al., 2012; Jin et al., 2010; Lorenzetti et al., 2014; Martini et al., 2007; Tsai et al., 2013). Variations have also been reported in some early lytic genes (BHRF1, BNLF2a) and late lytic gene (BLLF1) (Horst et al., 2012; Jing et al., 2010; Kawaguchi et al., 2009).

1.5 EBV relevant diseases

1.5.1 Infectious mononucleosis (IM)

Normally, the first awareness of EBV acute infection is IM, which occurs mostly in adolescents or adults (Dunmire et al., 2015). The incidence of IM is high, around 1/50,000 per year in the general population and 1/1000 in young adults (Moffat, 2001).

Symptoms of IM commence after an incubation period of around 6 weeks, and typically includes fever, lymphadenopathy and pharyngitis (Hoagland, 1955). By the time patients experience symptoms and arrive at the clinic, the infection is mostly resolving, however, in rare cases, IM causes life-threatening complications (Hadinoto et al., 2008; Wemel et al., 2017).

During acute infection, the host immune system cannot control EBV, so the memory compartment begins to be filled up with the latently infected B cells. The levels of virus-infected cells are extremely high in the peripheral blood (Hochberg et al., 2004). The commonly used serological diagnosis antigens include VCA, EA-D and EBNAs, but VCA-IgM titre is the most accurate tool for primary EBV infection (Moffat, 2001).

The infected cells are immediately attacked and killed by cytotoxic (CD8+) T cells (CTLs) that recognise the EBV early lytic antigens. Consequently, this destruction of large numbers of infected B cells by CTLs causes inflammatory symptoms (Callan et al., 1998). Eventually, the level of infected memory B cells drops to a low point, thus the acute infection is limited. However, EBV does not stop shedding and continues to stay with the host for a lifetime after acute infection.

1.5.2 Burkitt's lymphoma (BL)

BL was firstly described by a British surgeon, Dr Burkitt in Uganda in the 1950s. It is a rare and highly aggressive B cell lymphoma occurring in young children between 2 and 14 years in sub-Saharan Africa region (Burkitt and O'Conor, 1961) and the first human cancer with a viral aetiology described over 50 years ago.

Serological surveys for EBV viral capsid antigen (VCA), early antigen-diffuse (EA-D) and EBNA-1 on patients determined the EBV infection in BL. Epidemiology studies also indicated that EBV is a risk factor, playing a specific role in the development of BL (Dethe et al., 1978).

At the molecular level, the viral genome and viral protein EBNA-1 along with viral non-coding microRNAs are present in all cancer cells and EBV is clonal within the tumours. This clonality provides evidence for EBV being causal for BL (zur Hausen et al., 1970; Neri et al., 1991; Lindahl et al., 1974; Tao et al., 1998). EBNA-1 is reported to induce lymphomas in mouse models, suggesting a direct role of EBV for oncogenesis (Wilson et al., 1996).

Besides EBV infection, there are other factors playing roles in the development of BL, and the most important one is malaria (Biggar et al., 1981). Compared to the children from the holoendemic malaria transmission area, children from sporadic malaria area have a lower level of EBV-associated IgG antibody (Piriou et al., 2009). Recently, more studies had identified that malaria may regulate an enzyme activation-induced cytidine deaminase (AID). AID is required for C-MYC translocation which is an important feature for BL (Erikson et al., 1983). A cohort study on Kenyan children demonstrated that malaria-exposed children with detectable EBV viral load had higher AID expression level in peripheral blood compared to children with undetectable EBV (Wilmore et al., 2015). The reason for AID increasing in EBV viral load could be EBV prefers infecting B cells with mutated immunoglobulin, which is also AID-dependent (Heath et al., 2012).

1.5.3 Hodgkin's lymphoma (HL)

Hodgkin's lymphoma (HL) is one of the most common lymphomas and develops from germinal centre B-lymphocytes. In the Western world, the annual incidence of HL is approximately 2-3/100,000 people per year. While in Asia, the incidence of HL is low (Bray et al., 2015).

Detection of the increased antibody titres of EBV antigens in HL patients provides the hypothesis that EBV might be involved in the pathogenesis of HL (Levine et al., 1971). The rates of EBV infection in the HL cases vary between 20 and 50% from North American and Europe (Glaser et al., 1997; Pallesen et al., 1991). However, a higher rate is detected in African or other under-developed countries (Weinreb et al., 1996; Chang et al., 1993). It is also reported that the number of EBV positive cases is higher in older people and children under the age of 10 years (Jarrett et al., 1991).

European American Lymphoma (REAL)/World Health Organization (WHO) classifies HL into two subtypes, classical HL and nodular lymphocyte predominant (NLP) HL (Swerdlow SH, 2016). EBV contributes to the pathogenesis of classical HL. The main feature of classical HL is the presence of

the cancer hallmark cells, Hodgkin and Reed-Sternberg (HRS) cells which illustrate peculiar morphology and unusual phenotype (Kuppers, 2009). EBV-infected HRS cells express many latent viral genes, including EBNA1, LMP1 and LMP2A/B, non-coding EBERs and microRNAs (Deacon et al., 1993), and these EBV gene products may be responsible for the survival of HRS progenitors. LMP1 activates NF-KB, phosphatidylinositol-3-kinase (PI3K)/AKT pathways, which are identified constitutively expressed in HRS cells (Bargou et al., 1997; Dutton et al., 2005). LMP2A functions as a B cell receptor (BCR) substitution, promoting B cell development in the absence of BCR signalling (Caldwell et al., 1998). LMP2A also interferes with the expression of many B cell transcription factors to regulate the gene expression changes in HRS cells which may important for the survival and development of HRS cells (Portis et al., 2003).

1.5.4 Nasopharyngeal Carcinoma (NPC)

Apart from lymphomas, EBV has been reported to cause a major epithelial carcinoma, NPC, which is a tumour that derived from the squamous epithelium. This cancer is highly prevalent in southern China, Southeast Asia, and North Africa. The distinctive geographic distribution of NPC suggests that both environmental factors and genetic features were involved in the development of this cancer (Chang and Adami, 2006).

It is reported that 100% of undifferentiated NPC is EBV associated, however, studies also showed that differentiated tumours are EBV related (Raab-Traub et al., 1987). Studies identified the most relevant risk factors of NPC are EBV infection and consumption of salted-preserved food suggesting a complex aetiology of NPC (Yu et al., 1986). NPC patients have high antibody titres to the EBV antigens, VCA and E-AD (Henle et al., 1970). The viral genome is also detectable in the malignant epithelial cells of NPC (Wolf et al., 1974).

In EBV infected NPCs, expression of EBNA1, LMP1, LMP2 and high expression levels of EBERs and BART RNA transcripts are detected, which may play

important roles in the tumorigenesis of NPC (Brooks et al., 1992; Marquitz and Raab-Traub, 2012).

1.5.5 Gastric carcinoma

Gastric carcinoma has high incidence and it is one of the leading causes of cancer death in the world (Ferlay et al., 2015). There are geographical variations in the incidences of gastric cancer, with high rates in Eastern Europe, and Eastern Asia, and relatively low rates in Northern Europe, some African countries and North American whites and it is twice common in men than in women (Bray et al., 2015). The risk factors for gastric carcinoma are smoking, certain diets, alcohol and infection with *Helicobacter pylori* (Venerito et al., 2014).

The first evidence of EBV relevant to gastric carcinoma was reported in 1990 by the detection of the virus in lymphoepithelioma-like gastric carcinoma cells (Burke et al., 1990). Later on, more studies found EBV in gastric carcinoma cells which were not restricted to lymphoepithelioma-like gastric carcinoma (Martinez-Lopez et al., 2014). More than 80% of lymphoepithelioma-like gastric carcinomas and around 10% of other common types of gastric carcinomas are positive for EBV (Camargo et al., 2011).

In molecular biology study, EBV viral DNA and EBNA 1 can be detected in EBV-associated gastric carcinoma (Imai et al., 1994). Other EBV genes are also detectable in EBV positive gastric carcinoma, including EBV encoded RNAs, LMP1 and LMP2. EBV positive gastric adenocarcinoma tissue cells contain more viral load than EBV infected B cells (Ryan et al., 2009).

Genome-wide studies show a whole image of gene regulation in EBV positive gastric carcinoma. EBV positive gastric carcinoma often has PIK3CA and ARID1A mutation compared to EBV negative carcinomas. It also shows an amplified 9p24.1 locus linked to the overexpression of JAK2, PD-L1 and PD-L2 (Gulley, 2015; Cancer Genome Atlas Research, 2014; Liu et al., 2016a). A special feature for EBV positive gastric carcinoma is the hypermethylation of the

human genome, and the methylated positions are different from other gastric carcinoma types, for example, CDKN2A (p16) hyper-methylation is only seen in EBV positive gastric carcinoma (Gulley, 2015).

1.5.6 Non-Hodgkin's lymphoma

1.5.6.1 Diffuse large B cell lymphoma (DLBCL)

DLBCL is the most common non-Hodgkin's lymphoma among adults, although no large population case studies about the prevalence of EBV in DLBCL are available, small studies reveal less than 5% in western countries and 10-15% in Asian and South America (Heslop, 2005; Beltran et al., 2011; Hofscheier et al., 2011; Park et al., 2007).

There are different subtypes of DLBCL related to EBV, some are relevant to immunosuppression status, for example, acquired immune deficiency syndrome (AIDS) related DLBCL, T cell-rich DLBCL, however, the EBV-positive DLBCL of the elderly is the type used as the EBV-positive DLBCL model because it is not associated with concomitant immunosuppression or co-infection with other viruses (Sabattini et al., 2010). In 2017, WHO revised the classification and removed elderly, so the cases of DLBCL that showed clonal B cells and EBV positive but not specific to other named EBV-positive groups are named as EBV-positive DLBCL, NOS (Grimm and O'Malley, 2018).

EBV latent genes EBNA1 and LMP1 are expressed in 90% of the EBV positive DLBCL (Oyama et al., 2003; Oyama et al., 2007; Nguyen-Van et al., 2011). NF-KB signalling pathway is up-regulated in EBV- positive DLBCL. NF-KB and STAT3 regulated gene sets are accumulated in EBV-positive DLBCL as well (Kato et al., 2014). These studies revealed pathogenic mechanisms of EBV and identified drugable targets for the treatment of the DLBCL.

1.5.6.2 NK/T-cell lymphoma (NKTL)

EBV is associated with many NK/T cell lymphomas, including aggressive NK-cell leukaemia, extranodal NK/T cell lymphoma nasal type, and systematic EBV positive T-cell lymphoma of childhood. Nearly all of the cases are associated with EBV (Kimura and Fujiwara, 2018).

NK/T cell lymphoma is a rare disease. The mechanism of EBV in NK/T cell is still not clarified. In the primary infection, EBV infects B cells and epithelial cells in oral tonsils and may also infect some NK/T cells (Hudnall et al., 2005). Some transcription factors are involved in the EBV induced NK/T cell proliferation, including NF-κB and STAT3 (Takada et al., 2017; Onozawa et al., 2017).

A sequencing study through 384 samples from EBV associated lymphomas observed a high frequency of PD-L1/PD-L2 involving genetic alterations in 22% EBV associated lymphomas, including extranodal NK/T-cell lymphoma (ENKTL, 23%), aggressive NK-cell leukemia (57%), systemic EBV-positive T-cell lymphoproliferative disorder (17%). This feature suggests a role of evasion from cellular immunity in the development of these lymphomas and further provides a possible treatment for the NK/T cell lymphomas, which contain these genetic variations (Kataoka et al., 2019).

1.5.7 Posttransplant lymphoproliferative disorder (PTLD)

PTLD is a series of abnormal lymphoid proliferations related to organ transplant immunosuppression treatment. Most of the PTLD cases are related to EBV, including B cell-derived, and T cell and NK cell lymphoproliferation (Samant and Kothadia, 2018). The incidence of PTLD is variable and depends on the type of organ received as well as the immunosuppression treatment used. If an EBV seronegative recipient gets an organ from an EBV seropositive donor, this is the most significant risk factor for developing PTLD. That is why the higher rates of EBV positive PTLD are found in paediatric patients than adults (Schober et al., 2013; Rausch et al., 2016). Under immunosuppression status, EBV specific T

cells response is suppressed and EBV viral load is continuously at a high level, which could be the main reason for B cell proliferation and lymphomas (Sokal et al., 1997; Baldanti et al., 2000).

1.5.8 Other diseases

EBV is relevant to many other diseases, for example, autoimmune diseases, such as Multiple Sclerosis (MS). It is reported that MS risk is strongly associated with the history of IM (Thacker et al., 2006; Handel et al., 2010). However, it is still controversial about MS and EBV infection, and molecular relevance is still unclear.

EBV is also reported as a risk factor for breast cancer. However, limited evidence is found to support this relationship (Glaser et al., 2017).

It is important to understand the characteristics of EBV, especially in the context of different diseases, which will provide us with more information to discover drugs to treat EBV associated diseases.

1.6 EBV primary infection

It is broadly believed that EBV spreads through saliva with close contacts and the virus enters through the epithelium that underlies the nasopharynx (Cohen, 2000). Under the epithelium, the lymphoid system surrounds the nasopharyngeal and pharynx is called Waldeyer's ring. For EBV, in saliva, it is thought to infect the oral epithelial cells and then infects naïve B cells that reside below. However, how the EBV crosses epithelial cell is still unclear, evidence shows that the virus may cross passively through the process of transcytosis (Tugizov et al., 2013).

1.7 EBV Entry

The entry of EBV into B cells and epithelial cells are different. As EBV is first recognised as a B lymphotropic virus, the entry of B cells was studied well. The

first step for the virus to enter B cells is attaching, which is through viral protein, glycoprotein gp350 and cellular protein, complement receptor type 2 (CR2, CD21). Fusion in B cells requires four EBV glycoproteins gH, gL, gB, gp42 and cellular protein, HLA class II (Connolly et al., 2011; Mullen et al., 2002).

In epithelial cells, EBV also can use CD21 to entry the tonsillar epithelial cells, however, CD21 is not always expressed in other types of epithelial cells, then EBV can use gH, gL to bind to a subset of integrin for entry (Wang et al., 1998; Chesnokova and Hutt-Fletcher, 2011). Entry through gH, gL is not as efficient as CD21, and the reason could be that gH, gL bind to integrins, which reduces its function for fusion. In addition, fusion for EBV in epithelial cells is different from B cells, they use glycoprotein gH, gL and gB but not gp42, also epithelial cells do not express HLA class II proteins constitutively, they still use integrins (Chesnokova and Hutt-Fletcher, 2011). Recently a study reported that the integrins are not the primary receptors for EBV entry to HEK293 cells, ephrin receptor tyrosine kinase A2 (EphA2) is the receptor for the EBV entry to epithelial cells, which is also the receptor for KSHV entry (Chen et al., 2018; Hahn et al., 2012).

1.8 EBV latency

Once EBV encounters resting B cells *in vivo*, the virus could transform those cells and drive them into proliferating lymphoblast (Thompson and Kurzrock, 2004). This represents the first step in the establishment of their life-long viral latency, that is, the viral genome exists in host cells without the production of infectious viral particles. EBV enters into the host cell nucleus as naked linear DNA genome covered by protein capsid, then they will circulate as minichromosome in the nucleus (Liashkovich et al., 2011). This is the key step for protecting the ends of the viral DNA and establishing a structure that is able to complete the life cycle. However, the main mechanisms of this circularisation and assembly are still unclear (Deng et al., 2012). Then the virus will establish the appropriate nucleosome positions and epigenetic modifications.

During the latency, the viral genomes stayed in the host cells, as multi-copy non-integrated circular genomes that have similar chromatin structures and features of the host chromosome, which enables them to be transcribed and replicated by the host cell machinery once per cell cycle (Lieberman, 2013).

EBV establishes four distinct latency transcription types, latency type 0, I, II, III **(Figure 1.3)**. The most restrictive latency is type 0, which is observed in non-cycling, resting memory B cells, in this type only EBV non-coding RNAs are expressed, including EBERs, BARTs and miRNAs (Shaknovich et al., 2006). Type I latency is found in proliferating memory B cells and Burkitt's lymphoma cells, which involves the expression of Epstein-Barr nuclear antigen I (EBNA1) and some non-coding RNAs. Type II latency is defined by expression of latency membrane proteins (LMP1, LMP2A or LMP2B) in addition to type I products, it is observed in Hodgkin's lymphomas and epithelial cell carcinomas. Type III latency is observed in highly proliferating B cells and immortalised B cell lines, in this type all the viral latency genes are detectable, including EBNA1, EBNA2, EBNA3A, 3B, 3C, LMP1, LMP2A, 2B and EBV non-coding RNAs (Vockerodt et al., 2015).

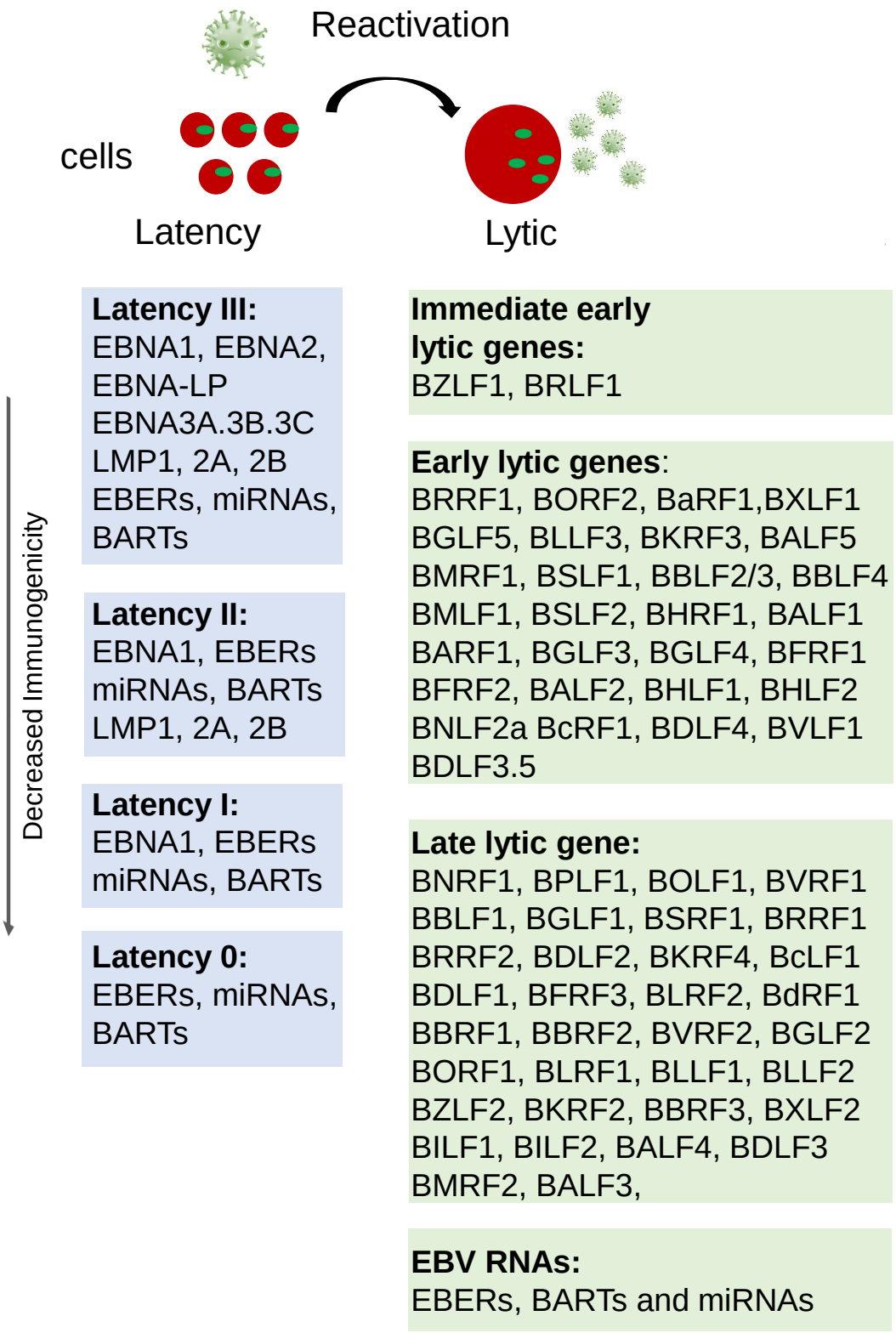

Figure 1.3 Diagram of EBV life cycles and gene expression. EBV has two life cycles, latency and lytic cycle. Latency 0 only expresses some EBV non-coding RNAs. Latency I expresses EBNA1 and non-coding RNAs. Latency II expresses EBNA1, LMP1, LMP2A, LMP2B and non-coding RNAs. latency III expresses all latency proteins including EBNA1, EBNA2, EBNA-LP, EBNA2A, 3B, 3C, LMP1, LMP2A, LMP2B and non-coding RNAs. Genes expressed at different stages of the lytic cycle are also listed on the right. (reviewed by Young et al., 2007).

There are different models to explain the EBV persistence during latency *in vivo.* The germinal centre model has been established for a long time. As shown in **Figure 1.4**, EBV establishes its primary infection in epithelial cells and then crosses the barrier to use the lymphoid tissue of Waldeyer's ring. Then it infects naïve B cells and transforms them into B cell blasts which show latency III features. Transformed B cell blasts induce a G protein-coupled receptor, it recognises lipid signals and migrates toward the germinal centre, and then the latent genes driving proliferation are turned off through different signalling pathways and the cells switch to latency II status. Afterwards, the cells in the germinal centre provide two signals, T cell help and BCR, to rescue the cells from the germinal centre into resting memory B cells. At this state, only latency protein EBNA1 expressed, which allows EBV to maintain replication of its viral genome with the cells but not the virus. Under certain circumstances, the EBV infected resting B cell will be triggered by signals to differentiate into plasma cells and undergo viral lytic replication (Thorley-Lawson, 2015).

1.8.1 EBNA1

EBNA1 is the only gene expressed in all the latency types (except latency 0) and its encoded protein is the first identified EBV latency protein (Reedman and Klein, 1973). The only viral protein required for the EBV latency DNA replication is EBNA1, which binds to oriP and initiates the EBV DNA replication dependant on host cell cycle (Yates et al., 1984; Yates et al., 1985). However, EBNA1 alone is not sufficient to activate DNA replication, EBNA1 recruits cellular origin recognition complex (ORC) to oriP and help initiate DNA replication, and this is dependent on the host replication machinery (Schepers et al., 2001).

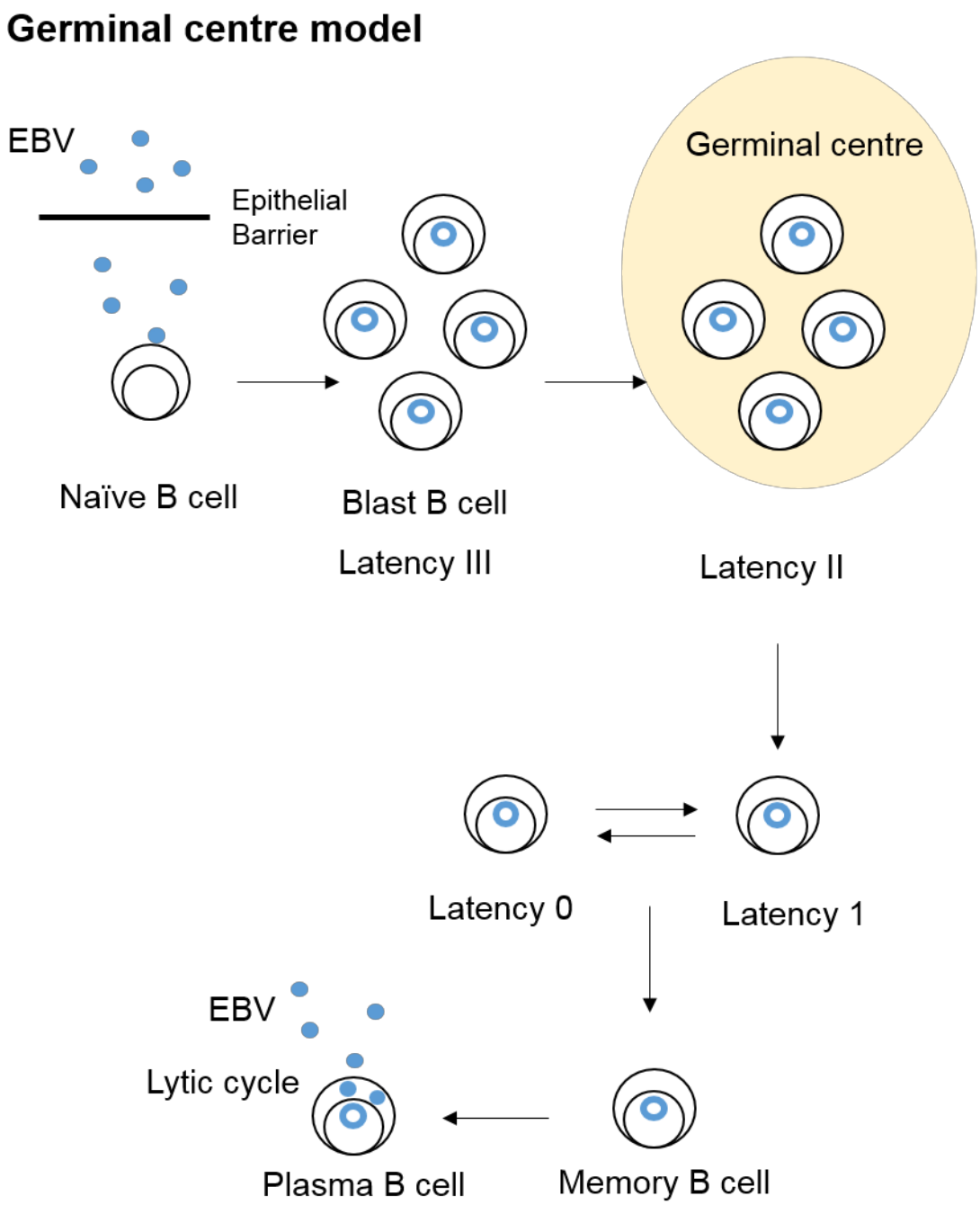

Figure 1.4 Germinal centre model of EBV establishing latencies in B cells. Once EBV transformed the Naïve B cells, all the latent genes will be expressed in this stage termed latency III, then EBV infected B cells will enter the germinal centre and establish latency II which has fewer latency genes expressed, this will provide signals for B cell survival and differentiation to memory B cells. EBV-infected memory B cells silence the latent gene expression to skip immune recognition, at this stage, only EBV non-coding RNAs can be detected, which is Latency 0, and when EBNA1 protein is expressed during cell division, EBV will replicate its genome once per cell cycle, this stage called Latency I. Under certain circumstances, the EBV infected resting B cell will be triggered by signals to differentiate into plasma cells and undergo viral lytic replication (adapt from Vockerodt 2015, Fox 2011).

EBNA1 is also required for mitotic segregation of the EBV episome, which is important for EBV to partition the episomes to the daughter cells during cell division. EBNA1 can tether the EBV episomes to the cellular mitotic chromosomes through EBNA1-chromosome interaction (Kanda et al., 2001; Harris et al., 1985). EBNA1 acts as a viral transcription factor by regulating the expression of other EBNAs and LMP genes during latency (Sugden and Warren, 1989; Mackey and Sugden, 1999).

1.8.2 EBNA2 and EBNA-LP

EBNA2 and EBNA-LP are the two early latency genes expressed during EBV infection of resting human primary B cells and are essential for EBV-driven B cell immortalisation (Cohen et al., 1989; Hammerschmidt and Sugden, 1989; Alfieri et al., 1991). EBNA2 is a transcription factor and is responsible for other viral and cellular gene expression. EBNA-LP works as an EBNA2 co-activator. Expression EBNA2 along with EBNA-LP in primary B-cells induces the expression of the cellular cyclin D2 gene (Sinclair et al., 1994).

EBNA2 is not able to bind to DNA directly, so adaptor proteins are used to bind DNA such as RBPJ and PU.1 (Johannsen et al., 1995). So far, the well-known adaptor protein of EBNA2 is the cellular protein RBPJ, which is a sequence-specific DNA binding protein that recruits a co-repressor complex to the promoter or enhancer region of the target genes to repress the transcription. EBNA2 competes with this complex and relieves this repression (Hsieh and Hayward, 1995). Genome-wide studies using EBV-infected B cells or EBNA2 expressing B cells revealed a gene regulation map of EBNA2 on the human genome (Zhao et al., 2011; Lucchesi et al., 2008; Calender et al., 1990). Known EBNA2 targeted genes such as RUNX1, RUNX3, CXCR7, PIK3R1, AML-2 and MYC were identified (Kempkes and Ling, 2015). EBNA2 activates the oncogene cMYC during B cell transformation by binding to the enhancer region and promoting long-range chromatin looping during the EBV gene mediated transcription (Wood et al., 2016).

1.8.3 EBNA3

Epstein-Barr virus nuclear antigens EBNA3A, EBNA3B and EBNA3C belong to one family that is expressed during latency III. EBNA3 transcripts are spliced from a long primary transcript that initiated at a single latency promoter. EBNA3A and 3C are required for B cell transformation while EBNA3B is nonessential (Tomkinson et al., 1993). EBNA3s bind to the same site on RBPJ as EBNA2 and reporter assay showed EBNA3s could inhibit EBNA2 mediated activation of viral promoters, suggesting EBNA3s may work as a regulator of the genes that EBNA2 activated (Robertson et al., 1996).

Genome-wide studies for EBNA3s revealed their function of host gene regulation and chromatin modulation (McClellan et al., 2013; Harth-Hertle et al., 2013). EBNA3A and 3C regulate and silence BCL2L11 through inactivating the enhancer region of this gene by chromatin looping (Wood et al., 2016).

EBNA3A and 3C also play a role in cell cycle regulation. Studies showed EBNA3C to influence LMP1 expression only in G1 phase and modulate a G1 arrest checkpoint in B cells (Maruo et al., 2006; Allday and Farrell, 1994). A few studies reported EBNA3C associated with many proteins involved in the regulation of cell cycle progression, including MDM2, p53, cyclin D1, cyclin A, Chk2 (Choudhuri et al., 2007; Knight and Robertson, 2004; Saha et al., 2009; Saha et al., 2011). A controlled level of EBNA3A is favoured for the LCL proliferation, and overexpression of EBNA3A reduces the expression level of MYC and cyclin D2 and causes a G0/G1 arrest (Cooper et al., 2003).

EBNA3B acts as a tumour suppressor. An EBNA3B knocked out virus-transformed B cell line has a growth advantage compared to wild type virus-transformed cell line *in vitro* and *in vivo*, EBNA3B also up-regulates CXCL10, which might be able to increase T cell-mediated killing (White et al., 2012).

1.8.4 LMP1 and LMP2

Latency membrane genes including LMP1 and LMP2 are expressed in latency II and III EBV infected cells (Cohen, 2000). LMP1 expression is detectable as early as four days after EBV infection in B cells and it is induced by EBNA2 (Allday et al., 1989). During latency II where EBNA2 is not expressed, the cytokine-induced activity of signal transducers and activators of transcription (STAT) are responsible for LMP1 expression (Chen et al., 2003).

LMP1 is important for B cell and epithelial cell transformation (Kaye et al., 1993; Baichwal and Sugden, 1988). LMP1 also influences the chromatin by up-regulating the expression of the DNA methyltransferase DNMT1 and by forming a transcriptional repression complex at E-cadherin promoter (Tsai et al., 2006). Global studies of LMP1 gene regulations revealed many LMP1 regulated genes, including many transcription factors, cytokines and chemokine receptors (Lo et al., 2001; Morris et al., 2008).

Two different LMP2 gene transcripts are expressed from separate promoters (Laux et al., 1988b). LMP2A promoter has EBNA2 responsive element as well as RBPJ and PU.1 binding site. It also can be activated by the Notch signalling pathway (Anderson and Longnecker, 2008). LMP2A mimics BCR and interferes with the EBV lytic activation by inhibiting the activation of protein tyrosine kinases, suggesting a role of LMP2A in maintaining EBV latency within the host cells (Miller et al., 1995). LMP2B may work as a regulator of LMP2A, it restores BCR signalling when co-expression with LMP2A and blocks phosphorylation of LMP2A (Rovedo and Longnecker, 2007).

1.8.5 EBV encoded RNAs

EBV encoded RNAs (EBERs) including EBER1 and EBER2, are highly abundantly expressed as non-polyadenylated RNA polymerase III transcripts in all EBV infected cells (Lerner et al., 1981). They are used as biomarkers for detecting EBV infection in clinical samples (Weiss et al., 1991). The biological roles of EBERs are still unclear, it is reported that EBERs are not necessary for

B cell transformation (Swaminathan et al., 1991), however, EBER2 depletion results in decreased EBV lytic replication, suggesting it plays a role in viral replication (Lee et al., 2015). Deletion of EBER1 or EBER 2 individually in B95-8 strain is relevant to different cellular gene expression changes in LCLs, suggesting they play an important role in cellular gene regulation (Gregorovic et al., 2011). EBERs interact with many cellular proteins. EBER1 recruits human ribosomal protein rL22 to the nucleus suggesting EBER1 may modulate translation (Fok et al., 2006). EBER2 interacts with transcription factor of B cell lymphocyte development PAX5 and together regulates the expression of other genes (Lee et al., 2015).

1.8.6 BamHI-A Rightward Transcripts (BARTs)

BARTs are another group of stable viral RNA transcripts expressed in all kinds of infected cells. They were first detected in NPC cells, and later, it is found that BARTs are detectable in both lytic and latent infection in the peripheral blood of EBV infected people, and in B and T cell lymphoma cells.

The EBV B95.8 strain has a deletion of the BARTs region, but it is still able to transform B cells. This suggests BARTs are dispensable for B cell transformation (Robertson et al., 1994). In NPC, BARTs are consistently highly abundant, that suggests they might play important roles in NPC pathogenesis (Marquitz and Raab-Traub, 2012).

The entire BART locus is around 20kbp including seven exons and two promoters P1 and P2. Upon infection of B cells, transcription from P1 is detectable soon after infection whereas P2 is delayed. These promoters are regulated by a few cellular transcription factors, P1 promoter contains AP-1 and IRF sites can be negatively regulated by interferon regulatory factor 7 (IRF7) and IRF5, P2 promoter contains c-Myc and C/EBP binding sites and can be positively regulated by these two proteins (Chen et al., 2005).

Some studies reported that BARTs have protein-coding potential, several ORFs were identified, including BARF0, RK-BARF0, RPMS1 and A73. However, the evidence for the existence of the encoded proteins is still controversial (Marquitz and Raab-Traub, 2012).

1.8.7 EBV microRNAs (miRNAs)

EBV was the first virus reported to encode miRNAs and five miRNAs were identified from EBV b95-8 infected B cells. However, the deletion of the BART region of the B95-8 strain contains more miRNAs and later on many miRNAs in this region were identified from other strains (Zhu et al., 2009; Grundhoff et al., 2006).

EBV miRNAs are fully dependent on the cellular processing machinery. miRNAs are expressed in all the latency types and lytic cycle, however, the expression level of EBV miRNAs varies in different tissues and tumours. Different latency types express different miRNAs, this is because BHRF1 miRNAs transcribe from major latency promoters, Cp and Wp, while BART miRNAs transcribe from BART P1 and P2 promoters. High levels of BHRF1 miRNAs are detected in latency III cell lines where the Cp and Wp are active while they are nearly non-detectable in latency I and II cells (Amoroso et al., 2011; Cai et al., 2006). BART miRNAs are expressed in all the latency types and lytic cycle. However, the expression level varies depending on the infected cell type. Especially high levels of BART miRNAs are found in latency II infected cells, such as NPC and gastric cancers, but low levels in latency I BL cell line. Many BART and BHRF1 miRNAs are found to be up-regulated upon lytic reactivation (Cai et al., 2006).

Functions of EBV miRNAs were recently studied. BHRF1 miRNAs can be detected by 2 days post-infection of primary B cells *in vitro* and the levels continue to increase during the transformation (Amoroso et al., 2011). BHRF1 miRNAs mutants cause a reduction of LCLs growth and a reduction of EBV transforming capacity compared to wild type virus (Feederle et al., 2011). However, EBV strains lacking the BART region and BHRF1 miRNA knockout viruses are able to

transform B cells in vitro suggests they are not essential for B cell transformation and also they had little effect on virus-induced oncogenesis *in vivo* (Wahl et al., 2013).

EBV miRNAs target multiple viral mRNAs at 3'UTRs, including latent genes LMP1, LMP2A and EBNA2, as well as lytic genes such as BHRF1, BALF5, BNRF1 and BALF2 (Skalsky et al., 2014; Riley et al., 2012).

Besides viral genes, EBV miRNAs also target cellular genes including targets involved in immune evasion, apoptosis and many important signalling pathways. miR-BHRF1-3 was reported up-regulates a T cell-attracting chemokine CXCL11 mRNA levels in EBV infected BL cells, inhibition of miR-BHRF1-3 enhanced mRNA levels of CXCL11 (Xia et al., 2008). BART miRNAs down-regulate BIM (BCL2L11) expression level in order to inhibit the apoptosis through binding to the BIM 3'UTR (Marquitz et al., 2011). Multiple EBV miRNAs modulate immune recognition of recently infected primary B cells. The secretion of IL-6, TNF and IL-12p40 were significantly less in wild type B95-8 EBV-infected cells than miRNAs knockout EBV-infected cells suggesting an inhibition of EBV miRNAs in secretion of proinflammatory cytokines. EBV miRNA target IL12B in order to prevent Th1 differentiation of naïve $CD4^+$ T cells, and further affect the antigen presentation and recognition of infected B cells by EBV-specific $CD4^+$ T cells (Tagawa et al., 2016). It is also reported that EBV miRNAs target peptide transporter subunit TAP2, reduce the levels of TAP1 subunit, MHC class I and EBNA1, which reduce the immune surveillance by virus-specific $CD8^+$ T cells (Albanese et al., 2016).

1.9 EBV lytic cycle

EBV lytic replication occurs in EBV primary infection or some cells containing latent infected EBV strains. Lytic cycle is required for the production of progeny virus. Once lytic cycle is induced, all EBV lytic genes, including immediate early genes, early genes and late genes are expressed and each cell produces more copies of viral genomes, assembles and releases them as virions. This is termed

the viral lytic cycle and is associated with the expression of full EBV genome (**Figure 1.3**). The lytic form of EBV infection is essential to pass EBV to new hosts as well as cell to cell spread. However, lytic replication only occurs at primary infection in the oral cavity and in a small percentage of host cells harbouring EBV.

1.9.1 Zp regulation during lytic reactivation

All EBV lytic genes are expressed in a temporally regulated manner. The activation of EBV immediate early gene BZLF1 promoter (Zp) is the first trigger during lytic activation and the expression of Zta is the key to control the EBV lytic switch (Binne et al., 2002).

The mechanisms that trigger EBV lytic reactivation *in vivo* are still unclear, in B cells, antigen- mediated activation of B cell receptor (BCR) leads to cascades of signal transduction, which can cause the activation of Zp.

In vitro, many reagents or chemicals can reactivate lytic cycle of EBV, one of these reactivation methods is cross-linking BCR with anti-immunoglobulin, IgG or IgM, to mimic the physiological antigen triggered Zp activation (Takada, 1984). Histone deacetylase inhibitors (HDACi) are another group of reagents that are able to trigger lytic reactivation *in vitro*. It is known that silencing of Zp is mediated by epigenetic histone modifications. During latency, the histone deacetylated state is found at Zp (Jenkins et al., 2000). Several HDACis initiate lytic cycle by triggering histone hyperacetylation of Zp, for example, suberoylanilide hydroxamic acid (SAHA), sodium butyrate and trichostatin A (TSA) (Chang and Liu, 2000). Calcium ionophores and 12-0-tetradecanoyl phorbol-13-acetate (TPA) are also commonly used for lytic cycle stimulation through activation of calcium signalling (Ca^{2+}) and protein kinase C (PKC) pathway, which are also the downstream pathways triggered by BCR (Faggioni et al., 1986). All the *in vitro* induction approaches give us a way to manipulate EBV lytic reactivation to investigate the switch from latency to lytic form in the EBV infected cell.

A few cis-elements were identified in Zp, including ZI-ZV and SMAD-binding elements (SBEs) that were regulated by different viral and cellular factors.

Zp is positively regulated during lytic reactivation by some motifs. ZI has four elements, ZIA-ZID, which can be induced recognised by two families of transcription factors, specificity protein 1 (Sp1) and myocyte enhancer factor 2D (MEF2D). During lytic induction via HDACi, protein kinase C delta (PKCδ) is the key factor. It phosphorylates Sp1, leads to the phosphorylated Sp1 binding to ZID, and in the end mediates Zp activation (Tsai et al., 2011). MEF2D is another factor that regulates Zp. During latency, MEF2D recruits class II HDAC to Zp in order to silence Zp (Gruffat et al., 2002b). Upon induction of lytic, MEF2D is de-phosphorylated via a cyclosporine A-sensitive Ca^{2+} signalling pathway, and this results in its binding to ZIA, ZIB and ZID directly and causes the activation of Zp. (Liu et al., 1997; Bryant and Farrell, 2002). Insert mutations in ZI motifs can disrupt the Zta expression upon inducing reagents, which also suggests ZI motifs are important for Zp initiation (Murata et al., 2013).

ZII element is a TPA responsive element near the TATA box of Zp and it is essential for the activation of Zp (Murata et al., 2013). It shows CREB/AP-1 binding sites features and can be recognised by many bZIP proteins including c-fos and c-jun (Flemington and Speck, 1990b).

ZIII A and ZIIIB motifs are Zta responsive elements (ZREs), Zta binding to these motifs could auto-activate Zp resulting in full activation (Flemington and Speck, 1990a). Zta can interact with CCAAT/enhancer binding protein α (C/EBPα) to activate ZII and ZIIIB co-operatively through direct binding to the motifs (Wu et al., 2004).

Five SBEs were identified in the Zp, which induce Zp activation through the canonical TGF-β signalling pathway. Mutation in any of the five SBEs decreases efficiency of Zp activation. SMAD4, one of the TGF- β signalling factor, was identified as a possible mediator of the activation of Zp via binding of SBEs elements (Liang et al., 2002; Iempridee et al., 2011).

Zp is negatively regulated by different factors. ZIIR, ZV and ZV' elements regulate Zp negatively within -221 to +12 region of Zp. The ZIIR element is located immediately upstream of CRE/AP-1 motif, mutation of this region results in an increase of Zp activity, however, the proteins that are involved in the regulation of this element is still unclear (Liu et al., 1998). It is identified that zinc finger E-box-binding proteins ZEB1 and ZEB2 bind to ZV and ZV'. In correlation of this, the human gastric carcinoma cell line AGS cells, which has little or is absent of ZEB1, shows spontaneous lytic reactivation (Feng et al., 2007). Latently infected epithelial HEK293 cells with the EBV ZV mutation, similarly shows spontaneous lytic reactivation, and this mutant leads to production of infectious virus upon induction of TPA while no virus production in wild type cells (Yu et al., 2007). Targeting ZEB1 and ZEB2 by microRNAs also leads to the increasing of lytic gene expression (Ellis-Connell et al., 2010).

1.9.2 Immediate-early lytic genes

Two immediate-early genes, BZLF1 and BRLF1, are the first viral genes expressed following lytic induction. Transcription of these two genes results in expression of two EBV lytic early transcription activator proteins, Zta (also known as ZEBRA, Z and EB1) and Rta (R, EB2) (Lieberman and Berk, 1990; Miller et al., 2007). Zta plays a primary role in EBV lytic initiation. It assembles the lytic replication machinery by interacting with many core viral replication proteins and targets them to the origin of lytic replication OriLyt (Liao et al., 2005; Zhang et al., 1996; Countryman and Miller, 1985). However, both Zta and Rta are required to complete lytic replication and produce viral particles. Expression of Rta in the Zta knockout cell line or expression of Zta in the Rta knockout cell line is not able to complete lytic replication (Feederle et al., 2000).

As transcription factors, Zta and Rta activate separate classes of early lytic genes, and together, the two proteins synergize to activate transcription of some lytic genes (Ragoczy and Miller, 1999; Young et al., 2007). How Zta and Rta work together is still unclear, there is evidence that a complex of Zta, Rta and cellular protein MCAF1 are involved in this co-operation (Chang et al., 2010).

1.9.2.1 Protein Zta in lytic replication: Structure and function

Zta belongs to the activating protein 1 (AP-1) family of transcription factors. AP-1 members share a basic leucine zipper (bZIP) domain, so it is also called bZIP family. Zta shows sequence similarity to all the AP-1 families, including c-Jun, ATF/CREB, and Maf, especially to c-Fos protein (Shaulian, 2010; Farrell et al., 1989).

Zta has 245 amino acid residues. The structure of Zta consists of three regions, including an N-terminal transactivation domain, a DNA binding domain and a dimerization region (bZIP) and C-terminal tail (**Figure 1.5A**) (Sinclair, 2003; Petosa et al., 2006).

Human c-Fos and c-Jun proteins are able to heterodimerise and bind to DNA through the bZIP domain. However, Zta has an unusual bZIP domain, which lacks the characteristic heptad repeats of leucine residues, so Zta only forms homodimers but fails to heterodimerise with cellular AP-1 proteins (Chang et al., 1990; Wu et al., 2004).

Further, Muller's group demonstrated the crystal structure of Zta C-terminal fragment (residues 175-220), which is shown in **Figure 1.5B**. Like other AP-1 proteins, the Zta homodimer embraces the DNA with its two long bZIP helices, with the basic region of each helix contacting the major groove and the zipper region forming a coiled-coil while residues from C-terminal to the bZIP helix form an additionally structured motif, the C-terminal tail (Petosa et al., 2006; Sinclair, 2006). C-terminal tail stabilises the coiled-coil through numerous interactions and greatly enlarges the dimer interface. Based on this, recent structure research demonstrated that Zta might interact with NF-κB and p53 through its C-terminal region (Dreyfus et al., 2011).

AP-1 family members are able to bind to a 7-bp AP-1 site through their DNA binding domain. Zta is able to bind to AP-1 like binding motifs known as Zta responsive elements (ZREs) (Lieberman and Berk, 1990; Farrell et al., 1989).

A

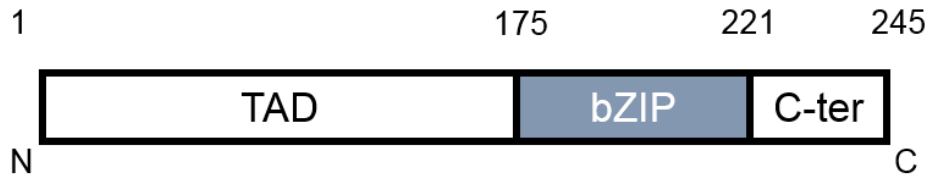

B

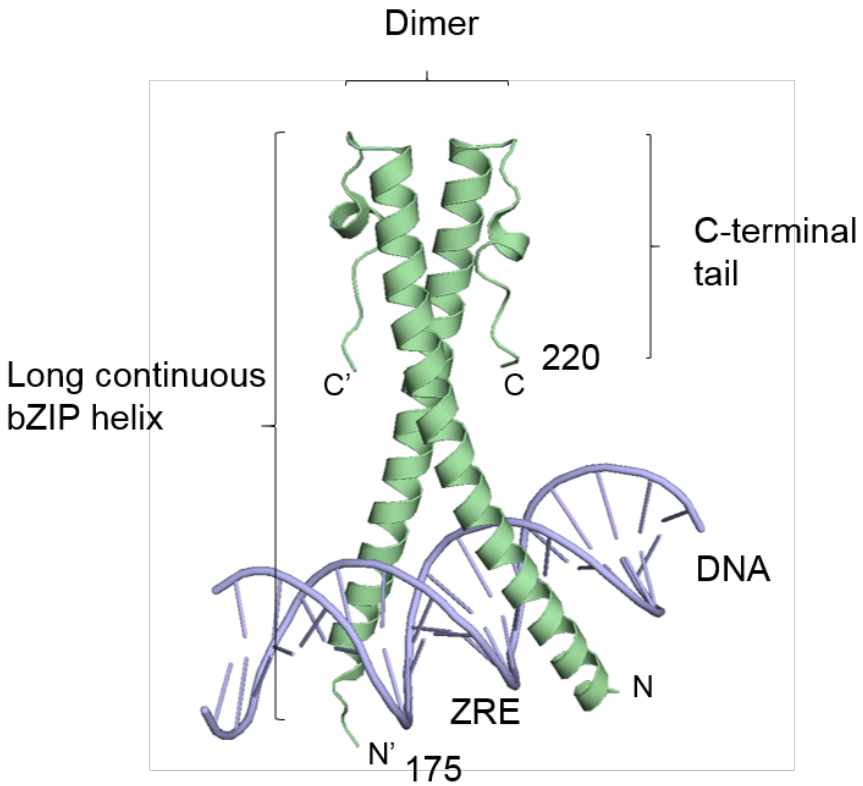

Figure 1.5 Illustrating the structures of Zta and Zta-DNA binding complex. A. Domain structure of Zta protein contains the transcriptional activation domain (TAD), dimerization and DNA binding domain (bZIP) plus C-terminal tail (C-ter). **B**. Crystal structure of Zta bZIP domain with DNA. The coiled-coil bends toward the DNA, with one bZIP helix curved and the other essentially straight. (Petosa et al., 2006, PDB 2C9L).

There are different classes of ZREs that Zta can interact with. Class I ZREs are the common AP-1 like motif, such as TGAGTCA and TGAGCAA, which can be found in BMRF1 promoter region. Both Class II and Class III ZREs contain a CpG motif, which can be methylated. Class III ZRE is dependent on DNA methylation, such as TGTGCGA, which can also be found in BMRF1 promoter region. DNA methylation enhances Zta binding to Class II ZREs, such as TGAGCGA, which located in Rp and BARF1 promoter region (Bergbauer et al., 2010; Bhende et al., 2004; Flower et al., 2011).

Although the EBV genome is highly methylated during latency and the methylation of DNA generally means the inhibition of transcription, Zta binds to methylated ZREs with greater affinity than non-methylated ZREs. *In vitro* binding assay shows Zta has higher affinity to the certain methylated ZREs (Hong et al., 2017). However, *in vivo*, the situation is more complex. When looking at the CpG ZRE in the context of the genome, Zta binds to CpG ZRE only when the genome is highly methylated. This suggests that at the early stage of the lytic cycle, the EBV genome is predominantly methylated, and Zta binds to all types of ZREs. However, during the full lytic cycle, the EBV genome becomes less methylated, and this causes less binding of Zta to CpG ZREs (Ramasubramanyan et al., 2012; Sinclair, 2013).

Zta activates immediate-early and early EBV gene promoters through directly binding Zta to ZRE motifs within the promoter regions or working with other transcription factors. Genome-wide studies identified most of the Zta interacting promoters in EBV genes, including BZLF1, BRLF1, BMRF1, BMLF1, BALF2 and so on, it is also identified some late genes that regulated by Zta, such as BKRF4, BLLF2, and BRRF1 (Ramasubramanyan et al., 2012). In addition to function in activating lytic genes, Zta also down-regulates latency-associated promoters, Cp and Wp (Kenney et al., 1989).

Apart from regulating viral genes, Zta transcriptionally activates certain cellular genes, some are important for EBV pathogenesis while some are involved in different cellular functions, such as cell cycle regulation and immune response.

Zta regulates expression of some cytokines, such as Interleukins (including Interleukin-8 (IL-8), Interleukin-10 (IL-10) and Interleukin-13 (IL-13)) and TGF-beta. Zta up-regulates the expression level of IL-8 and IL-10 gene by directly binding to the ZREs in their promoter regions (Mahot et al., 2003; Hsu et al., 2008). Zta up-regulates IL-13 in the EBV negative B cells and inhibition of Zta represses the IL-13 expression level in LCLs (Tsai et al., 2009). Zta induces the expression level of transforming growth factor igh3 (TGF- βigh3) and TGF- β1, it also increases the secretion of TGF- β1 into the medium (Cayrol and Flemington, 1995). The regulation of cytokines by Zta shows a feature that Zta may potentially change the host cell immune response during the lytic cycle and may enhance cell proliferation of EBV-positive tumour cells.

In addition to cytokines, Zta can regulate other cellular genes with different functions. Zta up-regulates the tyrosine kinase TKT (also called DDR2) both on mRNA and protein levels, and further causes the up-regulation of matrix metalloproteinase 1 (MMP-1), which is over-expressed in many tumour cells (Lu et al., 2000). Zta also up-regulates matrix metalloproteinases 3 (MMP-3) by directly binding to the promoter region, and MMP-3 is necessary for the Zta promoted cell migration (Lan et al., 2013). Zta genome-wide study reveals a whole regulation map of Zta with the human genome and shows Zta binds to 278 cellular genes during EBV lytic cycle (Ramasubramanyan et al., 2015a).

There is increasing evidence showing that Zta affects the host cell cycle and this effect is based on different mechanisms. Zta causes a G1/S block in some cell types by down-regulating cyclin A and c-myc and up-regulating p21 (Wu et al., 2003). However, in some cells like HeLa cells, Zta blocks both the G2 and the M phases (Mauser et al., 2002). Zta also inhibits the transcriptional function of p53, which is an important host defence and tumour suppressor gene that induces cellular apoptosis and inhibit viral replication (Sato et al., 2009).

1.9.2.2 Role of Rta in EBV lytic reactivation

All gammaherpesviruses encode a transcription factor similar to Rta. EBV Rta is essential for latency lytic switch in both EBV infected B cells and epithelial cells (Feederle et al., 2000; Ragoczy et al., 1998). Rta consists of three domains, an amino-terminal DNA recognition domain, a dimerisation domain and a transcription activation domain (Manet et al., 1991). Rta regulates several lytic promoters through direct interaction with a DNA motif called Rta response elements (RREs) (Heilmann et al., 2012), it also interacts with cellular transcription factors Sp1, TBP, TFIIB during transcription activation (Manet et al., 1993). During the lytic cycle, Rta alone or synergistically works with Zta to regulate a series of early lytic gene expression and also plays an important role in DNA replication.

1.9.3 Early lytic genes expression

Six early lytic genes encode core viral replication proteins, including the single-stranded DNA-binding protein (BALF2), DNA polymerase processivity factor (BMRF1), DNA polymerase (BALF5), helicase (BBLF4), primase (BSLF1), primase-associated factor (BBLF2/3). These proteins assemble the DNA replication machinery with Zta and help lytic DNA replication (Baumann et al., 1999; Gao et al., 1998). BMRF1 is a polymerase processivity factor during replication, however, it also shows a transcription regulation role to activate BHLF1 gene promoter together with Zta (Zhang et al., 1996).

There are other early lytic genes that play roles in viral gene expression, DNA replication or important for cellular functions such as apoptosis or immune response. Some of them are described in detail here as examples.

BMLF1 is an mRNA export factor. It shuttles between nucleus and cytoplasm to help transport un-spliced EBV mRNA, including those core replication gene mRNAs (Semmes et al., 1998).

Apoptosis regulator BCL-2 related genes BHRF1 and BALF1 are also expressed at the early lytic time. BHRF1 acts as an anti-apoptotic factor to delay host cell apoptosis during EBV lytic replication and helps the virus to complete the replication and virion assembly (Dawson et al., 1998). However, it is not essential for viral replication (Marchini et al., 1991). BALF1 can compete with the effects of BHRF1 as an antagonist of apoptosis (Bellows et al., 2002).

BARF1 gene encodes a protein that can act as a colony stimulating factor receptor, which is secreted into the medium of the cultured cells (Strockbine et al., 1998). It binds to the human colony stimulating factor 1 (CSF-1) and inhibits its function, suggesting BARF1 protein may play a role in modulation of host immune responses to EBV infection (Cohen and Lekstrom, 1999). BARF1 can work as an oncogene and transform cells when stably expressed in cultured B cells. (Cohen and Lekstrom, 1999). In EBV positive epithelial tumours NPC and gastric carcinoma, BARF1 products are detected by 85% and 100% in each disease indicating BARF1 can be an oncogene in these tumours (Decaussin et al., 2000; zur Hausen et al., 2000). Recently a study reported a BARF1- specific antibody was designed as an immunotherapeutic drug for the treatment of EBV related tumour, which showed promising results in the cells as well as animal models, this provided a new cancer therapy possibility for those tumours (Turrini et al., 2017).

BGLF4 is a serine/threonine protein kinase encoded by the EBV genome. BGLF4 targets substrates at the same site that cellular kinase cyclin-dependent kinase 1 (CDK1) does, suggesting BGLF4 may function similarly to CDK1 (Lee et al., 2008). BGLF4 modulates the function of nuclear pore complex to help the nuclear import of some EBV lytic proteins, at the same time, to inhibit the cellular protein nuclear transportation, this suggests a function of BGLF4 in virion assembly and egress (Chang et al., 2015). A phosphoproteomic study has revealed a whole protein phosphorylation regulation map of BGLF4, showed significant enrichment of signalling pathways including the DNA damage response, mitosis and cell cycle. It also found 22 proteins associated with the nuclear pore complex, which support the evidence of its role in nuclear transportation (Li et al., 2015). BGLF4

is also important for EBV late gene expression. Ectopic expression of BGLF4 in cells stimulates the mRNA levels of six late genes and this is dependent on its kinase activity. Knocking down of BGLF4 obviously decreased the late gene expression (El-Guindy et al., 2014).

1.9.4 Lytic DNA replication

EBV lytic DNA replication starts with Zta binding to oriLyt and it initiates EBV genome replication, resulting in around 100-fold genome amplification (Hammerschmidt and Sugden, 1988). Although EBV latent replication depends on cellular replication machinery, Lytic DNA replication uses a viral system, and it is independent of cellular DNA replication.

The initiation of lytic replication depends on Zta binding to the ZREs within upstream (ZRE1-4) and downstream (ZRE5-7) elements of oriLyt, which has been described in **session 1.4.1**. In addition, initiation of oriLyt requires a GC-rich BHLF1 RNA to form an RNA-DNA hybrid at oriLyt. This is essential for the unwinding of DNA and recruiting BALF2 to oriLyt (Rennekamp and Lieberman, 2011).

Cellular DNA replication process requires several enzymes and proteins, including DNA polymerase, DNA helicase, DNA primase and ligase, single-strand binding proteins, DNA topoisomerases, clamp and a processivity factor. During replication, all the components create a replication fork and perform the DNA synthesis from 5’-3’ direction on both strands (Bell and Dutta, 2002).

EBV lytic replication has a similar process while using its own enzymes. Once DNA replication is initiated, the core viral lytic replication proteins will be recruited to oriLyt. These replication units form replication compartments or called replisome, which include BALF2, BMRF1, BALF5, BBLF4, BSLF1, and BBLF2/3 (Baumann et al., 1999; Gao et al., 1998). Over-expression of six replication proteins can partly restore the capacity of replication-defective Zta mutants and

enhances Zta binding to oriLyt, which suggests these proteins are essential for EBV lytic replication (El-Guindy et al., 2010).

Name	Function in lytic replication
BALF2	Single-strand DNA binding protein
BMRF1	DNA polymerase processivity factor; a transcriptional coactivator of BZLF1 (Zhang et al., 1996)
BALF5	Polymerase, interacts with the helicase–primase complex (Fujii et al., 2000)
BBLF4	Helicase
BSLF1	Primase
BBLF2/3	Primase-associated protein; BBLF4, BSLF1, and BBLF2/3 form the helicase–primase complex (Gao et al., 1998)
BZLF1	Origin-binding protein, also binds to replication proteins. Viral transcription factor

Table 1.1 Core Lytic replication proteins and their functions.

The process of EBV lytic replication is illustrated here. Zta and BHLF1 RNA bind to oriLyt, which initiates the DNA replication. All the members that are essential for replication are recruited to oriLyt and together to assemble replication compartments. Then helicase BBLF4 unwinds the DNA and forms a replication fork. Single-strand DNA binding protein BALF2 binds to each single strand DNA in order to and prevent the double strand from re-annealing after unwinding

(Tsurumi et al., 1998). The helicase interacts with primase (BBLF4-BSLF1) to stabilise the replication compartments, and co-localise with primase-associated protein BBLF2/3 to form a complex (Gao et al., 1998). BBLF2/3-BBLF4-BSLF1 complex recruits and interacts with polymerase BALF5 to provide a start point for BALF5 (Fujii et al., 2000), then BALF5 synthesises new DNA strands by adding nucleotides to the template strand. The DNA polymerase processivity factor BMRF1 interacts with BALF5 to enhance its polymerase activity (Tsurumi et al., 1993; Kiehl and Dorsky, 1995; Murayama et al., 2009). A model showing the main members in replication compartments at oriLyt is illustrated in **Figure 1.6**.

Rta is also essential for EBV lytic replication, it binds to the enhancer region of oriLyt *in vivo* and co-localises to replication compartments. The C-terminal amino acids are essential for the function of Rta in replication. Rta works with Zta to express the BHLF1 transcripts that are required for the lytic replication (El-Guindy et al., 2013).

BGLF4 is reported to be co-localised with EBV lytic replication compartments and associated with the extensive phosphorylation of BMRF1 during lytic replication *in vivo*. BGLF4 also phosphorylates BMRF1 *in vitro*. This suggests an involvement of BGLF4 in lytic DNA replication (Chen et al., 2000).

Two cellular factors are involved in the lytic DNA replication, Sp1 and ZBP-89. They are both transcription factors and binding to the downstream TD element in the oriLyt region. In addition, they also recruit BMRF1 and BALF5 to the oriLyt through direct binding in order to assemble the replication compartments (Baumann et al., 1999).

The protein interaction and DNA replication compartments are illustrated in **Figure 1.6**.

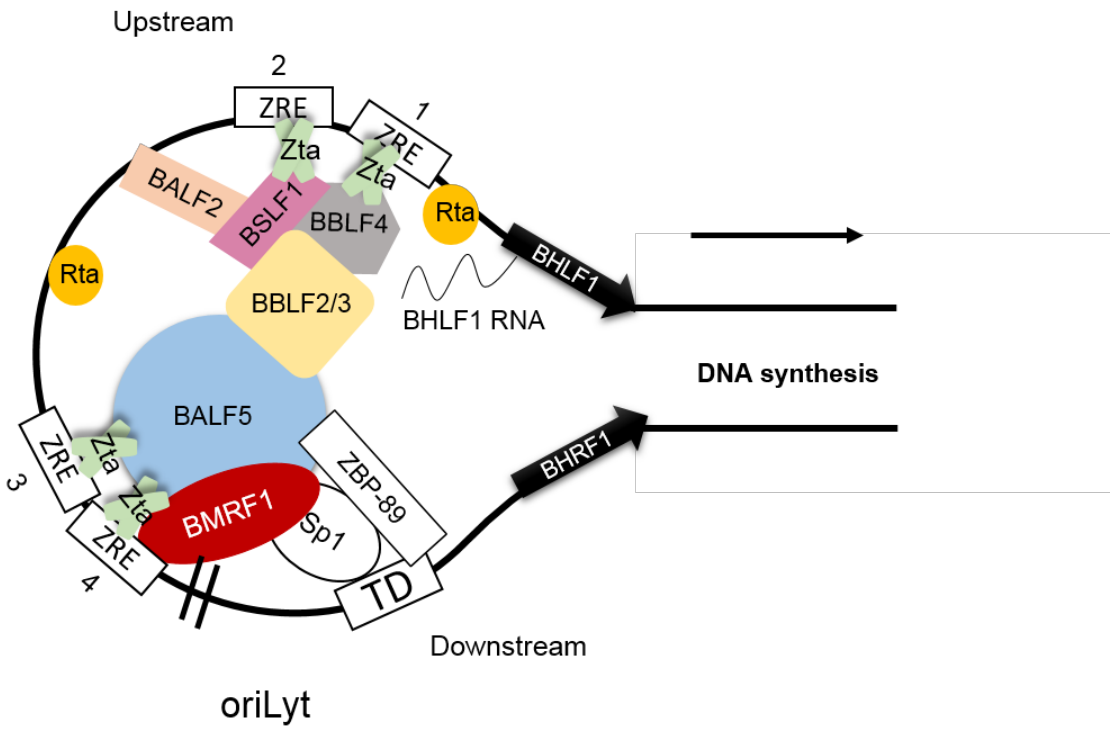

Figure 1.6 Model of replication compartments assembled at oriLyt (adapt from Baumann et al., 1999). When induced lytic cycle, Zta binds to ZREs located in the upstream component to initiates lytic replication and recruits core replication proteins to oryLyt. Zta interacts with DNA polymerase accessory factor BMRF1 through bZIP domain (Zhang et al., 1996), and interacts with helicase BBLF4 and primase sub-complex BSLF1-BBLF2/3 through transcription activation domain (Gao et al., 1998; Liao et al., 2001). Zta also interacts with polymerase BALF5 through transcription activation domain (Baumann et al., 1999). Protein-protein interactions are also seen among the core replication proteins. BBLF4, BSLF1 and BBLF2/3 interact together to form a primase-helicase complex (Gao et al., 1998). BALF2 and BALF5 interact with this complex (Gao et al., 1998; Fujii et al., 2000), BMRF1 interacts with BALF5 to enhance the polymerase activity (Murayama et al., 2009). Rta is required for lytic replication, it is required for the BHLF1 transcripts, which initiates lytic replication with Zta (El-Guindy et al., 2013). Cellular protein Sp1 and ZBP-89 bind to the TD element located downstream of oriLyt, and they interact with viral proteins BMRF1 and BALF5 (Baumann et al., 1999).

The termini of the EBV genome contain a variable number of oriented 538-bp terminal repeats (TRs). The TRs are involved in the circularisation event of the genome, a region of 159 bp in a single TR contains the cis-acting signals, and it is essential for cleavage and packaging of the EBV virion DNA (Zimmermann and Hammerschmidt, 1995).

At the end of replication, a linear EBV genome is synthesised as a continuous strand, cleaved and packaged into the capsid.

1.9.5 Late lytic genes expression

EBV encodes around 36 late genes including genes that encode viral structure proteins, glycoproteins such as gp350, gH, gL, tegument proteins that are important for EBV capsid assembly, DNA packaging proteins in capsids as well as viral attaching and fusion proteins during infection (Yuan et al., 2006).

DNA replication is one factor that is necessary for late gene expression. Disruption of DNA replication can stop late gene expression (El-Guindy et al., 2010).

Another important factor to regulate the late gene expression is the expression of viral serine/threonine Kinase BGLF4. Most late gene expression is dependent on its function. RNA-seq studies showed BGLF4 controls expression of 31 late genes, including BcLF1, BFRF3 and BLRF2 (El-Guindy et al., 2014).

Some early gene products are also involved in late gene expression. Recently, a study revealed a complex, named viral preinitiation complex (vPIC), which is required for the activation of an EBV late gene promoter. EBV early gene BcRF1 encodes a TATA box binding protein (TBP)-like protein. It recruits five other early proteins, including BFRF2, BGLF3, BVLF1, BDLF4 and BDLF3.5 to assemble the vPIC, which are required for the late gene expression. vPIC interacts with RNA polymerase-II and together regulate late gene expression (Aubry et al., 2014).

Rta and Zta are also associated with a few late gene promoters through the genome-wide studies and regulate the expression of late genes (Heilmann et al., 2012; Ramasubramanyan et al., 2012).

Figure 1.7 illustrates a summary of the different stages of lytic reactivation.

1.10 Zta interacting proteins

EBV encoded proteins work together or interact with host proteins in order to perform their functions. As a transcription factor, Zta needs to regulate viral and host gene expression through interacting with other proteins. Previous studies have found a few proteins that Zta interacts with, including EBV proteins as well as cellular proteins.

1.10.1 Zta interacts with EBV proteins

Zta was identified to interact with BMRF1 through BMRF1 first 45 amino acids and Zta bZIP domain by *in vitro* binding assay, and Zta can be co-immunoprecipitated by BMRF1 in lytic cycle inducted cells *in vivo*. BMRF1 interacts with Zta and enhances the transcription activation of Zta to the BMRF1 promoter. However, this direct interaction is not required for BMRF1 and BZLF1 to activate BHLF1 promoter, which suggests a promoter-specific manner for this interaction (Zhang et al., 1996).

BBLF4, BSLF1, and BBLF2/3 form the helicase-primase complex during lytic replication, Zta transcription activation domain 1-133 amino acid (aa) binds to this complex and helps to stabilise the replication complex (Gao et al., 1998). Further mapping study has mapped the region between 22-86 aa to be required for Zta to interact with BBLF4 both *in vitro* and *in vivo* (Liao et al., 2001).

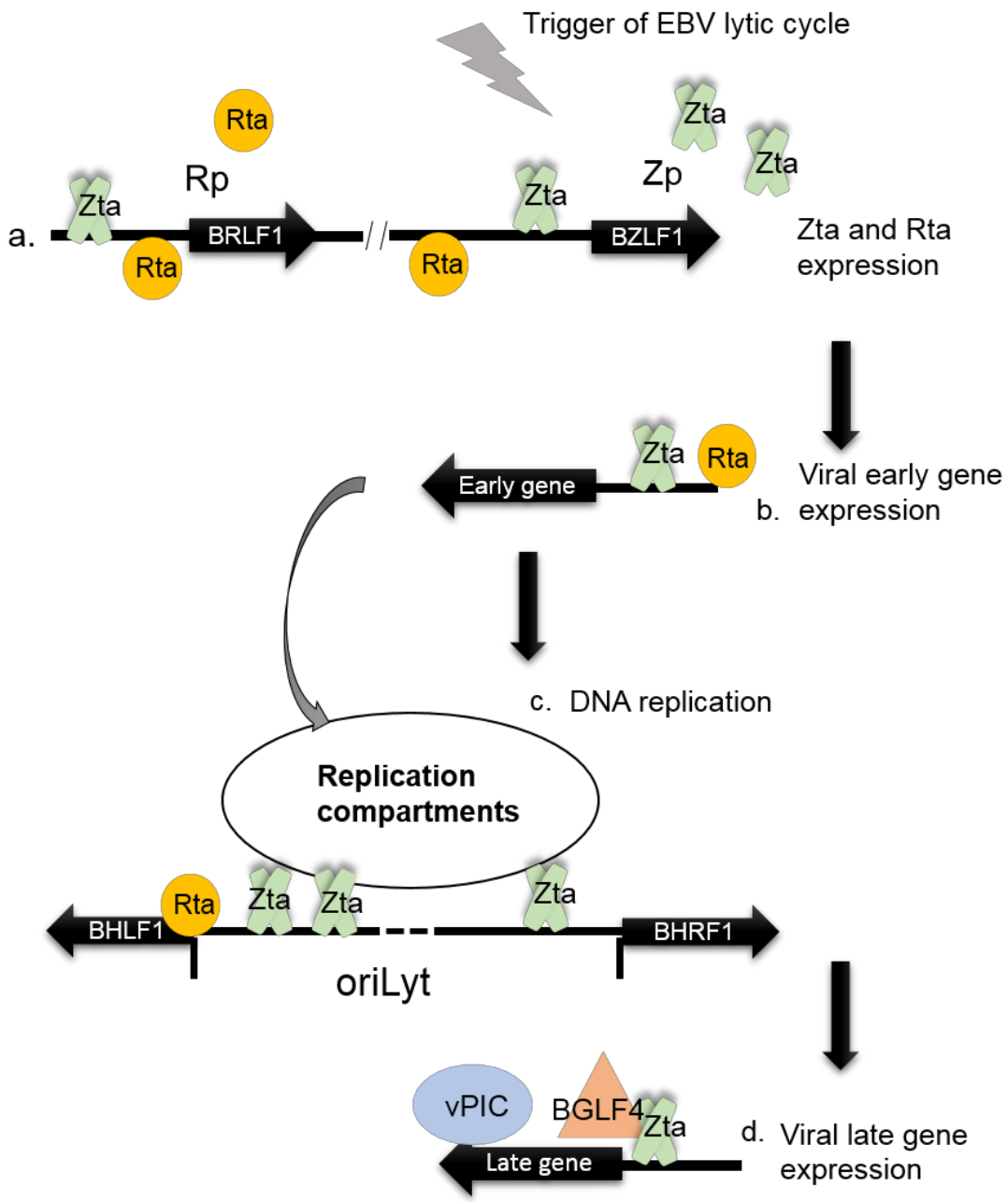

Figure 1.7 Different stages of EBV lytic reactivation. When triggered lytic cycle, transcription factors Zta and Rta expressed by the regulation of the Zp and Rp (a). As transcription factors, Zta and Rta activate a subset of early lytic genes on their own binding to target gene promoters or through synergy (b). Then Zta binds to ZREs located upstream of oriLyt to initiate EBV lytic DNA replication and recruits other early genes to oriLyt to assemble the lytic replication machinery (c). Following viral replication, late genes expressed, which are regulated by BGLF4 and the viral pre-initiation complex (vPIC) (d).

Zta also binds to EBV polymerase BALF5, GST pull-down assay *in vitro* and expression plasmids co-immunoprecipitation (co-IP) assay *in vivo* were used to study this interaction. The *in vitro* mapping study identified region 26-88 aa in the transcription activation domain is required for this interaction (Baumann et al., 1999).

BGLF4, which is an EBV protein kinase, phosphorylates Zta both *in vitro* and *in vivo*. It interacts and co-localises with Zta in the viral replication compartments to regulate EBV lytic replication. The binding of Zta to BGLF4 was shown by the co-IP assays, which were performed in the cells that over-expressed each protein as well as in the cells that were induced to EBV lytic cycle by TPA (Asai et al., 2006).

1.10.2 Zta interacts with cellular proteins

Zta shows a synergistic transcriptional effect on promoter sites with TATA box binding protein TFIID (also named TBP). Zta directly binds to TFIID to stabilise its association with EBV BHLF1 promoter. *In vitro,* purified 94-141 aa truncated Zta binds to TFIID suggests this interaction is through Zta N-terminus of transactivation domain (Lieberman and Berk, 1991).

Retinoid X receptor α (RXRα) interacts with Zta. It inhibits the transcription activity of Zta to activate the BMRF1 promoter through preventing Zta binding to the AP-1 motif. On the contrary, Zta can inhibit RXRα induced activation of a cellular RARβ promoter (Sista et al., 1993).

Zta interacts with transcription factor NF- κB subunit p65. p65 inhibits the ability of Zta to activate EBV early BHRF1 promoter in HeLa cells. Zta co-immunoprecipitates with endogenous p65 in sodium butyrate and TPA induced lytic cells but not in un-induced cells *in vivo*. *In vitro* binding study shows Rel homology domain of p65 is required to bind to the bZIP domain of Zta (Gutsch et al., 1994).

Human cellular tumour antigen p53 interacts with Zta *in vitro* and *in vivo*. Overexpression of p53 inhibits Zta's transcription ability to activate EBV early lytic BMRF1 and BHRF1 promoter. *In vitro* binding study shows this interaction is through C-terminus of p53 binding to Zta bZIP domain. P53 is also found to inhibit EBV lytic reactivation when co-transfected with Zta into D98/ HE-R-1 cell line, which is a fusion of a HeLa cell subclone (D98) with the EBV-positive Burkitt's lymphoma cell line P3HR-1. The expression of p53 also inhibits the anti-IgG induction of EBV lytic cycle in Akata cells. On the other side, Zta inhibits p53-dependent transactivation, suggests Zta may influence the function of p53 through direct binding. (Zhang et al., 1994).

C/EBPα is a transcription factor that belongs to the bZIP family. A co-IP study in EBV lytic cycle induced Akata cells shows C/EBPα interacts with Zta *in vivo*. *In vitro* mapping study shows Zta directly interacts with C/EBPα through its bZIP domain. Zta and C/EBPα co-operatively up-regulates the expression level of p21 and cause the G1 arrest during EBV lytic reactivation together (Wu et al., 2003). They also directly bind to ZII and ZIIIB of Zp during EBV lytic initiation and co-operatively regulate Zp expression (Wu et al., 2004).

Zta binds to transcriptional coactivator CREB binding protein (CBP) through its transactivation domain, this interaction increases protein EA-D expression level and enhances the transcription activity of Zta to BHLF1 promotor. Zta interacts with CBP was validated by an *in vitro* GST pull-down assay. On the other hand, Zta is identified to strongly enhance the histone acetyltransferase activity of CBP through this interaction (Chen et al., 2001; Zerby et al., 1999).

CREB-regulated transcription coactivator 2 (CTCR2) binds to Zta during EBV lytic initiation and co-activates Zp with Zta and CREB. Knocking down of endogenous CTCR2 could decrease Zta expression level triggered by TPA/ionophore in EBV positive gastric cancer cell line GTC-4 and EBV positive B cell line Akata. A co-IP study shows a CTCR2 interacts with Zta under an over-expression condition in HEK293T cells, and the coil-coil domain of CTCR2 is required for this binding (Murata et al., 2009).

Pax5 is a cellular transcription factor that regulates many B cell specific genes that are required for B cell development. Expression of Pax5 inhibits EBV lytic replication and inhibits Zta regulated early lytic promoters (BMRF1p and BRLF1p). This may be through the Pax5 binding to Zta. GST pull-down assay mapped to the DNA-binding domain of both proteins were required for this interaction (Raver et al., 2013). Oct-2 is another B-cell specific transcription factor that shows a similar inhibitory feature to EBV lytic replication and the transactivation of Zta. A co-IP assay showed an interaction between Zta and Oct2 *in vivo*, GST-pull down assay also showed a directly binding of Zta DNA binding domain to Oct-2 POU domain (179-343 aa) (Robinson et al., 2012). This also indicates a mechanism of inhibition of EBV lytic cycle by host proteins

Zta interacts with the cellular DNA damage response protein 53BP1 during EBV lytic cycle. Zta binds to 53BP1 both *in vitro* and *in vivo* through its C-terminal region. Knocking down of 53BP1 reduces EBV lytic replication in LCL#3 cells suggesting 53BP1 contributes to the EBV lytic replication (Bailey et al., 2009).

It is reported that Zta binds to cellular protein DNA-dependent protein kinase Ku80 using mass spectrometry by Sinclair lab for the first time. Later on, Chang's group verifies this interaction by GST pull-down assay and *in vivo* co-IP. *In vitro* mapping study shows Zta binds to 425 aa region in N-terminus of Ku80 through its C-terminal region. Ku80 binds to Zta and enhances Zta's transcription ability to activate BHLF1 promoter (Bailey et al., 2009; Chen et al., 2011).

Zta interacts with PKC targeting protein receptor for activated C kinase 1 (RACK1). Yeast interaction trap assay showed a direct interaction between these two proteins, GST pull-down study mapped Zta transcription activation domain is necessary for this interaction. However, RACK1 doesn't affect the transcription activity of Zta and on the other side, this interaction does not functionally influence PKC mediated phosphorylation of Zta. RACK1 might be a scaffolding protein to recruit Zta to PKC (Baumann et al., 2000).

Zta is reported to synergistically work with Rta and forms a complex via a cellular protein MBD1-containing chromatin-associated factor 1 (MCAF1). ChIP-qPCR suggests that Zta, Rta and MCAF1 bind to the same ZRE in BHRF1 and BMRF1 promoter region *in vivo* and they also co-localise at the same area in the cells, this interaction is through Zta and Rta directly binding to the region 562-816 aa of MCAF1 (Chang et al., 2010).

Zta can be SUMOylated at lysine 12 by SUMO-1, 2 or 3, which suppressed the transcription activity. Cellular protein RanBPM suppresses the SUMOylating of Zta through directly interacting with Zta. The interaction was validation in a co-IP assay in 293T co-transfected cells, GST pull-down assay showed the interaction was between 194-245 aa region of Zta and RanBPM SPRY domain (Yang et al., 2015).

From all the interaction studies, Zta shows a preference for interacting with cellular transcription factors, and this is mostly because Zta needs co-regulators to perform its transcription activity. Zta also shows the possibility to influence the function of some transcription factors during host gene regulation. In addition, Zta is able to interact with the protein kinase and DNA damage related proteins, which suggests a role of Zta in different cellular regulations. Most studies focused on how cellular proteins influence viral functions, however, some studies also investigate how Zta influence the functions of host cells. It is important to study the influences on both sides and doing so we can obtain a full image about how EBV lytic cycle interact with host cells through Zta.

1.11 EBV lytic cycle and cancers

EBV lytic cycle contributes to the incidence and tumorigenesis of EBV associated cancers.

EBV lytic activation increases viral load in the blood, which increases the chances for EBV to infect more cells within the body, and this also increases the chances to develop an EBV associated cancer in the cell.

In addition, The EBV lytic genes may play a role in cancer development. A subset of EBV infected cells with lytic replication features was detected by biopsy in BL and NPC tissues suggesting lytic cycle may promote tumour growth in those cancers (Xue et al., 2002; Zheng et al., 2015). The EBV strain M81 from NPC patients can switch to lytic cycle spontaneously and this causes the high viral load in the NPC cancer cells and increased antibody titres against EBV proteins in the peripheral blood, for example, EA-D IgA and VCA IgA (Tsai et al., 2013).

Animal tumorigenesis experiment shows wide type virus has higher chance to cause lymphomas than BZLF1 knockout virus, suggesting EBV lytic infection is important in the development of B cell lymphomas (Ma et al., 2011).

The role of EBV lytic infection in B cell immortalisation remains controversial. A previous study showed that BZLF1 knockout virus transforms B cells as efficiently as wide type virus, suggesting no role of lytic in B cell transformation. (Katsumura et al., 2009). However, recently it was reported that EBV lytic proteins can enhance the B cell immortalisation by inducing IL-13 as a paracrine mechanism (Katsumura et al., 2012).

There is no doubt that EBV lytic cycle plays a role in maintaining and spreading the virus in the host cells, and obviously there are different features for lytic in B cells and in epithelial cells, more studies are needed to answer these questions.

1.12 EBV vaccines

The best way to prevent a virus-associated disease is to vaccinate human beings. Scientists also want to design a vaccine to control the EBV infection, which can firstly prevent the primary infection of EBV such as IM and also control the latency establishment, further, to control the EBV associated malignancies. Although a few methods have been established, only one of them reached phase II clinical trial, and until now, there is no EBV vaccine on the market.

The first target for designing the EBV vaccine is EBV glycoprotein gp350. From the early studies, people found that immunised individuals with neutralised antibodies for cell membrane antigens could stop infection in primary B cells (Pearson et al., 1970). Later on, the membrane antigen gp350 was isolated and used for the induction of a gp350 neutralisation antibody as a vaccine. A few clinical studies have performed, one method showed a promising results in adults studies, its placebo-controlled double-blinded phase II study, which showed a high seroconversion, 98.7% by 6 months, and also showed a reduced incidence of IM (Sokal et al., 2007). However, a phase III clinical trial is needed to test the efficiency of this vaccine. In addition, new studies to improve the gp350 antibody titres are still underdevelopment.

Recently an EBV virus-like particle (VLP) was developed, which combined more targets but contained no viral DNA, in order to get more neutralising antibody. Animal studies showed that VLPs could induce high antibody titres that were able to neutralise EBV infection *in vitro* (Ruiss et al., 2011).

A T cell-mediated vaccine is another direction for designing the EBV vaccine, which can be used for prevention or treatment of IM, PTLD and some EBV associated cancers. The design of vaccine is based on latency proteins, including EBNA1, EBNA3, LMP1 and LMP2. However, all the studies are still underdevelopment (Bollard et al., 2012).

A new study used gH/gL and gp42 complex as the vaccine target, unlike the gp350 vaccine, which only protects B cells from infection, antibodies elicited from viral-fusion machinery EBV gH/gL or gH/gL/gp42 neutralises both epithelial cell and B cell infection. This new vaccine candidate still needs further study and clinical trials (Bu et al., 2019).

One limitation on the identification of EBV vaccine is from the unclear EBV primary infection. However, more vaccines will be designed with the development of the studies in EBV. In addition, the current clinical trial results do show that the vaccines are able to decrease the EBV infection of IM and EBV associated

cancers. The advantages of vaccination for EBV is obvious, however, we still have to consider whether the vaccination of the whole population has more benefits since the majority of people live with EBV for the lifetime without developing EBV associated diseases.

1.13 Lytic induction treatment in EBV-positive cancers

EBV is associated with many malignant tumours. Although there might be a risk to spread the virus, EBV lytic induction is now used as a new strategy for treating EBV positive tumours. Lytic induction strategy is to combine an EBV lytic induction reagent with the antiviral drugs as well as chemotherapy.

These antiviral drugs including ganciclovir (GCV) and acyclovir (ACV) are guanine nucleoside analogues that are widely used to inhibit the lytic replication of herpesviruses. They need to be phosphorylated in the cell by a protein kinase and work as a nucleotide that incorporated into viral DNA and stops the lytic replication. Studies in other herpesvirus revealed that a virally encoded kinase activates those drugs much better than cellular nucleoside kinases. Although in HSV-1 and HSV-2, thymidine kinase mediates the drug activation, in EBV, protein kinase BGLF4 is required and responsible for the phosphorylation of those drugs (Meng et al., 2010).

Comparing with chemotherapy alone, a combination of lytic induction reagents valproic acid plus antiviral drug GCV results in the best antitumour response among tested regiments (Hsu et al., 2015). Some chemotherapy drugs such as 5-FU or cis-Platinum can also induce EBV lytic cycle during the treatment and when combined with GCV for treatment, the EBV positive NPC tumour was inhibited more efficiently than conventional chemotherapy (Feng et al., 2002). Recently low toxicity and highly effective new types of small molecules that can induce EBV lytic cycle in EBV positive cancer cells were identified. Combining antiviral drugs with these compounds shows promising effects for killing tumour cells (Tikhmyanova et al., 2014).

1.14 Aims of the project

How EBV exploits the host cell machinery is the most important remaining question related to EBV replication. Previous studies have shown some viral and cellular proteins interact with Zta and some of these interactions play important roles for cellular and viral gene regulation, viral DNA replication and host immune response.

In this project, we asked which proteins interact with Zta during EBV lytic replication and whether this influences the function of Zta, and on the other hand, whether Zta will regulate other proteins. To study this, an unbiased approach was first needed in order to find a whole map of the Zta interactome.

- Establishing an affinity pull-down approach combined with quantitative mass spectrometry to obtain a possible series of target proteins that may interact directly or indirectly with Zta.
- HEK293-BZLF1-KO cell line (Feederle et al., 2000), which is HEK 293 cells harbouring a recombinant EBV plasmid with a deletion of the BZLF1 gene would be used in this study, which allowed for the introduction of Zta.
- A chromatin immunoprecipitation (ChIP) method would be optimised to isolate the Zta interactome.
- The interactome would be identified by mass spectrometry and the relevance of interacting proteins would be elucidated.

2 Materials and Methods

2.1 Materials

2.1.1 Plasmids

Name	Method	Source
pcDNA3	Transfection of cells	Invitrogen
pcDNA3- hisZta	Transfection of cells	(Bailey et al., 2009)
pCpGL-BHLF1	Luciferase assay	(Bergbauer et al., 2010)
pCpGL-BHLF1 mutant	Luciferase assay	(Ramasubramanyan et al., 2015a)
pGL3-IL2	Luciferase assay	A gift from Jerry Crabtree (Addgene plasmid # 17870; http://n2t.net/addgene:17870; RRID:Addgene_17870).

Table 2.1: Plasmid DNA constructs used in different experiments.

2.1.2 Primers

2.1.2.1 qPCR primers

Name	Sequence (5'-3')
B-Globin	(a) AGTCCTTCTTGGCTAGTCTGTTGA (b) CTTTGGCGCGGATCCTC
BALF5	(a) GGCAACCCTAAGGTGAAGGC (b) GGTGAGCCAGGCCATCACTA

Table 2.2: qPCR primers used for EBV genome load detection.

2.1.2.2 EMSA primers

DNA probe Name	Sequence (5'-3')	Fluorescent dye
BMLF1 AP-1 F	GATCCA**TGACTCA**GAGGAAAACATACG	IRDye800
BMLF1 AP-1 R	CGTATGTTTTCCTC**TGAGTCA**TGGATC	None
ARRE2 WT F	ACGCCTTCTGTA**TGAAACA**GT**TTTTCC**TCC	IRDye800
ARRE2 WT R	GGA**GGAAAA**AC**TGTTTCA**TACAGAAGGCGT	None

Table 2.3: EMSA primers

2.1.3 Cell lines

Name	Culture medium	Reference or Source
Akata EBV positive	RPMI1640	(Takada, 1984)
293-BZLF1-KO	RPMI1640	(Feederle et al., 2000)
HEK293	DMEM	ATCC
DG-75	RPMI1640	ATCC

Table 2.4: Cell lines used in different experiments.

2.1.4 Antibodies

Antibody (Primary)	Species	Application	Source
BZ1 anti-Zta	Mouse, monoclonal	WB/Flow cytometry	(Young et al., 1991)
SCZ anti-Zta	Goat, polyclonal	ChIP/ IP	Santa Cruz Biotechnology
EBV VCA gp125	Mouse, monoclonal	Flow cytometry	Merck
GFP	Rabbit, Polyclonal	WB	Invitrogen
Actin	Rabbit, polyclonal	WB	Merck, Sigma
HSC70	Mouse, monoclonal	WB	Santa Cruz Biotechnology
PARP1	Mouse, monoclonal	WB	Santa Cruz Biotechnology
TAF6	Mouse, monoclonal	WB	Santa Cruz Biotechnology
NFATC1	Mouse, monoclonal	WB	Santa Cruz Biotechnology
NFATC2	Mouse, monoclonal	WB	Santa Cruz Biotechnology
MEF2B	Mouse, monoclonal	WB	Santa Cruz Biotechnology

FAM96B	Mouse, monoclonal	WB	Santa Cruz Biotechnology
TXN	Mouse, monoclonal	WB	Santa Cruz Biotechnology
RUNX3	Mouse, monoclonal	WB	Santa Cruz Biotechnology
MMS19	Mouse, monoclonal	WB	Santa Cruz Biotechnology

Table 2.5: Primary antibodies used in different experiments.

Antibody (Secondary)	Species	Application	Source
VeriBlot for IP Detection Reagent (HRP) anti-multi species		WB	abcam
IR Dye α-rabbit 800CW	Donkey	WB	LICOR
IR Dye α-mouse 800CW	Goat	WB	LICOR
IR Dye α-mouse 680RD	Goat	WB	LICOR
Alexa Fluor 647 anti-mouse	Donkey	Flow cytometry	abcam

Table 2.6 Secondary antibodies used in different experiments.

2.1.5 Reagents and materials

Reagents and solutions	Application	Source
VER-155008	Hsp70 inhibitor	TOCRIS
FK506	Ca2+ signaling and NFATs inhibitor	Merck, Sigma
Anti-human IgG	Induce EBV lytic cycle in cell culture	Agilent, Dako
Hygromycin B	Cell culture, cell selection	Merck, Sigma

Ionomycin	Ca2+ signaling activation	Merck, Sigma
PMA/TPA (12-O-Tetradecanoylphorbol 13-acetate)	PKC activation	Merck, Sigma
RPMI1640	Cell culture	Gibco
DMEM	Cell culture	Gibco
Penicillin/Streptomycin/Glutamine	Cell culture	Gibco
GlutaMAX	Cell culture	Gibco
Fetal Bovine Serum (FBS)	Cell culture	Gibco
Nunc cell culture flasks (T25, T75, T175), filter caps	Cell culture	Thermo Scientific
6-well, 12-well and 96-well plate, flat bottom	Cell culture	Thermo Scientific
Trypsin	Cell culture	Gibco
D-PBS	Cell culture	Gibco
Dimethyl Sulfoxide (DMSO)	Cell culture	Merck, Sigma
Formaldehyde	Cross-linking cells	Merck, Sigma
PBS tablets	WB	Oxoid
4-12% pre-cast Bis-tris gel	Protein gel/ WB	Invitrogen
10% pre-cast Bis-tris gel	Protein gel/ WB	Invitrogen
12% pre-cast Bis-tris gel	Protein gel/ WB	Invitrogen
SimplyBlue Safestain	Protein gel	Invitrogen
Coomassie InstantBlue	Protein gel	expedeon
MOPS SDS running buffer (20X)	Protein gel/ WB	Invitrogen
MES SDS running buffer (20X)	Protein gel/ WB	Invitrogen
BSA	Protein gel	Merck, Sigma
BSA 100X	EMSA	NEB

CellLytic MT cell lysis reagent	Protein extraction	Merck, Sigma
Benzonase Nuclease	Protein extraction	Merck, Sigma
Protease inhibitor EDTA-free	Protein extraction and IP	Roche
PMSF (Phenylmethanesulfonyl fluoride)	Protein extraction and IP	Merck, Sigma
Trypsin (Mass spectrometry grade)	Mass spectrometry	Promega
Trifluoroacetic acid (TFA)	Ingel digest/Mass spectrometry	Thermo Scientific
Acetonitrile	Ingel digest/Mass spectrometry	Merck, Sigma
DTT (dithiothreitol)	Protein sample preparation	Merck, Sigma
Iodoacetamide	In-gel digest	Merck, Sigma
Odyssey Blocking buffer	WB	LI-COR
ECL solution	WB	LI-COR
Gotaq qPCR Master Mix	qPCR	Promega
Gel shift binding buffer 5X	EMSA	Promega
Orange loading dye	EMSA	LI-COR
DSP (dithiobis(succinimidyl propionate))	Cross-linking/IP	Thermo Scientific
BS3 (bis(sulfosuccinimidyl)suberate)	Cross-linking/IP	Thermo Scientific
DMP (Dimethyl pimelimidate dihydrochloride)	Cross-linking/IP	Merck, Sigma
Dynabeads Protein G	IP	Invitrogen
alarma-blue reagent	Cell viability assay	Invitrogen

siRNA Buffer 5X	siRNA Knock-down	Dharmacon
passive cell lysis buffer 5X	Luciferase assay	Promega

Table 2.7: Purchased reagents and materials.

2.1.6 Solutions

Method	solutions	composition or Source
ChIP	Cell lysis buffer	85 mM KCl, 0.5% NP-40, and 5 mM PIPES pH 8.0
	SDS lysis buffer	1% SDS, 10 mM EDTA, 50 mM Tris pH 8.0
	IP Dilution Buffer	0.01% SDS, 1.1% Triton X-100, 1.2 mM EDTA, 16.7 mM Tris pH 8.0, 167 mM NaCl
	Low salt wash buffer	0.1% SDS, 1% Triton X-100, 2 mM EDTA, 20 mM Tris pH 8.0, 150 mM NaCl
	High salt wash buffer	0.1% SDS, 1% Triton X-100, 2 mM EDTA, 20 mM Tris pH 8.0, 500 mM NaCl
	LiCl wash buffer	250 mM LiCl, 1% NP-40, 1% Na-deoxycholate, 1 mM EDTA, 10 mM Tris pH 8.0
	TE buffer	10 mM Tris pH 8.0, 5 mM EDTA
Cross-linking IP or Co-IP	Cell lysis buffer	85 mM KCl, 0.5% NP-40, and 5 mM PIPES pH 8.0

	IP Dilution Buffer	0.5% Triton X-100, 0.5 mM EDTA, 20 mM Tris pH 8.0, 150 mM NaCl
	Low salt wash buffer	0.5% Triton X-100, 0.5 mM EDTA, 20 mM Tris pH 8.0, 150 mM NaCl
	High salt wash buffer	0.5% Triton X-100, 0.5 mM EDTA, 20 mM Tris pH 8.0, 500 mM NaCl
	LiCl wash buffer	250 mM LiCl, 1% NP-40, 1% Na-deoxycholate, 1 mM EDTA, 10 mM Tris pH 8.0
	Co-IP wash buffer	10 mM Tris/Cl pH 7.5; 150 mM NaCl; 0.5 mM EDTA
Western blot	Transfer buffer	0.025MTris, 0.192M Glycine, 15% methanol (v/v)
	Blocking buffer	5% skimmed milk (w/v), in PBS-Tween.
	PBS Tween	PBS with 0.1% Tween
	Laemmli Protein sample buffer 2X	2% SDS, 10% glycerol, 5% 2-mercaptoethanol, 0.002% bromphenol blue, 0.0625 Tris-HCL (Sigma protocol)
Flow cytometry	Wash medium	0.1% NaN3 (v/v), 5% FBS (v/v), in PBS.
Cell culture	Freezing media	85% FCS supplemented with 15% DMSO

Table2.8: All the solutions prepared in different experiments.

2.1.7 Kits

Kit	Source	Use
QIAquick DNA Purification Kit	Qiagen	DNA purification
QIAprep Mini-Prep	Qiagen	Expression of vectors
QIAprep Maxi-Prep	Qiagen	Expression of vectors
Effectene Transfection Kit	Qiagen	Transfection
Cell Fixation & Cell Permeabilization Kit	Invitrogen	Flow cytometry
Luciferase Assay System	Promega	Luciferase Assay
Neon Transfection system 100ul tip kit	Invitrogen	Transfection Knock-down

Table 2.9: Commercial kits.

2.2 Methods

2.2.1 Cell culture

HEK293 cell line is a human embryonic kidney cell line. Adherent cells were cultured in DMEM (Gibco) media with 10% FBS (Gibco), 100 units/mL penicillin, 100 µg/mL streptomycin and 2 mM L-glutamine (Gibco).

293-BZLF1-KO cell line is human embryonic kidney cells transformed with a hygromycin-resistant EBV bacmid containing a deletion of the BZLF1 gene (Feederle et al., 2000). Cells were cultured in RPMI1640 (Gibco) with 10% FBS, 100 units/mL penicillin, 100 µg/mL streptomycin and 2 mM L-glutamine. Cells were selected by 100ug/ml hygromycin (Invitrogen) for maintaining knockout genome.

Akata group I cell line is EBV positive Burkett's lymphoma cell line, DG-75 cell line is EBV negative Burkitt's lymphoma cell line, both cell lines were suspension cells cultured in RPMI 1640 with 10% FBS, 100 units/mL penicillin, 100 µg/mL streptomycin and 2 mM L-glutamine.

All the cell lines were cultured in an incubator (Thermo Scientific) at 37°C with 5% CO_2.

For long-term storage of cell lines, cells were washed by PBS and then re-suspended in freezing media with around 2-5 x 10^6 cells/ml. Cells were frozen at -80°C in Mr. Frosty (Thermo Scientific) Freezing Container before storage in liquid nitrogen.

2.2.2 Lytic cycle induction

To induce lytic cycle in Akata cells, 2 x 10^6 cells/ml cells were re-suspended in media and 1.3µl/ml anti-IgG (Agilent, Dako) was added in the media, then

incubated for 24 hours and harvested for analysis. For 48 hours of induction, cells were diluted 1:2 after 24 hours in order to maintain cells with fresh media.

To induce lytic cycle in 293-BZLF1-KO cells, expression plasmid pcDNA3-hisZta was used by transient transfection for 48-96 hours, and then cells were pelleted for the analysis.

2.2.3 Transfection

Effectene transfection reagent was used for pcDNA3 or pcDNA3-hisZta plasmids transfected into HEK293 or 293-BZLF1-KO cells.

For small-scale transfection, 5 x 10^5 cells were plated one day before in small flask for each transfection. 2ug DNA was added to 150µl of EC buffer and 16µl enhancer, after vortexing for 2 seconds, the mixture was incubated for 5 minutes. 25µl of effectene was added and vortexed for 10 seconds and then incubated for 10 minutes. 1 ml of media was added into the mixture and then added back to the cells. Cells were incubated for 48 hours or 96 hours before being harvested.

For large-scale transfection, 4 x 10^6 cells were plated one day before in large flask for each transfection. 16ug DNA was added to 150µl of EC buffer and 128µl of enhancer, after vortexing for 2 seconds, the mixture was incubated for 5 minutes. 40µl of effectene was added and vortexed for 10 seconds, and then incubated for 10 minutes. 1 ml of media was added into the mixture and then added back to the cells. Cells were incubated for 48 hours or 96 hours before being harvested.

Electroporation transfection (Bio-Rad Gene Pulser II) was used for transfections in DG-75 cells. 1 x 10^7 cells were used for one transfection condition. Cells were washed by D-PBS and re-suspended in serum-free media, 5ug of each plasmid DNA was added to cells, the mixture was then transferred to a 4mm gap cuvette (VWR), and the electroporation was performed under condition 260V, 950µF.

2.2.4 Transformation/ Maxi Prep

100ng of plasmid DNA was added to Top10 chemically competent E.Coli cells. The cells were incubated on ice for 5 minutes before adding preheated LB media (42°C), heat shocked at 42°C for 30 seconds and incubated on ice for 2 minutes. Cells were streaked onto the pre-warmed LB agar plates, which containing 100µg/ml of ampicillin, and incubated at 37°C overnight.

A single colony was picked and added to 5ml of LB media containing 100µg/ml ampicillin and incubated in a ThermoScientific MaxQ4000 shaker at 37°C shaking (225rpm) for 8 hours. The start culture was then diluted (1:500) in LB media containing 100µg/ml of ampicillin and incubated at 37°C shaking overnight. The second day the cells were pelleted and used for the Maxi-prep. The rest steps followed the Qiagen maxi-prep kit manufacturers' protocol. The plasmid stock was then quantified as dsDNA concentration by an Eppendorf Biophotometer or Nanodrop.

2.2.5 Chromatin immunoprecipitation (ChIP)

Culturing cells were spun down and re-suspended in 1% formaldehyde (Sigma) solution ($1x10^7$/ml) for 15 minutes at room temperature, with shaking on a rotating wheel. Then glycine was added with a final concentration 125mM to stop crosslinking for 5 minutes. After washes with cold D-PBS (Gibco), cells were ready for ChIP.

Cells were re-suspended in cell lysis buffer for 10 minutes at 4°C. After centrifugation, the nuclear pellets will be washed once and then re-suspended in SDS lysis buffer. Chromatin from nuclei was sonicated on ice (10s sonication with 10s pulses; 30% amplitude output on a Branson model 250 Micro-tip). Then the chromatin was diluted 10-fold with IP dilution buffer. 50µl of each diluted chromatin was taken as the input sample.

10 µg of the Zta antibody (Santa Cruz) or control goat IgG (Santa Cruz) was added in the chromatin and incubated overnight at 4 °C on a rotating wheel. The second day, 25µl of dynabeads (Invitrogen) was added into each condition for 3 hours at 4 °C on a rotating wheel. After incubation, 50µl of chromatin from each tube was taken as the flow through samples.

Then the beads were washed in low salt, high salt, LiCl wash buffer and TE buffer each for 5 minutes. 30µl of Laemmli sample buffer 2X was added to the beads and incubated at 95 °C for 10 minutes to reverse crosslinking and elute the proteins from the beads. 50µl of sample buffer 2X was added into each input and flow through samples and incubated at 95 °C for 10 minutes. Proteins were now ready for protein gel and western blotting.

2.2.6 Cross-linked Immunoprecipitation (x-IP) and co-immunoprecipitation (Co-IP)

For x-IP, cells were harvested and re-suspended in 0.2mM DSP (Thermo Scientific) /PBS solution (1 x 10^7/ml) for 30 minutes at room temperature, then stopped the reaction by adding Tris solution pH 7.5 to get a final concentration 50mM and incubated for 15 minutes, then cells were washed by D-PBS (Gibco). For Co-IP, cells were harvested and washed by D-PBS directly.

Then the cells were re-suspended in cell lysis buffer for 10 minutes at 4°C. After centrifugation, the nuclear pellets were then re-suspended in cell lytic reagent (Sigma) with 250U/ml of Benzonase (Sigma). The nuclear extracts were then diluted in IP dilution buffer, 50µl of each condition was taken as the input sample. 10ug SCZ Zta antibody or control goat IgG were added into the nuclear extracts and incubated overnight at 4 °C on a rotating wheel. The second day, 25µl of dynabeads were added and incubated for 3 hours at 4 °C on a rotating wheel. After incubation, 50µl of chromatin from each tube was taken as the flow through samples.

Then the beads were washed by low salt, high salt, lithium and Co-IP wash buffer each for 5 minutes. Then proteins were eluted in 2x Laemmli sample buffer for 10 min at 95 °C to elute the proteins from the beads. 50µl of sample buffer 2X was added into each input and flow through samples and incubated at 95 °C for 10 minutes. Proteins were now ready for protein gel and western blotting.

The x-IP for TMT labelling mass spectrometry, 10µg of Zta and control antibody were cross-linked to the 25µl of dynabeads by BS3 (Thermo Scientific) first, then cross-linked antibody beads were added to the nuclear extracts and incubated overnight. The wash steps were performed on the second day as described before. 5% of the beads were isolated and the proteins were eluted by 2x sample buffer for 10 min at 95 °C. The rest of the beads were frozen at -20 °C and then sent for further mass spectrometry analysis.

2.2.7 SDS-PAGE and Western blotting

Protein samples were separated on 4-12%, 10% or 12% Bis-Tris NuPAGE gel in morpholinepropanesulfonic acid (MOPS) or MES buffer. Gel electrophoresis was performed at 200V. Then the gel was used for Coomassie blue directly or continue to be used for western blotting.

Proteins were then transferred onto a nitrocellulose membrane using a wet transfer protocol for 90 minutes at 75V and then the membrane was blocked in blocking buffer.

The membrane was incubated with primary antibodies at 4°C overnight, including BZ1 antibody (a kind gift from Martin Rowe lab, mouse 1:200), Actin antibody (Sigma Rabbit 1:1000), MEF2B (Santa cruz, mouse, 1:100), FAM96B (Santa cruz, mouse, 1:100), TXN (Santa cruz, mouse, 1:100), RUNX3 (a kind gift from West lab, santa cruz 1:200), TAF6 (Santa cruz, mouse, 1:500). PARP1 (Santa cruz, mouse, 1:200), MMS19 (Santa cruz, mouse, 1:200), NFATC1 (Santa cruz,

mouse, 1:200), NFATC2 (Santa cruz, mouse, 1:200) and GFP (Invitrogen, rabbit, 1:1000).

The second day, after washes by PBS-Tween for 3 times, the membrane was incubated by fluorescent Donkey anti Rabbit (800CW, 1:5000-1:10,000) or Goat anti Mouse (680RD, 1:5000-1:10,000) secondary antibodies (LI-COR) for 1 hour at room temperature followed with another 3 times washes by PBS-Tween. Then the membrane was exposed directly to the Odyssey Fc imager (LI-COR). After detection at 700nm and 800nm channels by the Odyssey Fc system, the specific bands were detected.

Secondary IP specific HRP antibody (Abcam) was used for some of the IP western blotting analysis. Signals were activated by ECL solution (LI-COR) and exposed directly to the Odyssey Fc imager (LI-COR) at ECL channel.

2.2.8 Liquid Chromatography-Tandem Mass Spectrometry (LC-MS)

LC-MS analysis protocol used in University of Sussex:

The gel was stained with Coomassie InstantBlue (Expedeon) for 1 hour and washed with distilled water 3 times for 10 minutes or SimplyBlue SafeStain (Invitrogen) for 1 hour and washed with distilled water 2 times for 1 hour. After that, the protein bands or gel lanes were cut into pieces on a clean board with a scalpel, and gel pieces were then stored in -20°C freezer or subjected to in-gel digestion.

The gel was washed with 50µl of 50% acetonitrile in 25mM NH_4HCO_3 (Sigma) on a shaker for 3 times, then gel pieces were subjected to SpeedVac concentrator with no heat for 5 minutes. The gel pieces were heated by the addition of 50µl 10mM dithiothreitol (DTT) at 50°C for 45 minutes. After this, alkylation performed

by the addition of 50μl 50mM iodoacetamide (Sigma) in 25mM NH_4HCO_3 in a box avoiding light, incubating for another 45 minutes. The gel was washed three times with 50μl of 50% acetonitrile in 25mM NH_4HCO_3 on a shaker, and then dry them by SpeedVac with no heat for 5 minutes in the end. 12.5ng/μl trypsin (Promega) was added to each tube and incubated on ice for 10 minutes. 25mM NH_4HCO_3 was added on the top of gel pieces and incubated at 37°C overnight.

Trifluoroacetic acid (TFA) (Thermo Scientific) was added to the tube to get a final concentration of 0.5%, after vortexing and centrifugation, the liquid with peptides was moved into clean tubes. The rest gel pieces were added the 1X volume of acetonitrile and vortexed at room temperature for 15 minutes. Then the supernatant was transferred into the tubes containing peptides. The peptides were applied to Speedvac with heating until the supernatant was reduced into about 8μl per tube, then they were stored into -20°C until further analysis.

Then samples were further analysed by a Dionex Ultimate 3000 nano LC system coupled to an LTQ-Orbitrap Velos mass spectrometer (Thermo Scientific). The instrument was controlled by Xcalibur software (Thermo Scientific). When obtained the raw files of all the samples, MaxQuant was used to search the proteins using a FASTA file combined human genome database with the EBV 3 strains database.

The MaxQuant setting parameters were listed down below:

Parameter	**Value**
Fixed mdifications	Carbamidomethyl (C)
Include contaminants	TRUE
PSM FDR	0.01
Protein FDR	0.01
Site FDR	0.01
Use Normalized Ratios For Occupancy	TRUE
Min. peptide Length	7
Min. score for unmodified peptides	0
Min. score for modified peptides	40

Min. delta score for unmodified peptides	0
Min. delta score for modified peptides	6
Min. unique peptides	0
Min. razor peptides	1
Min. peptides	1
Use only unmodified peptides and	TRUE
Modifications included in protein quantification	Oxidation (M);Acetyl (Protein N-term)
Peptides used for protein quantification	Razor
Discard unmodified counterpart peptides	TRUE
Min. ratio count	2
Use delta score	FALSE
iBAQ	TRUE
iBAQ log fit	TRUE
Match between runs	TRUE
Matching time window [min]	0.7
Alignment time window [min]	20
Find dependent peptides	FALSE
Decoy mode	revert
Include contaminants	TRUE
Advanced ratios	TRUE
Second peptides	TRUE
Stabilize large LFQ ratios	TRUE
Separate LFQ in parameter groups	FALSE
Require MS/MS for LFQ comparisons	TRUE
Calculate peak properties	FALSE
Main search max. combinations	200
Advanced site intensities	TRUE
Top x mass window [Da]	100
Max. peptide mass [Da]	4600
Min. peptide length for unspecific search	8
Max. peptide length for unspecific search	25
Razor protein FDR	TRUE
Disable MD5	FALSE
Max mods in site table	3
Match unidentified features	FALSE

Table 2.10: MaxQuant parameters used for label-free mass spectrometry analysis.

LC-MS analysis in University of Bristol:

Samples on the beads were reduced, alkylated and digested with trypsin (2.5µg trypsin per sample; 37°C, overnight). The resulting peptides were labelled with Tandem Mass Tag (TMT) ten-plex reagents according to the manufacturer's protocol (Thermo Fisher Scientific) and the labelled samples pooled.

The pooled sample was evaporated to dryness and resuspended in buffer A (20 mM ammonium hydroxide, pH 10) prior to fractionation by high pH reversed-phase chromatography using an Ultimate 3000 liquid chromatography system (Thermo Fisher Scientific). In brief, the sample was loaded onto an XBridge BEH C18 Column (130Å, 3.5 µm, 2.1 mm X 150 mm, Waters, UK) in buffer A and peptides eluted with an increasing gradient of buffer B (20 mM Ammonium Hydroxide in acetonitrile, pH 10) from 0-95% over 60 minutes. The resulting fractions (four in total) were evaporated to dryness and resuspended in 1% formic acid prior to analysis by nano-LC MSMS using an Orbitrap Fusion Tribrid mass spectrometer (Thermo Scientific).

High pH RP fractions were further fractionated using an Ultimate 3000 nano HPLC system in line with an Orbitrap Fusion Tribrid mass spectrometer (Thermo Scientific). In brief, peptides in 1% (vol/vol) formic acid was injected onto an Acclaim PepMap C18 nano-trap column (Thermo Scientific). After washing with 0.5% (vol/vol) acetonitrile 0.1% (vol/vol) formic acid, peptides were resolved on a 250 mm × 75 µm Acclaim PepMap C18 reverse phase analytical column (Thermo Scientific) over a 150 min organic gradient, using 7 gradient segments (1-6% solvent B over 1min., 6-15% B over 58min., 15-32%B over 58min., 32-40%B over 5min., 40-90%B over 1min., held at 90%B for 6min and then reduced to 1%B over 1min.) with a flow rate of 300 nl min−1. Solvent A was 0.1% formic acid and Solvent B was aqueous 80% acetonitrile in 0.1% formic acid. Peptides were ionized by nano-electrospray ionization at 2.0kV using a stainless steel emitter with an internal diameter of 30 µm (Thermo Scientific) and a capillary temperature of 275°C.

Then samples were further analysed by an Ultimate 3000 nanoHPLC system in line with an Orbitrap Fusion Tribrid mass spectrometer (Thermo Scientific) the

instrument was controlled by Xcalibur 2.0 software (Thermo Scientific) and operated in data-dependent acquisition mode using an SPS-MS3 workflow. FTMS1 spectra were collected at a resolution of 120 000, with automatic gain control (AGC) target of 200 000 and a max injection time of 50ms. Precursors were filtered with an intensity threshold of 5000, according to charge state (to include charge states 2-7) and with monoisotopic precursor selection. Previously interrogated precursors were excluded using a dynamic window (60s +/-10ppm). The MS2 precursors were isolated with a quadrupole mass filter set to a width of 1.2m/z. ITMS2 spectra were collected with an AGC target of 10 000, a max injection time of 70ms and CID collision energy of 35%. For FTMS3 analysis, the Orbitrap was operated at 50 000 resolution with an AGC target of 50 000 and a max injection time of 105ms. Precursors were fragmented by high-energy collision dissociation (HCD) at a normalised collision energy of 60% to ensure maximal TMT reporter ion yield. Synchronous Precursor Selection (SPS) was enabled to include up to 5 MS2 fragment ions in the FTMS3 scan.

2.2.9 Database Search and Protein Quantification

FASTA files containing the human proteome alongside the EBV proteome came from UniProt/SwissProt database. Protein interactors from the cross-linking ChIPs were Identified and quantified by MaxQuant (version 1.5.3.30) (Cox and Mann, 2008), TMT labelled mass spec analysis were identified and quantified by Proteome discoverer. Data were visualized by Perseus (version 1.5.5.0) (Tyanova et al., 2016) and R studio (RStudio Team (2015). RStudio: Integrated Development for R. RStudio, Inc., Boston, MA URL http://www.rstudio.com/).

2.2.10 alamar-Blue cell viability Assay

Akata cells, DG75 cells or 293-BZLF1-KO cells were cultured in 96-well plates. Cells were treated with different drugs (VER155008, FK506) at different

concentrations for 24-48 hours. alamarBlue cell viability reagent (Invitrogen) was added as 10% of the sample volume into the 96-well plate, followed an overnight incubation at 37ºC, fluorescence was measured by Glomax (Promega) under an excitation wavelength of 520nm (green) and an emission at 580-640nm.

2.2.11 Genomic DNA purification

Genomic DNA was extracted from the cells using the Qiagen DNA kit following the protocol provided by Qiagen.

2.2.12 Real-time quantitative PCR (qPCR)

The quantitative polymerase chain reaction was used to measure EBV viral load in cells. CYBR green (Promega) intercalates with double-stranded DNA and the SYBR will fluoresce, and then detected by the qPCR machine (StepOnePlus, Applied Biosystems) controlled by StepOne. Viral lytic gene BALF5 primer was used to detect the amplified viral genome, beta-globin was used as an internal control. A standard curve was constructed by using serial dilutions 1:2 or 1:4 of a 100ng sample with one primer set.

A master mix of reagents was used in each sample of the 96-well plate. A master mix is including 12.5µl SYBR green, 9.5µl dH2O, 0.5µl of 10µM forward and reverse primer mix. 2.5µl of each sample were plated in triplicates with the master mix. The qPCR reaction conditions include:

Temperature	Time	
95 °	10 minutes	
95 °	15 seconds	
60 °	1 minute	40 cycles
95 °	15 seconds	
60 °	1 minute	

qPCR results were analysed by StepOne software (Applied Biosystems) the melting curve was analysed to ensure the results are at good quality.

2.2.13 Flow cytometry

1 x 10^6 of induced and un-induced Akata cells were used in each condition. Cell Fixation & Cell Permeabilization Kit (Invitrogen) was used for treating the cells. Cells were re-suspended in 100µl of D-PBS. 100µl of reagent A was added and incubated for 15 minutes, then washed once by the wash medium. After, 100µl of reagent B was added with BZ1 or VCA antibody or control antibody into each tube and incubated for 20 minutes at room temperature. Cells were washed once, and then another 100µl of reagent B was added with Alexa Fluor secondary antibody (diluted 1:100 in wash medium) and incubated for 20 minutes at room temperature. After washing by wash medium, the cells were re-suspended in 500µl wash medium and ready for the flow cytometry analysis. Cells were detected by BD Accuri C6 Flow cytometer (Beckton Dickinson) and Zta or VCA positive cells were identified by BD CSampler software (Beckton Dickinson).

2.2.14 siRNA Knockdown

siRNA Knockdown was performed by Neon transfection system (100µl Neon kit) in DG-75 cells, NFATC1 and C2 siRNA smart pool (Dharmacon) were used, non-targeting siRNA pool #1 (Dharmacon) was used as a control. Other plasmids were delivered with siRNA into the cells at the same time.

5 x 10^6 cells were harvested and washed by D-PBS and resuspended in 104µl Buffer T. 6µl DNA and RNA mix in each condition was prepared before adding to the cells. Electroporation was performed at 1300v, 30 msec, and 1 pulse in 100µl Neon tip. Whole media without antibiotics was used for culturing the cells. 24 hours post-transfection, ionomycin (final concentration 1µM) and PMA (final concentration 20ng/ml) were added in the certain conditions, after another 48 hours, cell were harvested and washed by D-PBS. Then 1/10 of the cells were used for western blotting and the rest of the cells were used for luciferase assay.

The volume and concentration of DNA and RNA list below:

Name	Volume	Stock concentration	Final concentration/amount
Non-Targeting siRNA	4µl	5µM	200µM
Human NFATC1 siRNA	2µl	5µM	100µM
Human NFATC2 siRNA	2µl	5µM	100µM
BHLF1 reporter	1µl	250ng/µl	250ng
pcDNA3	1µl	250ng/µl	250ng
hisZta	1µl	250ng/µl	250ng

Table 2.11 DNA and RNA used in siRNA knockdown assay.

Each siRNA pools list below:

Name	Target sequence	Type and source

Non-Targeting siRNA pool #1	UAGCGACUAAACACAUCAA UAAGGCUAUGAAGAGAUAC AUGUAUUGGCCUGUAUUAG AUGAACGUGAAUUGCUCAA	Dharmacon, siGENOME
Human NFATC1 siRNA-SMARTpool	UCAGAAACUCCGACAUUGA GGACAGCUAUCCGGUCGUG GUUGAGAUCCCGCCAUUUC AGGAAGAACACACGGGUAC	Dharmacon, siGENOME
Human NFATC2 siRNA-SMARTpool	CCAAUAAUGUCACCUCGAA GCAGAAUCGUCUCUUUACA GCGGGGAUCUUGAAGCUUA UCAUGUACUGCGAGAAUUU	Dharmacon, siGENOME

Table 2.12 siRNA pools used in siRNA knockdown experiment.

2.2.15 Luciferase reporter assay

1 x 10^7 cell numbers of DG-75 cells were used and transfected by electroporation (Bio-Rad) in each condition for 48 hours. BHLF1 wild type promoter, BHLF1 mutated promoter or pGL3-NFAT IL-2 promoter construct with pcDNA3 or pcDNA3-hisZta expression vector were used in different experiments, the details were described in transfection session (**2.2.3**).

For siRNA knockdown luciferase assay, the transfection is described in that session (**2.2.14**)

Cells were harvested and washed in 10 ml D-PBS, then 1/10 of the cells were used for western blotting and the rest of the cells were used for luciferase assay. 90µl of 1X passive cell lysis buffer (Promega) was added to the cell pellets and incubated 30minutes on the ice and 30 minutes at room temperature. Then cells were centrifuged and the supernatant was transferred to clean tubes. For luciferase activity analysis, 10µl of each sample was pipetted into a white 96-well plate. Samples were prepared as triplicates. Glomax (Promega) multi-detection machine with the autosampler, which allows auto dispensing the luciferase activation reagent (Promega), was used for the detection, settings are 50µl of luciferase activation reagent per well and reading for 10 seconds with a delay for 2 seconds after adding the reagent.

Normalization of luciferase assay by BCA assay. 5µl samples from each condition were then diluted 1:5 in PBS and added in a 96-well plate, 200µl of freshly made BCA reaction solution was added in each well and the plate was incubated at 37°C for 30 minutes avoiding light. Then the plate was read by a plate-reader (Glomax explorer, Promega) at a wavelength of 560 nm. The reading of each well was matched to each of the luciferase reading, and used for the normalisation of the total protein levels.

2.2.16 Electrophoretic mobility shift assay (EMSA)

Fluorescent 5'-IRDye 800 labelled ARRE2 binding motif and BMLF1 AP-1 site forward strands (IDT) and unlabelled reverse strands were used. To prepare a working stock (20µM), 10µl labelled forward strand (100µM stock) with a 30µl reverse strand(100µM stock) were annealed in 10µl TE buffer at 95°C for 5 minutes, 65°C 10minutes and then cooling down at room temperature for 1 hour.

1 µM of each DNA probe was used as a working concentration for the EMSA. His-GFP-bZIP and control GFP protein 1mg/ml were used for the binding assay. 8µl of EMSA binding buffer was prepared for one reaction using 5X Gel shift binding buffer (Promega), DTT, BSA and dH2O. Then 1µl of each protein was added and incubated with different probes for 20 minutes at room temperature.

The binding buffer reaction was listed below for each condition:

EMSA Binding buffer	Final concentration	Amount
5X Gel shift binding buffer (Promega)	1X	1.6µl
DTT 100mM	4mM	0.32µl
BSA 10mg/ml (Biolabs)	1mg/ml	0.8µl

dH2O		5.28µl
Probe 1µM		1µl
Protein		1µl
Total volume		10µl

Table 2.13 reagents and buffer used in EMSA assay.

Meanwhile, pre-cast native 6% DNA retardation gel (Invitrogen) was pre-run in 0.5X TBE buffer (Invitrogen) at 100V for 15 minutes.

After the 20 minutes' reaction, each sample was mixed with 1µl of loading dye (10x orange dye, LI-COR). 11µl of each sample was loaded on the gel and run at constant 100V for 60 minutes at room temperature. Once finished running, the gel was exposed directly to the Odyssey Fc imager (LI-COR) at 800nm channel for 10 minutes.

2.2.17 Bioinformatics analysis

The Gene Ontology (GO) analysis was obtained from The Database for Annotation, Visualization and Integrated Discovery (DAVID) (https://david.ncifcrf.gov/) (Dennis et al., 2003). The protein-protein interaction prediction was analysed by STRING database version 11.0 (http://string-db.org) (Szklarczyk et al., 2015). NFATC1 ChIP-seq data was obtained from ENCODE database (UCSC Accession: wgEncodeEH002307) and processed in Genomic Regions Enrichment of Annotations Tool (GREAT) version 3.0.0 (McLean et al., 2010).

3 Identifying Zta interactome during lytic cycle in an overexpressed condition

3.1 Introduction

As a transcription factor, Zta regulates both viral and host gene expression, and it is the key protein for EBV genome replication during the lytic cycle. Zta cooperates with other EBV proteins as well as host co-regulators for transcription regulation and DNA replication. As introduced in chapter one, a few viral and cellular proteins were reported to interact with Zta thereby influencing the function of each other. However, a global map of the Zta interactome during EBV lytic reactivation is still missing.

Previous studies managed to combine affinity pull-down assays with quantitative mass spectrometry analysis to identify interactome for different proteins. Two different quantitative methods for mass spectrometry have been used widely. The first method uses stable isotope labelling with amino acids in cell culture (SILAC), which labels the proteins during cell culture. The second method uses the chemical labelling method, which directly labels digested peptides, such as tandem mass tag (TMT) labelling and Isobaric tags for relative and absolute quantitation (iTRAQ). Recently, with the development of computer software, label-free quantitation became an accurate method for proteomics studies, which is extensively used in different fields (Mohammed et al., 2016; Ersing et al., 2017; Cox et al., 2014; Traylen et al., 2015).

Each quantitative method has its pros and cons and with the development of new mass spectrometer instruments, quantitative mass spectrometry became a promising method to study protein interactome under different conditions.

With the improvement of the resolution of the mass spectrometer, label-free has becoming the first choice for many studies, although SILAC or chemical labelling quantitation still have obvious benefits for protein studies. Label-free studies

reduce sample preparation time and is comparatively economical than other methods to obtain valuable information (Cox et al., 2014).

Recently, chromatin immunoprecipitation (ChIP) method was combined with mass spectrometry to study protein-protein interactions, which needs short sample preparation time and gives high quality data (Mohammed et al., 2016). Previous study in our laboratory used genome-wide chromatin immunoprecipitation coupled to next-generation DNA sequencing (ChIP-seq) to establish a map of Zta interactions across the human genome (Ramasubramanyan et al., 2015a). In this chapter, a revised ChIP method from our lab is established in an EBV positive cell line and coupled with label-free quantitative mass spectrometry in order to identify proteins that interact with EBV immediate early lytic protein Zta.

3.2 Results

3.2.1 Establishment of ChIP-western blotting conditions in 293-BZLF1-KO cell line.

To combine the ChIP protocol from our lab with label-free mass spectrometry, a revised procedure is illustrated (**Figure 3.1)**. Based on this protocol, chromatin and proteins were cross-linked by 1% formaldehyde solution in both control cells and Zta expressed EBV lytic cells, chromatin extraction was then followed with sonication, chromatin immunoprecipitation, protein elution, SDS-PAGE gel, in-gel digestion and mass spectrometry.

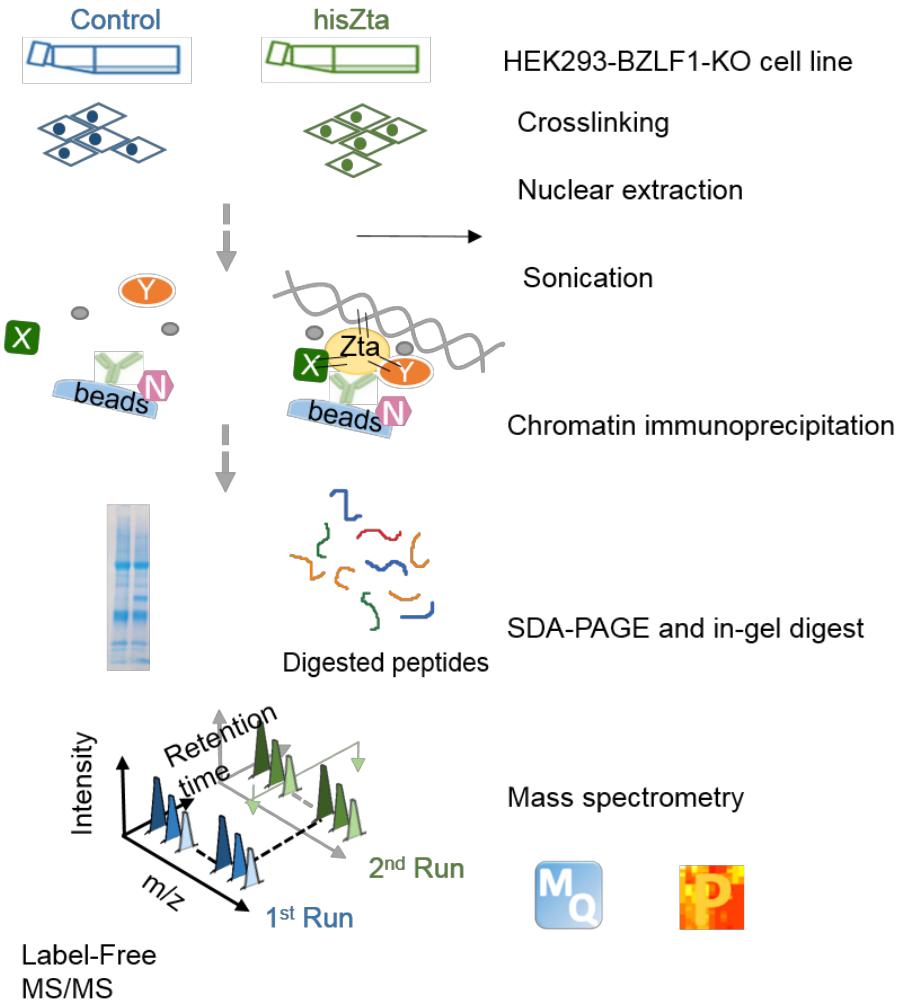

Figure 3.1 Whole scheme of ChIP label-Free quantification Mass Spectrometry. 293-BZLF1-KO cells were cultured and transfected with hisZta and the control vector (pcDNA3) for 96 hours. Cells were cross-linked by 1% formaldehyde. The nucleus was lysed by SDS lysis buffer and sonicated to extract short chromatin fragments with proteins. Zta antibody (SCZ) coupled with magnetic protein G beads were used for pull-down. Protein X and Y represent the potential targets that interact with Zta, and protein N represents one of the non-specific proteins. After a series of washing steps, the eluted proteins were separated by SDS-PAGE and stained by Coomassie blue. Then protein gel lanes were cut into small pieces and mass spectrometry analysis was performed after trypsin digestion.

To establish the experiment conditions, 293-BZLF1-KO cell line was used, which is a human embryonic kidney cell line (HEK293) harbouring EBV genome with deletion of BZLF1 gene (Feederle et al., 2000). These cells contain the EBV genome, however, the virus cannot go through the lytic cycle automatically. When exogenous Zta is expressed in these cells, the lytic cycle can be established, which triggers the lytic replication, followed by assembly and production of viral particles. Thereby allowing us to control lytic cycle reactivation.

A polyhistidine tagged Zta plasmid (hisZta) was used to express Zta in 293-BZLF1-KO cells and an empty pcDNA3 vector was used as a control. 293-BZLF1-KO cells were transiently transfected with hisZta and control vector for 96 hours to express the hisZta protein and to trigger the EBV lytic cycle. hisZta expression level was analysed by western blotting using a Zta antibody BZ1 (**Figure 3.2A**). EBV viral load was analysed by real-time quantitative PCR (qPCR) in order to verify the viral copies after lytic reactivation. Primers for the EBV DNA polymerase gene BALF5 were used to detect the EBV genome and primers for the human gene β-globin were used to detect human genome and normalise for cell numbers. Cells transfected with an empty vector were used as a control group to identify the amount of EBV genome load before transfection, the results are shown as fold-change compared to the control group (**Figure 3.2B**).

The EBV viral load result suggested that the EBV lytic cycle had been activated by expression of hisZta and the cells could be used for the further ChIP experiments.

In order to question hisZta pull-down efficiency, a chromatin extract was prepared and sonicated DNA was analysed on an agarose gel, chromatin length between 100bp-1000bp were identified (**Figure 3.3**).

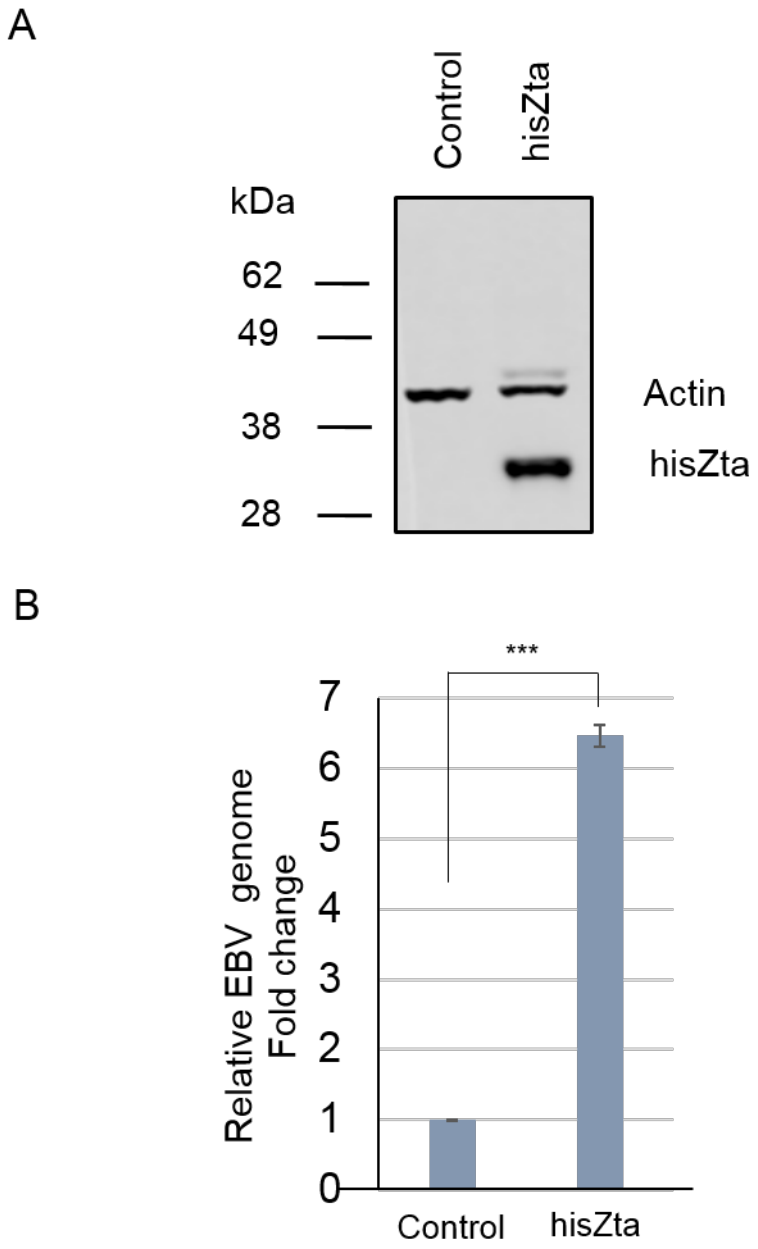

Figure 3.2 Zta expression level and EBV viral load in 293-BZLF1-KO cells. Cells were transfected with control vector or hisZta to express Zta protein and trigger the lytic cycle for 96 hours. Cells were lysed by protein sample buffer and genomic DNA was extracted. **A.** Western blotting of Zta. Actin was used as a loading control. **B.** The EBV viral load was measured by qPCR, the EBV genome was normalised by the human genome and shown as fold-change compared to the control group. (***) indicates $p<0.001$.

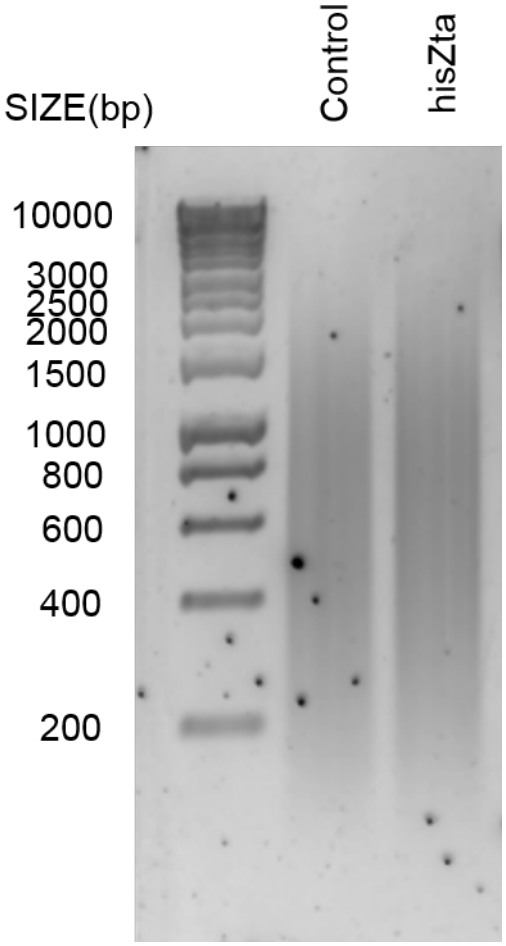

Figure 3.3 Sonication of chromatin checked by agarose gel. Purified chromatin from sonicated nuclear extracts was loaded on 1% agarose gel. Chromatin length between 100bp-1000bp were identified.

The chromatin was further used for the ChIP. hisZta and its binding partners were pulled down by Zta antibody SCZ (goat) and magnetic beads, after a series of washing steps, all the proteins binding to the beads were eluted in 2X protein sample buffer. Input (Nuclear extracts), unbound, first wash, first and second immunoprecipitation (IP) eluate samples were collected and prepared for western blotting (**Figure 3.4A**). A mouse Zta antibody BZ1 was used here to detect hisZta. hisZta level was quantified by ImageStudio software (LI-COR), the value was adjusted by loading percentage and each sample was normalised to input (**Figure 3.4B**). Compared with the hisZta in the input (shown as 100%), 50% of hisZta was left in the un-bound, 30% of the bound hisZta was collected in the first eluate from beads by ChIP, and 5% of hisZta were collected in the second eluate. This suggests that the ChIP procedure worked. The first elution was efficient. Therefore, the second elution was not included in further studies. This condition was appropriate for future large-scale experiments.

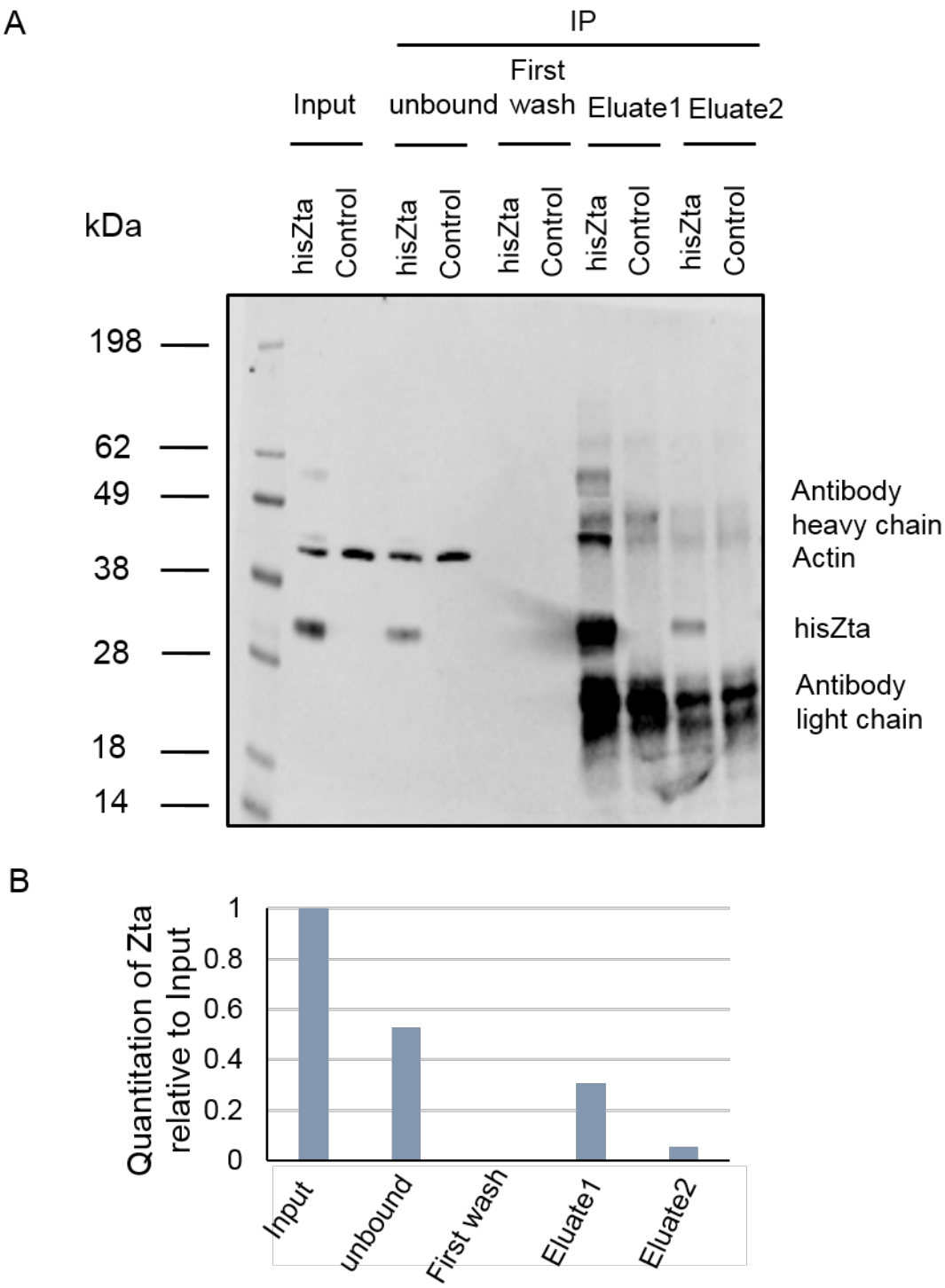

Figure 3.4 Zta ChIP-western blotting in 293-BZLF1-KO cell line. 293-BZLF1-KO cells were transfected with hisZta and control vector for 96 hours, 1% formaldehyde cross-linked cell nuclear extracts were used for the ChIP, Zta and its binding proteins were immunoprecipitated by antibody and magnetic beads. To establish the ChIP condition and compare the pull-down efficiency, Input (nuclear extracts), unbound, first wash, first and the second eluate was collected and prepared for western blotting. **A.** Western blotting of Zta. Actin was used as a loading control. **B.** Quantitation of Zta. The quantitation was converted by loading volume and normalised to the Input.

3.2.2 In-gel digestion and mass spectrometry setting up.

After establishing the ChIP condition, next I had to establish a good mass spectrometry setup for the ChIP. The first step was in-gel digestion, which allowed the proteins to be digested into short peptides by trypsin prior to the liquid chromatography (LC) and mass spectrometry. To test this, input and IP samples obtained from ChIP were loaded along with 100ng BSA on the SDS-PAGE gel, and then the gel was stained by Coomassie blue (**Figure 3.5**). A band between 28kDa to 38kDa could only be detected in Zta IP samples whereas no band was seen in the control samples, which indicated it was the band of hisZta. BSA was run together on the gel and shown as a single band around 60 kDa, which was used as a positive control for in-gel digestion and mass spectrometry.

In-gel digestion was performed and followed by mass spectrometry in order to set up the instrument running condition and to check the digestion efficiency. The IP lanes were cut into four parts and sliced into small pieces, and then in-gel digestion was performed in the lab (**Figure 3.6)**. Each sample was then sent for mass spectrometry analysis. The Mascot search engine (Perkins et al., 1999) was used to analyse the single run of each sample, BSA and bait protein hisZta were matched to the database.

BSA sample showed 83% of sequence coverage with a score 2903 when matched to the database, which suggests the digestion worked and mass spectrometer was functioning well (**Figure 3.7**). Our bait protein Zta showed 33% sequence coverage with a decent score of 578 (**Figure 3.8**). Considering the lack of arginine and lysine residues in the middle of Zta sequence, which cannot be digested by trypsin, the mass spectrometer may not be able to fragment such long undigested peptides, the coverage percentage here was still acceptable, it was good enough and we were ready to proceed to further large-scale experiments.

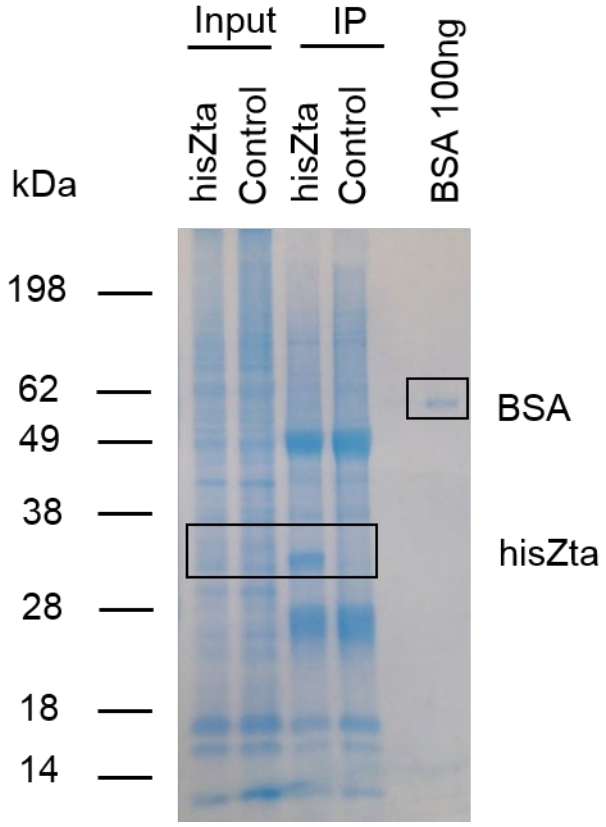

Figure 3.5 Coomassie blue for Immunoprecipitation of Zta in 293-BZLF1-KO cells. Input, IP samples and 100ng bovine serum albumin (BSA) were separated by SDS-PAGE gel and stained by Coomassie blue. Zta and BSA bands were highlighted in the black boxes.

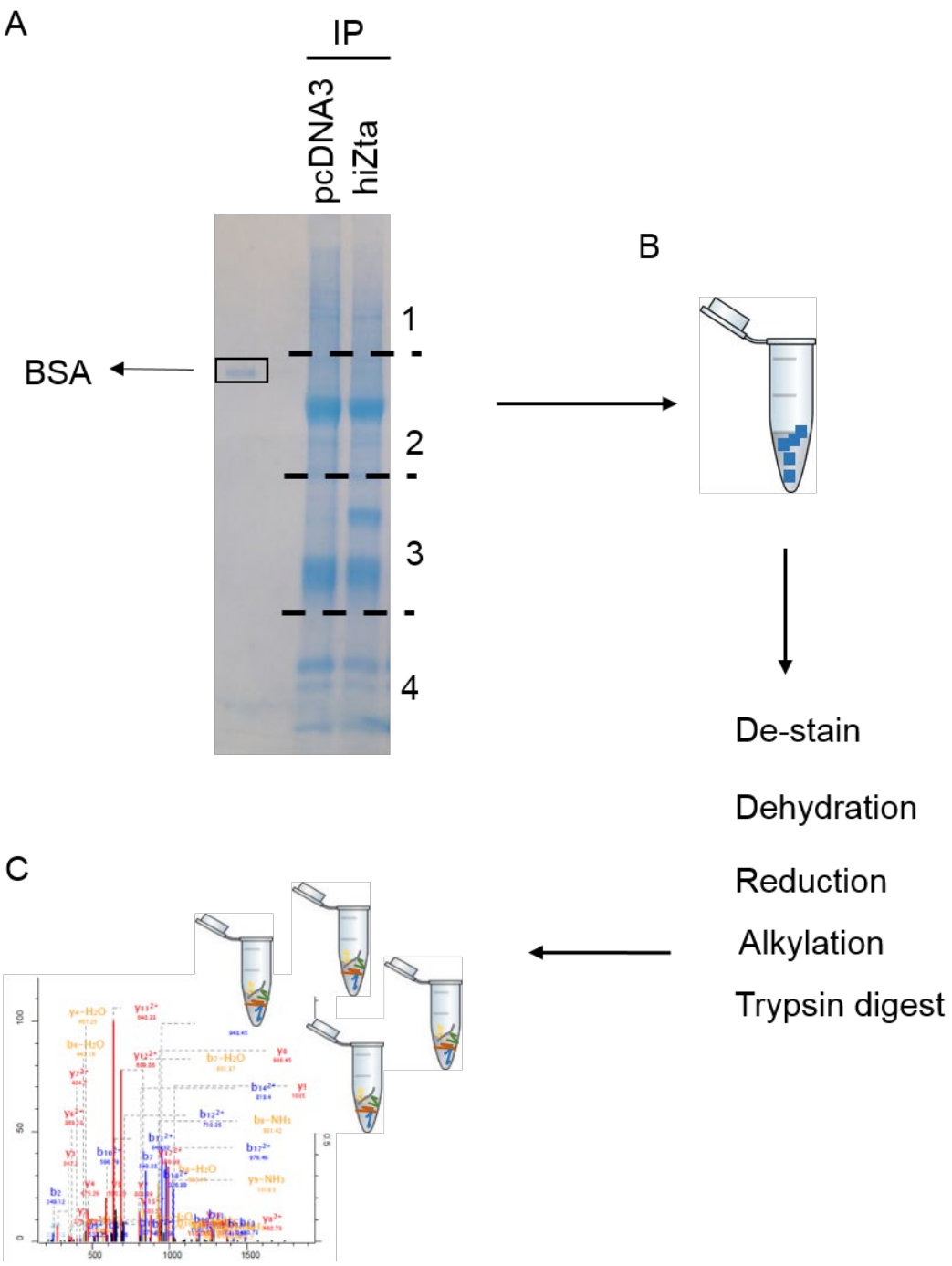

Figure 3.6 Diagram of In-gel digest and mass spectrometry analysis. IP lanes and BSA band were cut out from the gel and sliced into small pieces. Each lane was separated into four different tubes as shown in the figure. In-gel digest steps de-stain, dehydration, reduction, alkylation and trypsin digestion were performed, and then digested peptides were loaded on LC-Mass spectrometer.

MATRIX SCIENCE Mascot Search Results

Protein View

Match to: **P02769|ALBU_BOVIN** Score: **2903**
Serum albumin OS=Bos taurus GN=ALB PE=1 SV=4
Found in search of C:\IP MS\YZ_ingel_IP_2016-04-26\YZ_2016-04-26_Ingel_BSA

Nominal mass (M_r): **71244**; Calculated pI value: **5.82**
NCBI BLAST search of P02769|ALBU_BOVIN against nr
Unformatted sequence string for pasting into other applications

Taxonomy: Bos taurus

Fixed modifications: Carbamidomethyl (C)
Variable modifications: Oxidation (M)
Cleavage by Trypsin: cuts C-term side of KR unless next residue is P
Sequence Coverage: **83%**

Matched peptides shown in **Bold Red**

```
  1 MKWVTFISLL LLFSSAYSRG VFRRDTHKSE IAHRFKDLGE EHFKGLVLIA
 51 FSQYLQQCPF DEHVKLVNEL TEFAKTCVAD ESHAGCEKSL HTLFGDELCK
101 VASLRETYGD MADCCEKQEP ERNECFLSHK DDSPDLPKLK PDPNTLCDEF
151 KADEKKFWGK YLYEIARRHP YFYAPELLYY ANKYNGVFQE CCQAEDKGAC
201 LLPKIETMRE KVLASSARQR LRCASIQKFG ERALKAWSVA RLSQKFPKAE
251 FVEVTKLVTD LTKVHKECCH GDLLECADDR ADLAKYICDN QDTISSKLKE
301 CCDKPLLEKS HCIAEVEKDA IPENLPPLTA DFAEDKDVCK NYQEAKDAFL
351 GSFLYEYSRR HPEYAVSVLL RLAKEYEATL EECCAKDDPH ACYSTVFDKL
401 KHLVDEPQNL IKQNCDQFEK LGEYGFQNAL IVRYTRKVPQ VSTPTLVEVS
451 RSLGKVGTRC CTKPESERMP CTEDYLSLIL NRLCVLHEKT PVSEKVTKCC
501 TESLVNRRPC FSALTPDETY VPKAFDEKLF TFHADICTLP DTEKQIKKQT
551 ALVELLKHKP KATEEQLKTV MENFVAFVDK CCAADDKEAC FAVEGPKLVV
601 STQTALA
```

Figure 3.7 Peptides matched to BSA and analysed by Mascot. Digested peptides were detected by the mass spectrometer and the raw file was matched to the database by Mascot. 83% sequences of BSA protein were matched to the database and the matched peptides were highlighted in bold red.

Mascot Search Results

Protein View

Match to: **P03206|BZLF1_EBVB9** Score: **578**
Trans-activator protein BZLF1 OS=Epstein-Barr virus (strain B95-8) GN=BZLF1 PE=1 SV=2
Found in search of C:\Yaqi Zhou\IP MS\YZ_2016-04-26_Ingel_4ZTA_s13_16_ITMS_CID.mgf

Nominal mass (M_r): **27129**; Calculated pI value: **5.25**
NCBI BLAST search of P03206|BZLF1_EBVB9 against nr
Unformatted sequence string for pasting into other applications

Taxonomy: Human herpesvirus 4 (strain B95-8)

Fixed modifications: Carbamidomethyl (C)
Variable modifications: Oxidation (M)
Cleavage by Trypsin: cuts C-term side of KR unless next residue is P
Sequence Coverage: **33%**

Matched peptides shown in Bold Red

```
  1 MMDPNSTSED VKFTPDPYQV PFVQAFDQAT RVYQDLGGPS QAPLPCVLWP
 51 VLPEPLPQGQ LTAYHVSTAP TGSWFSAPQP APENAYQAYA APQLFPVSDI
101 TQNQQTNQAG GEAPQPGDNS TVQTAAAVVF ACPGANQGQQ LADIGVPQPA
151 PVAAPARRTR KPQQPESLEE CDSELEIKRY KNRVASRKCR AKFKQLLQHY
201 REVAAAKSSE NDRLRLLLKQ MCPSLDVDSI IPRTPDVLHE DLLNF
```

Figure 3.8 Peptides matched to Zta and analysed by Mascot. Digested peptides were detected by the mass spectrometer and the raw file was matched to EBV B95-8 strain database by Mascot. 33% sequences of BZLF1 were matched and the matched peptides were highlighted in bold red.

3.2.3 Identifying proteins that interact with Zta during EBV lytic cycle.

Since all the conditions were established and validated, the large-scale experiment of ChIP-MS was performed. Three biological replicates of ChIP were finished first. 8.3% of each IP sample were analysed by western blotting along with input in order to ask whether the Zta pull-down was successful (**Figure 3.9A**). Western blotting showed the bait protein hisZta was pulled down by ChIP in each repeat successfully suggesting that the experiment could proceed to the next step.

Then the rest of the IP samples were run on the gel and stained by Coomassie blue (**figure 3.9B**). Each group was cut into five slices and then each slice was cut into small pieces, after this, trypsin digestion was performed. The digested peptides from each sample were analysed by LC-mass spectrometry one by one, and the raw data was analysed in triplicate in order to obtain a statistically analysed result by MaxQuant software (Cox et al., 2014). In the MaxQuant settings, label-free quantitation was chosen, the rest of the run methods and settings were described in **Chapter 2**. Database of the proteomes of three EBV isolates (B95-8, GD1 and AG876) and the human genome, obtained from UniProt was used in MaxQuant for protein searching and matching. Perseus software (Tyanova et al., 2016) was used to process the MaxQuant output results and visualise each protein by scatter plot (**Figure 3.10**).

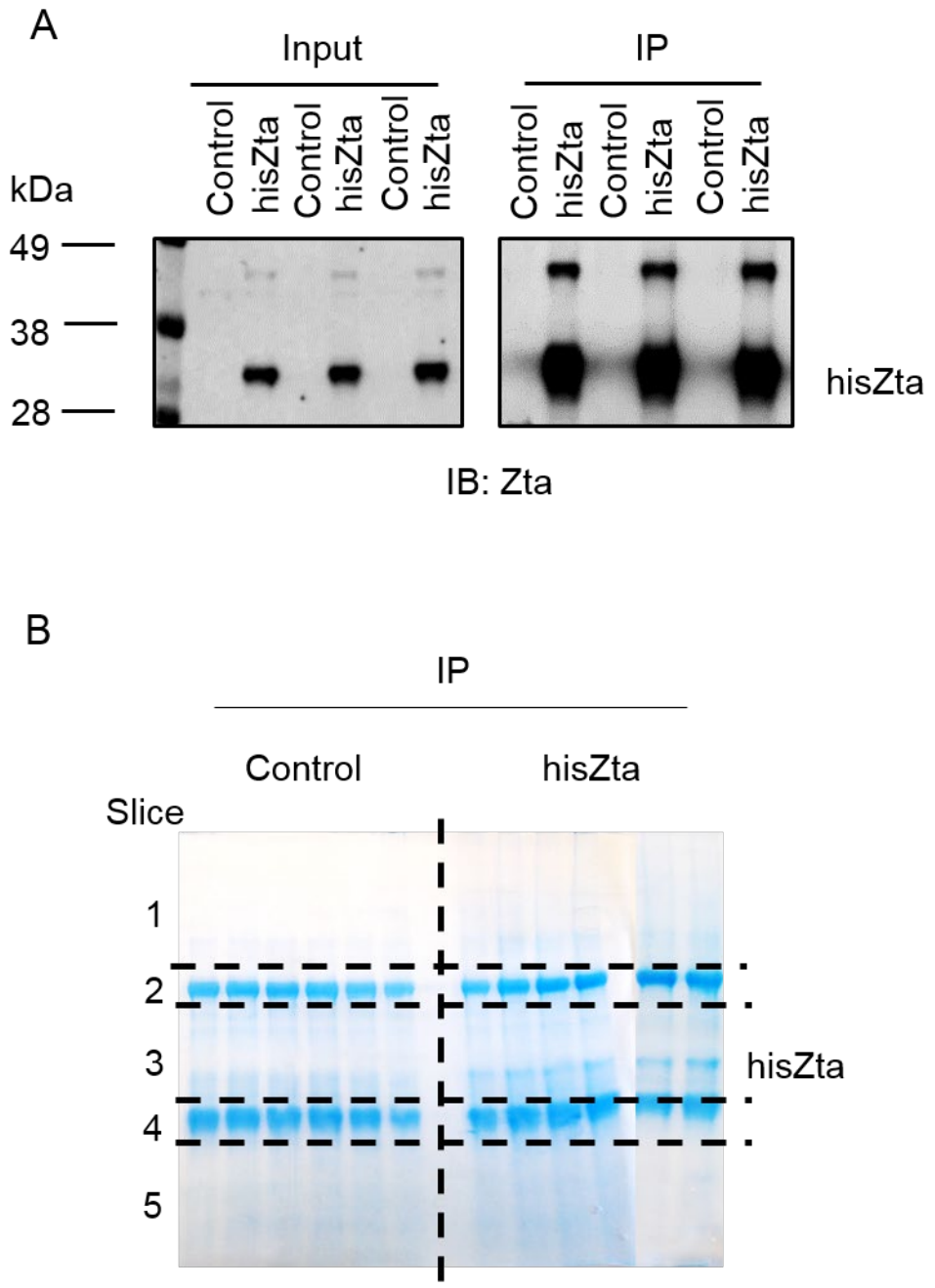

Figure 3.9 Three biological replicates of Zta ChIP-western blotting in 293BZLF1-KO cells. 293-BZLF1-KO cells were transfected with hisZta and control vector for 96 hours, 1% formaldehyde cross-linked cell nuclear extracts were used for the ChIP, Zta and its binding proteins were immunoprecipitated by antibody and magnetic beads. Then the proteins were eluted in the sample buffer. **A.** 8.3% of each IP sample were analysed by western blotting along with input by western blotting for hisZta. **B.** The rest of the IP samples were run on the gel. Coomassie blue was shown one of the single control or hisZta IP eluate, gels were cut into pieces and each condition was divided into 5 tubes for the in-gel digest.

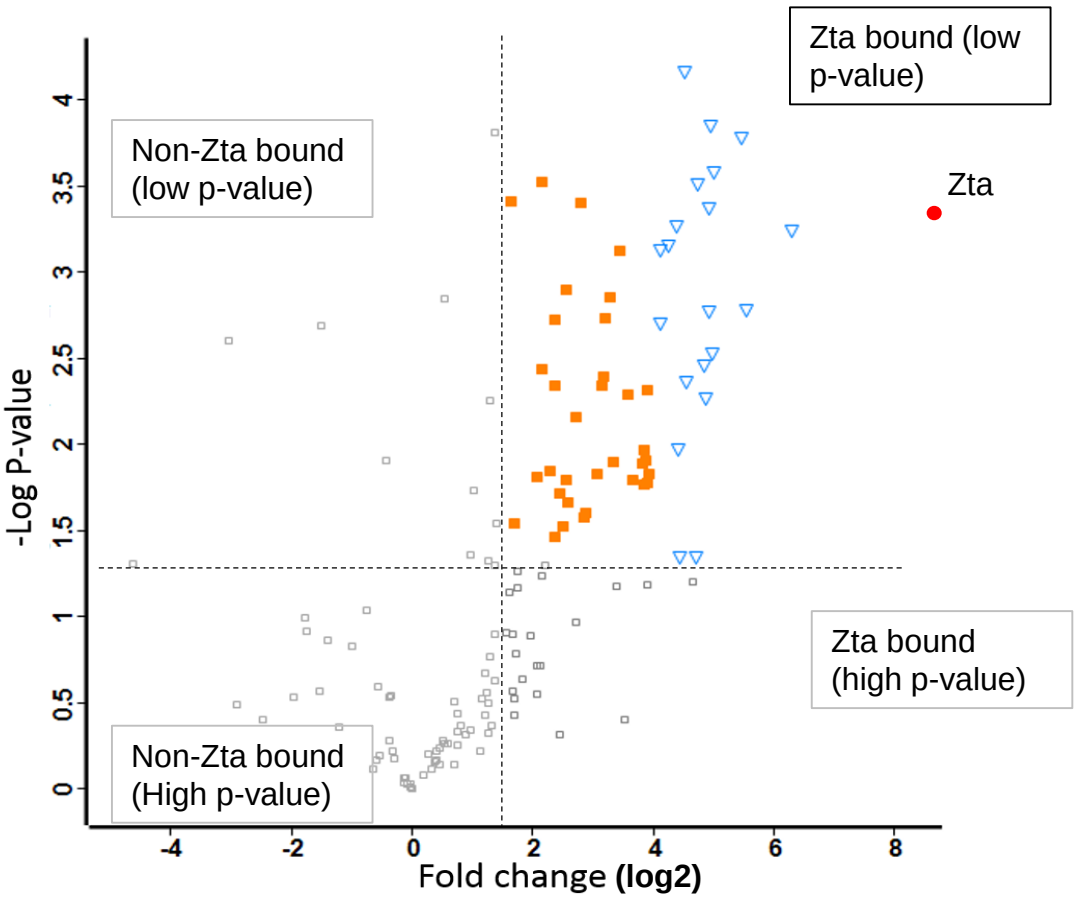

Figure 3.10 Zta ChIP label-free Mass spectrometry results searched and plotted by MaxQuant and Perseus. Proteins searched by MaxQuant were plotted by fold-change (Zta/Control) against -Log (P-value). Bait Protein Zta was highlighted in red with the highest fold-change. Fifty-four cellular proteins (blue and orange) were found as significant ($p<0.05$) changed proteins (fold-change ≥1.5) and 20 cellular proteins (blue) with higher fold-change (fold-change ≥4). No other EBV proteins were identified in this experiment apart from Zta.

Three biological repeats were analysed and measured, the results were shown as fold-change over control group and student's t-test was used to calculate if the difference was statistically significant. Scatter plot was used to plot the protein log2 fold-change (X-axis) against to the T-test –log p-value (Y-axis) of each gene, 1.5-fold (log2) changed genes were highlighted by colours and 4-fold (log2) changed genes were highlighted in blue triangles as the most significant proteins that may interact with Zta (**Figure 3.10)**. 4-fold changed proteins (**table 3.1**) and 1.5-fold to 4-fold changed proteins (**table 3.2**) were listed. Proteins with high fold changes and low p-value were listed as the best candidate proteins that interact with Zta. Also another method to evaluate the possibility of the interacting proteins or contaminations found by mass spectrometry was used, known as CRAPome (Mellacheruvu et al., 2013). It is a database that provides contaminant information for affinity pull-down studies, different pull-down negative control data is collected from mass spectrometry and provided for searching. The score shown in the CRAPome is listed in the separate column (**Table 3.1 and 3.2**)**,** which shows the numbers of the control experiments containing this protein among all the negative control experiments in the database.

Gene functional annotation analysis was used through The Database for Annotation, Visualization and Integrated Discovery (DAVID) website in order to analyse all the significantly changed proteins (Dennis et al., 2003), proteins were grouped and enriched by functions (**Figure 3.11)**. From all the 54 proteins above 1.5-fold changes, mRNA metabolic process, DNA packaging, response to unfolded protein, DNA repair and translational elongation were on the top list (**Figure 3.11A**). When I focused on the 4-fold change proteins, RNA splicing proteins were still the most enriched group with a score 8.35, I also see nucleolus protein, and proteins that respond to unfolded proteins (**Figure 3.11B**).

Gene name	Description	Unique peptides	Difference/Fold-change	CRAPome Num of Expt. (found/total)
HNRNPC	Heterogeneous nuclear ribonucleoproteins C1/C2	11	6.307797	180 / 411
HNRNPH1	Heterogeneous nuclear ribonucleoprotein H	6	5.539114	263 / 411
PARP1	Poly [ADP-ribose] polymerase 1	15	5.453821	182 / 411
TUBB4B	Tubulin beta-4B chain	1	5.010109	376 / 411
DHX9	ATP-dependent RNA helicase A	19	4.985822	205 / 411
SFPQ	Splicing factor, proline- and glutamine-rich	8	4.959501	201 / 411
RACK1	Receptor of activated protein C kinase 1	6	4.938445	135 / 411
NONO	Non-POU domain-containing octamer-binding protein	7	4.923285	220 / 411
DDX39B	Spliceosome RNA helicase DDX39B	7	4.88415	138 / 411
HSPA8	Heat shock cognate 71 kDa protein	8	4.843933	396 / 411
PCBP1	Poly(rC)-binding protein 1	3	4.747019	194 / 411
HNRNPM	Heterogeneous nuclear ribonucleoprotein M	13	4.709555	220 / 411
DDX17	Probable ATP-dependent RNA helicase	7	4.537481	238 / 411
PCBP2	Poly(rC)-binding protein 2	2	4.535346	189 / 411
HNRNPK	Heterogeneous nuclear ribonucleoprotein K	17	4.44713	288 / 411
HSP90AB1	Heat shock protein HSP 90-beta	3	4.414055	277 / 411
TUBA1B	Tubulin alpha-1B chain	1	4.395084	389 / 411
HNRNPL	Heterogeneous nuclear ribonucleoprotein L	10	4.246385	190 / 411
HSPA1A	Heat shock 70 kDa protein 1A	9	4.125194	395 / 411
ILF2	Interleukin enhancer-binding factor 2	4	4.122527	152 / 411

Table 3.1 4-fold changed Proteins found to interact with Zta by mass spectrometry. Proteins were ranked by the difference of fold-change. Gene name, description, unique matched peptide and CRAPome search results were listed in the table.

Gene name	Description	Unique peptides	Difference/Fold-change	CRAPome Num of Expt. (found/total)
H3F3B	Histone H3.3	1	3.93	139 / 411
NPM1	Nucleophosmin	4	3.91	252 / 411
NCL	Nucleolin	11	3.90	261 / 411
RBMX	RNA-binding motif protein, X chromosome	4	3.89	169 / 411
HNRNPA3	Heterogeneous nuclear ribonucleoprotein A3	8	3.85	183 / 411
RPS3	40S ribosomal protein S3	6	3.85	266 / 411
HNRNPU	Heterogeneous nuclear ribonucleoprotein U	14	3.82	280 / 411
HIST1H1C	Histone H1.2	1	3.67	301 / 411
LMNA	Prelamin-A/C	7	3.57	92 / 411
HNRNPAB	Heterogeneous nuclear ribonucleoprotein A/B	4	3.46	206 / 411
MATR3	Matrin-3	8	3.34	171 / 411
XRCC6	X-ray repair cross-complementing protein 6	6	3.29	176 / 411
HNRNPD	Heterogeneous nuclear ribonucleoprotein D0	4	3.20	216/411
LMNB1	Lamin-B1	16	3.17	117 / 411
HNRNPA1	Heterogeneous nuclear ribonucleoprotein A1	12	3.14	268 / 411
IGF2BP1	Insulin-like growth factor 2 mRNA-binding protein 1	4	3.06	114 / 411
ENO1	Alpha-enolase	4	2.88	223 / 411
HIST2H2BE	Histone H2B type 2-E	1	2.86	227 / 411
HNRNPA2B1	Heterogeneous nuclear ribonucleoproteins A2/B1	14	2.81	262 / 411
PKM	Pyruvate kinase PKM	2	2.73	249 / 411

Gene name	Description	Unique peptides	Difference/Fold-change	CRAPome Num of Expt. (found/total)
HIST2H3D	Histone H3.2	1	2.59	142 / 411
SRSF3	Serine/arginine-rich splicing factor 3	1	2.56	197 / 411
HNRNPR	Heterogeneous nuclear ribonucleoprotein R	1	2.55	188 / 411
VDAC2	Voltage-dependent anion-selective channel protein 2	4	2.51	58 / 411
SNRPD1	Small nuclear ribonucleoprotein Sm D1	2	2.46	193 / 411
TOP2A	DNA topoisomerase 2-alpha	3	2.37	69 / 411
RAN	GTP-binding nuclear protein Ran	2	2.37	154 / 411
HSPD1	60 kDa heat shock protein, mitochondrial	4	2.36	231 / 411
EEF2	Elongation factor 2	3	2.28	207 / 411
VIM	Vimentin	32	2.16	257 / 411
MYH9	Myosin-9	2	2.15	203 / 411
EEF1A1	Elongation factor 1-alpha 1	7	2.07	350 / 411
PABPC1	Polyadenylate-binding protein 1	1	1.69	172 / 411
UBB	Polyubiquitin-B	3	1.65	233 / 411

Table 3.2 1.5-fold to 4-fold changed proteins found to interact with Zta by mass spectrometry. Proteins were ranked by the difference of fold- change. Gene name, description, unique matched peptide and CRAPome search results were listed in the table.

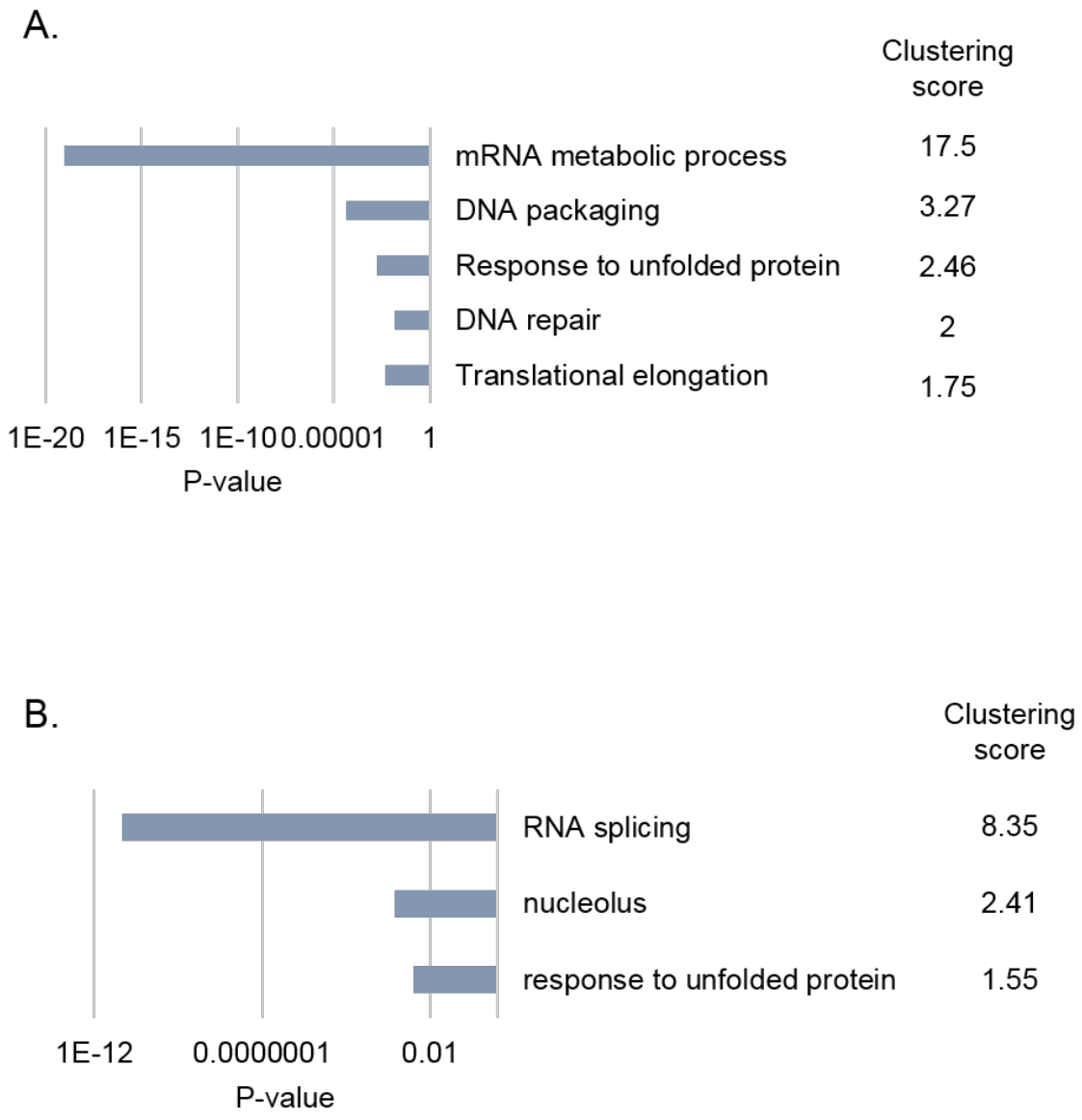

Figure 3.11 Gene functional annotation analysis of proteins interact with Zta from mass spectrometry using the DAVID database. Gene annotation analysis was shown with p-value and ranked by clustering scores. **A.** All 54 proteins above 1.5-fold change. **B.** The 20 proteins with 4-fold change.

STRING networks showed functional networks of all the significant proteins found from mass spectrometry grouped by functional annotations, functional clusters were shown in different coloured nodes (Szklarczyk et al., 2015). This gave us a clear image of the potential Zta interacting protein network. The 4-fold change proteins were shown first (**Figure 3.12),** most mRNA metabolic process proteins were grouped as a complex, some proteins in this complex were also involved in different processes, such as regulation of transcription, cytokine production and viral relevant process. Additionally, analysis of all the 54 proteins above 1.5-fold changes (**Figure 3.13)** showed that the mRNA metabolic process proteins were still the core of the network form a huge complex. However, DNA metabolic process proteins and DNA repair-related proteins were also shown in the network. Some proteins were grouped together with connection by the lines, but with high FDR value, they were not highlighted by colours.

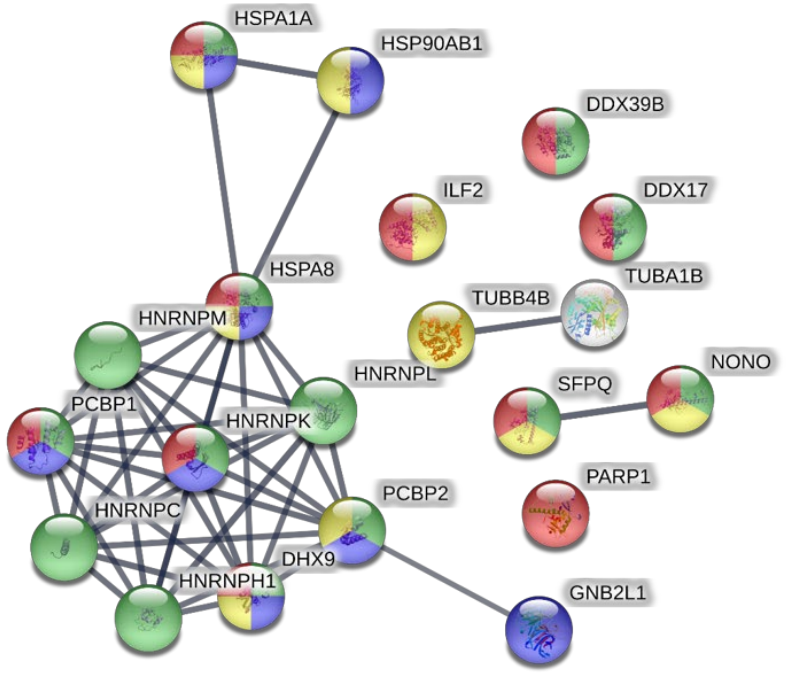

	FDR		FDR
Regulation of transcription	0.0031	mRNA metabolic process	2.25e-14
Viral process	2.61e-06	Regulation of cytokine production	0.0021

Figure 3.12 Network of protein-protein interactions by STRING for 4-fold change proteins. Proteins above 4-fold change were analysed by STRING. Nodes with different colours represent the biological process GO categories. Line thickness indicates the strength of data support. The minimum required interaction score is 0.7 (high confidence).

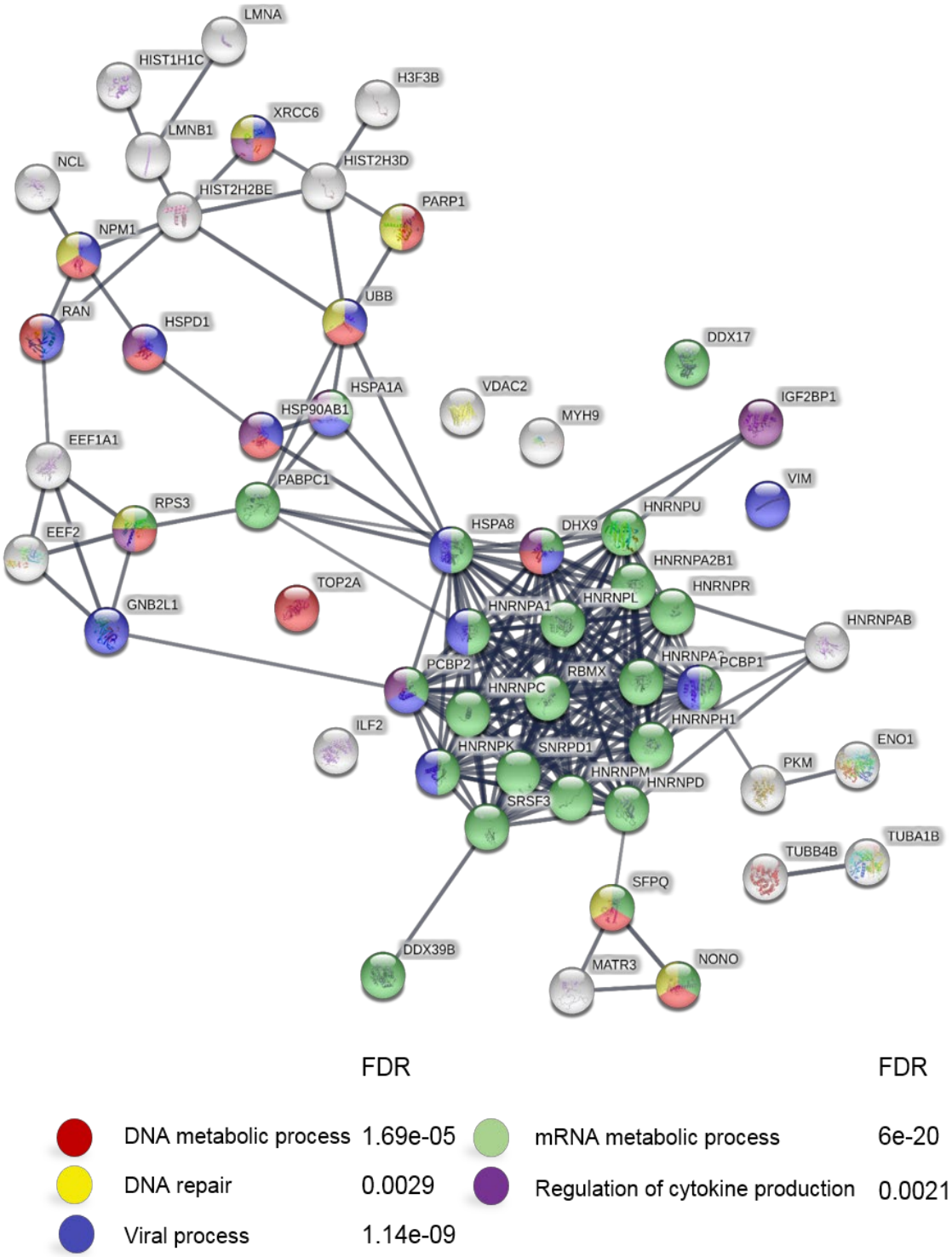

Figure 3.13 Network of protein-protein interactions by STRING for 1.5-fold change proteins. All proteins above 1.5 fold-change were analysed by STRING. Nodes with different colours represent the biological process GO categories. Most proteins in the network were shown here. Line thickness indicates the strength of data support. The minimum required interaction score is 0.7 (high confidence).

3.3 Discussion

293-BZLF1-KO cells provided us an EBV positive background and with the expression of Zta, it is able to establish EBV lytic replication. Previously, our lab determined the EBV genome load after transfection of Zta in this cell line and identified high viral copies in the cells after 72 hours of transfection. Therefore, in this study, 96 hours post-transfection was chosen to induce the lytic replication and to express hisZta.

Pull-down efficiency of nuclear co-associating proteins is a problem due to the harsh conditions required to extract DNA-bound proteins. Therefore, I had to revise the protocol based on a previous ChIP experiment in our lab (Ramasubramanyan et al., 2015a), which cross-links proteins to DNA prior to extraction, and which would be suitable for protein pull-down study. To achieve an acceptable level of Zta pull-down, an antibody with magnetic beads was used. The IP result gave us an efficient elution of Zta, and I used Actin as a negative control to question non-specific binding (**Figure 3.3**). In this IP, Actin was only seen in input and flow through but not in the IP elution, suggesting the wash steps to be efficient.

Proteins were matched to both EBV and human database because two species co-existed and studied at the same time. There are some published EBV proteins that interact with Zta in previous studies, for example, BMRF1, BGLF4, unfortunately, apart from our bait protein Zta, no other EBV proteins were identified that interact with Zta from this study.

The CRAPome database was used as a method to consider the quality of proteins found by mass spectrometry. The proteins with high scores suggest potential non-specific binding, however, it does not mean these proteins are contaminants. I also have to consider the quantitative fold-change of those proteins compared to the control group from mass spectrometry. Literature searches of the protein function is also necessary to evaluate the possibility of

each target. Further, to validate each potential target, ChIP-western blotting will be used to question each target.

One of the cellular proteins found from our experiment has been reported as a Zta interacting protein, RACK1. It is an anchoring protein that binds to protein kinases C (PKC) and it is important for PKC translocation. Previous study showed, in EBV infected monocytes, EBV reduced the activity of PKC, and this was through Zta binding to RACK1. Zta co-immunoprecipitated with RACK1 when co-expressed in a 293T cell line using expression plasmids (Tardif et al., 2002). *In vitro* binding assays also showed the interaction between these two proteins. However, this interaction did not influence Zta's transactivation function, and it was not relevant to the PKC dependent phosphorylation or nuclear translocation of Zta (Baumann et al., 2000).

Poly [ADP-ribose. polymerase 1 (PARP-1) was another protein with high fold-changes found from mass spectrometry. It is an enzyme that belongs to PARP family and is an important protein involved in DNA repair, it initiates recruitment of the DNA-repair machinery to the site of damage (Satoh and Lindahl, 1992), it also plays roles in chromatin modification and transcriptional regulation (Ray Chaudhuri and Nussenzweig, 2017). It is over-expressed in different cancers such as breast, gastric and also in lymphoma (Ossovskaya et al., 2010; Pournazari et al., 2014; Liu et al., 2016b). PARP1 has been reported to be repressed by a related herpesvirus KSHV lytic protein and it restricted KSHV lytic cycle through regulation of KSHV Rta (Chung et al., 2015). The previous study has shown EBV-infected B cells had higher PAR levels than EBV-negative B cells, suggesting PARP families may play a role in latency maintaining and silencing lytic switch (Martin et al., 2016). It is reported that PARP1 inhibitor 3-ABA showed a protective effect during EBV lytic reactivation in B cells and reduced apoptosis during EBV lytic cycle (Mattiussi et al., 2007). Recently, Tempera group reported that PARP1 bind to EBV BZLF1 promoter to restrict EBV lytic cycle. Knocking down of PARP1 induced EBV viral copies and Zta expression was sufficient to decrease PARP activity (Lupey-Green et al., 2017). These studies suggest that

PARP1 is involved in EBV lytic replication and it will be worth investigating the functional relationship between PARP1 and Zta as well as EBV lytic cycle.

Gene annotation analysis and STRING analysis (**Figure 3.10, 3.11 and 3.12**) showed that a few groups of proteins potentially interacted with Zta and suggesting that Zta may play roles in different cellular functional pathways, including DNA repair, cell cycle and regulation of cytokine production. Zta has been known to interact with DNA damage response protein 53BP1 during lytic cycle (Bailey et al., 2009). It also reported that Zta regulated cell cycle during lytic replication (Wu et al., 2003; Mauser et al., 2002). This suggests that the functions of proteins I identified are consistent with the roles Zta may play in the cells and it is possible that Zta regulates different functions through interacting with those proteins.

Although a few promising proteins were identified by mass spectrometry, the disadvantages of the whole experiment was obvious. Firstly, it was the high Zta expression level. The exogenous vector for Zta gave us a clear expression of Zta and combined with the BZLF1 knockout cell line, I could establish an EBV lytic cycle. However, overexpression of the bait protein could artificially change many situations *in vivo*. When I went through the protein list in the table (**Table 3.1 and 3.2**) that was found from mass spectrometry, many chaperones and stress response proteins were detected, and from the CRAPome analysis, most of the proteins were highly seen as non-specific binding proteins. This does not mean the proteins I found were non-specific ones, however, a huge amount of chaperones and stress response proteins might mask other proteins that interact with Zta. This may also explain why no other EBV proteins were identified in this study, as the expression level of those EBV proteins might be too low to be detected. Secondly, the EBV lytic cycle induced a change of many cell-signalling pathways, and the whole cell background may have changed. Although the formaldehyde crosslinking method had been used to stabilise the protein and DNA interaction status which also cross-linked some proteins (Mohammed et al., 2016), it might not be able to cross-link all protein-protein interactions. This suggests that a longer chain cross-linker may be needed for further studies to be

able to identify more Zta interacting proteins. In addition, the resolution of mass spectrometer instrument could be another reason to affect the result, using a new model with higher resolution, maybe will give us better results.

Above all, in this chapter, a Zta pull-down assay was established and used to combine with mass spectrometry analysis, 54 cellular proteins were found that interact with Zta in 293-BZLF1-KO cells. RACK1 was previously identified as Zta interacting protein by a different binding study. PARP-1 was a promising target for validation and follow up. However, I found no EBV proteins other than Zta. Most of the proteins with high fold-changes were also suspect contaminations, but I cannot confirm this without further validation experiments. This suggested that there were disadvantages to this study. To avoid this, a more specific system needs to be used, which would contain the EBV genome but can be induced into the lytic cycle without the need to overexpress Zta. Furthermore, a longer chain protein-protein cross-linker may be considered to replace formaldehyde in order to stabilise the protein-protein interactions during lytic cycle.

4 Identifying Zta interactome during lytic cycle by mimicking a physiological condition

4.1 Introduction

After the initial experiments, I decided to use an alternative method, which mimicked a physiological situation to induce the lytic cycle and express Zta to avoid the overexpression impact of Zta. As introduced in the previous chapter, EBV can establish its lifelong latency in B cell lymphomas such as Burkitt's lymphoma *in vivo*. Previous studies have managed to induce EBV lytic cycle in Raji cells and B95-8 cells using 12-O-Tetradecanoylphorbol-13-acetate (PMA/TPA) (Oh et al., 2003; Laux et al., 1988a), and EBV positive Burkitt's lymphoma cell line Akata cells by cross-linking surface B cell receptor (BCR) using anti-human immunoglobulin IgG (Ramasubramanyan et al., 2012; Takada, 1984). The latter method provides more physiologically relevant route to induce EBV lytic replication.

Formaldehyde is most widely used cross-linker that has good performance for DNA and protein interaction studies, however, it might not be the first choice for protein-protein interaction studies. A few in cell protein-protein cross-linkers were evaluated and used to stabilise the protein-protein interaction in the cells (Xue et al., 2016; Smith et al., 2012). Recently there were studies using different cross-linking combination conditions to improve pull-down assays and also to increase the efficiency of detecting binding partners of the bait protein by mass spectrometry (Engelen et al., 2015).

Post-extraction chemical labelling mass spectrometry analysis was used in clinical sample studies widely, especially isobaric tags such as tandem mass tags (TMT) (Wiese et al., 2007; Thompson et al., 2003), with the high-resolution mass spectrometer, TMT labelling could maximally compare 11 samples at one time, and this makes it valuable for multi-sample studies. Although label-free quantification worked to some degree for my first experiment in **Chapter 3**, the TMT labelling methods may give us more sensitive quantitation results.

4.2 Results

4.2.1 Establish induction condition for EBV lytic cycle in Akata EBV positive BL cell line.

Two anti-human IgG products from different companies were used for my test, cells were plated in a 24-well-plate and treated with increasing concentrations of each anti-IgG for 24 hours. Cells were harvested at 24 and 48 hours post-treatment and lysates prepared for western blotting to detect Zta, untreated cells were used as a negative control and previous anti-IgG induced Akata cell protein lysate from our lab was used as a positive control, Actin was used as a loading control (**Figure 4.1**). The result showed 1.3µl/ml IgG (highlighted in red) from DAKO and 24 hours induction time was the best condition to express Zta. This concentration was used for all of the lytic cycle induction studies in Akata cells in this chapter.

Flow cytometry analysis was used to determine the lytic cell proportion. Akata cells were treated with anti-IgG for 24 hours, followed by wash and prepared for flow cytometry. Zta and EBV late lytic protein VCA were labelled separately by fluorescent antibody then detected by flow cytometry (**Figure 4.2** and **4.3**). The result shows around 5% of the total cells were induced and expressed Zta. The percentage of VCA expressed cells was around 3%.

Until then I established lytic cycle induction, although the percentage showed by flow cytometry was low, my goal was to enrich Zta and its binding proteins using pull-down assays, increasing the cell numbers for the pull-down assays could solve this problem.

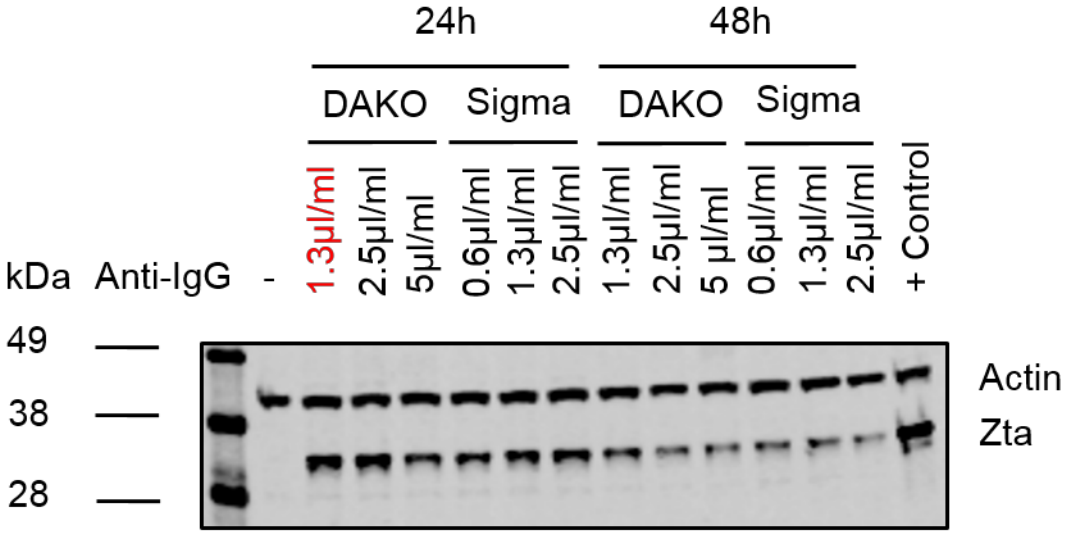

Figure 4.1 Select appropriate condition for EBV lytic cycle induction in Akata cells. Different concentrations of rabbit anti-human IgG from DAKO or Sigma (Merck) were used for induction condition selection at two time points. The positive control was from previous induced Akata cells in our lab. Western blotting was used for Zta expression level, Actin was used as a loading control.

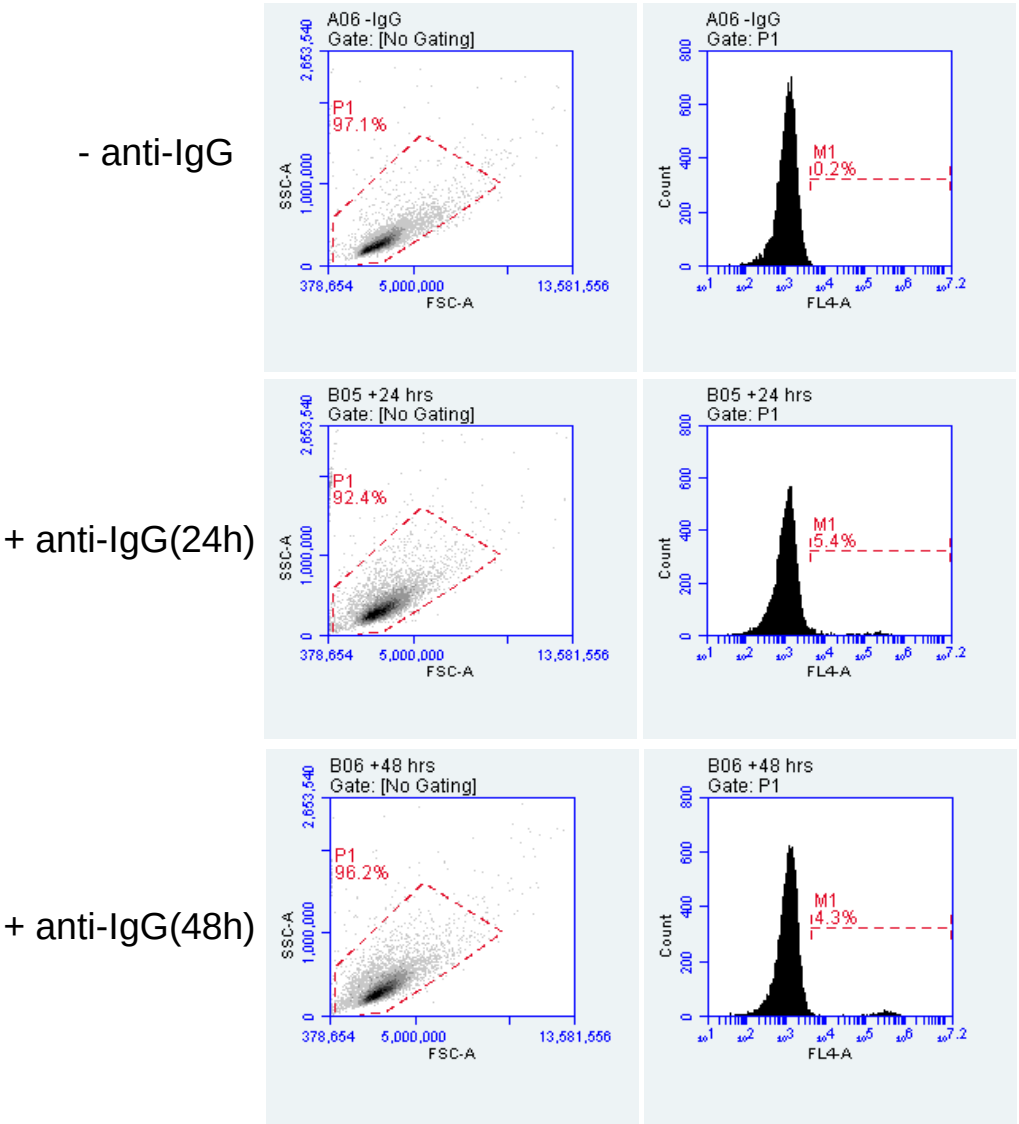

Figure 4.2 Zta expressed cells detection after IgG induction in Akata cells. Akata cells were induced by anti-IgG for 24 hours and 48 hours. Both un-induced and induced cells were fixed, permeabilized and labelled by Zta antibody BZ1 and secondary anti-mouse Alexa 647 antibody. Cells were analysed by flow cytometry and gated. The percentage of Zta expressed cells were shown compared to the un-induced cells.

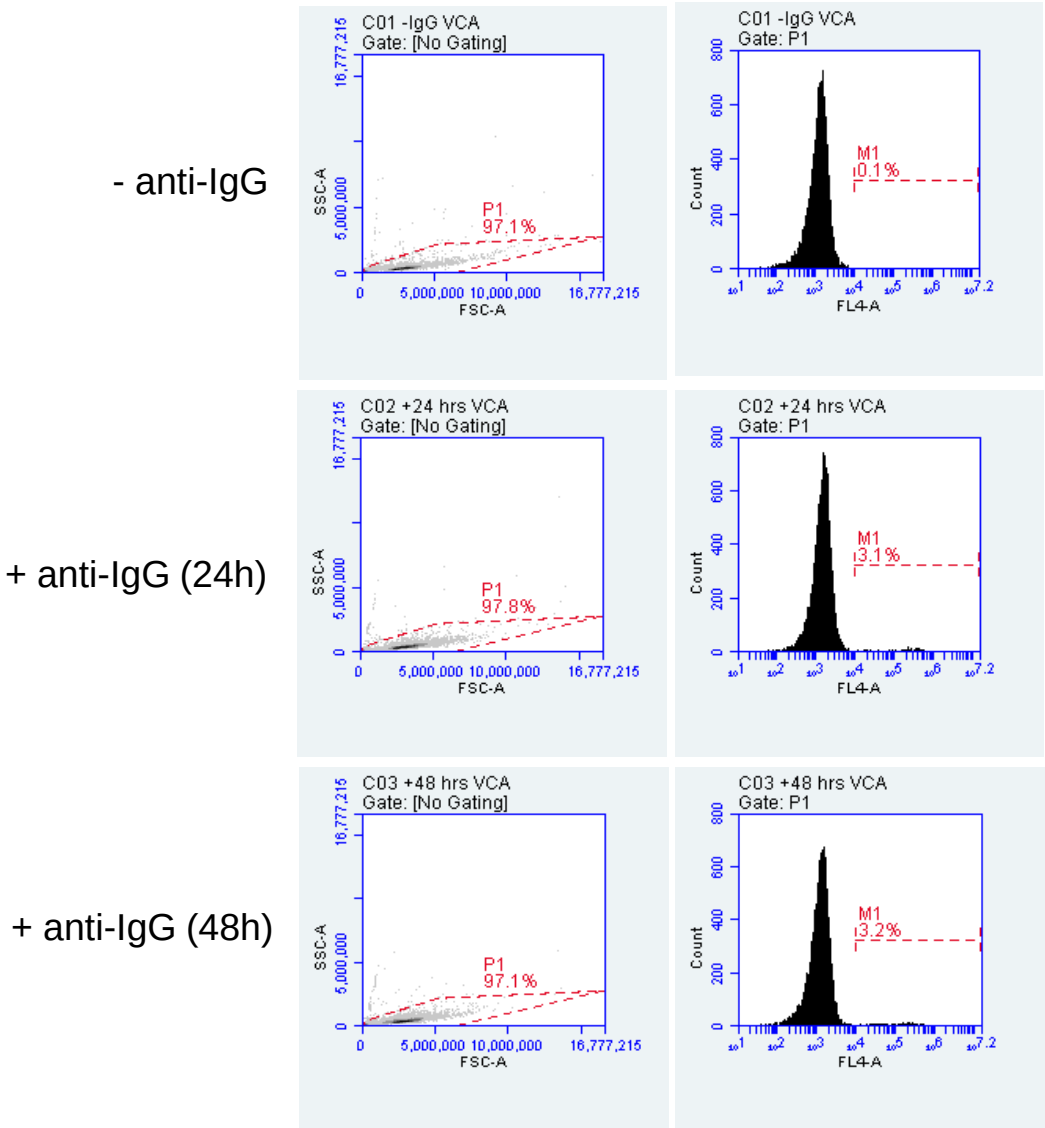

Figure 4.3 EBV-VCA protein expressed cells detection after IgG induction in Akata cells. Akata cells were induced by anti-IgG for 24 hours and 48 hours. Both un-induced and induced cells were fixed, permeabilised and labelled by EBV-VCA antibody and secondary anti-mouse Alexa 647 antibody. Cells were analysed by flow cytometry and gated. The percentage of VCA expressed cells were shown compared to the un-induced cells.

4.2.2 Determine a suitable concentration of new in-cell cross-linker DSP (dithiobis(succinimidyl propionate)).

In order to establish a suitable pull-down assay condition, a reversible protein-protein cross-linker DSP was chosen, which has much longer spacer arm (12 Å) than formaldehyde (2 Å). Next, the optimal concentration of DSP was needed to be determined, which could efficiently stabilise protein-protein interactions while could not capture too many non-specific binding proteins. Since DSP can be quenched and reversed by DTT, an experiment was designed to answer this question (**Figure 4.4**).

Akata cells were treated with anti-IgG for 24 hours, cells were then cross-linked by increasing concentrations of DSP solution at room temperature for 30 minutes, the cross-linking reaction was stopped by adding Tris. Cells were harvested and lysed by protein sample buffer without reducing reagent and prepared for western blotting. Half of each sample was taken and recovered by 50mM DTT. DSP un-treated and DTT quenched cells were lysed and used as controls.

Western blotting was performed for Zta. Since Zta could form a dimer, Zta dimer and monomer bands were used to evaluate the cross-linking situation (**Figure 4.4**). Zta dimer was observed in 0.1mM DSP treated condition, additionally, a small amount of Zta was seen as the monomer. With the increasing concentration of DSP, especially above 1mM, Zta only could be detected as a dimer, but dark smears were also seen on the top of the lanes, which suggested most of the interacting proteins were cross-linked with Zta and couldn't run through the gel without reducing reagent. When the cross-linking was reversed by 50mM DTT, most Zta was recovered to the monomer. The groups cross-linked by higher concentrations of DSP were not recovered as well as low concentration DSP treated ones. Above all, considering the cross-linking efficiency and the possibility to be recovered, 0.2mM was chosen for further pull-down experiment.

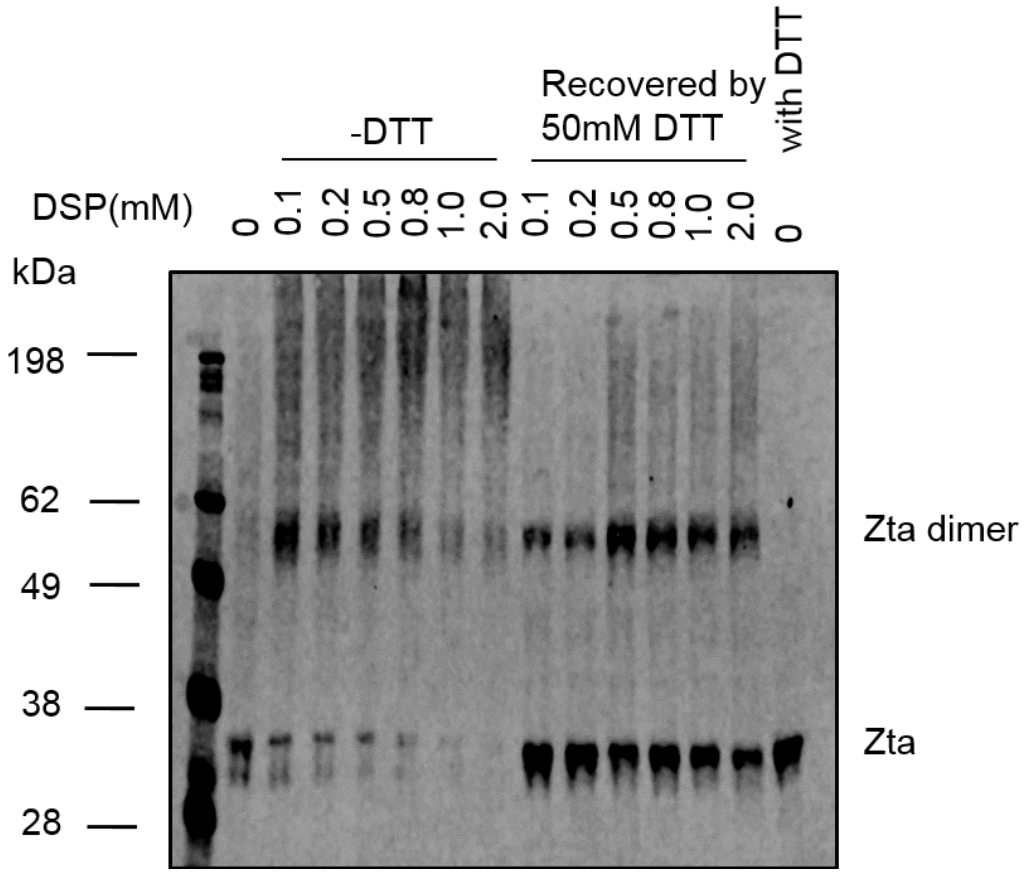

Figure 4.4 DSP cross-linking titration in EBV positive Akata cell line. Akata cells were incubated with different concentrations of DSP/PBS solution for 30 minutes, then cross-linking was stopped by Tris solution. DSP Non-cross-linked (leftmost) and DTT quenched (rightmost) cells were used as controls. Cells were lysed in 2X sample buffer without reducing reagent (DTT or β-Mercaptoethanol). Half of the cross-linked samples from each group were then reversed by exposure to 50mM DTT. Then Western blotting was performed for Zta.

4.2.3 Establishment of Zta pull-down condition in Akata cells

In order to reduce antibody chain contamination in the elute proteins or digested peptides, two non-cleavable cross-linkers were tested to couple antibody to the beads before pull down. DMP (Merck Sigma) and BS3 (Fisher) were used and compared to each other, a certain amount of beads and antibody were incubated for 2 hours, and then cross-linkers were added and antibody coupled beads were washed following the protocols for each condition.

Besides with the cross-linked antibody were added to nuclear extracts (input) that were from hisZta transfected 293-BZLF1-KO cells. After overnight incubation, beads were washed proteins were eluted, half of the samples were run by SDS-PAGE gel and stained by Coomassie blue (**Figure 4.5**). IP using BS3 cross-linked antibody and beads gave us less antibody chain bands than DMP cross-linked ones, which suggested BS3 was a better reagent for antibody beads cross-linking to avoid antibody eluting in the samples. However, hisZta bands could not be seen clearly at the predicted region in both IP. In order to measure Zta level, rest half of the samples were analysed by western blotting for hisZta (**Figure 4.6**). hisZta was detected, which suggested pull down to be successful and no huge difference of Zta bands between two groups using different cross-linkers was observed. However, considering the BS3 group had a lower amount of antibody chains in the IP samples by Coomassie blue, it was chosen and used for future experiments. Two different amounts of antibody was used to test whether the beads had all the antibody bound (**Figure 4.5** and **Figure 4.6**). There was no big difference between 10ug and 15ug groups according to the Zta pull down levels, suggesting 10 µg was enough to conjugate all the beads or bind to all of the Zta in the extract, it was not necessary to use more antibody for future experiments.

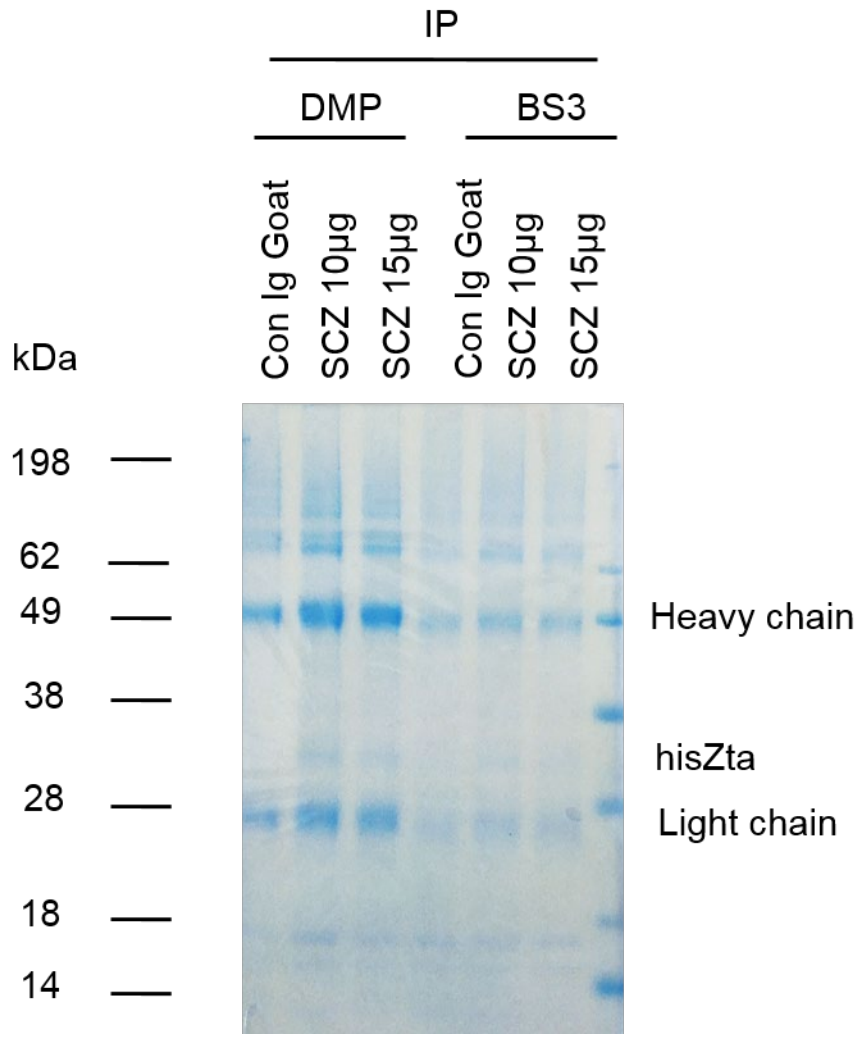

Figure 4.5 Antibody cross-linked to beads comparison (Coomassie gel). 293-BZLF1-KO cells were transfected with hisZta or control vector for 96 hours and cross-linked by formaldehyde. Then cross-linked cell nuclear extracts were sonicated and used for each IP. 10ug antibody (SCZ) and control antibody were bind to 25µl beads and cross-linked by DMP or BS3 separately prior to the IP. Then prepared antibody beads were added in the sonicated nuclear extracts. Protein eluates were separated by SDS-PAGE gel and stained by Coomassie blue. Zta, antibody heavy and light chain were labelled in the figure.

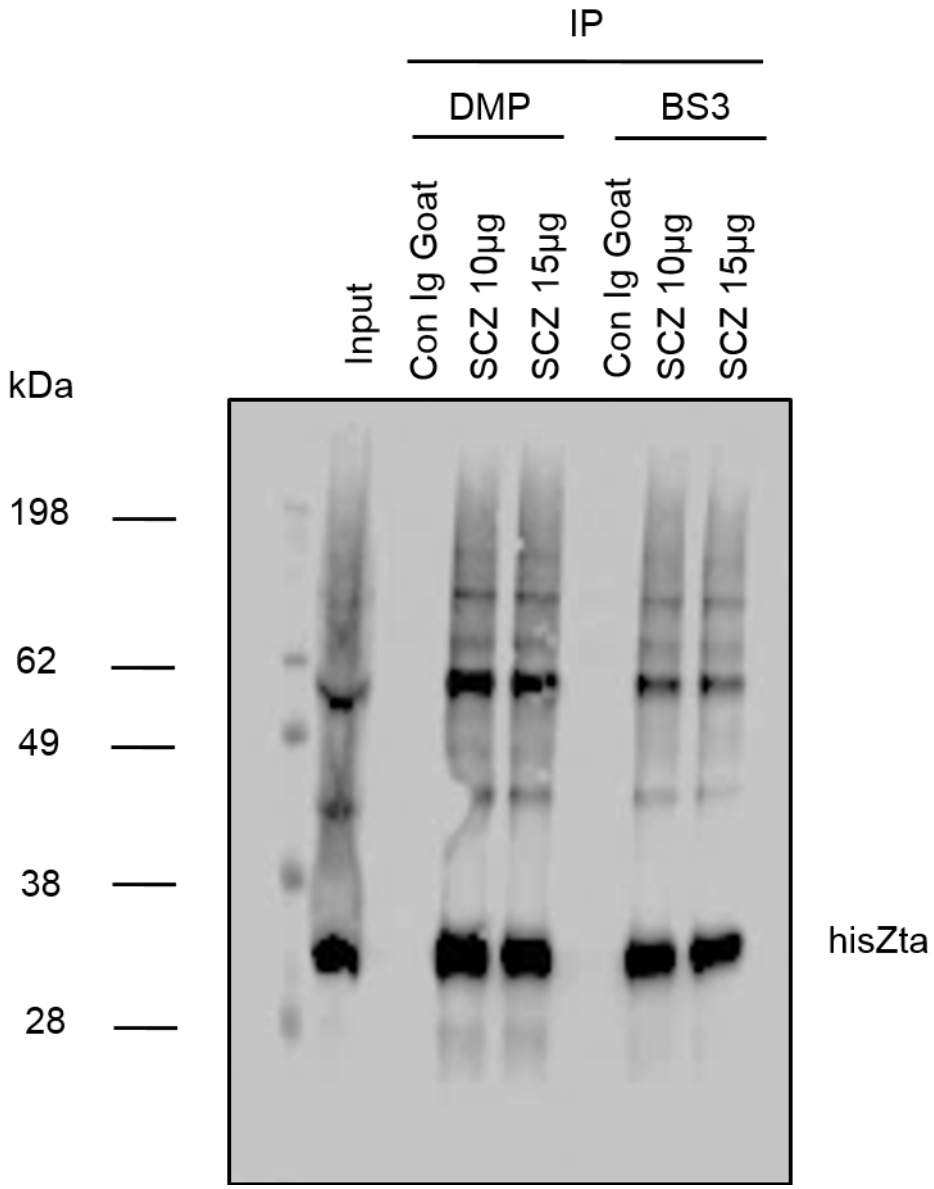

Figure 4.6 Antibody cross-linked to beads comparison (Western blotting). 293-BZLF1-KO cells were transfected with hisZta or control vector for 96 hours and cross-linked by formaldehyde. Then cross-linked cell nuclear extracts were sonicated and used for each IP. 10ug antibody (SCZ) and control antibody were bind to 25µl beads and cross-linked by DMP or BS3 separately prior to the IP. Then prepared antibody coupled beads were added in the sonicated nuclear extracts. Protein eluates after IP were then analysed by western blotting for Zta.

Next, the new Zta pull-down condition was tested in Akata cells. Instead of sonication, Benzonase nuclease was used to break DNA. Uninduced Akata cells were used as a control group. Cells were cross-linked by 0.2mM DSP, then nucleus was extracted and used for IP, antibody were coupled to magnetic beads before immunoprecipitation steps by BS3. In order to evaluate IP efficiency, input, flow through (FT) and IP eluate was collected and prepared for western blotting (**Figure 4.7A**). The blot was probed for Zta and quantitated by ImageStudio software (LI-COR), the values were converted by loading volume and normalised to the input **(Figure 4.7B)**. As shown in the bar chart, around 30% of Zta was pulled down, and the percentage was similar to the Zta pull down in 293-BZLF1-KO cells, which has been described in **Chapter 3**. A reduction in flow through was also seen, which again suggested Zta was efficiently pull down in this IP experiment.

4.2.4 Large-scale Zta pull-down and TMT labelling mass spectrometry analysis in Akata cells

After establishing the appropriate conditions, I moved forward to the large-scale IP and TMT labelling mass spectrometry analysis. The whole experiment scheme is shown (**Figure 4.8**). Group A was un-induced Akata cells, group B and group C were anti-IgG induced Akata cells. Zta antibody (SCZ) coupled beads were used in group A and B, control Goat IgG coupled beads were used in group C for the pull-down. So Zta pull-down was performed in group B, two other pull-downs performed in group A and C were used as controls.

Before doing a large-scale experiment, a small number of cells from the same batch of each group were harvested for western blotting and qPCR in order to check the Zta expression level and EBV viral load (**Figure 4.9**).

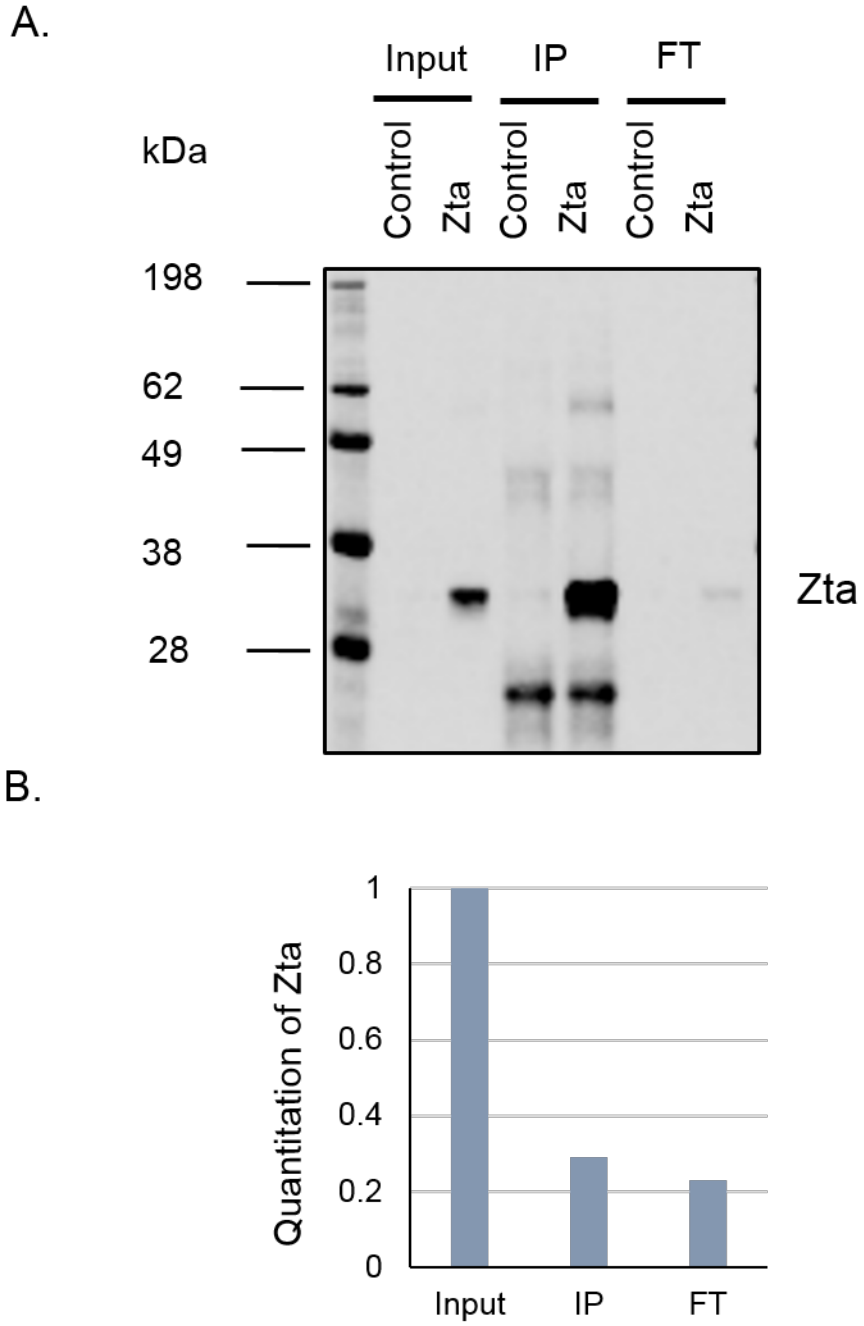

Figure 4.7 Zta pull down western blotting in Akata cell line. 0.2mM DSP was used for in-cell cross-linking in Akata cells, Cell Lytic reagent with benzonase nuclease was used to prepare the nuclear extracts, 10ug antibody (SCZ) and 25ul beads was cross-linked together by BS3 prior to the immunoprecipitation steps. To test the pull-down efficiency in Akata cells using this revised protocol, input, flow through (FT), and IP eluate was collected and prepared for western blot. **A.** Western blotting for Zta. **B.** Quantitation of Zta. The quantitation was converted by loading volume and normalized to Input.

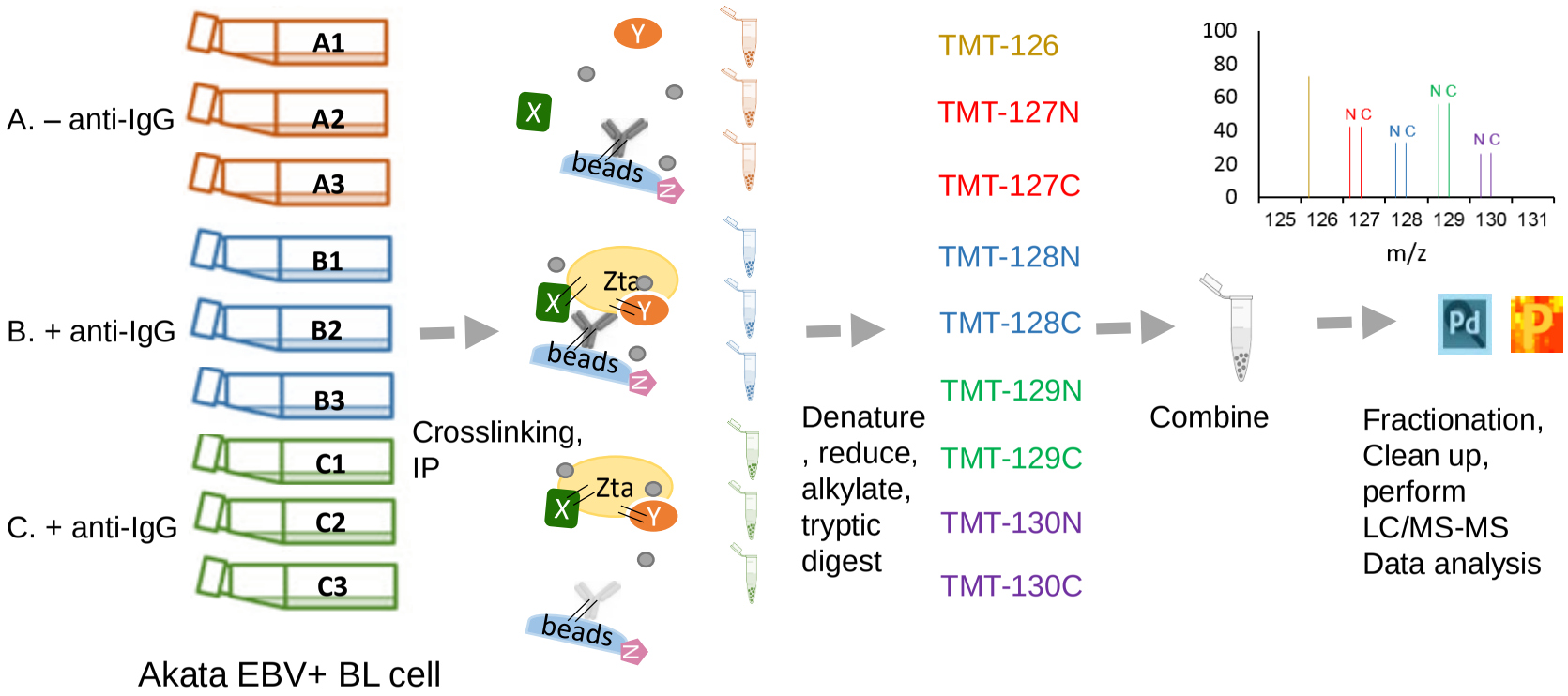

Figure 4.8 Scheme of IP-TMT labelling Mass spectrometry analysis in Akata cells. Lytic reactivation of Akata cells was triggered by anti-IgG for 24 hours. Cells were cross-linked by 0.2mM DSP. Zta antibody (SCZ) and control goat IgG coupled with magnetic protein G beads, cross-linked by BS3 and used for IP. Each IP group was performed as triplicates. Protein X and Y represent the potential targets that interact with Zta, protein N represent one of the non-specific proteins binding to antibody or beads. Proteins bind antibody-beads from each group were digested by trypsin, then digested peptides were mixed, fractionated and analyzed by mass spectrometer. Data were analyzed by Proteome discoverer, and Perseus.

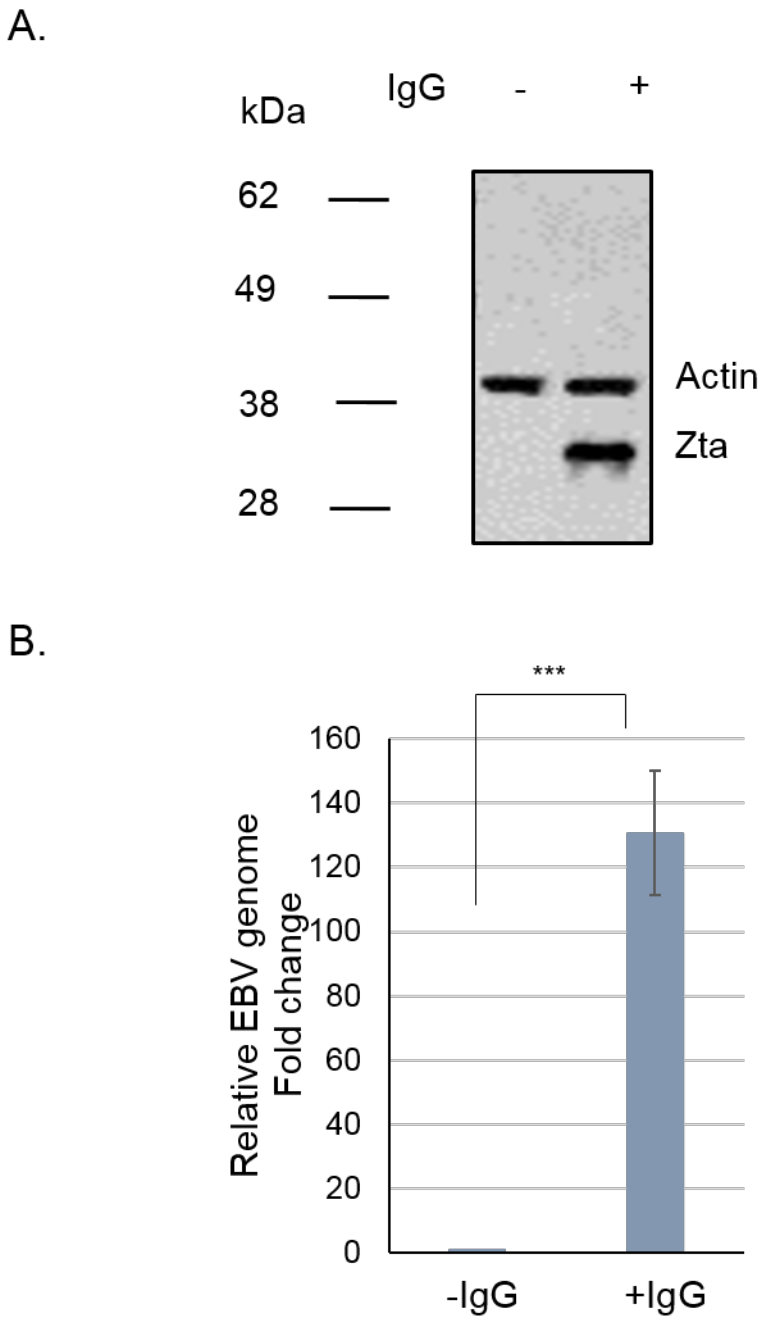

Figure 4.9. Zta expression level and EBV viral load in Akata cells. Cells were induced by anti-human IgG to express Zta and trigger the lytic cycle for 24 hours. Cells were lysed by protein sample buffer and total Genomic DNA was extracted. **A.** Western blotting of Zta, actin was used as a loading control. **B.** EBV viral load was measured by qPCR, EBV genome was normalized to the human genome and shown as fold-change compared to the control group.

Reagents were all scaled up according to the cell numbers, and biological triplicates of the whole experiment was performed for each group. In the end, nine tubes with washed antibody and beads bound proteins were collected, 5% of the total beads were taken out from each tube and the proteins were eluted in the 2X protein sample buffer for western blotting analysis. Rest of the beads were stored in the freezer and would be used for mass spectrometry analysis. Western blotting was performed for Zta (**Figure 4.10**), this showed that the pull-down worked. The beads were sent to the mass spectrometry facility at the University of Bristol. TMT labelling and Mass spectrometry analysis were performed by the facility. The tandem mass tags used in my experiment were listed (**Figure 4.11**).

4.2.5 Proteins found from mass spectrometry that interact with Zta

The mass spectrometry raw files were processed and quantified using Proteome Discoverer software v2.1 in the University of Bristol, they were searched against the UniProt Human database (140000 entries) plus EBV B95-8 and GD1 database using the SEQUEST algorithm. Then two TMT ratios were generated to compare condition B (induced cells Zta IP) to A (un-induced cells Zta IP) and B (induced cells Zta IP) to C (Induced cells con IgG IP) separately, the ratio was generated for 3 replicates of each condition. Further analysis was based on these data. All the proteins found without ratio were excluded and only proteins with TMT ratios and low FDR were included for further consideration. Then the ratios were transformed to log2 value, and log2 value above one was considered as two-fold changes.

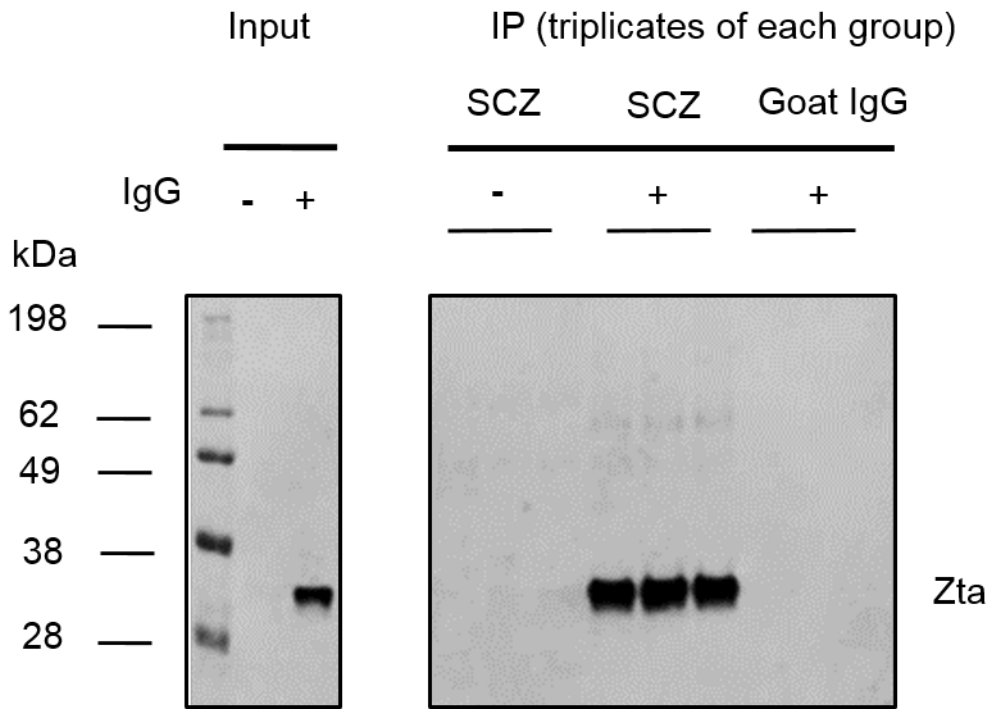

Figure 4.10. IP sample confirmation before mass spectrometry. 10% of beads taken from each sample were eluted by protein sample buffer, Input and IP eluates from each group were then analyzed by western blotting for Zta.

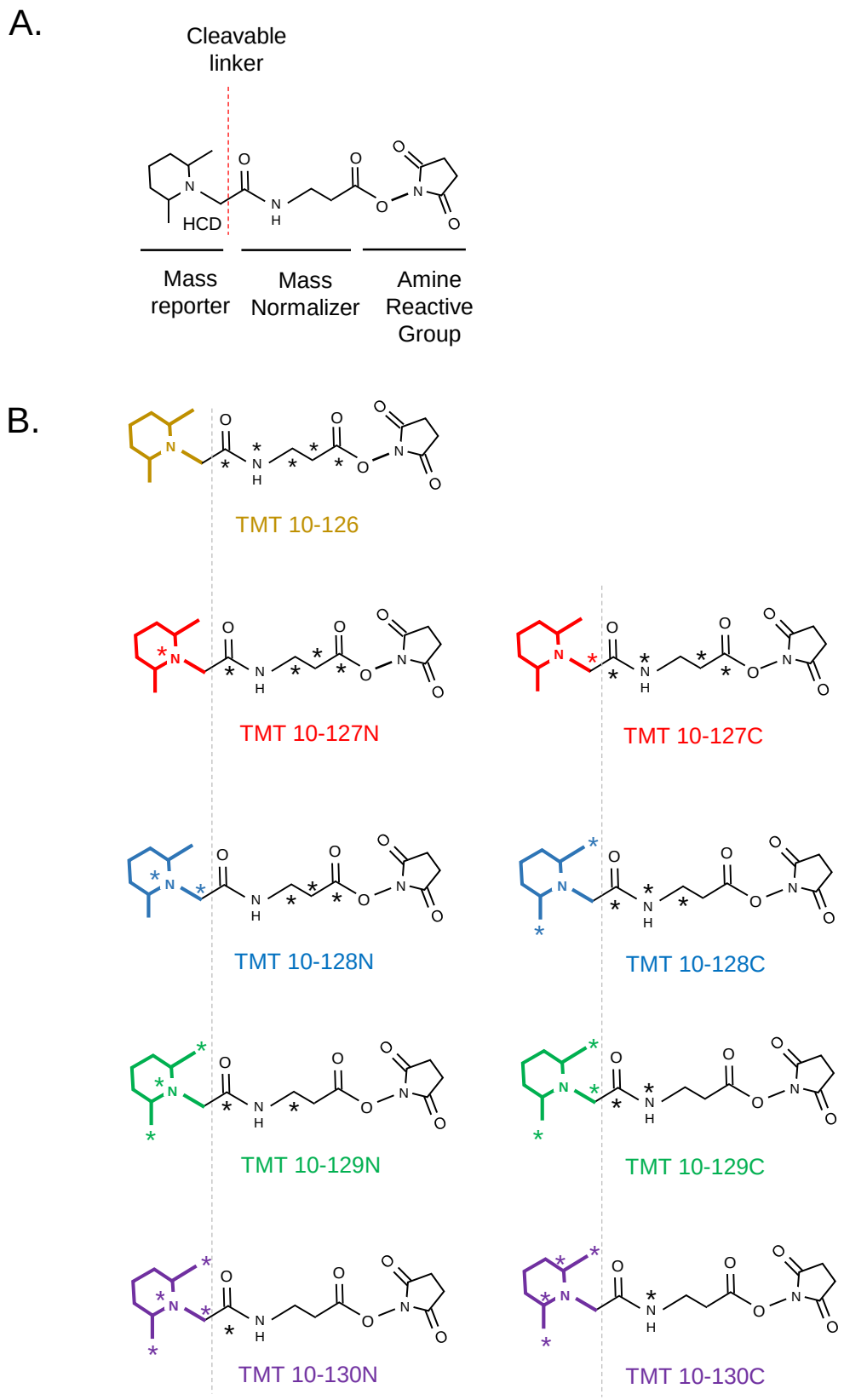

Figure 4.11. Chemical structures of the TMT Labelling Reagents. A. Chemical structure and functional regions of the reagent, and the MS/MS fragmentation sites by higher energy collision dissociation (HCD). **B**. Structure and mass difference of 9 tags used from ThermoFisher TMT 10plex labelling kit (adapted from Thermo Fisher). Isotope positions (*)

Proteins were ranked by 2 different ratios separately and together (**Figure 4.12**), all the proteins with ratios were plotted in the scatter plot, 267 proteins, including 252 human and 15 viral proteins were considered as significant targets shown 2-fold changes to one control, 44 proteins including 37 human and 7 viral proteins had significantly high ratios in Zta IP compared to both controls, 7 viral proteins and 37 human proteins were listed (**Table 4.1 and 4.2**). Among the 7 viral proteins, BALF5 and BGLF4, were the viral proteins that were known to interact with Zta. All the 252 human proteins were analysed by DAVID database, the top enriched gene clusters were listed (**Figure 4.13A**). mRNA splicing proteins were enriched with the highest score 8.22 and lowest p-value, followed with transcription and chromatin remodelling proteins, got the score 7.65 and 7.06 respectively and with a low p-value. Proteins related to cell-cell adhesion, chromosome segregation and protein folding were also enriched as a bit lower score. The 37 most enriched proteins were then analysed independently (**Figure 4.13B**), the top cluster with highest score 3.7 and the low p-value was transcription relevant proteins, which possibly acts as a transcription activator or repressor of Zta during lytic cycle.

Network analysis of STRING was performed with clusters of different biological functions. A total of 252 cellular protein network was analysed first (**Figure 4.14**). Nodes represented different proteins and the clusters with low FDR were selected and shown by different colours, which represented different functions. The proteins that were not grouped were excluded in the image. From the whole picture, some protein complexes were shown with different functions, transcription relevant proteins were grouped in two main areas with red nodes. RNA splicing proteins were also grouped in yellow nodes. Another big group of proteins were relevant to programmed cell death. Chromatin remodelling, DNA metabolic process, protein folding and cell cycle relevant protein were also shown in the network with low FDR.

Group A : Un-induced cells Zta IP
Group B : Induced cells Zta IP
Group C : Induced cells con IgG IP

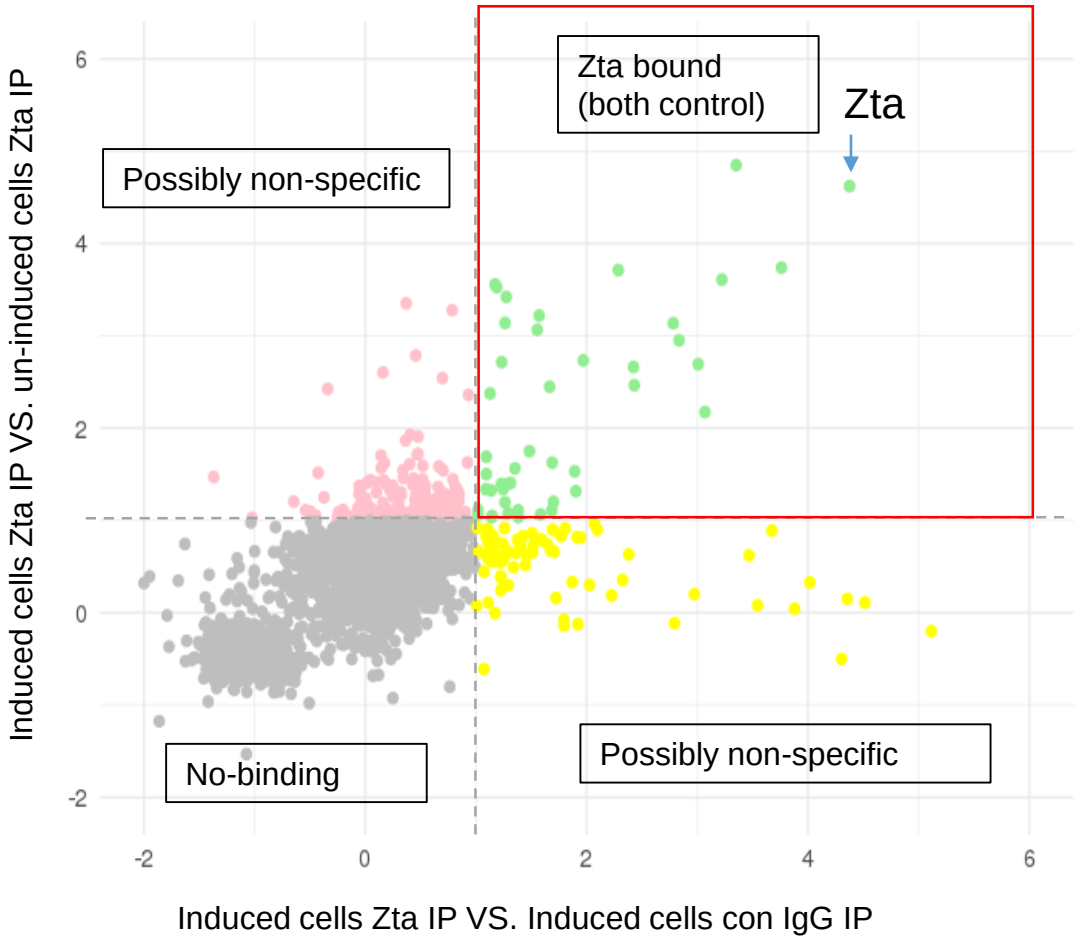

Figure 4.12. Scatter plot of proteins quantified in each group. Zta associated protein ratios were generated by comparing to each control (B VS. A or B VS. C). Zta as a bait protein had the highest ratio compared to both controls. 252 human+15 viral proteins were highlighted as significant hits shown 2-fold changes compare to one control (Pink, yellow and Green). 7 viral and 37 human proteins (Green) were significant in Zta IP compared to both controls (≥2-fold). There were chances that the targets in the pink and yellow were nonspecific Zta interacting targets.

Known binding proteins

Gene name	Description	Unique peptide	Log2 Ratio: (B) / (A)	Log2 Ratio: (B) / (C)
BALF5	DNA polymerase	5	3.14	1.26
BGLF4	Serine/threonine-protein kinase	5	3.53	1.19

Unknown binding proteins

Gene name	Description	Unique peptide	Log2 Ratio: (B) / (A)	Log2 Ratio: (B) / (C)
BBRF1	Portal protein	1	4.85	3.35
BVRF2	Capsid scaffolding protein	12	3.71	2.29
BALF2	Major DNA-binding protein	17	3.56	1.17
BcLF1	Major capsid protein	17	3.42	1.27
BMLF1	mRNA export factor ICP27 homolog	6	2.72	1.23

Table 4.1 Zta associated EBV proteins identified by mass spectrometry. The upper table showed 2 EBV proteins already known bind to Zta and on our top list, bottom table showed 5 potential EBV proteins found by mass spectrometry that may bind to Zta and also on our top list.

Gene name	Description	Unique peptide	Log2 Abundance Ratio: (B) / (A)	Log2 Abundance Ratio: (B) / (C)	Crapome Num of Expt. (found/total)
FAM96B	Mitotic spindle-associated MMXD complex subunit MIP18	2	3.74	3.76	20 / 411
SBSN	Suprabasin	3	3.61	3.22	41 / 411
TXN	Thioredoxin	2	3.22	1.57	174 / 411
TMED9	Transmembrane emp24 protein transport domain containing 9	1	3.14	2.78	11 / 411
BLMH	Bleomycin hydrolase	3	3.07	1.55	35 / 411
TIPRL	TIP41-like protein	2	2.95	2.84	27 / 411
NCOA5	Nuclear receptor coactivator 5	20	2.73	1.97	19 / 411
MMS19	MMS19 nucleotide excision repair protein homolog	7	2.69	3.01	25 / 411
TMED10	Full-length cDNA 5-PRIME end of clone CS0DF013YM24 of Fetal brain of Homo sapiens (Human) variant (Fragment)	2	2.66	2.42	19 / 411
FGFR2	Adenosylhomocysteinase	2	2.46	2.43	15 / 411
FBP11	Pre-mRNA-processing factor 40 homolog A (Fragment)	10	2.45	1.67	76 / 411
GGCT	Gamma-glutamylcyclotransferase	3	2.37	1.13	30 / 411
CIAO1	Probable cytosolic iron-sulfur protein assembly protein CIAO1	2	2.17	3.07	4 / 411
NFATC2	Nuclear factor of activated T-cells, cytoplasmic 2	6	1.75	1.48	4 / 411
HSPA8	Heat shock cognate 71 kDa protein (Fragment)	15	1.69	1.09	396 / 411
ARID1A	AT-rich interactive domain-containing protein 1A	2	1.63	1.69	24 / 411
RUNX3	Runt-related transcription factor	1	1.56	1.35	0 / 411
ADAMTSL1	ADAMTS-like protein 1	1	1.53	1.89	1 / 411
HSPA9	Stress-70 protein, mitochondrial	31	1.50	1.09	395 / 411
TLE3	Transducin-like enhancer protein 3	4	1.41	1.31	34 / 411
NFATC1	Nuclear factor of activated T-cells, cytoplasmic 1	5	1.39	1.23	0 / 411

Gene name	Description	Unique peptide	Log2 Abundance Ratio: (B) / (A)	Log2 Abundance Ratio: (B) / (C)	Crapome Num of Expt. (found/total)
TMED2	Transmembrane emp24 domain-containing protein 2	2	1.39	1.28	13 / 411
TAF6	Transcription initiation factor TFIID subunit 6	1	1.34	1.24	36 / 411
SRSF9	Serine/arginine-rich splicing factor 9	6	1.34	1.09	77 / 411
HMG20A	High mobility group protein 20A	2	1.33	1.14	7 / 411
PABPC1	Polyadenylate-binding protein 1	18	1.32	1.90	172 / 411
MEF2B	Myocyte-specific enhancer factor 2B	7	1.20	1.70	0 / 411
RBMXL1	RNA binding motif protein, X-linked-like-1	4	1.20	1.26	159 / 411
GATAD2B	cDNA FLJ37346 fis, clone BRAMY2021310, highly similar to Transcriptional repressor p66 beta	9	1.12	1.02	50 / 411
PABPC4	Polyadenylate-binding protein	12	1.11	1.38	142 / 411
YLPM1	YLP motif-containing protein 1	4	1.11	1.69	45 / 411
CPSF3L	Integrator complex subunit 11	4	1.08	1.29	4 / 411
KHDRBS1	KH domain-containing, RNA-binding, signal transduction-associated protein 1	14	1.07	1.58	138 / 411
RBMX	RNA-binding motif protein, X chromosome	9	1.06	1.02	169 / 411
TCF20	Transcription factor 20	23	1.05	1.15	29 / 411
SMARCD2	SWI/SNF-related matrix-associated actin-dependent regulator of chromatin subfamily D member 2	5	1.04	1.38	12 / 411
PHF14	PHD finger protein 14	14	1.04	1.14	6 / 411
PARP1	Poly [ADP-ribose] polymerase 1	52	1.44	0.52	182 / 411

Table 4.2. Zta associated cellular proteins compared to both controls (B VS. A and B VS. C). 37 human proteins associated with Zta compared to both controls (≥2-fold) were listed with gene name, description, log2 ratios. Crapome score was also listed as quality control for each protein. Targets highlighted by green colour were chosen for further validation. PARP1 only has high ratio compare to one group, however, it was the protein also found in **Chapter 3**, so chosen for the validation and list separately.

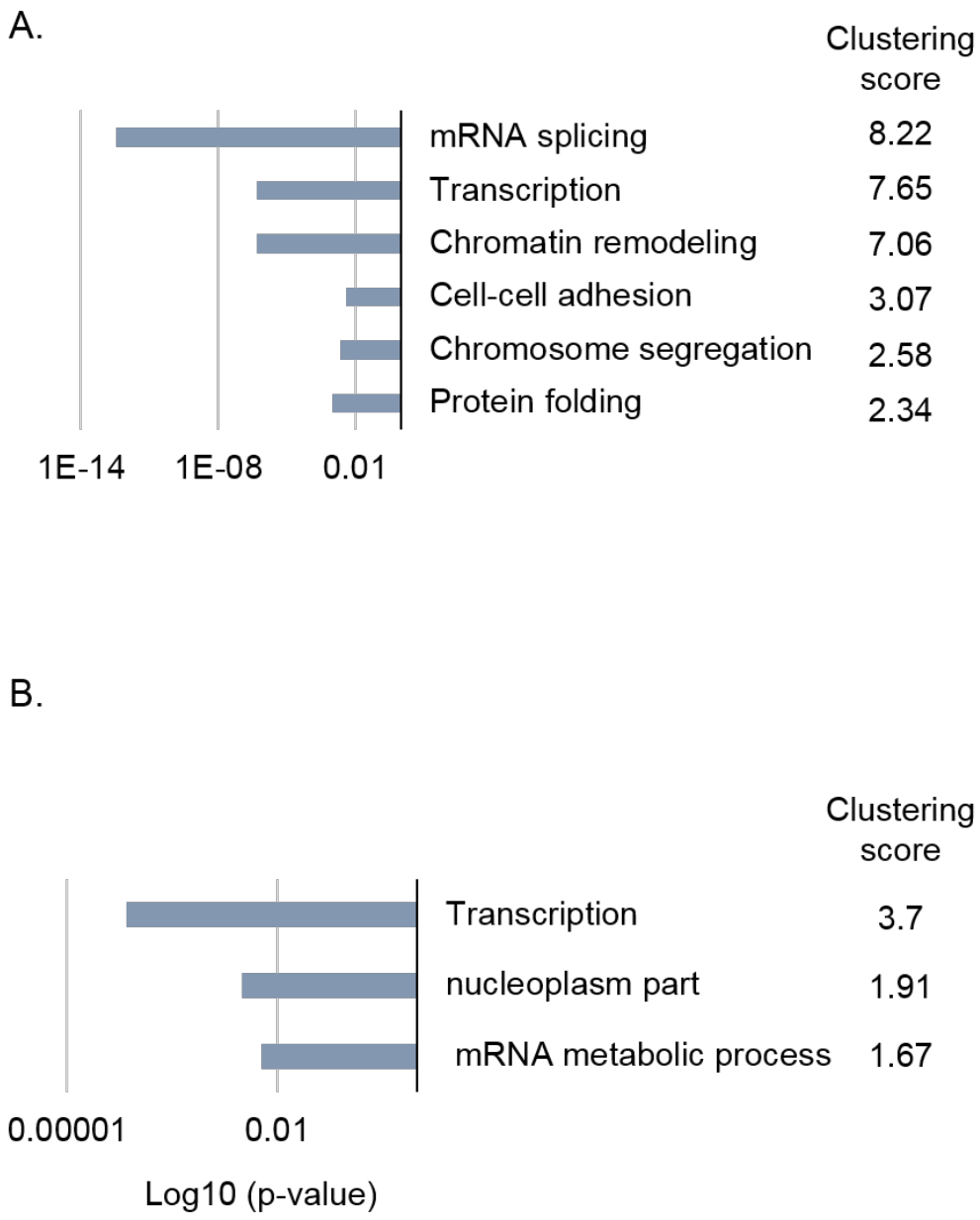

Figure 4.13 GO analysis for proteins associated with Zta. Gene ontology analysis of human proteins found that interact with Zta through DAVID database. Top enrichment groups with p-value and clustering scores were shown in the chart. **A.** All 252 human proteins. **B.** 37 enriched human proteins.

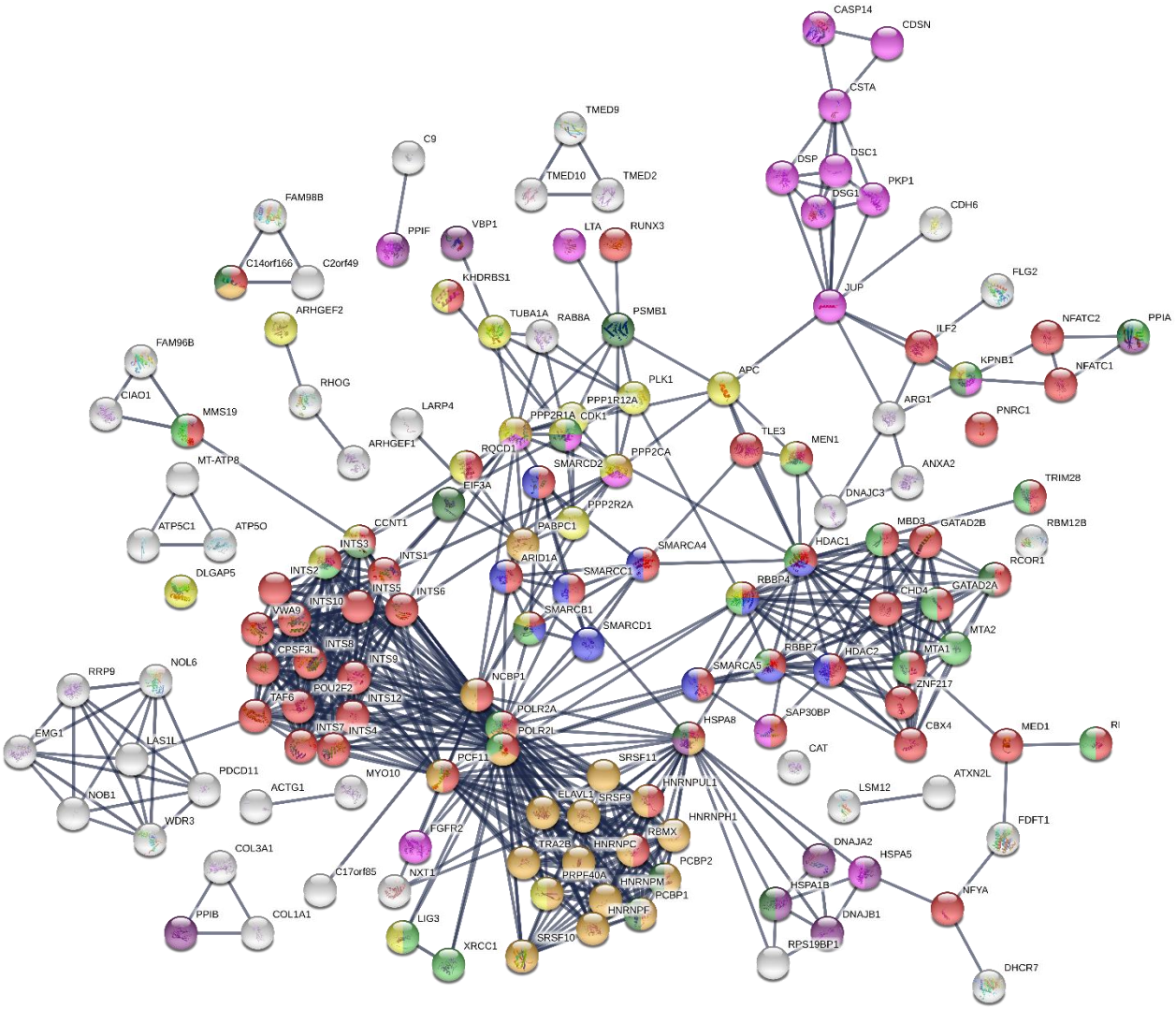

	FDR		FDR
Transcription	8.57e-16	Protein folding	0.00053
RNA splicing	1.63e-14	Programmed cell death	0.0011
Chromatin remodelling	6.00e-06	Viral process	0.0023
DNA metabolic process	0.00015	Cell cycle	0.0084

Figure 4.14. A network of protein-protein interactions by STRING for all identified cellular proteins. 252 human proteins associated with Zta compared to both controls (≥2-fold) were analyzed by STRING. Proteins which were not in the network were excluded in the image, Nodes with different colours represented biological process GO categories.

The most enriched 37 cellular proteins were also analysed separately (**Figure 4.15)**. Most of them were transcription factors, but some groups also showed specific functions, such as TMED proteins which are important for Golgi vesicle, iron-sulfur cluster assembly protein complex formed by MMS19, CIAO1 and FAM96B and calcium signalling regulated proteins, NFATs. Besides, many important transcription regulation proteins were also identified, such as TCF20, RUNX3, TXN, TAF6, which were all interesting for further investigation.

4.2.6 To investigate proteins that may interact with Zta.

After obtaining the information of significantly changed proteins in each group, some of them were chosen (highlighted in **Table 4.2**), and their association with Zta was questioned further. Cytosolic iron-sulfur assembly component 2B (FAM96B), nucleotide excision repair protein homolog (MMS19), a few transcription factors, runt-related transcription factor 3 (RUNX3), Myocyte-specific enhancer factor 2B (MEF2B), transcription initiation factor TFIID subunit 6 (TAF6), nuclear factor of activated T-cells, cytoplasmic 1 and cytoplasmic 2 (NFATC1 and NFATC2), cellular chaperone Heat shock cognate 71 kDa protein (HSPA8, HSC70) and DNA repair protein PARP1 were the proteins selected from the mass spectrometry list, most of them have high TMT ratios from the top 37 candidates. PARP1 was the one that had high ratio only in one comparison, however, PARP1 had high fold-changes found from mass spectrometry analysis in 293-BZLF1-KO cells in **Chapter 3**, and it was highly possible that PARP1 was a Zta interacting protein. By evaluating this target, I could also decide whether it is valuable to test the proteins that only have a high ratio in one comparison (shown in **Figure 4.12** and highlighted in pink and yellow).

First of all, antibodies of all these proteins was tested in three different cell lines, Akata, 293-BZLF1-KO and HEK293 cell lines. Most of the antibodies were the test samples from Insight Biotechnology. RUNX3 antibody was a kind gift from West lab. The total cell lysate from each cell line was used for western blotting and probed for different proteins (**Figure 4.16**).

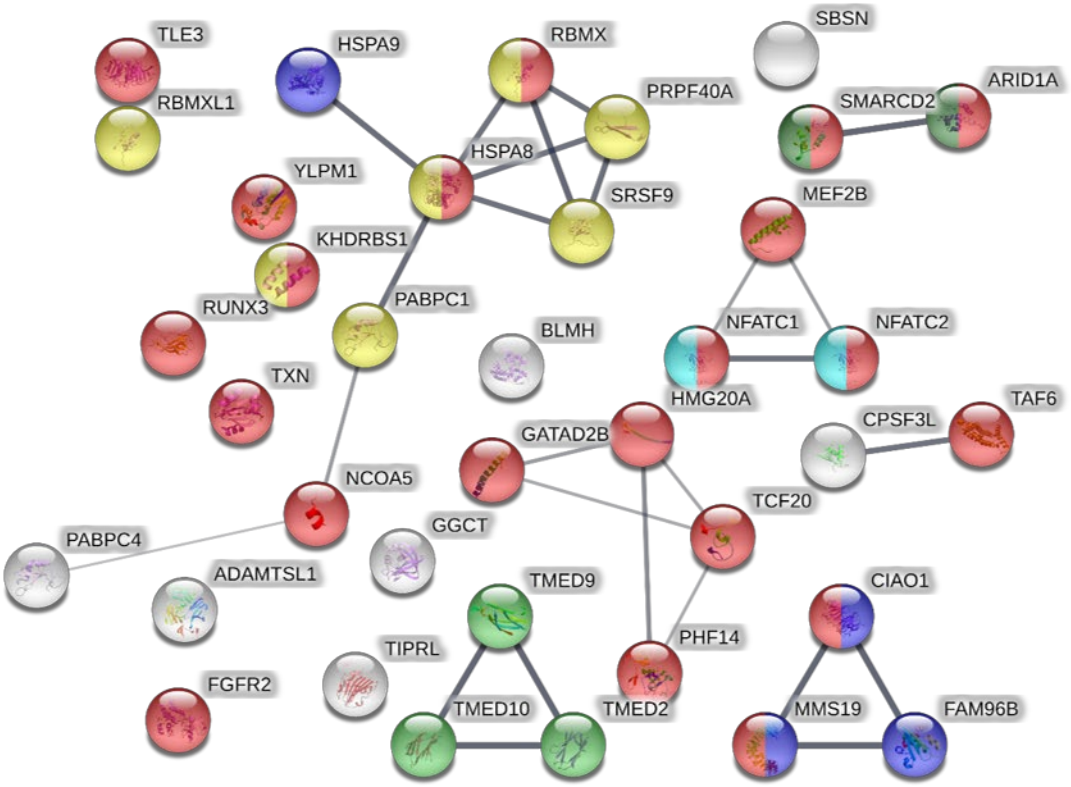

	FDR
Iron-sulphur cluster assembly	9.93e-06
COPI coating of Golgi vesicle	1.44e-05
Regulation of transcription	1.62e-05
mRNA processing	0.00053
Calcineurin-NFAT signalling cascade	0.004
Chromatin disassembly	0.0079

Figure 4.15. A network of protein-protein interactions by STRING for top identified proteins. 37 human proteins associated with Zta compared to both controls (≥2-fold) were analyzed by STRING. Nodes with different colours represented biological process GO categories.

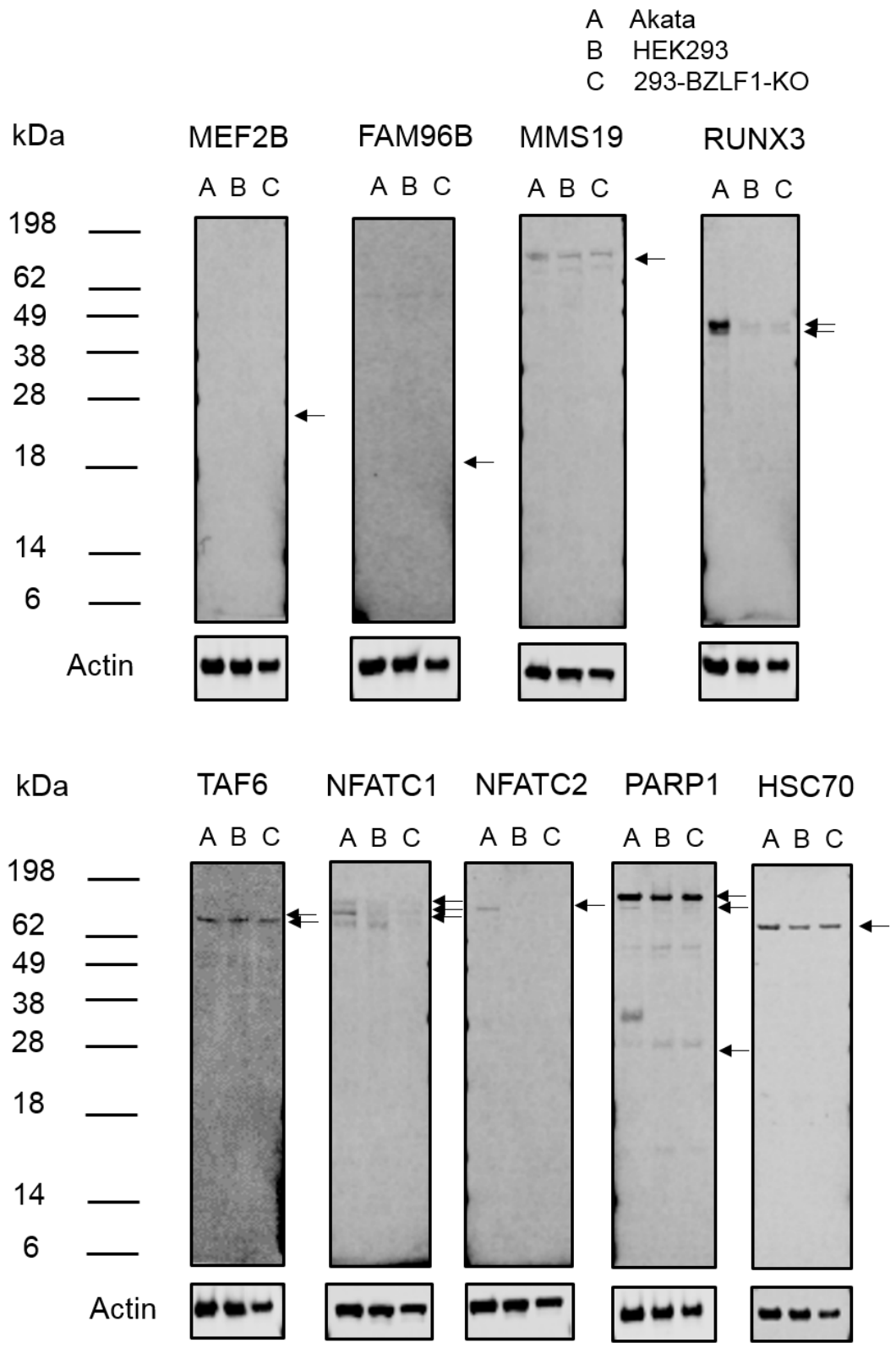

Figure 4.16 protein expression level in three cell lines. A few proteins were selected from mass spectrometry, western blotting was performed to detect each protein expression level in Akata cells, 293-BZLF1-KO and HEK293 cell lines. Actin was used as a loading control. The predicted size of each protein was labelled by arrows.

There was no band in MEF2B and FAM96B gels, and the predicted band for MEF2B was 25kDa, for FAM96B was 18kDa, so they were excluded for further IP. MMS19 gel showed one clearer band and a faint band in each cell line and both bands were between 62kDa and 198kDa, the predicted band size was 113kDa. RUNX3 gel showed two close strong bands in Akata cell, and only faint bands in other two cell lines around size 49kDa, the predicted band size of RUNX3 were 48/46kDa. TAF6 gel showed one band in each cell line between 62kDa and 198kDa, the prediction band size of TAF6 was 72/78kDa. NFATC1 gel showed 3 bands between 62kDa and 198kDa in Akata cells, only a faint band in other two cell lines. The predicted bands for NFATC1 isoforms were 90/110/140kDa. NFATC2 gel showed only one band in Akata cells, no band in other two cell lines, the predicted size for this protein was 135kDa. Actin was used as a loading control for each gel. PARP1 gel showed one strong band between 62kDa and 198kDa in each cell line, one lower band only showed in Akata cell line, another band between 28kDa and 38kDa in Akata cell line, and two faint bands between 49kDa and 62kDa, or around 28kDa in each cell line. The predicted band for PARP1 was 116kDa and cleaved PARP1 were 89 and 24kDa. HSC70 gel showed a single band in each sample at size 62 kDa. The predicted band size of HSC70 was 70kDa.

Then, Zta Immunoprecipitation was performed for a few times in Akata lytic cycle induced cells and western blotting was used to show the IP elution. 0.2mM DSP cross-linked cells nuclear extracts were used as a way to show the reproducibility for mass spectrometry. At the same time, a Co-IP with non-cross-linked cells was performed to show a more natural interaction *in vivo*. The eluted sample of each IP was separated into three for probing different targets, and Zta was only probed for once in each IP.

One IP elution was probed for MMS19 protein, MMS19 got 2.69 and 3.01 log2 TMT ratios from mass spectrometry (**Figure 4.17**). MMS19 band at the predicted size was only shown in input but not in IP of both experiments.

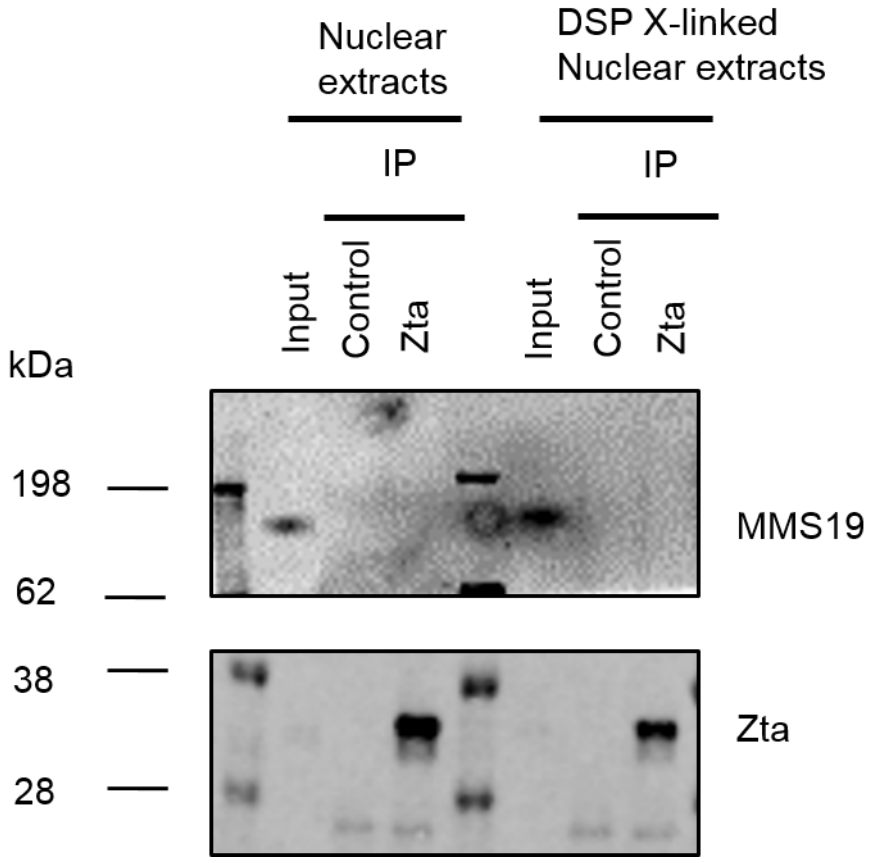

Figure 4.17. **IP in nuclear extracts or DSP cross-linked nuclear extracts for MMS19 in Akata cells.** Akata cells were induced to lytic cycle for 24 hours and cross-linked by DSP or not cross-linked, nuclear extracts were used for IP. Zta was pulled down by anti-Zta (SCZ) and magnetic beads, control Goat IgG was used for the control group. 1/3 of eluates were loaded into the gel and western blotted with antibody for MMS19 and Zta.

Another IP elution was probed for RUNX3 protein. RUNX3 got 1.56 and 1.35 log2 TMT ratios from mass spectrometry (**Figure 4.18**). RUNX3 was only detected in Input clearly at the predicted size, only a faint band was shown in Zta IP but not in control IP group in both experiments.

TAF6 got 1.34 and 1.24 log2 fold changes. An IP elution was probed for TAF6 (**Figure 4.19**), a single band at predicted size was detected in the input, a band at the same size was detected in both control and Zta IP, one extra upper band was detected in control and Zta IP but not in the input, which suggested it was a nonspecific band.

NFATC1 and C2 belong to the same family, NFATC2 got ratios 1.75 and 1.48, and NFATC1 got 1.39 and 1.23. NFATC1 IP showed it was only detected in the input, however, no obvious bands were seen in both IP samples, suggesting no interaction between NFATC1 and Zta were detected (**Figure 4.20**). NFATC2, on the other hand, was detected in input and only in Zta IP in both cross-linked and Co-IP (**Figure 4.21**), a repeated Co-IP was also shown at the bottom, this suggested NFATC2 interacts with Zta *in vivo*.

PARP1 got ratios 1.44 and 0.51 in Akata cells and showed 5.45 fold-changes in the first mass spectrometry analysis in 293-BZLF1-KO cells, that's the reason it was chosen for further IP validation (**Figure 4.22**). Two bands were shown in the input at the predicted range, the bottom band was considered as cleaved PARP1. A band was only detected in Zta IP but not in the control at the same size of the upper band in the input, which suggested PARP1 was immunoprecipitated by Zta.

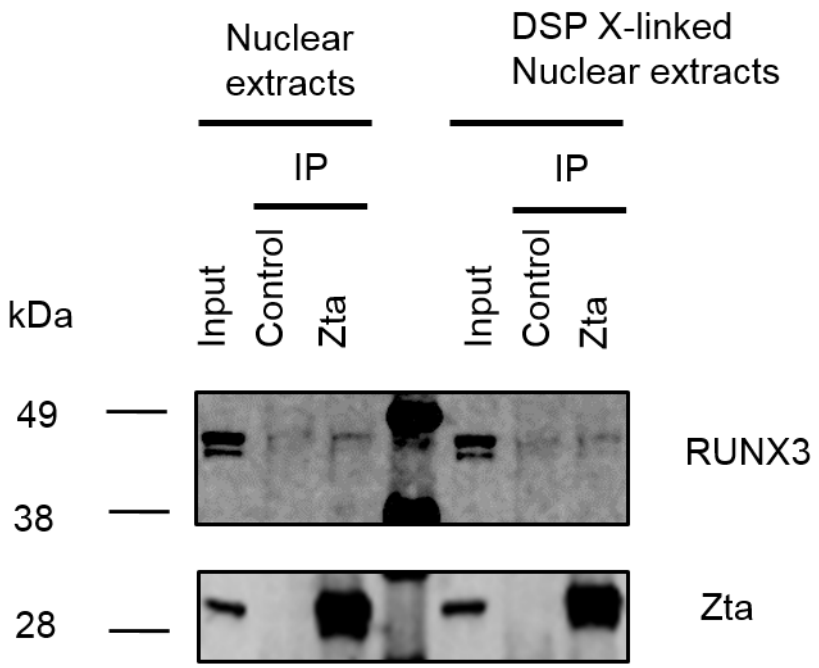

Figure 4.18. **IP in nuclear extracts or DSP cross-linked nuclear extracts for RUNX3 in Akata cells.** Akata cells were induced to lytic cycle for 24 hours and cross-linked by DSP, nuclear extracts were used for IP. Zta was pulled down by anti-Zta (SCZ) and magnetic beads, control Goat IgG was used for the control group. 1/3 of eluates were loaded into the gel and western blotted with antibody for RUNX3 and Zta.

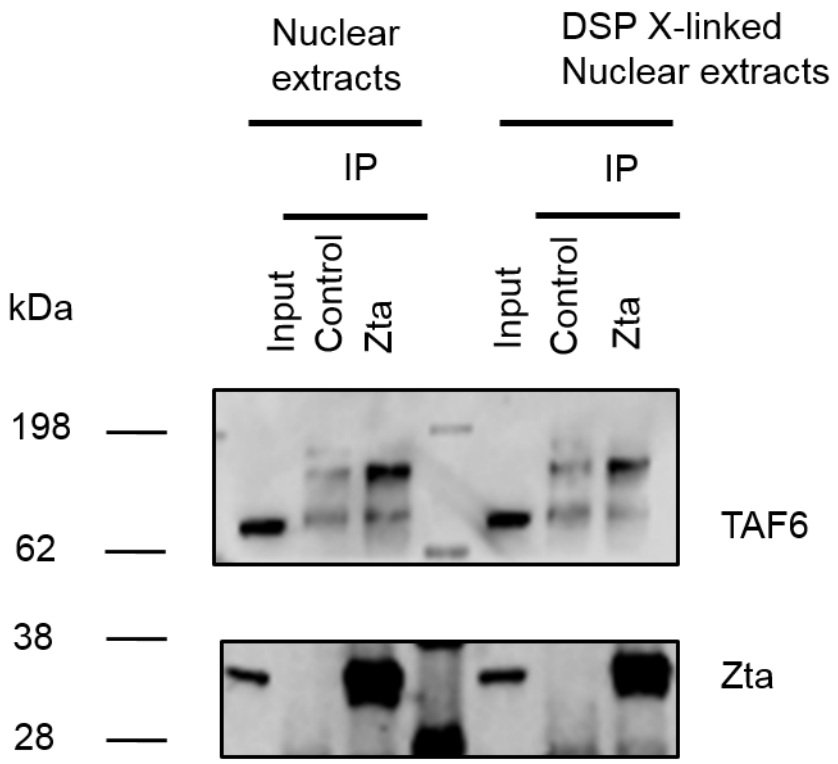

Figure 4.19. **IP in nuclear extracts or DSP cross-linked nuclear extracts for TAF6 in Akata cells.** Akata cells were induced to lytic cycle for 24 hours and cross-linked or not by DSP, nuclear extracts were used for IP. Zta was pulled down by anti-Zta (SCZ) and magnetic beads, control Goat IgG was used for the control group. 1/3 of eluates were loaded into the gel and western blotted with antibody for TAF6 and Zta.

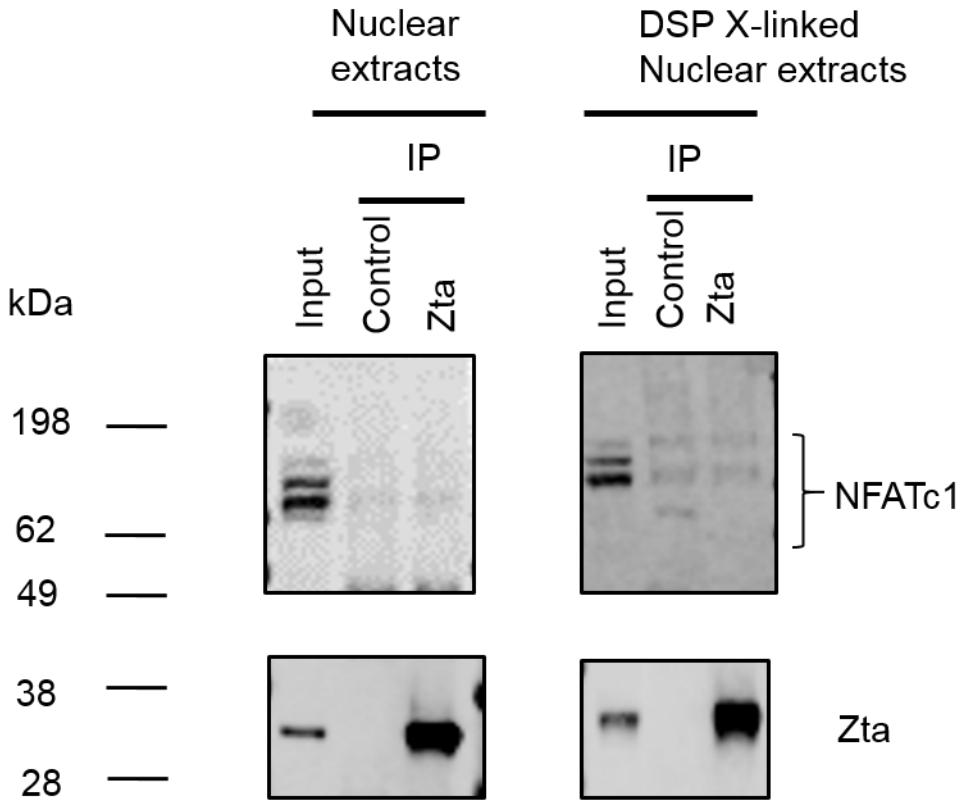

Figure 4.20. **IP in nuclear extracts or DSP cross-linked nuclear extracts for NFATc1 in Akata cells.** Akata cells were induced to lytic cycle for 24 hours and cross-linked or not by DSP, nuclear extracts were used for IP. Zta was pulled down by anti-Zta (SCZ) and magnetic beads, control Goat IgG was used for the control group. 1/3 of eluates were loaded into the gel and western blotted with antibody for NFATc1 and Zta.

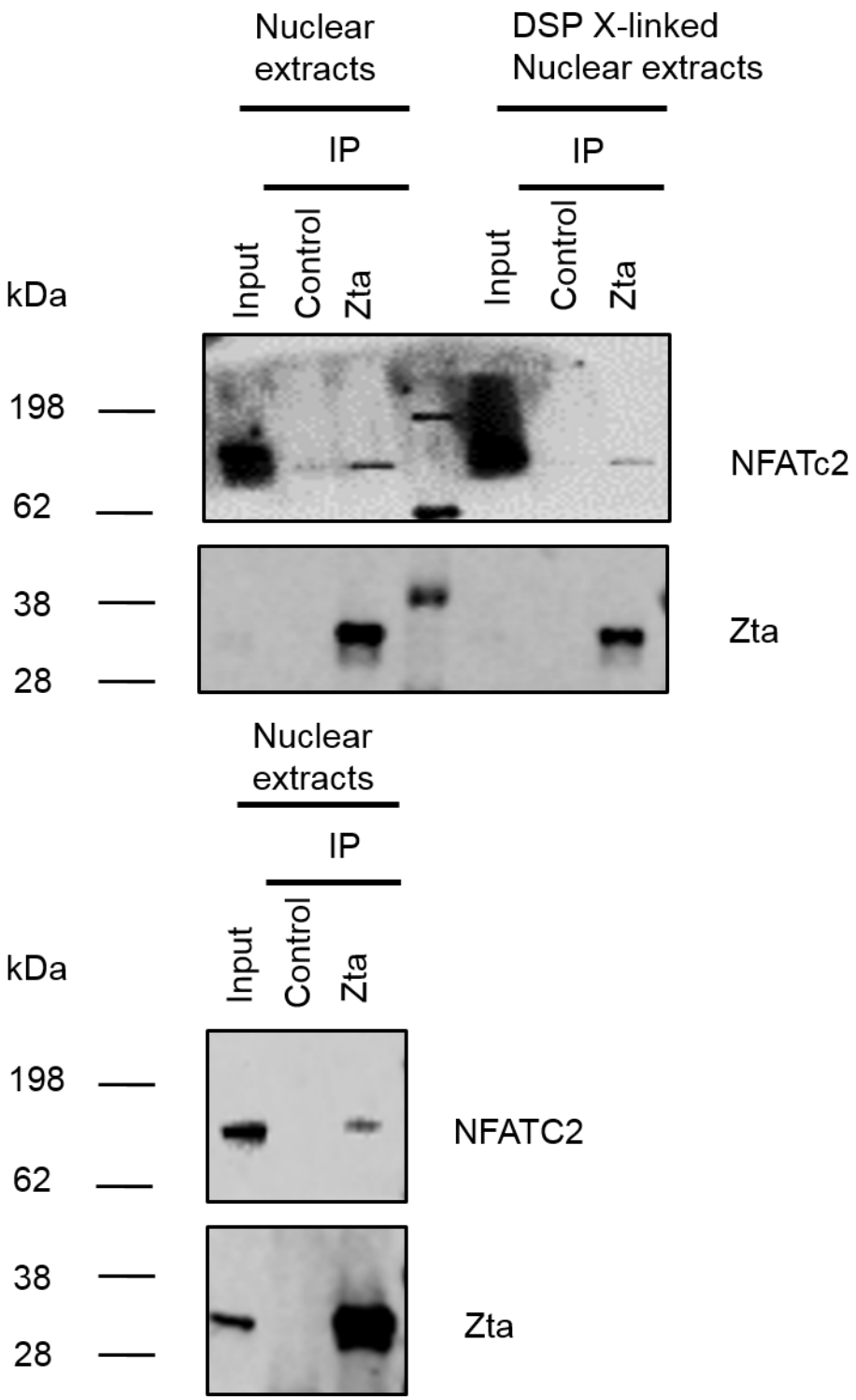

Figure 4.21 IP in nuclear extracts or DSP cross-linked nuclear extracts for NFATc2 in Akata cells. A. Akata cells were induced to lytic cycle for 24 hours and cross-linked or not by DSP, nuclear extracts were used for IP. Zta was pulled down by anti-Zta (SCZ) and magnetic beads, control Goat IgG was used for control group. 1/3 of eluates were loaded into the gel and western blotted with antibody for NFATc1 and Zta. A repeat IP for NFATc2 was also shown at the bottom.

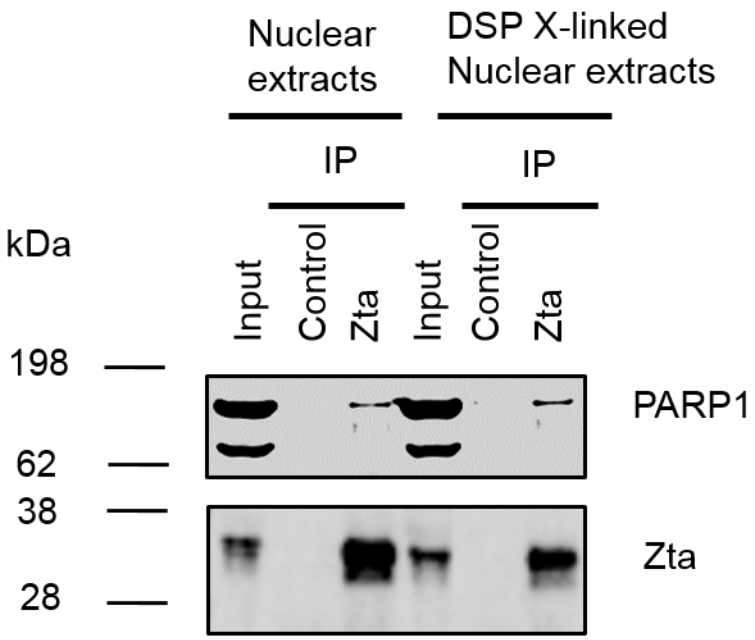

Figure 4.22. **IP in nuclear extracts or DSP cross-linked nuclear extracts for PARP1 in Akata cells.** Akata cells were induced to lytic cycle for 24 hours and cross-linked by DSP or not cross-linked, nuclear extracts were used for IP. Zta was pulled down by anti-Zta (SCZ) and magnetic beads, control Goat IgG was used for the control group. 1/3 of eluates were loaded into the gel and western blotted with antibody for PARP1 and Zta.

HSC70 was chosen because it was shown in both Akata and 293-BZLF1-KO mass spectrometry experiments. And it was reported as an important cellular chaperone in other herpesviruses. HSC70 got ratios 1.69 and 1.09 in Akata cells and 4.8-fold changes in 293-BZLF1-KO cells. In the co-IP results (**Figure 4.23),** it was shown a strong band at predicted size of HSC70 in the input, and also a band only in Zta IP but not in the control, which suggested it had been pulled down by Zta.

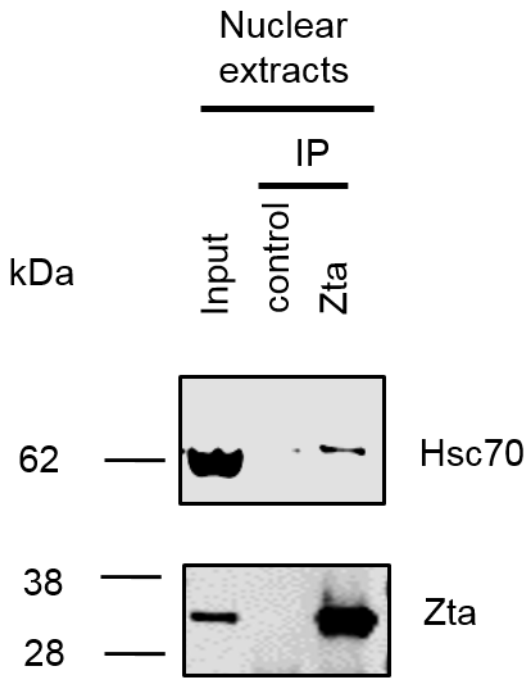

Figure 4.23. IP in nuclear extracts for HSC70 in Akata cells. Akata cells were induced to lytic cycle for 24 hours and cross-linked or not by DSP, nuclear extracts were used for IP. Zta was pull down by anti-Zta (SCZ) and magnetic beads, control Goat IgG was used for the control group. 1/3 of eluates were loaded into the gel and western blotted with antibody for HSC70 and Zta.

4.3 Discussion

With Akata EBV positive cells, it was possible to induce the lytic cycle by mimicking a physiological condition using anti-human IgG. The Zta expression level at different time points after induction reflects the different stages of lytic reactivation in the cells. It is reported that the primary induction response happens rapidly after cross-linking the B cell receptor on Akata cells, which reflected the early incidence at the Zp activation (Bryant and Farrell, 2002). However, Zta involved EBV genome replication happened at the late point. In order to study the Zta interactome during the lytic DNA replication, two late time points were selected and tested at the beginning.

Although from the flow cytometry data (**Figure 4.2 and 4.3**), the induction level was not high, more cell numbers were used to achieve a suitable Zta level and captured Zta interacting partners as much as possible.

An in-cell protein-protein cross-linker DSP was used, which is a cell-permeable cross-linker with a longer spacer arm than formaldehyde, and the disulfide bond in its spacer arm is cleavable by reducing reagents such as DTT. Then a suitable concentration of DSP was chosen and used for stabilizing the protein-protein interaction, a pull-down condition was also established in Akata cells.

Previously, our lab tried using SILAC labelling for a proteomic analysis by quantitative mass spectrometry in Akata cells, and it was successful. However, considering the large numbers of cells I would use and the restriction of labelling groups, SILAC was not a good method to choose. On the contrary, TMT labelling could combine all my biological repeats and run them together to reduce bias and also could obtain quantitative ratios of each protein, which was more accurate to look for protein interaction partners. However, the necessity of using HCD to collision the reporter iron and do an MS3 analysis suggested it was impossible to be done by the mass spectrometer instrument in the University of Sussex, that's why the labelling and this mass spectrometry running were performed in the University of Bristol mass spectrometry facility.

Two known Zta interacting viral proteins were found in my study, EBV polymerase (BALF5) was known to be recruited to the oriLyt by Zta during EBV lytic cycle and BALF5 can be co-immunoprecipitated with Zta (Baumann et al., 1999). BGLF4, which is EBV protein kinase, was also reported to phosphorylate, interact and work with Zta to further regulate EBV lytic replication (Asai et al., 2006).

Apart from these two, there were five viral proteins also detected as Zta interacting proteins from mass spectrometry with high ratios. BALF2 had been studied not to bind to Zta, but it was a member of the core replication complex recruited to the oriLyt by Zta during lytic replication, which suggested an indirect binding and explained why it showed up with Zta. One portal protein BBRF1 and two capsid relevant proteins, BVRF2 and BcLF1 were shown in the list, suggesting Zta may play a role in the capsid assembly or transport. mRNA export factor BMLF1 helps mRNA transportation during the lytic cycle. It was also seen in the list, suggested that Zta may play a role in mRNA regulation. The function of these proteins was not well characterised yet and they need further studies to figure out their relationship with Zta.

During lytic cycle, Zta works as a transcription factor to regulate viral and human gene expression, it is also the key factor to initiate the lytic DNA replication, so a lot of cellular proteins from different signalling pathways are involved in all these procedures. From GO protein clusters of all 252 cellular proteins (**Figure 4.13A, 4.14**), mRNA splicing proteins were obtained, such as PCBP1, HNRNPH1, and SRSF10. It is not known any roles of Zta in mRNA splicing yet, Zta could interact with EBV mRNA Export Factor BMLF1 and enhance its function, and also Zta could be involved directly in mRNA splicing by interacting with those proteins. There were also transcription factors like RUNX3, TAF6, and TCF20 identified, which could regulate the transcription activity of Zta. Chromosome segregation proteins were also found, which suggested Zta might play a role in the cell cycle.

From the protein-protein interaction network, I observed some proteins with similar functions to be grouped together, some could form complexes, suggesting a possibility that Zta could interact with one or more proteins in the complexes to

perform certain functions during lytic replication. To zoom in the 37 most significant proteins, transcription factors got the highest clustering score (**Figure 4.13B**). To see the details of each protein, I saw MMS19, CIAO1 and FAM96B, which could form the iron-sulphur cluster assembly complex. TMED2, TMED9 and TMED10, which could form vesicular protein trafficking complex. NFATC1 and C2, which were involved in Calcium-NFAT signalling cascade.

Validation of my experiment was firstly focused on the proteins involved in transcription and protein folding categories. Nine proteins were chosen and antibodies were obtained for testing, only the proteins, whose antibodies worked for western blotting, were chosen for further IP validations. Protein levels were detected in three cell lines, I didn't see any band in MEF2B and FAM96B tests (**Figure 4.16**), suggesting either the protein level was low in all three cell lines or both antibodies were not in high quality. So they were excluded for further studies.

MMS19 is a key component of the Iron-sulphur protein assembly complex, which plays a role in double-strand break DNA repair, also in chromosome segregation. It is reported that iron-sulphur complex is critical for improving the antiviral function of protein Viperin (RSAD2), which is an interferon-stimulated gene, interferes with numerous RNA and DNA viruses (Upadhyay et al., 2017). Zta interacts with this complex could be relevant to escaping or inhibiting the cellular antiviral process of EBV. However, MMS19 was not detected in the Zta IP group (**Figure 4.17**), therefore, its interaction with Zta could not be proven.

RUNX transcription factors are important in the development of many cancers. RUNX3 belongs to this family. RUNX3 is up-regulated by EBV latent protein EBNA2 and 3C in EBV positive B cells during latency (Spender et al., 2002; Jiang et al., 2014; Wang et al., 2015). From my IP results (**Figure 4.18**), two RUNX3 bands were shown clearly in both Inputs, a very faint band was detected in both Zta IP samples, which suggested RUNX3 may interact with Zta *in vivo.* But it was a position where the antibody chains could show. In future, more IPs between RUNX3 and Zta needs to be performed in the same cell line or in other cell lines in order to get a clear answer.

TAF6 is transcription initiation factor TFIID subunit 6, belongs to TFIID complex, Zta interacts with TFIID protein (TBP) through its transcription activation domain at the target gene promoter, and then recruit other proteins to initiate the transcription (Lieberman and Berk, 1991; Lieberman et al., 1997). TAF6 was seen in my top list and chosen for validation, the two IP western blotting results showed one band at size 70-80 kDa in Input, which was the right size for TAF6, however in IP lanes, bands were seen at the same size both in Zta and control IP, there was one upper band was detected in both control and Zta IP, it was stronger in Zta IP than in control IP, however I couldn't consider this band as TAF6 because no band was detected in the input at this size.

NFATC1 and C2 are two transcription factors from the same family, they are regulated and activated by calcium signalling pathway. NFATC1 showed no obvious interaction with Zta by IPs (**Figure 4.20**), but NFATC2 showed a clear interaction with Zta (**Figure 4.21**). Although first found in T cells, NFATs were identified playing roles in B cells and also involved in the regulation of EBV lytic cycle (Teixeira et al., 2016; Liu et al., 1997). Further investigation of Zta with calcium signalling and NFATs will be described in **Chapter 6**.

PARP1 is a DNA damage response protein and plays roles in host-viral interaction. PARP1 was the protein found from mass spectrometry analysis in 293-BZLF1-KO cells in **Chapter 3**, so although in Akata cells, one of the ratios didn't achieve two-fold, I chose it for IP-western blotting validation (**Figure 4.22**), un-cleaved PARP1 was pull down by Zta in both DSP cross-linked IP and Co-IP. Zta interacts with PARP1 could be a way to reverse the restriction of BZLF1 promoter by PARP1 (Lupey-Green et al., 2017). Zta is known to interact with another DNA damage response protein 53BP1, which suggests that Zta plays a role in DNA damage (Bailey et al., 2009). Interacting with PARP1 could be a way that Zta restricts PARP1 to recruits other DNA repair proteins to the damage sites. However, more evidence for physical binding between Zta and PARP1 is still needed, and also functional studies need to be designed to characterise the roles of this interaction during EBV lytic and DNA repair.

HSC70 is a cellular chaperone to help client protein's folding, assembly and trafficking, it has been reported that HSC70 is an important chaperone for viral replication in different herpesviruses (Baquero-Perez and Whitehouse, 2015; Salinas et al., 2016). Both mass spectrometry analysis has detected HSC70 as a Zta interacting protein, it got 4.84 fold-change in 293-BZLF1-KO cells and high TMT ratios in Akata cells. The Co-IP-western blotting validation showed that HSC70 interacted with Zta (**Figure 2.23**). Further investigation of Zta with HSC70 will be described in **Chapter 5**.

Above all, in this chapter, I successfully established a pull-down condition in Akata cells and used an unbiased TMT labelling mass spectrometry analysis. EBV and cellular proteins that interact with Zta were obtained and analysed by functional clustering. A few targets were chosen for validation. Proteins HSC70 and NFATC2 were chosen for further functional analysis in the next two chapters.

5 Heat shock cognate 71 kDa protein (Hsc70) contributes to EBV lytic reactivation

5.1 Introduction

Heat shock protein 70 families as the cellular chaperones are important for protein folding, assembly, trafficking and degradation, which play a role in the maintenance of protein homeostasis and help client proteins' survival of stress situations such as hypoxia, oxidative stress and pH changes. Increasing evidence suggests that the imbalance of protein homeostasis caused by this protein family leads to many diseases, including neurodegenerative disorders and cancers. This protein family is regarded to be the most conserved protein in evolution (Murphy, 2013; Fernandez-Fernandez et al., 2017; Hipp et al., 2014).

The human genome encodes 13 isoforms of Hsp70, Hsc70 (HSPA8) and Hsp70 (HSPA1A) are two of them. Hsc70 is constitutively expressed in cells while the Hsp70 is inducible by stress (Fernandez-Fernandez et al., 2017; Kampinga et al., 2009). The structure of Hsp70 proteins comprises an N-terminal nucleotide-binding domain (NBD) that displays ATPase function, a substrate-binding domain (SBD) to bind to client proteins and a C-terminal domain that helps co-chaperone binding (Flaherty et al., 1990; Zhu et al., 1996).

It is reported that Hsp70 and Hsc70 co-localised with Kaposi's sarcoma-associated herpesvirus (KSHV) replication and transcription compartments in the nucleus of cells during the lytic cycle. The inhibition of Hsp70 isoforms abolished viral gene transcription, viral protein synthesis and DNA replication (Baquero-Perez and Whitehouse, 2015). Some studies indicated that Hsp70 families were involved in murine gammaherpesvirus 68 (MHV68) and herpes simplex virus type 1 (HSV-1) replication. MHV68 latency-associated nuclear antigen (LANA) interacted with Hsc70 and recruited Hsc70 to the nucleus of infected cells. Hsp70 family inhibitor and Hsc70 shRNA knockdown blocked the MHV68 lytic replication and viral protein synthesis. Hsc70 and Hsp70 were recruited to HSV-1 replication compartments and helped the formation of the HSV-1 portal complex during HSV-

1 infection (Burch and Weller, 2004; Salinas et al., 2016). In EBV, it is reported that Hsp70 protein interacted with EBNA1 and an Hsp70 inhibitor 2-phenylethynesulfonamide reduced the EBV lytic replication and inhibited the proliferation and migration of EBV positive cancer cells (Wang et al., 2018). This suggests that as cellular chaperones, Hsp70 families play important roles during herpesvirus infection and lytic replication.

In chapter 3 and 4, two proteins (Hsp70 and Hsc70) from Hsp70 family were detected by mass spectrometry with high ratios as the proteins that interacted with Zta both in HEK293-BZLF-KO cells and Akata cells, and Hsc70 was validated to interact with Zta in Akata cells. In this chapter, further investigation of the interaction between Zta and Hsp70 proteins was performed, and an inhibitor called VER-155008 (Williamson et al., 2009; Schlecht et al., 2013), which is specific for binding to Hsp70 family ATPase domain, was used to study whether the Hsp70 family's function was involved in EBV lytic reactivation.

5.2 Results

5.2.1 Hsc70 interacts with Zta is not EBV dependent

Since Hsc70 was identified by two mass spectrometry analyses in two cell lines, and Hsc70 was validated to interact with Zta in Akata cells, first, I asked whether the interaction of Hsc70 with Zta could be validated in 293-BZLF1-KO cells during EBV lytic cycle.

hisZta was expressed in the cells for 96 hours to trigger the EBV lytic cycle. Then a Zta immunoprecipitation was performed and formaldehyde cross-linked nuclear extracts were used for this IP (**Figure 5.1**). The result shows Hsc70 bands were detected in input and Zta IP but not in the control, suggesting Hsc70 was pulled down by Zta.

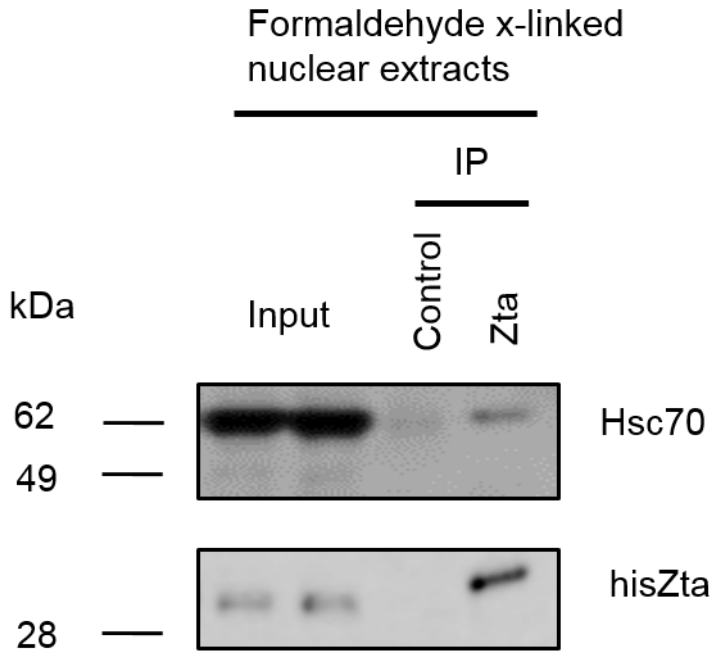

Figure 5.1 Zta **pull-down in nuclear extracts of formaldehyde cross-linked 293-BZLF1-KO cells for Hsc70.** 293-BZLF1-KO cells were transfected with hisZta and control vector, 96 hours post-transfection, formaldehyde x-linked nuclear extracts were used for IP, anti-Zta (SCZ) was used for Zta pull-down, goat anti-IgG was used as a control, western blotting was performed for Hsc70 and Zta.

Next, I asked whether this interaction was dependent on other EBV proteins. To answer this, another IP was performed in the nuclear extracts of formaldehyde cross-linked HEK293 cell line that does not contain the EBV genome. hisZta was expressed, 48 hours post-transfection, an IP was performed (**Figure 5.2**). The result shows Hsc70 was detected in the input and Zta IP, but not in the control, which meant Hsc70 was pulled down by Zta. This suggests that other EBV proteins are not required for this interaction, and it is not dependent on replication of the EBV genome.

5.2.2 Determine the viable range of VER-155008

Next, I asked whether the function of Hsc70 influenced the EBV lytic cycle since Zta was a key regulator for the EBV lytic switch. To answer this question, a small molecule inhibitor of the Hsp70 family, VER-155008 was used. Toxicity of this drug was tested by a cell viability assay and the drug range within 50% cell viability was chosen for further experiments. 293-BZLF1-KO cells were treated with different concentrations of VER-155008 for 48 hours (**Figure 5.3**) and Akata cells were treated for 24 hours (**Figure 5.4**), which were the time points used for further experiments. Untreated cells and 0.1% DMSO treated cells were used as controls.

The results indicated a decreasing metabolic activity with increasing concentrations of VER-155008. The inhibition showed a dose-dependent manner in both cell lines. 0-20 uM range was chosen for 293-BZLF1-KO cell line and 0-10 uM range was chosen for Akata cell line and both ranges were used for the further experiment.

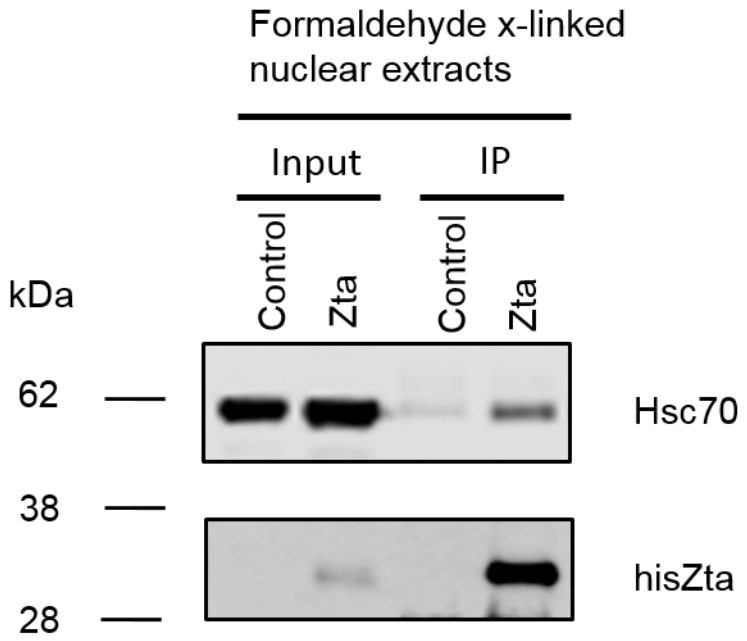

Figure 5.2 Zta pull-down in nuclear extracts of formaldehyde cross-linked HEK293 cells for Hsc70. HEK293 cells were transfected with hisZta and control vector, 48 hours post-transfection, formaldehyde x-linked nuclear extracts were used for IP, anti-Zta (SCZ) was used for Zta pull-down, goat anti-IgG was used as a control, western blotting was performed for Hsc70 and Zta.

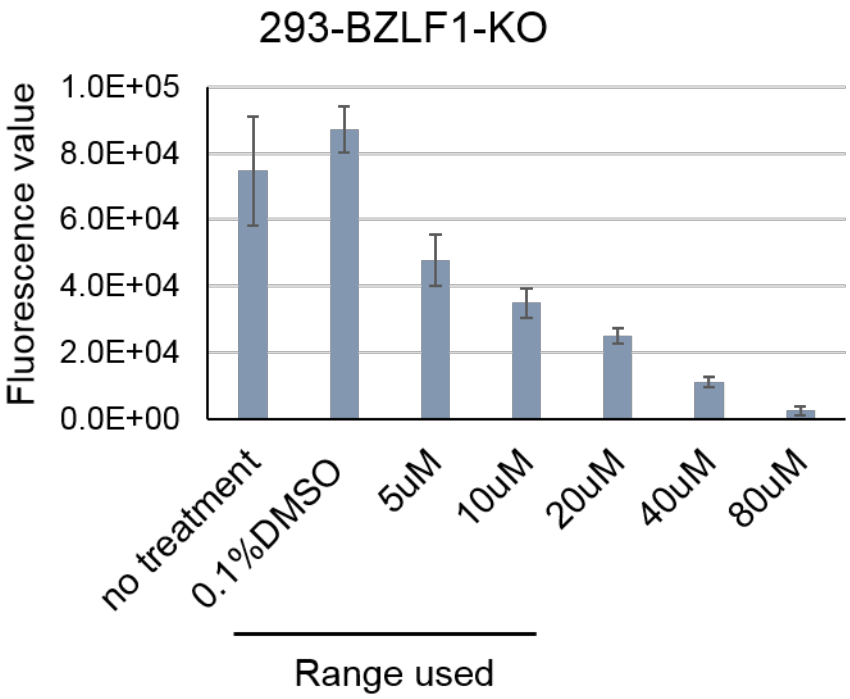

Figure 5.3 The viability of VER-155008 in 293-BZLF1-KO cells. Cells were treated with increasing concentrations of VER-155008 for 48 hours, untreated cells and solvent treated cells were used as controls, cell viability was detected by alamarBlue assay.

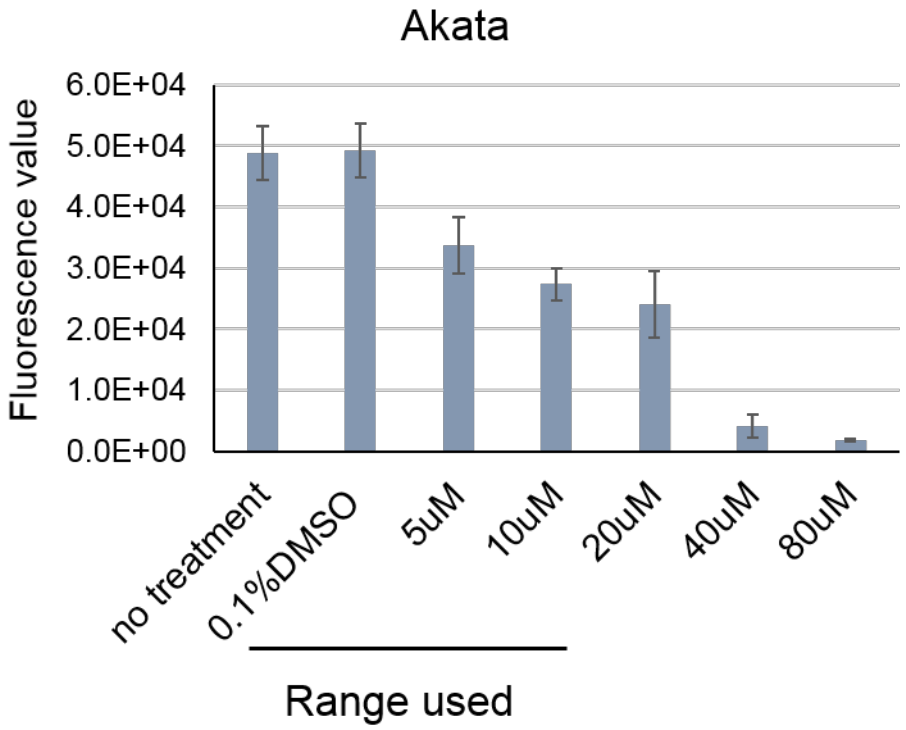

Figure 5.4 The viability of VER-155008 in Akata cells. Akata cells were treated with increasing concentrations of VER-155008 for 24 hours, untreated cells and solvent treated cells were used as controls, cell viability was detected by alamarBlue assay.

5.2.3 VER-155008 inhibits EBV lytic reactivation in 293-BZLF1-KO cells.

Would this inhibitor affect the EBV lytic activation in epithelial cells? To answer this question, the impact of this inhibitor on EBV replication was evaluated in 293-BZLF1-KO cells. hisZta was expressed for 48 hours in this cell line in order to induce lytic cycle, and cells were treated with 0 μM, 10 μM or 20 μM of VER-155008, un-induced and 0.1% DMSO treated cells were used as controls. 48 hours post-transfection, cells were harvested and EBV genome load was detected. EBV viral genome levels were normalised to human genome levels and shown as fold change compared to the control group (**Figure 5.5**). All the cells that express hisZta were triggered into the lytic cycle, however, when treated with 10 μM and 20 μM of VER-155008, EBV viral load was inhibited 2-3 times compared to the 0.1% DMSO treated group. This result suggested that blocking the Hsp70 family's function could partially inhibit EBV viral replication s.during the lytic cycle in 293-BZLF1-KO cells.

5.2.4 VER-155008 inhibits EBV lytic activation in Akata cells

Next, I asked whether this inhibition phenomenon could also be seen in EBV positive Burkett's lymphoma cells. So another drug treatment experiment was performed in Akata cells. Cells were treated with different concentrations (0-10uM) of VER-155008 and then the cells were induced into the lytic cycle by anti-IgG at the same time with the drug, un-induced and 0.1% DMSO treated cell groups were used as controls. Cells were harvested after 24 hours and EBV viral load was detected (**Figure 5.6**). The result showed that compared to untreated Akata lytic cells (0.1% DMSO), EBV genome load was partially inhibited by VER-155008, around 3-4 times, which suggested viral DNA synthesis had been partially blocked by this small molecule inhibitor in Akata cells. Given the interaction between Zta and Hsc70, it is suggested that Hsc70 may be required for the function of Zta.

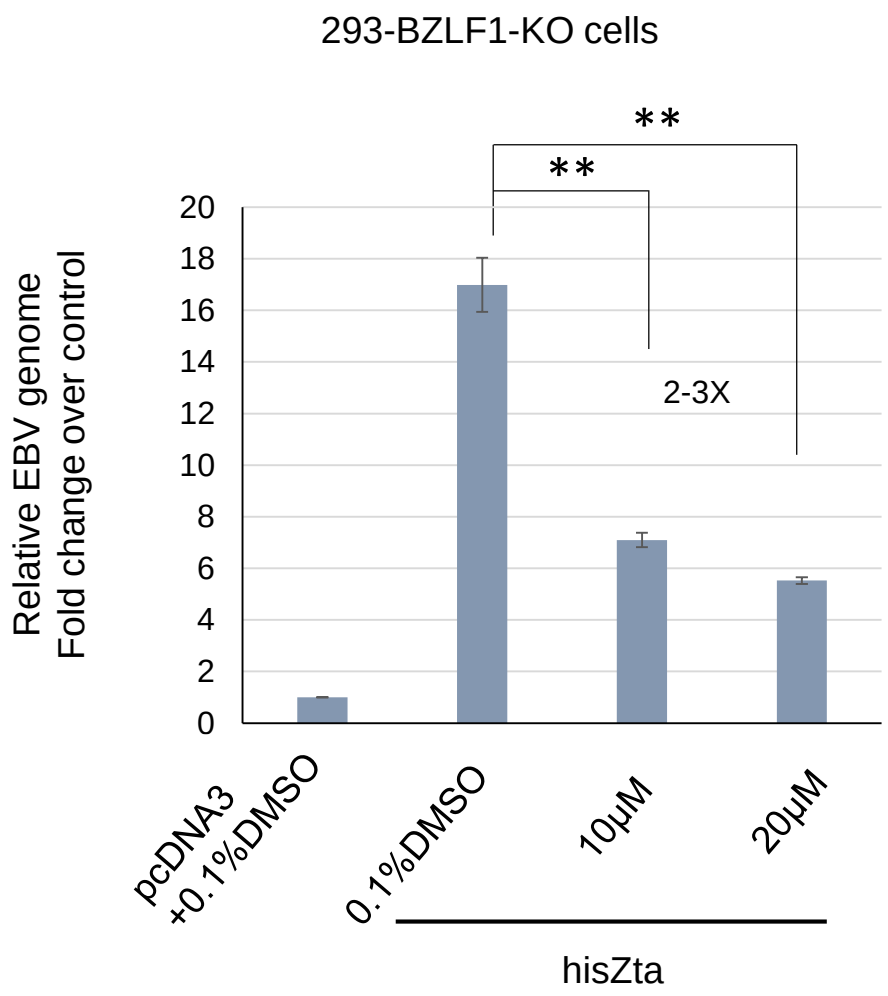

Figure 5.5 VER-155008 reduces EBV viral replication in 293-BZLF1-KO cells. 293-BZLF1-KO cells were transfected with hisZta to trigger the lytic cycle for 48 hours, empty vector (pcDNA3) was used as a control. Cells were treated with VER-155008 at the same time, the solvent was used as a control. Genomic DNA was extracted from each group and EBV genome level was analysed by qPCR, normalsed by human genome and shown as fold change compared to control group. Error bars represent the mean of triplicate reads ± SD. A t-test was used to show the statistical difference. (**) indicates $p<0.01$.

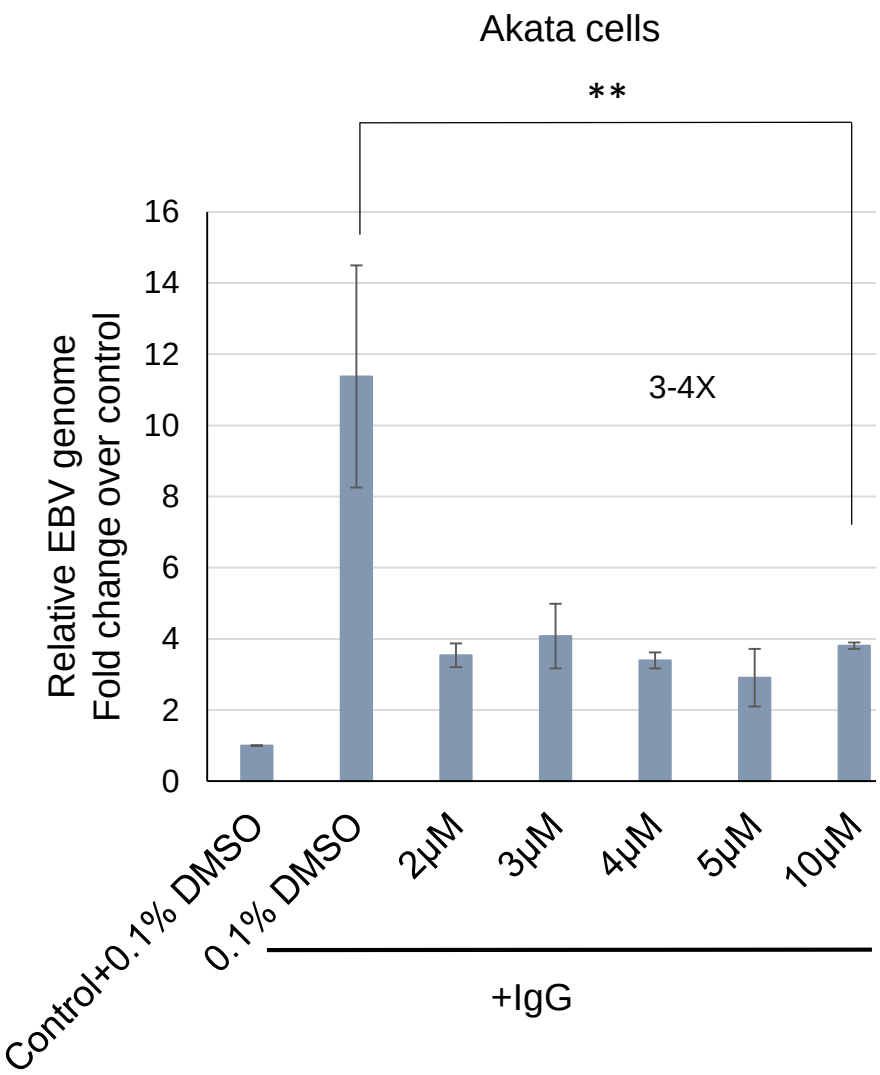

Figure 5.6 VER-155008 reduces EBV viral replication in Akata cells. Akata cells were induced to lytic cycle for 24 hours, and cells were treated with VER-155008 at the same time, the solvent was used as a control. Genomic DNA was extracted from each group and EBV genome level was analysed by qPCR, normalised by human genome and shown as fold change compared to control group. Error bars represent the mean of triplicate reads ± SD. A t-test was used to show the statistical difference. (**) indicates $p<0.01$.

5.2.5 Zta protein abundance was inhibited by VER-155008

Then I asked whether the inhibition the function of Hsp70 family would influence the abundance of Zta protein. Hsc70 and Zta protein levels in VER155008 treated 293-BZLF1-KO and Akata cell lines (**Figure 5.7** and **5.8**). Results were quantified by ImageStudio (LI-COR) and the abundance of Zta protein level was normalised to Actin. Hsc70 protein level was not changed after inhibitor addition in either cell lines (**Figure 5.7A and 5.8A**). However, a slight reduction of Zta abundance was seen in both experiments. In 293-BZLF1-KO cell line, around 1-2 times reduction (**Figure 5.7B**) was detected at 5-10uM treated groups compared to the control group and around 1-2 times reduction (**Figure 5.8B**) was seen in Akata cells, which suggests this inhibitor could slightly reduce the abundance of Zta protein during the EBV lytic reactivation.

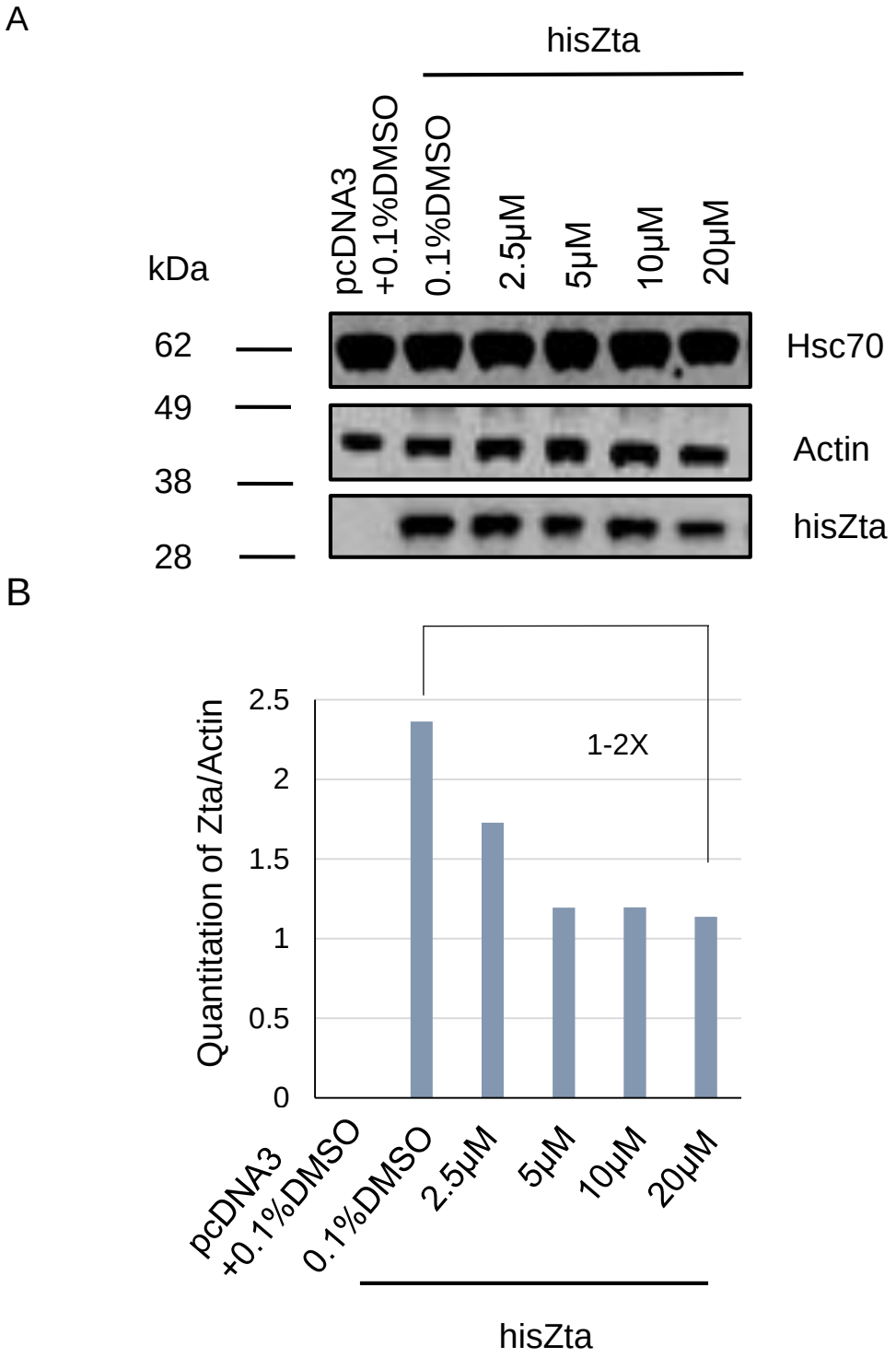

Figure 5.7 Protein level changes after treatment of VER-155008 in 293-BZLF1-KO cells. **A.** Western blotting analysis of cellular and Zta protein level in 293-BZLF1-KO cells after treated with VER-155008 in different concentrations for 48h. **B.** Quantification of Zta expression level normalised to Actin.

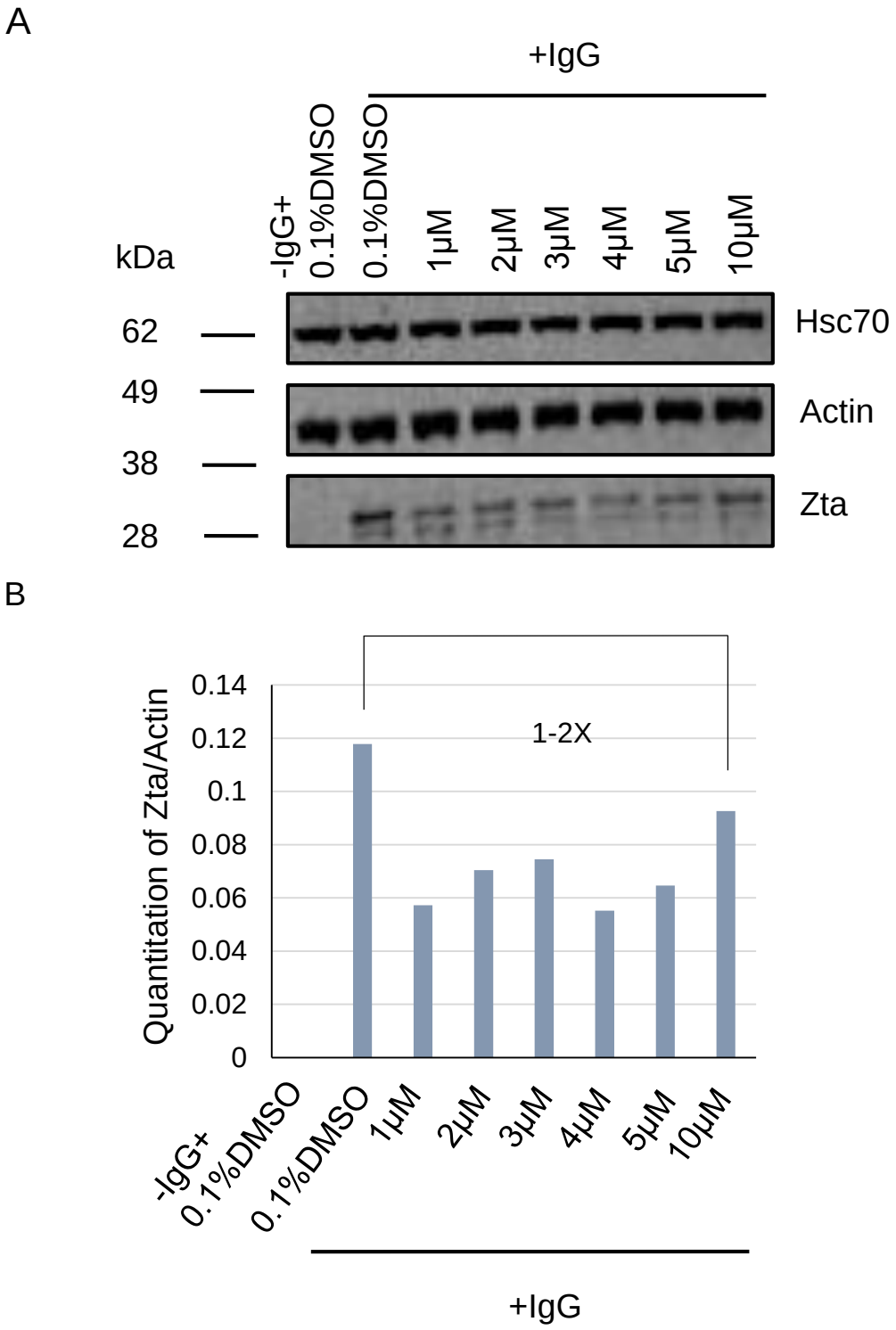

Figure 5.8 Protein level changes after treatment of VER-155008 in Akata cells. **A**. Western blotting analysis of cellular and Zta protein level in Akata cells after treated with VER-155008 in different concentrations for 24h. **B**. Quantification of Zta expression level normalised to Actin.

5.3 Discussion

Hsp70 families are involved in cancer initiation and tumorigenesis, and also regulate many cancer relevant signalling pathways, such as apoptosis and autophagy (Murphy, 2013). Overexpression of Hsp70 in T cells increases the chance of T cell lymphoma in transgenic mice, and this is thought to act through the inhibition of the apoptosis signalling pathway (Seo et al., 1996). The high expression level of Hsp70 is also a sign for hepatocellular and prostate cancer and it is also a marker for advanced disease and metastasis for colorectal carcinoma and breast cancer (Chuma et al., 2003; Abe et al., 2004; Hwang et al., 2003).

Previous studies in other herpes viruses have reported that Hsp70 and Hsc70 were important for viral replication and function, and Hsp70 family inhibitor VER-155008 could significantly decrease the synthesis of the new viral genome during viral replication in KSHV and MHV68 (Baquero-Perez and Whitehouse, 2015; Salinas et al., 2016). Recently, the Sun group published that when EBV genome replication is induced with TPA and sodium butyrate in EBV positive HONE/Akata cells, a different inhibitor called 2-phenylethynesulfonamide (PES), which was able to act on the SBD of Hsp70 family and block the interaction with co-chaperones and substrates, could reduce activation of EBV genomic DNA replication (Wang et al., 2018). This provides independent verification of our discovery. In addition, they reported that the PES induced cell cycle arrest and apoptosis in EBV positive cells (Wang et al., 2018). However, high doses of PES were required and these ablated Zta protein induction and the abundance of other cell and viral proteins, so maybe were unrelated to lytic cycle.

From our mass spectrometry results of the Zta interactome, implied that Hsp70 families have involved in EBV lytic reactivation. Hsc70 was tested that interacted with Zta in B cells in **Chapter 4** and I also tested the interaction in Hek293 cells in that chapter (**Figure 5.1**), suggesting this widely conserved cellular chaperone could be the main chaperone protein that helps Zta folding, assembly or trafficking. Pull-down results in HEK293 EBV negative cells showed that Hsc70

interacting with Zta does not need the assistance of other EBV proteins, this again suggested a basic chaperone function of Hsc70 during EBV lytic cycle.

The folding function of Hsp70 families with client proteins were illustrated (**Figure 5.9**)**.** Hsp70 proteins bind to unfolded client protein via SBD and help the client protein folding in an ATP-dependent manner. Next, the binding pocket closes and releases the folded protein, and then protein exchange ADP to ATP for the next substrate (Mayer, 2013). The inhibitor VER-155008 binds to the Hsp70 ATP binding domain. It is able to compete with ATP binding to the Hsp70 protein and inhibits its function (Massey et al., 2010; Schlecht et al., 2013). It is reported that this inhibitor could inhibit viral replication in different viruses, and also it is proved that this is a potential drug for different cancers, such as breast cancer, bladder cancer (Massey et al., 2010; Cavanaugh et al., 2015).

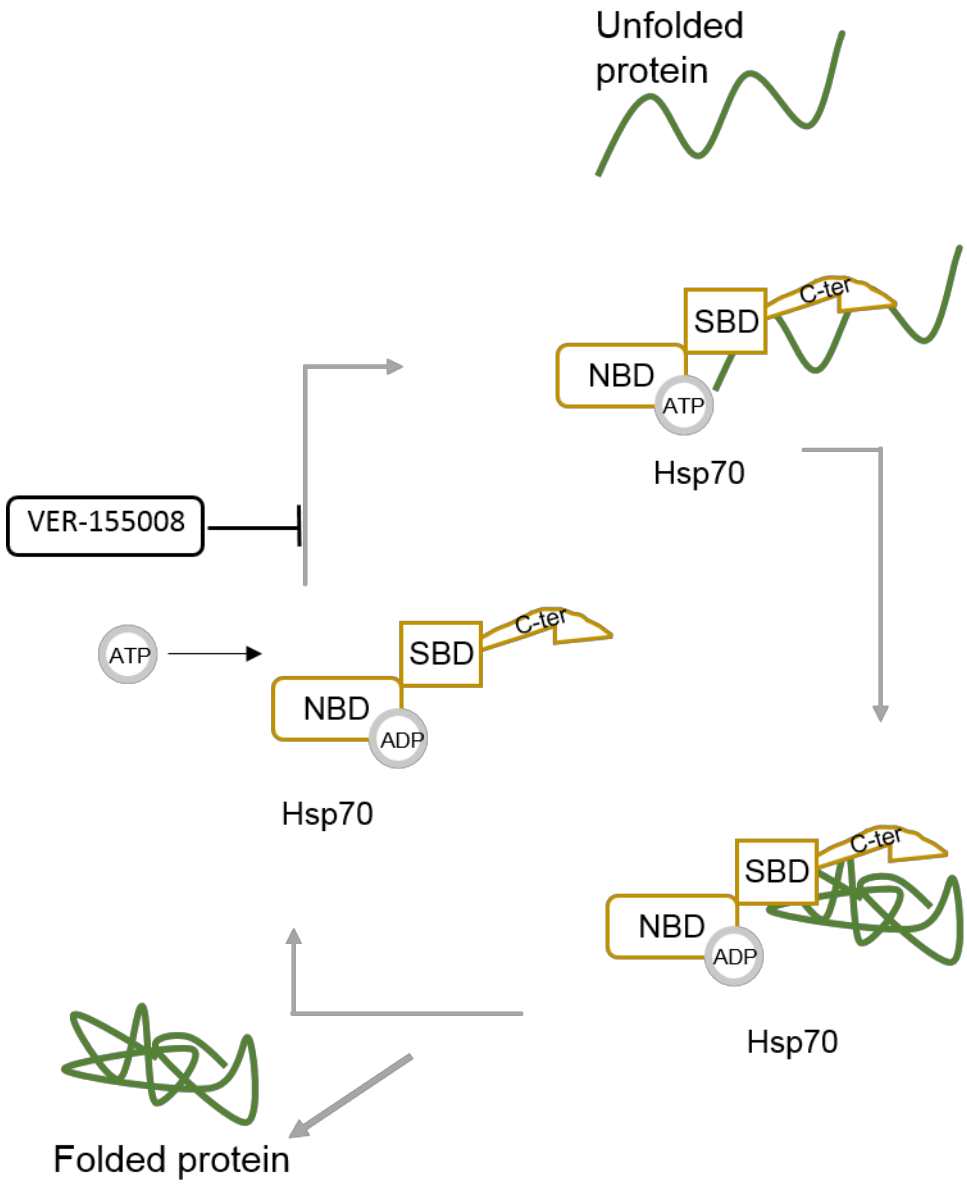

Figure 5.9 Function diagram of Hsp70 protein families. Hsp70 proteins comprise three domains, nucleotide-binding domain (NBD), substrate binding domain (SBD) and a C-terminal domain. Hsp70 families bind to unfolded protein (Green) and help them to fold using their ATPase pocket, then folded protein is released and the Hsp70 ATPase becomes the non-functional state, then they regain ATP and recover their function. VER-155008 is a small molecule inhibitor that binds to the Hsp70 ATP binding area and competes with ATP binding to the protein.

In this chapter, the contribution of the Hsp70 family to EBV lytic replication was investigated. Interrupting the ATP binding dependent function of Hsp70 family by VER-155008 reduced EBV lytic replication in two EBV positive cell lines.

The inhibition of EBV genome replication could be partly caused by the reduced abundance of Zta protein in two cell lines suggesting mixture factors were involved in this inhibition.

Since the interaction between Zta and Hsp70 family member Hsc70 was identified, Zta may be a client protein of Hsc70. One of the reasons that the lytic genome reduced in presence of VER155008 could be linked to the folding and assembly of Zta. Additionally, Hsc70 could affect the trafficking of Zta from the cytoplasm to the nucleus (Parra et al., 2016). Both of these situations would cause the inhibition of Zta inducted EBV lytic reactivation.

Although the interaction between Zta and Hsc70 is not EBV genome or lytic replication dependent, and no other EBV proteins were involved in the Zta-Hsc70 interaction, however, there is a possibility that Hsp70 family members are relevant to other viral protein synthesis and this might enhance the treatment efficiency of EBV replication. In addition, inhibition of the Hsp70 family might influence the assembly of cellular proteins especially the co-chaperones that are involved in EBV lytic replication or the Hsc70-Zta interaction. However, further investigation is needed to figure out the details.

To summarise, the heat shock protein 70 family member Hsc70 interacts with Zta, and blocking Hsp70 family's function reduces EBV lytic replication. This is partly due to a reduction in Zta abundance and the rest may be due to the inhibition of the function of Zta, including folding, assembly or trafficking. However, this is still unclear and would need further investigation. This conclusion shows functional conservation of the Hsp70 family, involvement in gamma herpes viruses during the viral lytic cycle.

6 The association of Calcium (Ca^{2+}) signalling pathway and EBV lytic cycle

6.1 Introduction

Ca2+ signalling is an important pathway during B cell receptor (BCR) activation and it regulates genes that are involved in EBV lytic activation. Few genes regulated by Ca^{2+} signalling pathway have been reported to regulate the BZLF1 promoter or interact with Zta during lytic cycle, such as Ca^{2+} /calmodulin-dependent kinase type IV/Gr (CaMKIV/Gr), TORC2 and MEF2D (Murata et al., 2009; Chatila et al., 1997; Liu et al., 1997).

NFATc1 and c2 belong to the NFAT protein family of transcription factors and play crucial roles in T cell activation and differentiation. They are also reported to be important for B cell differentiation (Muhammad et al., 2018). NFATs are cytoplasmic proteins and are regulated by the Ca^{2+}/calmodulin-dependent serine phosphatase, Calcineurin. When NFATs activated by the Ca^{2+} signalling pathway, they are dephosphorylated and followed by translocation to the nuclei where they act as transcription factors (Hogan et al., 2003).

NFATs have been reported to regulate EBV lytic activation. A previous study has shown Cyclosporin A (CsA) or Tacrolimus (FK506) can block Zta expression and EBV lytic activation in EBV positive BL cells (Goldfeld et al., 1995). Previous studies have shown the V3 polymorphism in the Zp promoter which affects Zp function (Correia et al., 2017). The Zp V3 has been shown to be overrepresented in NPC patients (Correia et al., 2018). The V3 form of Zp created an NFAT binding site on it, which enhances EBV lytic replication (Bristol et al., 2018). These studies indicate an important role of NFATs in the Zp activation and EBV lytic cycle.

In **chapter 4**, mass spectrometry studies identified NFATs to potentially interact with Zta, and the interaction of NFATc2 was further validated by Zta immunoprecipitation in Akata cells. Since NFATc1 and c2 are regulated by Ca^{2+} signalling pathway, in this chapter, whether activation of Ca^{2+} signalling pathway

and NFATs would regulate EBV lytic genes was asked and whether Zta would influence the function of NFATs was investigated.

6.2 Results

6.2.1 Calcineurin inhibitor FK506 can block the EBV lytic replication.

To investigate whether the Ca^{2+} signalling pathway and NFATs played a role in EBV lytic cycle, FK506 was used for inhibition of Calcineurin and NFATs during EBV lytic cycle activation.

FK506 or Tacrolimus is a Calcineurin inhibitor, which is an immunosuppressive drug used mainly after allogeneic organ transplant on the clinic. FK506 can form a complex with FKBP protein and inhibit Calcineurin function (Liu et al., 1991), based on this, it is used as an NFATs inhibitor widely.

To address this question, I first determined the viable range of FK506 by cell viability assay in Akata cells. Cells were treated with different concentrations of FK506 for 24 hours, which was the time for lytic cycle induction. 0.1% DMSO treated cells and untreated cells were used as controls. The viable range of FK506 in Akata cells was shown to be 0-10μM (**Figure 6.1A**).

After determining the FK506 viable condition in Akata cells, the cytotoxicity of 100μM FK506 with anti-IgG was then analysed in Akata cells, which would be the condition used for EBV lytic induction (**Figure 6.1B)**, no difference in cell viability was detected among different conditions.

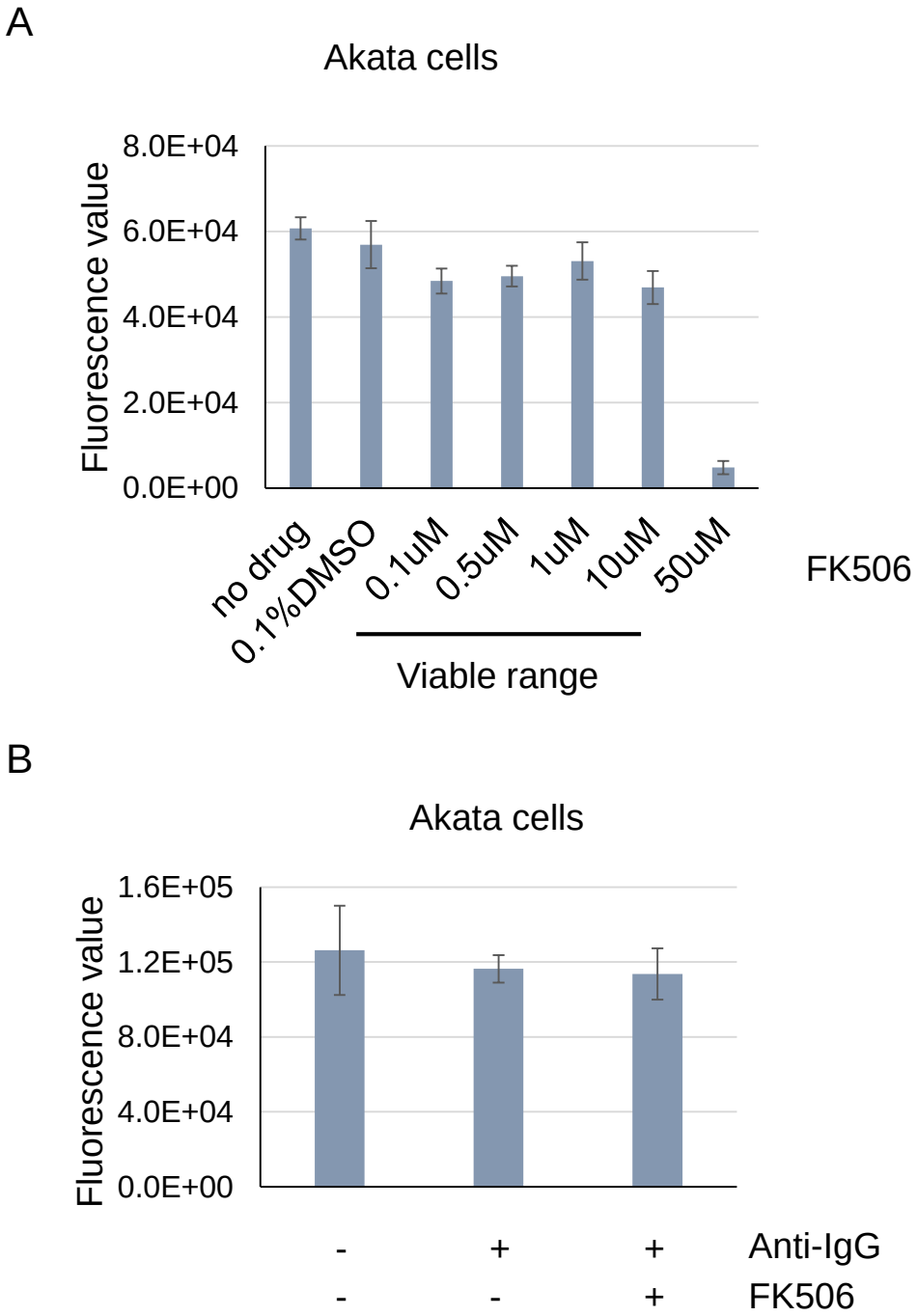

Figure 6.1 Testing the cytotoxicity of FK506 (Tacrolimus) in Akata cells. A. Akata cells were treated with increasing concentrations of FK506 for 24 hours, and cell viability was analysed by alamar-Blue assay, the viable range of FK506 was shown in the figure. **B.** Akata cells were treated with anti-IgG for 24 hours, 100nM FK506 with anti-IgG and untreated cells as the control, cell viability was analysed by alamar-Blue assay.

Time course experiment was performed for the induction of EBV lytic cycle in Akata cells. Untreated Cells and FK506 pre-treated cells were induced into the lytic cycle by anti-IgG and compared to un-induced cells, Zta protein expression was detectable after 4 hours of anti-IgG induction (**Figure 6.2A**), and the expression level increased steadily until 24 hours. However, FK506 treated cells (middle lane under each condition) barely showed expression of Zta for all the time points. EBV viral load dramatically increased after 24 hours of induction (**Figure 6.2B**). EBV lytic cycle was blocked completely by treatment with FK506, and this enhanced that the BZLF1 promoter activation is Ca^{2+} signalling pathway dependent.

6.2.2 Activation of the Ca^{2+} signalling pathway does not affect the ability of Zta to activate BHLF1.

To ask whether activation of the Ca^{2+} signalling pathway affected the transactivation of Zta, luciferase reporter assays were used in this session to answer this question.

The activation of the EBV early lytic gene BHLF1 by Zta has been characterised in previous studies (Ramasubramanyan et al., 2015b; Balan et al., 2016; Schepers et al., 1996; Hammerschmidt and Sugden, 1988). Zta activates BHLF1 through binding to the Zta responsive element in the promoter region of BHLF1. By using this, a luciferase reporter assay was designed to study Zta transcription activity. The BHLF1 promoter was placed upstream of a luciferase gene in pCpGL vector (BHLF1 WT). It contained four ZREs, which were used to study Zta transactivation. A mutant construct (BHLF1 Mut) with four ZRE sequences mutated was used as a control (**Figure 6.3A**). Expression Zta with these constructs could indicate whether the activation was trough Zta binding to four ZREs**.**

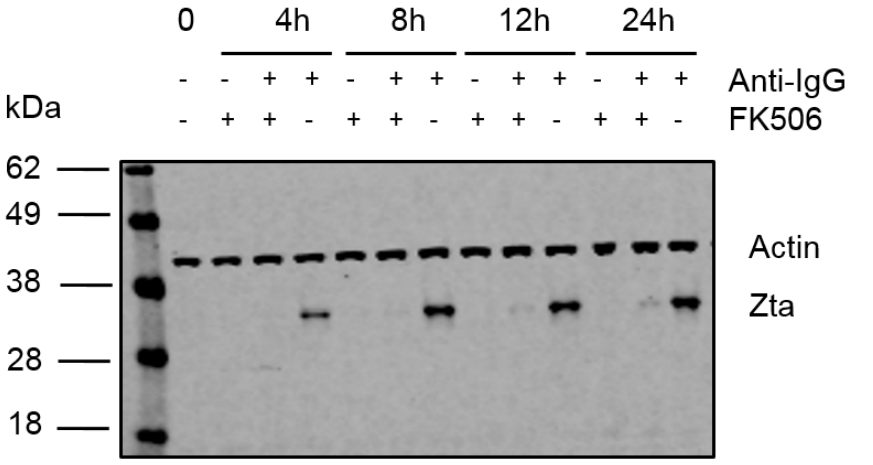

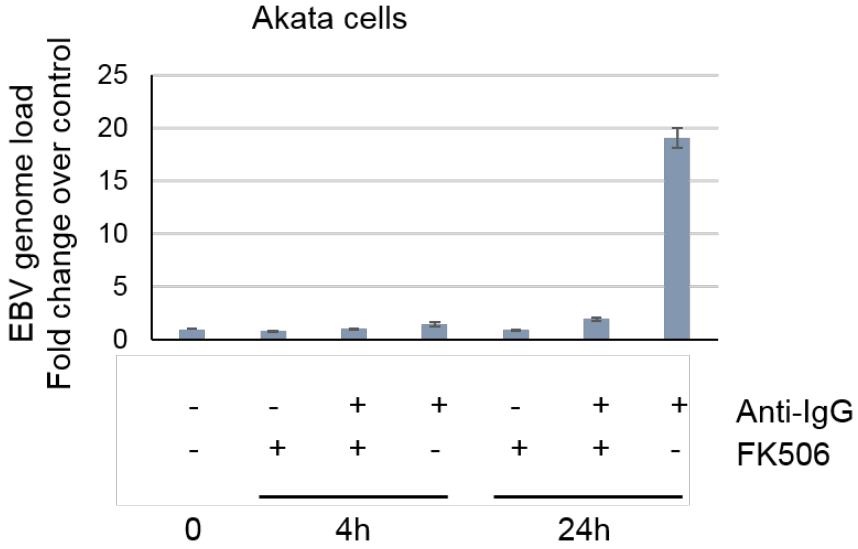

Figure 6.2 Zta expression level and EBV viral load changes when treated with FK506 in Akata cells. Akata cells were treated with 100nM FK506 1 hour before inducing to lytic cycle by anti-IgG for up to 24 hours. Cell pellets were collected after 0 hour, 4 hours, 8 hours, 12 hours and 24 hours. **A.** Western blotting for Zta was performed, Actin was used as a loading control. **B.** EBV viral load for cells induced for 4 hours and 24 hours were detected by qPCR, normalised to the human genome and shown as fold change compared to 0-hour control.

A

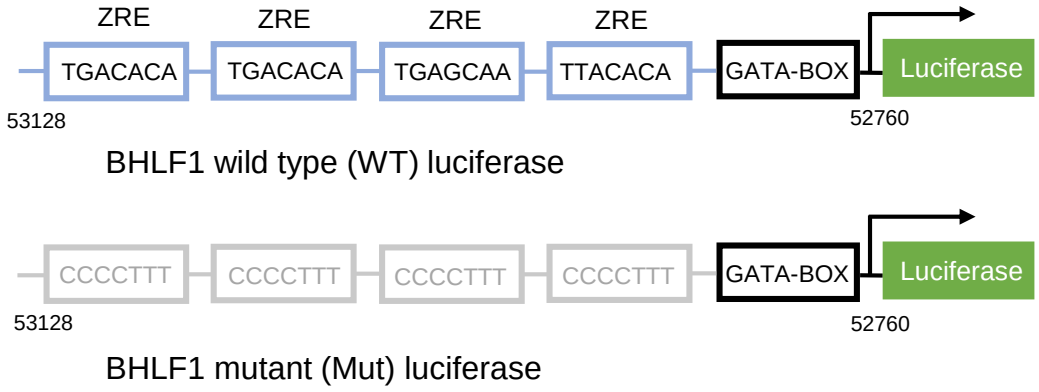
ZRE
ZRE
ZRE
ZRE
TGACACA
TGACACA
TGAGCAA
TTACACA
GATA-BOX
Luciferase
53128
52760
BHLF1 wild type (WT) luciferase
CCCCTTT
CCCCTTT
CCCCTTT
CCCCTTT
GATA-BOX
Luciferase
53128
52760
BHLF1 mutant (Mut) luciferase

B

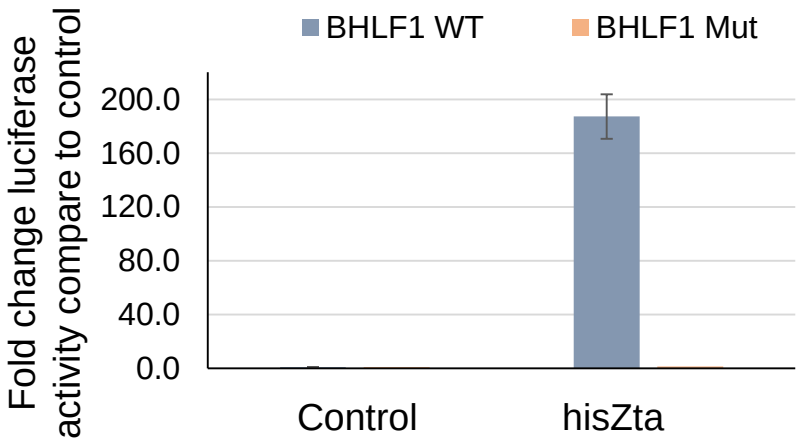
BHLF1 WT
BHLF1 Mut
Fold change luciferase activity compare to control
200.0
160.0
120.0
80.0
40.0
0.0
Control
hisZta

C

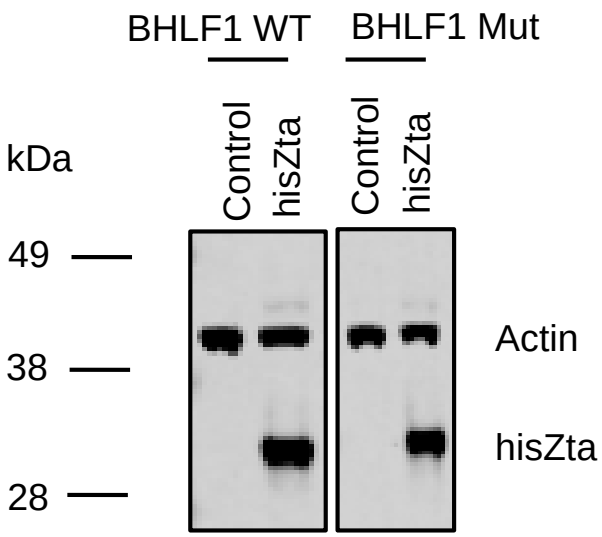
BHLF1 WT
BHLF1 Mut
kDa
Control
hisZta
Control
hisZta
49
38
28
Actin
hisZta

Figure 6.3 Transcription activity of Zta in B cells. pCpGL-BHLF1 wild type (WT) or pCpGL-BHLF1 mutant (Mut) luciferase constructs were co-transfected with either control vector or hisZta in DG-75 cells. Cells were harvested after 48 hours for western blotting and luciferase reporter assay. **A**. Schematic diagram of BHLF1 promoter with ZRE sequences and ZRE mutant. **B**. Luciferase reporter assay showed the activation of control vector or hisZta, results were normalised to total protein. Error bars represent the mean of triplicate readings ± SD. **C.** western blotting for Zta expression level in the reporter assay. Actin was used as a loading control.

BHLF1 WT and Mut constructs were co-transfected with hisZta (**Figure 6.3B and C)**, and the activation by Zta was detected only from BHLF1 WT promoter but not in the Mut. Western blotting for hisZta was detected and shown similar expression level.

In order to study the influence of Ca^{2+} signalling pathway on the ability of Zta to activate BHLF1, the BHLF1 WT construct was co-transfected with hisZta, and then the Ca^{2+} signalling pathway was induced by Ionomycin/PMA immediately after transfection. Transactivation by Zta was detected around 200 fold compared to control group (**Figure 6.4A)**, however, no obvious changes of transactivation by Zta was detected after induction with Ionomycin/PMA, western blotting showing similar expression level of hisZta in each condition (**Figure 6.4B**).

6.2.3 Reducing the abundance of NFAT proteins does not affect the transactivation ability of Zta to activate BHLF1.

Since NFATs are downstream members of the Ca^{2+} signalling pathway, next I asked whether NFAFs influenced Zta's transactivation ability to BHLF1. A knockdown assay of NFATc1 and c2 was performed. Following knockdown, a luciferase reporter assay was performed as described earlier. BHLF1 WT construct was co-transfected with hisZta in DG-75 cells, along with the NFATc1 and c2 siRNA or non-targeting control siRNA.

NFATc1 and NFATc2 were knocked down to about 30-50% of their normal protein levels (**Figure 6.5A.B**). However, knockdown of the NFATs did not show any prominent effect on transactivation by Zta (**Figure 6.5C**).

Considering both the Ca^{2+} signalling activation and the NFATs knockdown data, no influence of NFATs on transcription activation by Zta was detected.

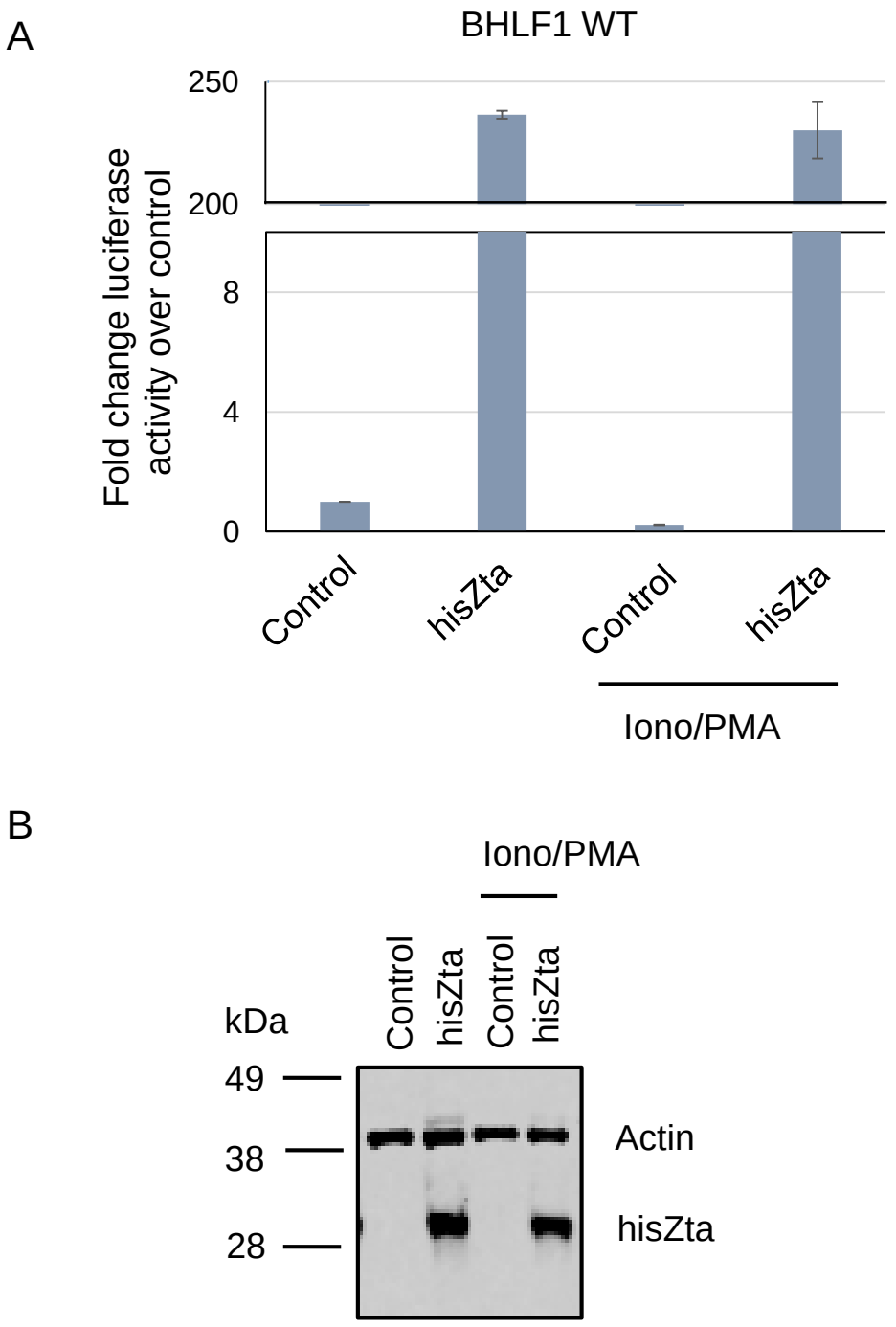

Figure 6.4 Transcription activity of hisZta is not regulated by activation of the calcium signalling pathway. pCpGL-BHLF1 WT luciferase construct was co-transfected with either hisZta or control vector in DG-75 cells, then treated with or without ionomycin/PMA immediately after transfection. 48 hours later, cells were harvested for luciferase reporter assay and western blotting. **A.** Luciferase reporter assay showed the activation of hisZta and control vector, results were normalised to total protein. Error bars represent the mean of triplicate readings ± SD. **B**. western blotting for Zta expression level in the reporter assay. Actin was probed as a loading control. Results showed a representative of three biological replicates.

A

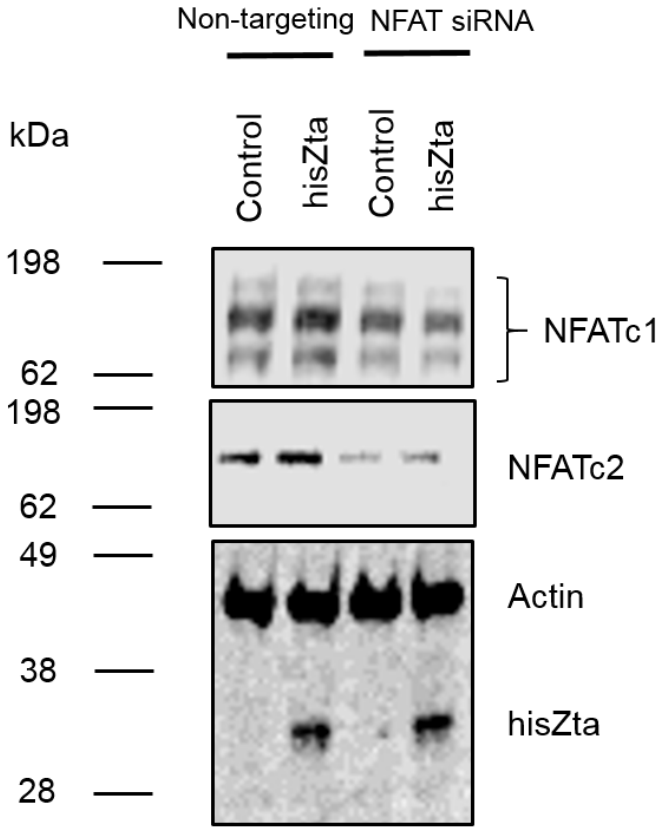
Non-targeting
NFAT siRNA
kDa
Control
hisZta
Control
hisZta
198
62
198
62
49
38
28
NFATc1
NFATc2
Actin
hisZta

B

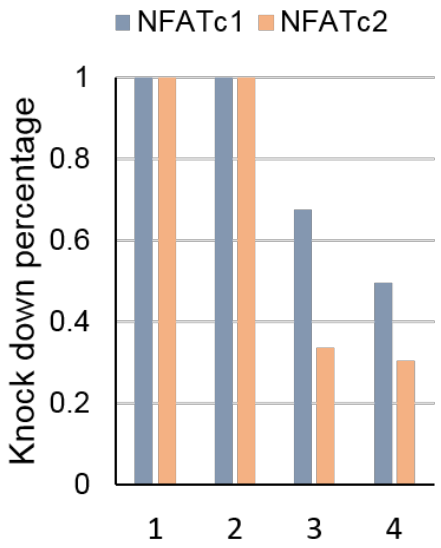
NFATc1
NFATc2
Knock down percentage
1
0.8
0.6
0.4
0.2
0
1
2
3
4

C.

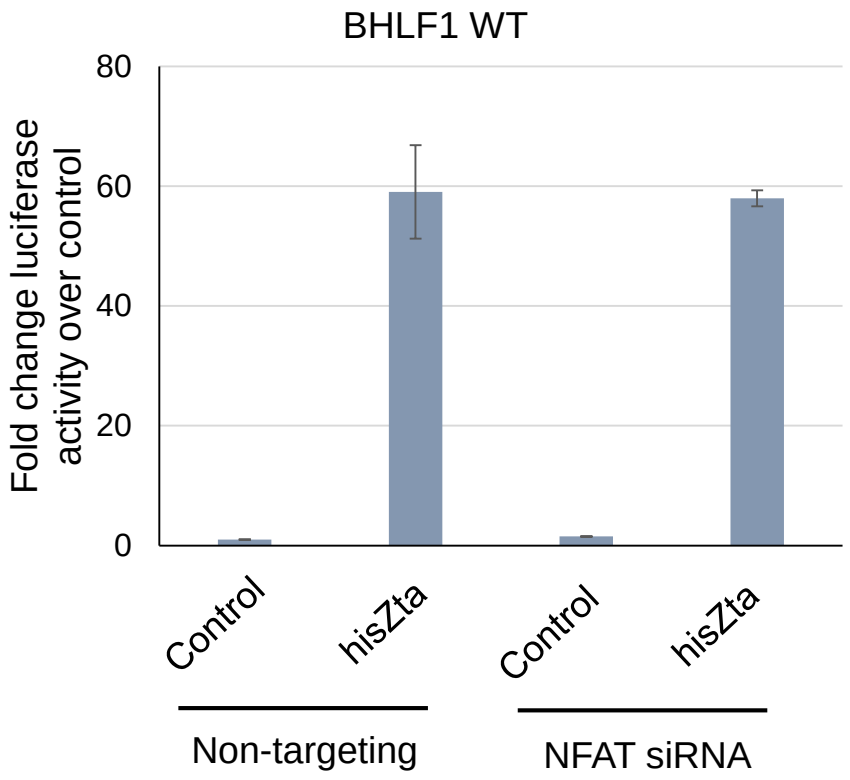

Figure 6.5 Transcription activity of Zta with NFAT proteins knocked down in DG-75 cells. pCpGL-BHLF1 WT luciferase construct was co-transfected with Zta or control vector, and NFATc1 and c2 siRNA smart pool or Non-targeting control siRNA by Neon electroporation in DG-75 cells, 48 hours post-transfection, cells were harvested for luciferase reporter assay and western blotting. **A**. Western blotting for Zta, NFATc1 and NFATc2, Actin was used as a loading control. **B**. Protein bands were quantified by LICOR imageStudio. Protein quantitation of NFATc1 and NFATc2 was normalised to Actin and plotted as knock-down percentage compared to the non-targeting group. **C.** Luciferase reporter assay showed the activation of hisZta and control vector, results were normalised to total protein. Results were shown as fold change compared with the control non-targeting group. Error bars represent the mean of triplicate reads ± SD. Results showed a representative of three biological replicates.

6.2.4 Zta interferes with transcription activation by NFATs on IL-2 promoter.

Although NFATs showed no obvious impact on transcription activity by Zta, another question was whether Zta influenced the transcription activity of NFATs. Previous studies have investigated NFAT proteins' transcription activity on the Interleukin-2 (IL-2) gene promoter. IL-2 is a cytokine gene expressed upon T cell stimulation and mainly regulated by NFAT and Activator protein 1 (AP-1) families. A construct with three NFAT/AP-1 composite elements (ARRE2), cloned upstream of the minimal IL-2 promoter, was used for a luciferase reporter assay (**Figure 6.6A**). FK506 was used as an inhibitor of Calcineurin and NFATs. The viability of DG-75 cells was studied upon treatment with FK506, and the viable range was identified (**Figure 6.6B**). Then DG-75 cells were transfected with pGL3-IL2 NFAT luciferase construct and control construct following which the cells were treated with ionomycin/PMA to induce Ca^{2+} signalling and activate NFATs. Cells treated with FK506 1 hour before transfection to block the Ca^{2+} signalling activation were used as a control (**Figure 6.6C**). The activation of transcription was detected after ionomycin/PMA induction, and 1 μM of FK506 could block this activation.

A

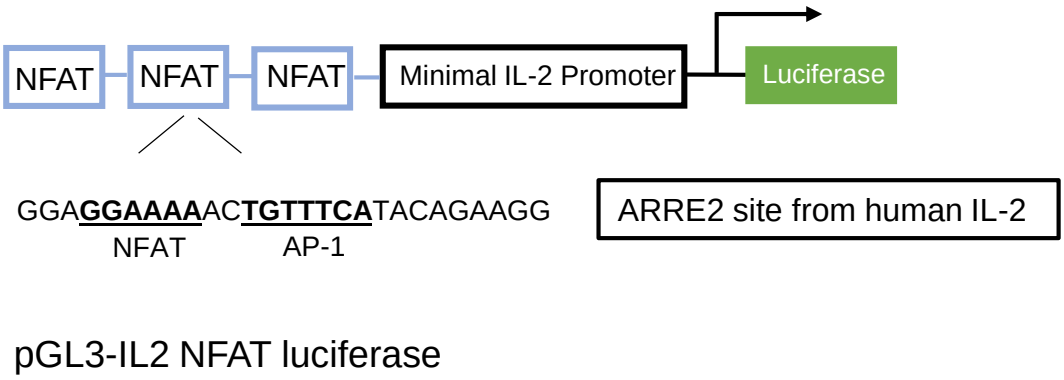

pGL3-IL2 NFAT luciferase

B

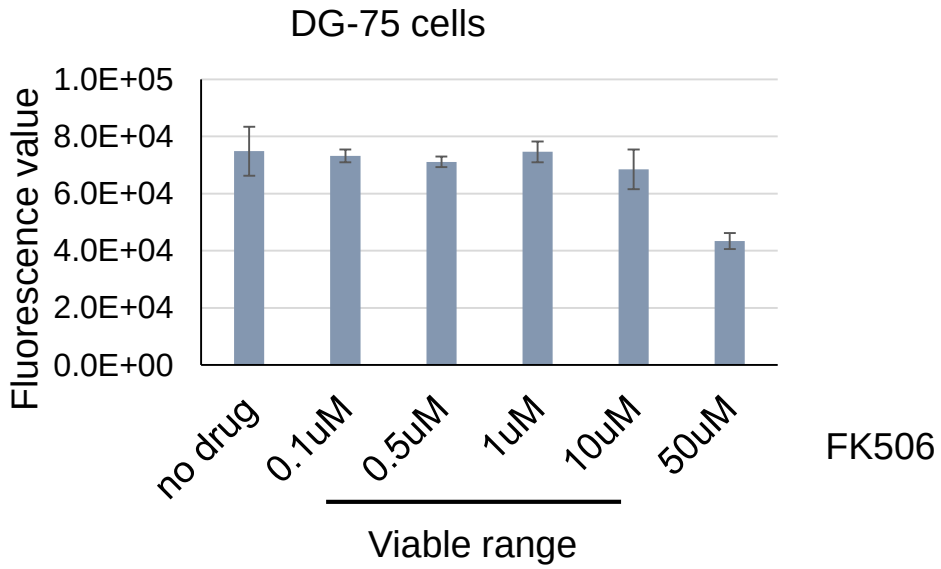

C

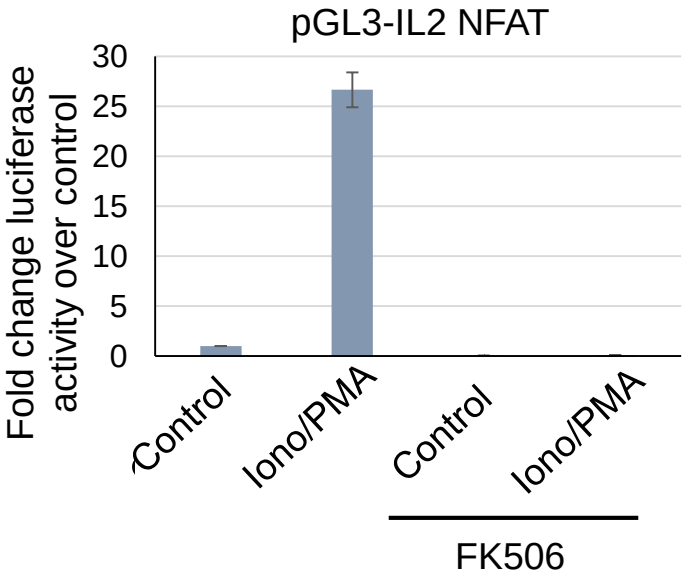

Figure 6.6 Transcription activity of NFAT protein in DG-75 cells. DG75 cells were transfected with pGL3-IL2 NFAT luciferase reporter construct after treated with 1μM FK506, NFAT proteins were activated by ionomycin/PMA immediately after transfection. After 48 hours, cells were harvested for luciferase reporter assay. **A**. A pGL3-IL2 luciferase reporter construct with three NFAT protein binding sites before the minimal IL-2 promoter. **B**. DG-75 cells were treated with increasing concentrations of FK506 for 48 hours, and then cell viability was analysed by alamar-Blue assay. Viable concentrations were labelled in the figure. **C**. Luciferase reporter assay shown the activation of each group. Results were normalised to total protein and showed as fold change compared with the control group. Error bars represent the mean of triplicate reads ± SD.

Based on this, another reporter assay was performed to ask whether Zta co-operated or interfered with NFAT transcription activity. pGL3-IL2 NFAT luciferase construct was co-transfected with hisZta and control vector (pcDNA3). Ca^{2+} signalling was induced by ionomycin/PMA, FK506 pre-treated cells were also used to block the Ca^{2+} signalling activation. This revealed that Zta expression alone could activate transcription by 20-fold (**Figure 6.7A**), and cells treated with ionomycin/PMA alone triggered higher activity, around 60-fold. When cells exposed to both hisZta and ionomycin/PMA, instead of synergy, it showed intermediate activation compared to ionomycin/PMA or Zta alone group. The Calcineurin and NFAT inhibitor FK506 completely blocked ionomycin/PMA activation. However, there was no impact on the activation by Zta. Western blotting showed a similar expression level of hisZta in each condition (**Figure 6.7B**).

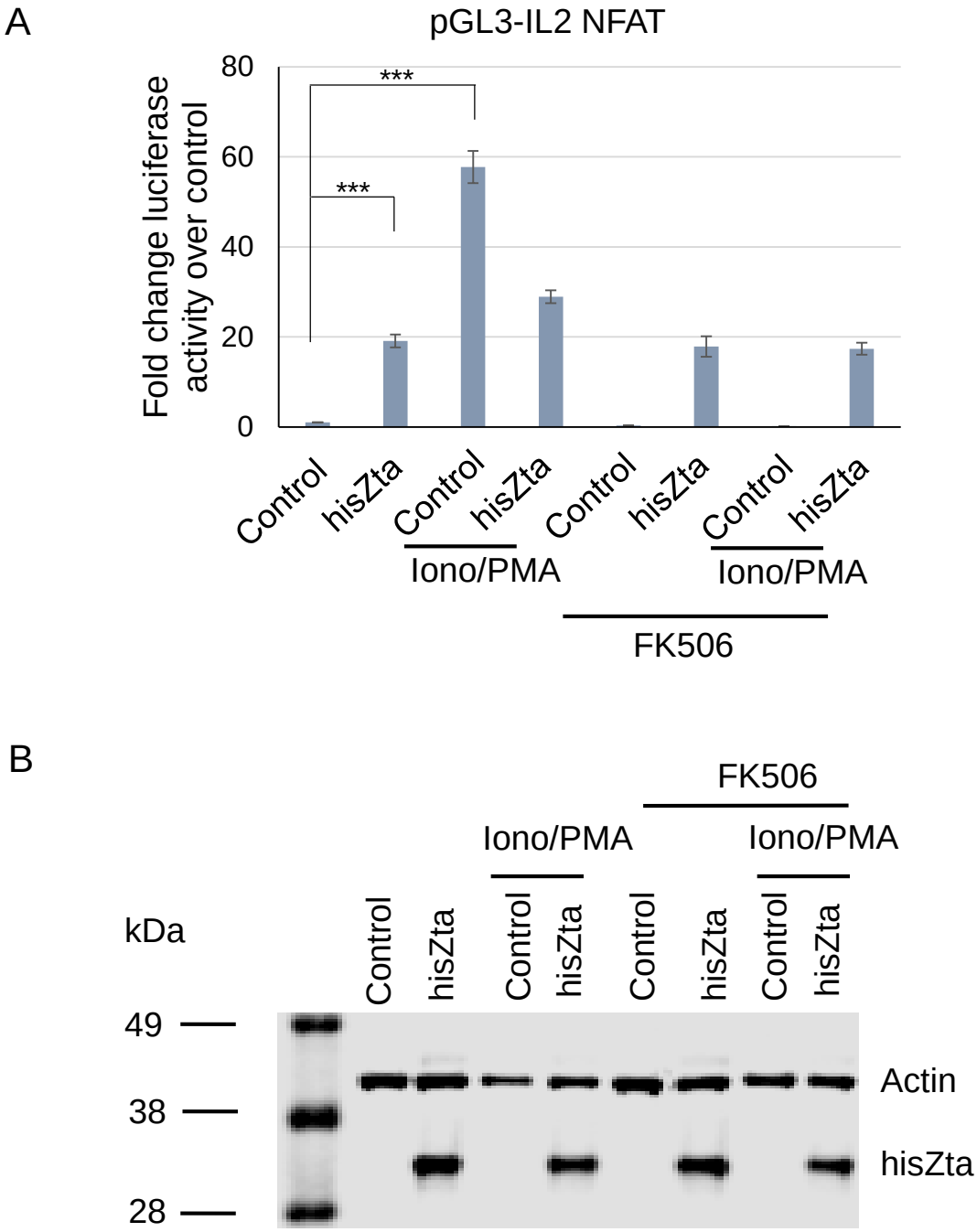

Figure 6.7 Zta interferes with NFAT transcription activity. pGL3-IL2 NFAT luciferase reporter construct was co-transfected with hisZta or control vector after treated with or without FK506 in DG75 cells. Ca2+ signalling was activated by ionomycin/PMA immediately after transfection. After 48 hours, cells were harvested for luciferase reporter assay and western blot. **A**. Luciferase reporter assay showed the activation of each group, results were normalised to total protein and shown as fold change compared with the control group. **B**. Western blotting for the Zta expression level in each group, Actin was used as a loading control. Error bars represent the mean of triplicate reads ± SD. Results showed a representative of three biological replicates. (***) indicates p<0.001

6.2.5 Zta bZIP domain binds to ARRE2 element weakly.

To figure out whether Zta was able to bind to the ARRE2 element directly, an *in vitro* protein-DNA binding assay was performed. An electrophoresis mobility shift assay (EMSA) was carried out using fluorescently labelled probes of ARRE2 element. An AP-1 site from BMLF1 promoter, which has been identified as a strong Zta binding site, was used as a positive control.

A recombinant Zta protein resembling His-GFP tagged basic leucine zipper (bZIP) domain of Zta (His-GFP-bZIP Zta) was used in this EMSA analysis, which was purified by previous group member Rajaei Almohammed.

The increasing amount of purified protein His-GFP-bZIP Zta was used to interact with each probe, and a GFP protein (1mg/ml) was used as a control. Then, the reaction mixtures under each condition were loaded into a DNA retardation gel. Strong DNA shift bands were detected in each His-GFP-bZIP Zta lanes with AP1-BMLF1 probe but not in GFP control (**Figure 6.8A**). Most of the probes were shifted with His-GFP-bZIP Zta at the highest protein concentration. However, only a very rare amount of ARRE2 probes was shifted with the highest concentration of His-GFP-bZIP Zta. Quantitation of the shifted bands was shown (**Figure 6.8B**). Western blotting showed the purified proteins that were used in this experiment (**Figure 6.8C**). Compared with ZRE in BMLF1 promoter, very weak evidence showed that His-GFP-bZIP Zta binds to ARRE2 element directly *in vitro*.

Therefore, it appeared that inhibition of Ca^{2+} signalling was sufficient to block EBV lytic reactivation while transcription activation through Zta was unaffected by Ca^{2+} signalling. Zta attenuated transcription activation through NFAT.

A

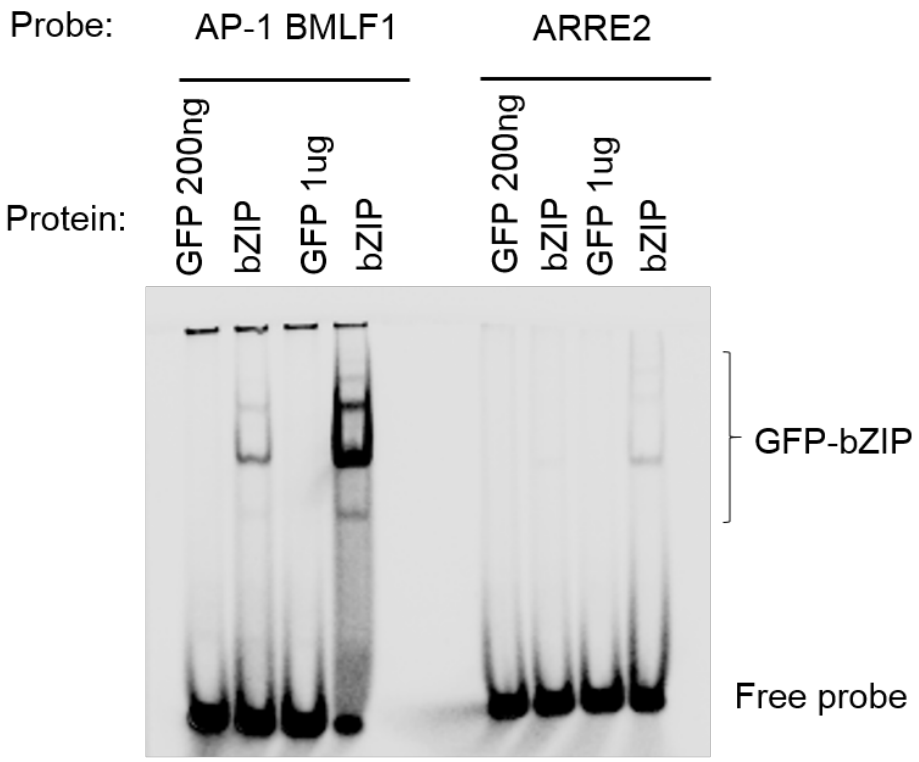
Probe:
AP-1 BMLF1
ARRE2
Protein:
GFP 200ng
bZIP
GFP 1ug
bZIP
GFP 200ng
bZIP
GFP 1ug
bZIP
GFP-bZIP
Free probe

B

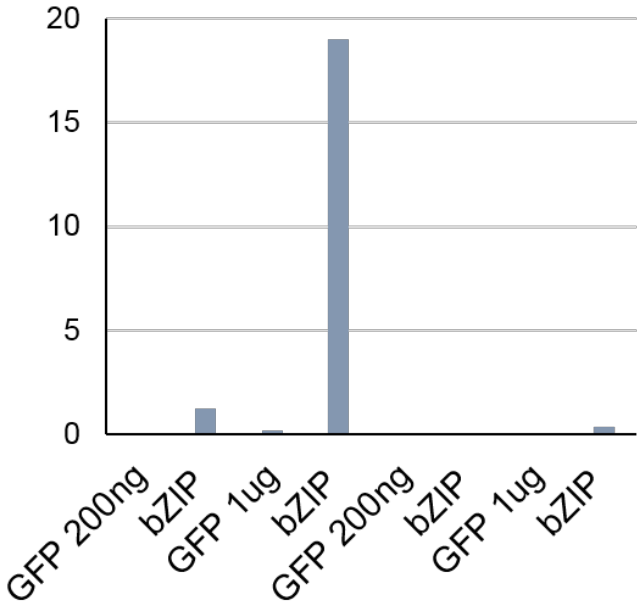
20
15
10
5
0
GFP 200ng
bZIP
GFP 1ug
bZIP
GFP 200ng
bZIP
GFP 1ug
bZIP

C

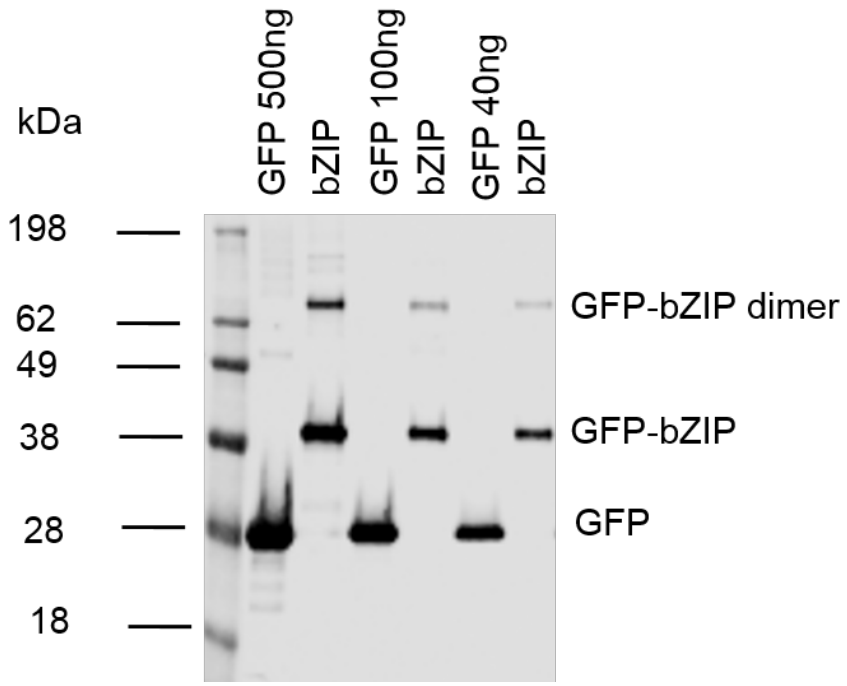

Figure 6.8 Zta bZIP domain binds to ARRE2 element weakly. The ability of purified GFP tagged Zta bZIP domain binds to fluorescently labelled ARRE2 element and a known AP-1 in BMLF1 gene promoter were analysed by electrophoresis mobility shift assay (EMSA). **A.** The increasing amount of Zta bZIP proteins were used with each probe, GFP was used as a control. **B.** quantitation of the shift in each condition. **C**. Western blotting shows the purified proteins used in this EMSA.

6.3 Discussion

The NFAT family of transcription factors contains five NFAT proteins, NFATc1-c4 are proteins regulated and activated by the Ca^{2+} signalling pathway, whereas NFAT5 is activated by osmotic stress (Lopez-Rodriguez et al., 1999). NFATs regulate cell differentiation and development in many different cell types and organ systems. Several studies have reported that NFATs involve in different cancers, such as B cell lymphomas, leukaemia, breast cancer, pancreatic and many others (Pham et al., 2005; Koenig et al., 2010). NFATc2 represses the expression of G0/G1 checkpoint kinase, cyclin-dependent kinase 4 (CDK4) and cyclin A2, and plays an important role in controlling cell-cycle progression (Baksh et al., 2002; Carvalho et al., 2007). NFATc2 also promotes tumour cells migration and invasion upon the regulation of relevant gene expression such as cyclooxygenase 2(COX2) (Yiu and Toker, 2006).

The function of NFATs has been well investigated in the immune system, especially in T cells. As transcription factors, NFATs regulate expression of different genes. Many of them are dependent on NFAT/AP-1 co-operation and binding to the NFAT/AP-1 composite, locating in the promoter regions of IL-2 (ARRE1 and ARRE2 site), IL-4, IL-5, FasL and enhancer regions of GM-CSF (GM330 element) (Macian et al., 2000; Rao et al., 1997).

This composite has a common feature, which includes an NFAT binding site with the core binding sequence GGAAA and a 7-bp AP-1 site that is able to be bind by bZIP families. A wide range of composite has been studied, which pairs elements with different binding ability in different genes. The weak NFAT sites with strong AP-1 site was identified in GM330 element of GM-CSF enhancer region; strong NFAT sites with weak AP-1 site, which was identified in murine IL-2 promoter; and also the weak AP-1 with weak NFAT site, as the ARRE2 site in human IL-2 promoter (Peterson et al., 1996; Rao et al., 1997; Johnson et al., 2004). The crystal structure of murine NFAT/AP-1 complex with ARRE2 motif gave us detailed information of this co-operation, also proved the feature that the

three components, NFAT, AP-1 and the DNA composite form a strong complex (Chen et al., 1998).

Although the function of NFATs in T cells has been well characterised, it is still unclear whether they have roles in B cells. Several studies showed that NFATs were involved in B cell development and functions using mice models (Berland and Wortis, 2003; Winslow et al., 2006). Besides, NFATc2 induced apoptosis of BL cells upon induction of the BCR signalling pathway (Kondo et al., 2003). Another study showed that NFATs were controlled and activated by the BCR stimulation through Ras-mediated activation of guanine nucleotide exchange factors for the GTPase Ral (de Gorter et al., 2007).

Involvement of Ca^{2+} signalling and NFATs in EBV infected cells was first identified in the early 90s. Speck's group found Calcineurin inhibitors CsA and FK506 could block the activation of EBV lytic cycle. They further used Zta promoter (Zp) luciferase construct co-expression with NFATs and Calcineurin to study their effects on Zp activation. They discovered that CsA-sensitive Zp was mediated through a calcineurin-regulated pathway through NFATc2 (Goldfeld et al., 1995; Liu et al., 1997). However, no NFAT binding site was found in the Zp suggested this might be an indirect regulation.

When study sequence variants in Zp, it was reported that the V3 form of Zp created an NFAT binding site in a sub-set of EBV positive BLs, gastric cancers and NPCs (Correia et al., 2018). The NFAT binding site enhanced Zp activity and increased the EBV lytic initiation upon BCR stimulation through NFAT activation, and it can be inhibited by both CysA and NFAT siRNA (Bristol et al., 2018). All these studies suggest that NFATs are important for EBV lytic replication.

In **Chapter 4**, NFATc1 and NFATc2 were shown to bind Zta by mass spectrometry, and I further validated the interaction of NFATc2 with Zta in cells. In this chapter, the functional relevance between Zta and NFAT was investigated. Two reporter promoters, BHLF1 and IL-2 promoter were used to unpick potential co-regulation between NFATs and Zta.

To address how NFATs affect the transcription activation by Zta, BHLF1 promoter was used, which is regulated by Zta through four ZREs and to only study the interaction of Zta and NFATs on this promoter. It is showed that this promoter was not activated by Ca^{2+} signalling and furthermore that Ca^{2+} signalling did not affect the regulation of BHLF1 by Zta (**Figure 6.4 and 6.5).** One of the possible explanations for this could be that the binding of Zta and NFAT did not affect Zta's transactivation. The other possibility could be that these proteins needed to bind to DNA in order to stabilise the interaction between them. In addition, it could be that the activation of NFAT was not enough to show the impact on this promoter.

The ionomycin/PMA caused basal signal decreased (**Figure 6.4A**), because along with the Ca^{2+} signalling pathway activation, the whole cell environment changed, other factors that were not known, might affect this construct. However, when Zta expressed, this inhibition was recovered and the activation can reach to the usual level.

The second promoter contained an NFAT/AP-1 composite (ARRE2) element from the human IL-2 promoter. This construct (pGL3-IL2 luciferase construct) has three NFAT/AP-1 composites (NFAT/AP-1*3) cloned into upstream of a minimal IL-2 promoter (Mattila et al., 1990; Clipstone and Crabtree, 1992). The previous study has shown that NFAT activation by Ca^{2+} signalling and AP-1 activation by PKC are required for the activation of these composites. NFAT or Fos-Jun expression alone does not show the activation in both murine and human IL-2 genes (Nguyen et al., 2010; Peterson et al., 1996). Therefore, in our study, both Ionomycin and PMA were used to activate the IL-2 promoter through NFAT/AP-1 composite (**Figure 6.6)**.

The activation that was triggered by ionomycin/PMA could be completely blocked by FK506 (**Figure 6.6**). This also approved that both NFAT and AP-1 proteins were needed for the composite activation.

Then the influence of Zta expression along with the Ca^{2+} signalling activation to this promoter was investigated. Surprisingly, instead of synergy, the expression

of Zta interfered with the transcription activation of Ionomycin/PMA treatment to this promoter.

The molecular mechanism by which Zta interferes with Ca^{2+} signalling activation to this promoter is still unclear. Then it was questioned whether there were any ZREs in the promoter region, where Zta could bind. After searching for known ZREs across the whole pGL3-IL2 luciferase construct (Flower et al., 2011), none of the ZREs was found in the promoter or upstream region, which suggested Zta may bind to unknown ZREs or to the AP-1 site in this ARRE2 element to activate the gene promoter when Zta expressed alone.

So then, EMSA assay was used to figure out whether Zta bind to ARRE2 element in vitro directly through the bZIP domain. Very weak binding of Zta bZIP to this ARRE2 element was detected (**Figure 6.8**), suggesting the activation on the IL-2 promoter by Zta is through an indirect manner but not binding to ARRE2 element directly.

There is a model with three situations that may happen on this promoter is shown to explain this mechanism (**Figure 6.9**). Following the stimulation with ionomycin and PMA, IL-2 promoter activated by NFAT and AP-1 interaction through ARRE2 element, which is inhibited by FK506 (**Figure 6.9a**). Following the expression of Zta, it activates IL-2 promoter, but this is not through ARRE2 element, and it is not blocked by FK506 (**Figure 6.9b**). Combining stimulation with ionomycin and PMA and expression of Zta, transcription is activated to an intermediate level. FK506 reduces the expression to the level seen when Zta is activated alone. Interaction of Zta with NFATC2 may account for this reduction (**Figure 6.9c**).

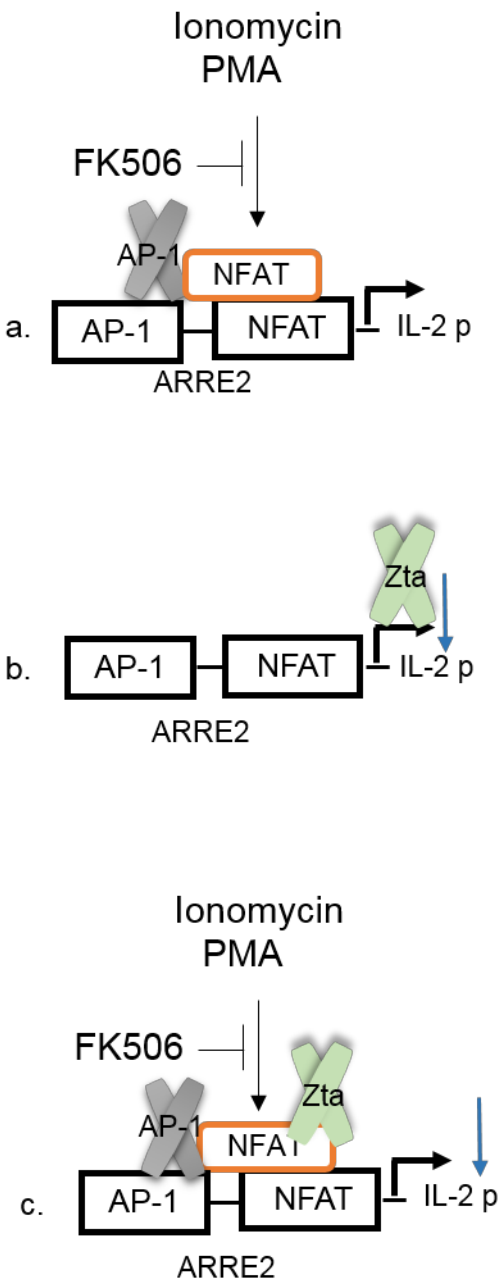

Figure 6.9 Impact of ionomycin, PMA and Zta on the IL2 promoter. The IL2 promoter and one ARRE2 element is shown with location of transcription factors (NFATC2, AP1 and Zta). **a.** Following the stimulation with ionomycin and PMA, IL-2 promoter activated by NFAT and AP-1 interaction through ARRE2 element, which is inhibited by FK506. **b.** Following expression of Zta, IL-2 promoter activated by Zta, which is not through ARRE2 element. **c.** Combining stimulation with ionomycin and PMA and expression of Zta, Zta binding to NFAT causes the interference of the transcription at IL-2 promoter.

NFAT/Fos-Jun DNA complex crystal structure is the only structure available now for NFAT and AP-1 co-operation (Chen et al., 1998). The same group used the NFATc2 mutant proteins that were unable to interact with Fos-Jun but did not affect the transcription activity of this complex to investigate whether the NFAT targeting genes are dependent on NFAT/AP-1 interaction (Macian et al., 2000). Apparently, NFAT/AP-1 co-operation was found to be essential for many NFAT dependent genes, such as IL-2, IL-3, IL-4, MIP-1α, and FasL, however, they are not essential for activation of TNFα or IL-13 (Macian et al., 2000). Based on the crystal structure and mutant studies, the residues that were shown to be required for NFAT Fos-Jun interaction were revealed (**Figure 6.10**). R468 of murine NFATc2 (R466 in human NFATC2) contacts with D170, E173 of Fos, and T535 in the murine NFATc2 (T533 in human NFATC2) contacts within a pocket formed by R285, R288 and K292 of Jun.

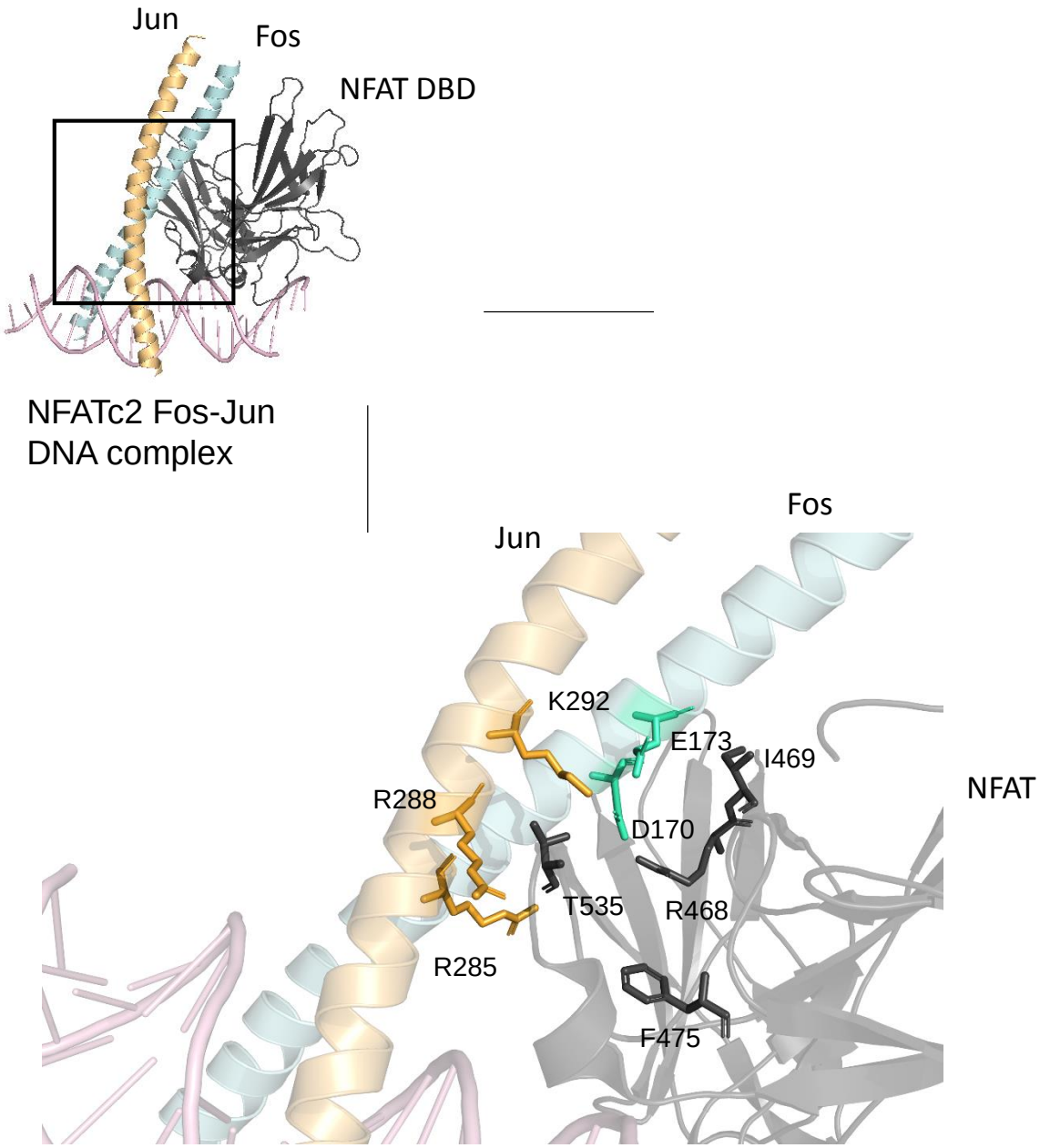

Figure 6.10 Structure of NFATc2 Fos-Jun DNA complex and interaction residues. Murine NFATc2 DNA binding region (DBD) and Fos-Jun bZIP domain heterodimer with DNA complex (PDB 1a02) was illustrated. Important interaction residues were highlighted, R468 of Murine NFATc2 (R466 in human NFATC2) contacts with D170 and E173 of Fos, T535 in the E'F loop of murine NFATc2 (T533 in human NFATC2) contacts within a pocket formed by R285, R288 and K292 of Jun. Besides, F475 and I469 of NFATc2 were also important for the interaction. Adapted from (Macian et al., 2000).

Although Fos, Jun and Zta in the same bZIP family, Zta has an unusual structure at its c-terminal tail region while the Fos and Jun proteins have a continuous coiled-coil structure (**Figure 6.11B**) (Petosa et al., 2006). Also, from sequence alignment (**Figure 6.11A**), the contact amino acids with NFAT in Fos-Jun are not conserved in Zta. When superimposing Zta bZIP with Fos-Jun bZIP (**Figure 6.11C**), the contact region is still within Zta bZIP domain and the Zta tail region could be involved in the interaction with NFATs. All of these suggested there might be a different interaction features between Zta, NFAT and DNA.

To summarise, NFATs inhibitor FK506 could block EBV lytic cycle in Akata cells during lytic activation, NFATs did not affect Zta transcription activity during EBV lytic cycle, however Zta can interfere with NFATs transcription activity, and this could be through Zta binding to NFATs during transcription regulation on NFATs regulated genes.

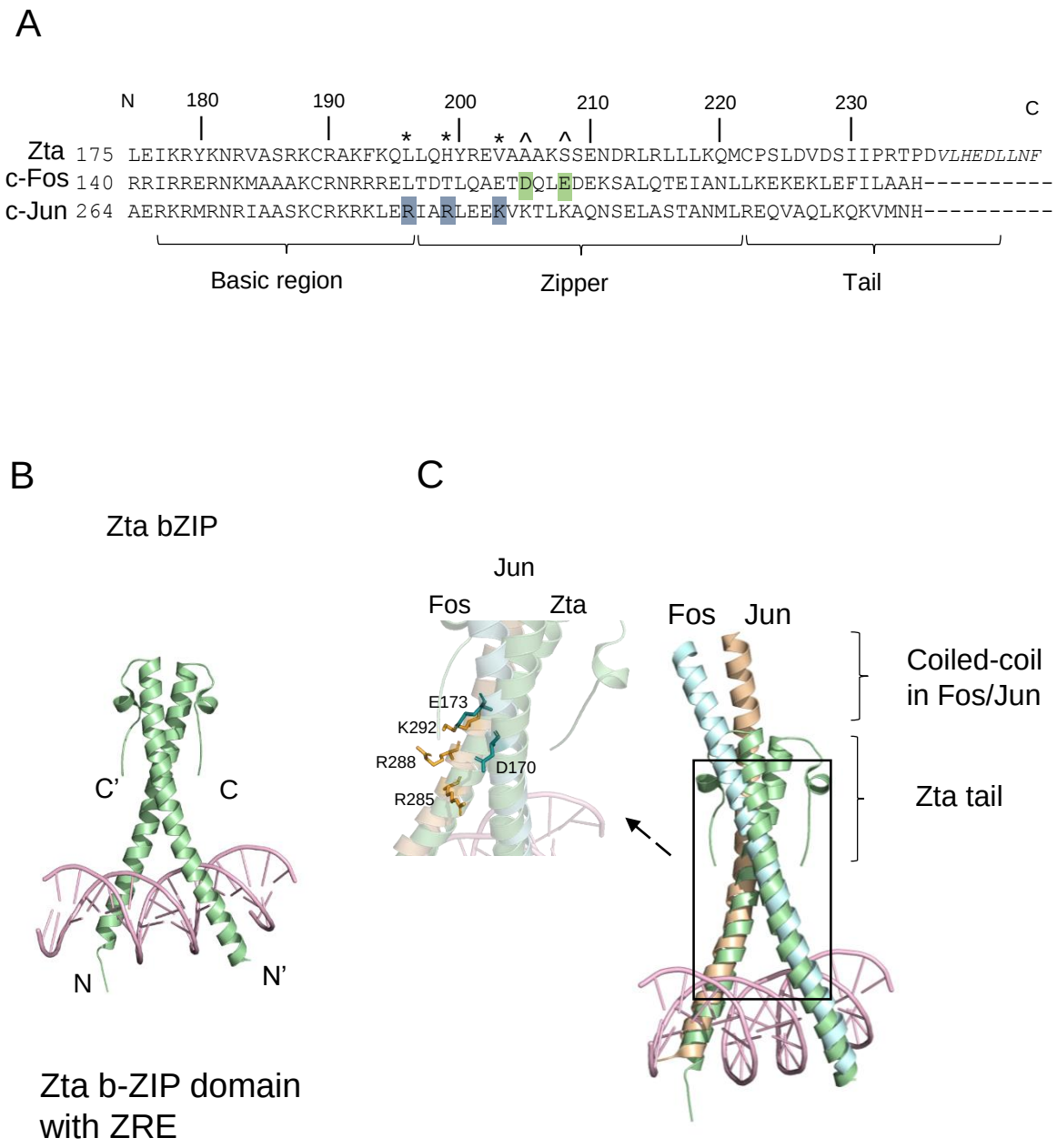

Figure 6.11 Structure of Zta-DNA complex. A. Sequence alignment of Zta, c-Fos, c-Jun bZIP domain. Basic region, zipper and tail were labelled. NFAT contacting residues in c-Fos (D170 and E173, labelled by ^) and c-Jun (R285, R288 and K292, labelled by *) were labelled. **B.** View of Zta DNA complex (PDB 2C9L), adapted from (Petosa et al., 2006). **C.** Zta homodimer (PDB 2C9L) superimposed with c-Fos/c-Jun hererodimer (PDB 1a02) and DNA. The NFAT contacting residues were highlighted on Fos-Jun helix.

7 Discussion

Characterising the host-viral interaction is an important component of studying viral function, especially a malignant causing virus. EBV, a human herpes virus, is living with most of the human population for their lifetime without harm. However, it is a potential risk factor for different tumours and diseases (Hjalgrim et al., 2007).

To understand the function of key EBV lytic regulator Zta and the proteins that interact with Zta gave us a hint of how virus crosstalk with the host. Through the studies of these interactions, to further understand how the viral proteins help EBV to survive and persist in the host cells. It is also a chance to identify biomarkers that are important for viral replication, persistence, and more importantly, to find drugable targets or develop a vaccine in order to treat the primary EBV infection as well as the EBV associated cancers.

To achieve this goal, I first established a Zta pull-down condition during the EBV lytic cycle in an EBV positive BZLF1 gene knock-out cell line based on a ChIP assay, using a label-free quantitative mass spectrometry analysis (described in **Chapter 3**). The label-free quantitation method performed by MaxQuant software was suitable for this study. A few cellular proteins were enriched as Zta interacting proteins. The relevance of this is shown by the identification of RACK1, which had been reported as a Zta interacting protein in the previous study (Baumann et al., 2000).

The high level of exogenous hisZta used in this method led to a concern this may not represent the physiological change. In addition, as no other EBV proteins apart from Zta were identified from mass spectrometry, this prompted a change of approach.

In order to improve this pull-down method, I decided to use another cell line. It was an EBV positive BL cell line that could be induced into the lytic cycle by using a physiologically relevant stimulant anti-IgG, which has been described in

Chapter 4. To stabilise the interaction during the lytic cycle, I used a protein-protein cross-linker DSP, which has a long spacer arm and widely used in protein-protein crosslinking studies. I also used benzonase nuclease to digest DNA in order to reduce the potential of purifying DNA binding proteins unspecifically to Zta-bound DNA. Two controls were chosen in this experiment to relate to potential non-specific interaction with the specific antibody and with lytic cycle proteins associating with the beads. The using of the TMT labelling method raised sensitivity and gave us a chance to combine all the controls and three biological replicates together for mass spectrometry.

Five viral proteins were identified with high ratios as Zta interacting viral proteins in addition to the known ones (BGLF4 and BALF5). Including a portal protein BBRF1, two capsid proteins BVRF2 and BcLF1, an mRNA export factor BMLF1 and a DNA binding protein BALF2.

Portal protein BBRF1 is an HSV-1 UL6 homolog (Baer et al., 1984; Cai et al., 2017). In HSV-1, UL6 protein is an important capsid portal protein. It is required for the encapsidation of viral DNA and DNA cleavage (Heming et al., 2017). Electron microscopy studies revealed the portal structures of HSV-1, twelve subunits of UL6 form the portal structure where the viral DNA enters and exits the capsid (Cardone et al., 2007; Newcomb et al., 2001). In EBV, it is reported that mutant virus with deletion of BBRF1 gene resulted in the formation of capsids without genome (empty capsids), which suggested a role of BBRF1 in EBV DNA packaging to the capsid (Pavlova et al., 2013). Transmission electron microscopy study in EBV revealed the features of EBV portals formed by BBRF1 *in vitro*, resembling HSV-1 UL6 but including a central channel with thirteen monomeric clip, stem and wing/crown domains, suggested the role of BBRF1 was similar to its homologs in other herpesviruses (Visalli et al., 2019). Zta was not identified by the mass spectrometry in the viral particles, suggested the function of Zta was possibly not involved in infection of cells, viral entry or DNA exiting from the viral particles (Johannsen et al., 2004). However, the interaction of Zta with portal protein I identified in our study suggested Zta might function in the viral DNA packaging and importing into the capsid.

Two capsid proteins BVRF2 and BcLF1 were also identified that were able to interact with Zta. BVRF2 (protease) and BcLF1 (Major capsid) are required for the EBV capsid assembly (Henson et al., 2009). Considering the studies of the HSV-1, during the viral replication, all the capsid proteins are transported into the nucleus through protein-protein interactions of each other, and form a procapsid. The protease then cleaves the scaffold proteins and releases them from the capsid, which is essential for the DNA packaging into the capsid and promotes the maturation of the capsid (Gao et al., 1994). Interaction of Zta with these two proteins in EBV suggested that Zta might be able to enhance their functions during the lytic cycle, which again suggested a role of Zta in DNA import and virion assembly.

BMLF1 as a homolog of HSV-1 ICP27, plays a role in mRNA transportation, it shuttles between cytoplasm and nucleus and interacts with RNA (Sergeant et al., 2008). It is essential for the production of infectious virions (Gruffat et al., 2002a). The interaction of Zta with BMLF1 that I observed suggested that Zta might be involved in mRNA processing or transportation. This is also consistent with the cellular targets found in mass spectrometry in **Chapter 3** and **4** that mRNA splicing and processing proteins were enriched with high scores.

BALF2 is one of the core lytic replication proteins and has been proved not interacted with Zta directly by a few immunoprecipitation studies (Fujii et al., 2000). However, surprisingly, it is detected by our mass spectrometry analysis, which suggested that as a part of the replication complex, BALF2 could be pulled down by Zta indirectly.

One of the limitations of studying interacting proteins is the lack of commercial antibodies. In order to perform the further investigation between Zta and capsid proteins, some constructs could be created to express tagged viral proteins *in vitro* and *in vivo*, which allows us to investigate their interactions with Zta using pull-down assays. Domain mapping study can be used to study their direct or indirect interactions with Zta. Point mutants that will disrupt the interactions can be generated and used to study the functions that are relevant to this interaction.

After validated the interaction of those proteins with Zta, functional studies could also be designed based on those constructs in order to investigate the role of this interaction during the EBV lytic replication. Super-resolution microscopy could be used to study whether Zta is involved in the portal and capsid assembly or the DNA packaging by showing the co-localisation of Zta with the capsid/portal proteins (Liao et al., 2001).

The cellular proteins I chose for validation in **Chapter 4** were from different functional groups. Some of them were proved by IP-western blotting to interact with Zta. However, considering the limitation and quality of the antibodies as well as the costs, it was not possible to assess many targets. Some promising targets were verified from mass spectrometry, including PARP1, Hsc70 and NFATc2.

The further studies were focused on the functional relevance between validated cellular proteins and the EBV lytic cycle. The functional relevance of PARP1 and EBV had already been studied in previous studies, so I focused on another two proteins. The first protein I studied in **Chapter 5** was Hsc70, I identified that Zta interacted with Hsc70 and an Hsp70 ATPase inhibitor was able to reduce EBV lytic reactivation. The interaction between Zta and Hsc70 suggested that Hsc70 could be the main chaperone that helped Zta folding, assembly and trafficking. As a dimeric nuclear protein, inhibition the function of Hsc70 also might impact Zta's folding as well as nuclear translocation, which then leads to the reduction of the EBV genome replication. And combined with the functions of Hsc70 in other herpesviruses, KSHV, HSV-1 and MHV-68, it is suggested a conserved role of Hsc70 as a cellular chaperone during herpesvirus replication (Baquero-Perez and Whitehouse, 2015; Salinas et al., 2016; Burch and Weller, 2004). Further investigation about Zta and Hsc70 could be focused on the *in vitro* binding studies, in order to find out the evidence about the direct interaction features, whether there are other co-chaperones involved in this interaction and the binding regions between two proteins.

Then I investigated Ca^{2+} signalling regulated NFAT proteins in **Chapter 6.** Both NFATc1 and NFATc2 were detected by mass spectrometry, and the IP-western

blotting validated that NFATc2 interacted with Zta. The previous study has reported that the NFAT inhibitor CsA and FK506 can block EBV lytic reactivation (Goldfeld et al., 1995). In our study, the induction of Zta expression and EBV viral replication were completely blocked by the FK506 during 24 hours' anti-IgG induction in Akata cells, suggesting an inhibition in lytic reactivation. Another study showed that a natural sequence variant in Zta promoter (Zp-V3), which has an NFAT binding site, increased the EBV lytic replication in response to the lytic induction of BCR ligation and ionomycin induction in BL cells. In addition, when comparing the gene sequencing data from EBV associated cancer samples from different regions, it is shown that this Zp-V3 variant is over-represented in EBV positive BLs and EBV infected gastric cancers (Bristol et al., 2018).

The increased possibility of lytic reactivation increases the chances of the virus to infect more cells and establish more latently infected cells. EBV lytic replication also increases the secretion of some cytokines, such as IL-6, VEGF, which are important for cell growth (Jones et al., 2007; Hong et al., 2005). Both reasons suggest the EBV lytic cycle may increase the development of EBV associated cancers and this further suggested NFATs could induce EBV lytic reactivation and might be important for the tumorigenesis of the EBV associated cancers.

Then I investigated the influence of transcription activity between NFATs and Zta, and identified that NFATs did not affect Zta's transcription activity, however, Zta can interfere with NFATs to activate an IL-2 promoter, which is a well-studied NFATs regulated gene. Three situations were identified through this study, following stimulation with ionomycin/PMA, transcription is activated through the interaction of NFATC2 and AP1 at the ARRE2 element. Moreover, this activation could be blocked by the drug FK506. Following expression of Zta alone, transcription is activated weakly through an indirect means that is not inhibited by FK506. Combining stimulation with ionomycin/PMA and expression of Zta, transcription is activated to an intermediate level. FK506 reduces the expression to the level seen when Zta is activation alone. This suggests the interaction of Zta with NFATC2 may account for the reduction in the impact of this stimulation.

In the study of Kenney's group, EMSA assay that using a probe contains an NFAT binding site and an AP-1 like ZIIIA motif (not the ARRE2 element), showed protein NFAT/AP-1 complex binding to this probe compared to the Zp wild type. Cold competitor DNA containing consensus binding sites for NFATs and AP-1 were able to compete with NFATs and AP-1 binding to the Zp-V3. This suggested that NFATs, which bind to the Zp-V3 NFAT binding site, recruited AP-1 to this region and bind to the adjacent ZIIIA motif. Luciferase assay also showed that NFATc1 and c-Fos could synergistically activate Zp-V3 but not Zp wild type suggesting that NFAT/AP-1 enhances the activation of Zp when the Zp-V3 is existed (Bristol et al., 2018).

It is reported that during the early time of the lytic cycle, Zta transcripts level goes to a peak level, then goes down after a few hours (Tierney et al., 2015). This could because the continuous high level of Zta causes damage to the cells (Zuo et al., 2011). Since Zta could interfere with NFATs to activate IL-2 promoter through NFAT/AP-1 composite, it is possible that under the situation of Zp-V3, Zta itself could interfere with the activation through NFAT/AP-1 together. This suggests a possible feedback loop of Zta to regulate the Zp expression with NFATs during EBV lytic reactivation (**Figure 7.1**).

During lytic infection, EBV infected cells express many antigens that can be detected by the host immune system, so in the infected cells, EBV like other herpesviruses, utilises different methods to evade the host immune responses, this process is termed host gene shutoff. One example is the repression of cellular gene mRNA levels during infection, which is through EBV early gene BGLF5 promoted mRNA degradation (Rowe et al., 2007). NFATs regulate the expression of many cellular cytokines, which are involved in the host immune responses. Zta interaction with NFATs suggests a way for Zta to block host immune responses through inhibition of NFATs regulated cytokine gene expression. However, the data I have at the moment was not enough to show the proof of Zta could influence NFATs regulated genes *in vivo*.

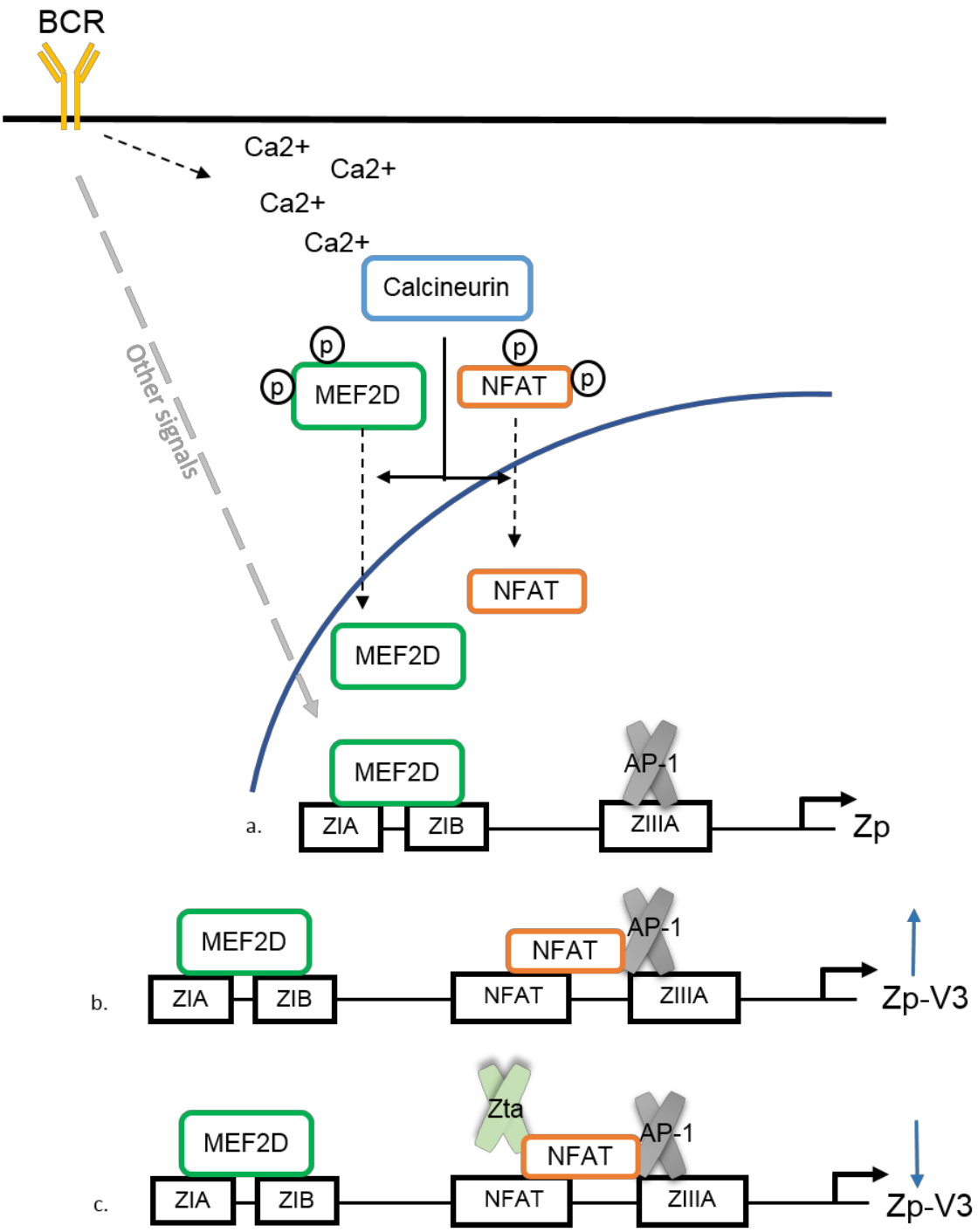

Figure 7.1 A model of Zp regulation by BCR signalling pathway. With activation of the BCR signalling pathway, NFATs and MEF2D will be activated and translocated into nuclear by dephosphorylation, activated proteins will regulate the Zp activation. **a.** Wild type Zp can be activated by AP-1 at ZIIIA and MEF2D at ZIA and ZIB. **b**. Zp-V3 creates a NFAT binding site, NFATs with AP-1 binding to the NFAT binding site and ZIIIA site, increases the activation of Zp. **c**. A possible situation that Zta binding to NFAT causes the interference of the transcription on the Zp-V3.

A few NFAT regulated cytokines and genes have been studied, such as IL-2, IL-3, IL-4, IL-13, TNF-α, TGF-β, GM-CSF and FasL (Rao et al., 1997). Some of these cytokines are not commonly expressed in B cells such as IL-4 (Kindler et al., 1995). Further studies can be started from the genes that are expressed in B cells, such as IL-2, IL-13 and FasL, which can be detected at mRNA level (IL-2, IL-13) or protein level (IL-2, FasL) in different B cells (Kindler et al., 1995; Fior et al., 1994; Hahne et al., 1996).

The previous study in our lab had determined the transcripts changes after Zta expression and lytic reactivation in Akata cell line by RNA-seq study (Ramasubramanyan et al., 2015a). Moreover, from ENCODE database, I obtained a ChIP-seq data of NFATc1 in an EBV positive B cell background (UCSC Accession: wgEncodeEH002307) and processed it by Genomic Regions Enrichment of Annotations Tool (GREAT, version 3.0.0) to get NFATc1 associated genes with distal up to 20kb (McLean et al., 2010). I compared the up-regulated or down-regulated genes from Zta RNA-seq results with NFATc1 associated genes (**Figure 7.2**), 165 out of total 1679 (9.8%) Zta up-regulated genes and 91 out of total 584 (15.6%) down-regulated genes were matched to NFATc1 10 kb list, 234 out of total 1679 (13.9%) Zta up-regulated genes and 113 out of total 584 (19.3%) down-regulated genes were matched to NFATc1 20 kb list. This huge difference strongly suggested that Zta could down regulate those genes through interacting with NFATs.

In future, the ChIP-qPCR study can be designed in the cells undergoing lytic cycle in order to study whether both proteins can co-bind to the same gene region. Luciferase reporter assays using promoter elements or mutants can be used to study the transcription ability of both proteins to those genes.

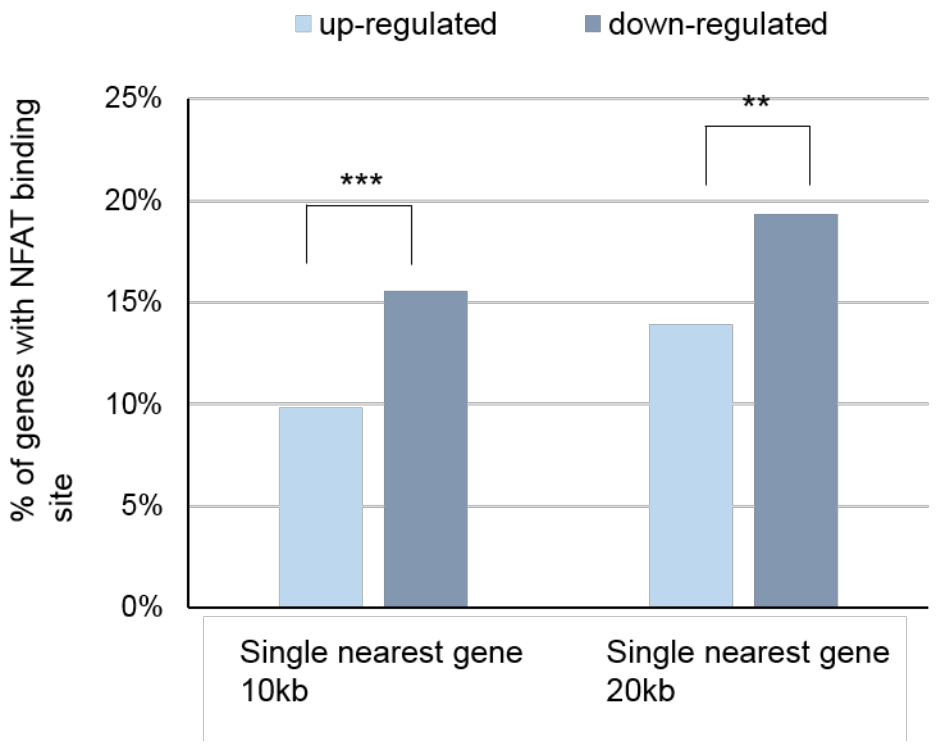

Figure 7.2 Intersection of NFAT binding sites and genes regulated following Zta expression. The NFAT binding data in human B-cells were extracted from Encode and transcriptome data from B-cells comparing differential expression after induction of Zta. Identification of the closes within 10 or 20Kb of each NFAT binding site was undertaken for the upregulated gene set and the down regulated gene set. The association is shown as % of each set of genes and the results of significant difference are shown following anova p-tests. ** p≤0.05; *** ≤ p0.01.

The main problem in our lytic reactivation system is that it is impossible to achieve a high proportion of lytic reactivated cells. The background from a huge proportion of cells might cover the changes in the small proportion of lytic cells. Some studies like pull-down studies for viral proteins, which can be isolated by antibody and beads and achieve high specificity. However, if I want to isolate cellular proteins and look for viral protein interactions, the background from non-lytic cells causes sensitivity problems. A few lytic cell enrichment methods have been used in previous works, in future, A cell system with a physical cell sorting method or using a lytic protein marker like a glycoprotein following fluorescence-activated cell sorting (FACS) can be used, in order to achieve a high percentage of lytic cells (Ersing et al., 2017; Ramasubramanyan et al., 2015a). Then a ChIP-qPCR study for NFATs and Zta can be performed in those cell systems.

In future, to further study the interaction between Zta and different interacting cellular proteins, the protein expression constructs, as well as different mutants can be designed and the domain-mapping studies undertaken *in vitro* and *in vivo* to identify the binding regions between Zta and those proteins. Then we would attempt to design different Zta mutants that do not bind to those proteins but still able to activate EBV lytic replication and used in cells to study the functional relevance of those interactions during EBV lytic cycle. For the cellular proteins, how Zta would influence the cellular functions through those proteins could be studied, such as cytokine profiling and immune response.

In this project, I successfully established pull-down conditions for EBV lytic transcription factor Zta. Combined with quantitative proteomics methods, I identified both EBV and cellular proteins that interact with Zta during EBV lytic reactivation. I also identified Zta interacts with cellular protein Hsc70 and the Hsp70 families contribute to lytic replication. In addition, I identified calcium-signalling pathway and NFATs involved in EBV lytic reactivation, Zta interacts with NFATc2 and is able to attenuate NFATs transcription activation. Further, I identified a feedback loop that limits Zta expression during lytic cycle trough NFATs and Zta interaction, which might be important to reduce the cytotoxicity caused by Zta during the EBV lytic cycle.

8 Bibliography

Abe M, Manola JB, Oh WK, et al. (2004) Plasma levels of heat shock protein 70 in patients with prostate cancer: a potential biomarker for prostate cancer. *Clin Prostate Cancer* 3: 49-53.

Albanese M, Tagawa T, Bouvet M, et al. (2016) Epstein-Barr virus microRNAs reduce immune surveillance by virus-specific CD8(+) T cells. *Proceedings of the National Academy of Sciences of the United States of America* 113: E6467-E6475.

Alfieri C, Birkenbach M and Kieff E. (1991) Early Events in Epstein-Barr-Virus Infection of Human Lymphocytes-B. *Virology* 181: 595-608.

Allday MJ, Crawford DH and Griffin BE. (1989) Epstein-Barr virus latent gene expression during the initiation of B cell immortalization. *J Gen Virol* 70 (Pt 7): 1755-1764.

Allday MJ and Farrell PJ. (1994) Epstein-Barr virus nuclear antigen EBNA3C/6 expression maintains the level of latent membrane protein 1 in G1-arrested cells. *J Virol* 68: 3491-3498.

Amoroso R, Fitzsimmons L, Thomas WA, et al. (2011) Quantitative Studies of Epstein-Barr Virus-Encoded MicroRNAs Provide Novel Insights into Their Regulation. *J Virol* 85: 996-1010.

Anderson LJ and Longnecker R. (2008) An auto-regulatory loop for EBV LMP2A involves activation of Notch. *Virology* 371: 257-266.

Apolloni A and Sculley TB. (1994) Detection of A-type and B-type Epstein-Barr virus in throat washings and lymphocytes. *Virology* 202: 978-981.

Asai R, Kato A, Kato K, et al. (2006) Epstein-Barr virus protein kinase BGLF4 is a virion tegument protein that dissociates from virions in a phosphorylation-dependent process and phosphorylates the viral immediate-early protein BZLF1. *J Virol* 80: 5125-5134.

Aubry V, Mure F, Mariame B, et al. (2014) Epstein-Barr virus late gene transcription depends on the assembly of a virus-specific preinitiation complex. *J Virol* 88: 12825-12838.

Baer R, Bankier AT, Biggin MD, et al. (1984) DNA sequence and expression of the B95-8 Epstein-Barr virus genome. *Nature* 310: 207-211.

Baichwal VR and Sugden B. (1988) Transformation of Balb 3T3 cells by the BNLF-1 gene of Epstein-Barr virus. *Oncogene* 2: 461-467.

Bailey SG, Verrall E, Schelcher C, et al. (2009) Functional interaction between Epstein-Barr virus replication protein Zta and host DNA damage response protein 53BP1. *J Virol* 83: 11116-11122.

Baksh S, Widlund HR, Frazer-Abel AA, et al. (2002) NFATc2-mediated repression of cyclin-dependent kinase 4 expression. *Mol Cell* 10: 1071-1081.

Balan N, Osborn K and Sinclair AJ. (2016) Repression of CIITA by the Epstein-Barr virus transcription factor Zta is independent of its dimerization and DNA binding. *Journal of General Virology* 97: 725-732.

Baldanti F, Grossi P, Furione M, et al. (2000) High levels of Epstein-Barr virus DNA in blood of solid-organ transplant recipients and their value in predicting posttransplant lymphoproliferative disorders. *Journal of Clinical Microbiology* 38: 613-619.

Baquero-Perez B and Whitehouse A. (2015) Hsp70 Isoforms Are Essential for the Formation of Kaposi's Sarcoma-Associated Herpesvirus Replication and Transcription Compartments. *PLoS Pathog* 11: e1005274.

Bargou RC, Emmerich F, Krappmann D, et al. (1997) Constitutive nuclear factor-kappa B-RelA activation is required for proliferation and survival of Hodgkin's disease tumor cells. *Journal of Clinical Investigation* 100: 2961-2969.

Baumann M, Feederle R, Kremmer E, et al. (1999) Cellular transcription factors recruit viral replication proteins to activate the Epstein-Barr virus origin of lytic DNA replication, oriLyt. *Embo Journal* 18: 6095-6105.

Baumann M, Gires O, Kolch W, et al. (2000) The PKC targeting protein RACK1 interacts with the Epstein-Barr virus activator protein BZLF1. *Eur J Biochem* 267: 3891-3901.

Bell SP and Dutta A. (2002) DNA replication in eukaryotic cells. *Annual Review of Biochemistry* 71: 333-374.

Bellows DS, Howell M, Pearson C, et al. (2002) Epstein-Barr virus BALF1 is a BCL-2-like antagonist of the herpesvirus antiapoptotic BCL-2 proteins. *J Virol* 76: 2469-2479.

Beltran BE, Castillo JJ, Morales D, et al. (2011) EBV-positive diffuse large B-cell lymphoma of the elderly: a case series from Peru. *Am J Hematol* 86: 663-667.

Bergbauer M, Kalla M, Schmeinck A, et al. (2010) CpG-Methylation Regulates a Class of Epstein-Barr Virus Promoters. *PLoS Pathog* 6.

Berland R and Wortis HH. (2003) Normal B-1a cell development requires B cell-intrinsic NFATc1 activity. *Proc Natl Acad Sci U S A* 100: 13459-13464.

Bhende PM, Seaman WT, Delecluse HJ, et al. (2004) The EBV lytic switch protein, Z, preferentially binds to and activates the methylated viral genome. *Nat Genet* 36: 1099-1104.

Biggar RJ, Lennette ET, Nkrumah FK, et al. (1981) Malaria, Sex, and Place of Residence as Factors in Antibody-Response to Epstein-Barr Virus in Ghana, West-Africa. *Lancet* 2: 115-118.

Binne UK, Amon W and Farrell PJ. (2002) Promoter sequences required for reactivation of Epstein-Barr virus from latency. *J Virol* 76: 10282-10289.

Bollard CM, Rooney CM and Heslop HE. (2012) T-cell therapy in the treatment of post-transplant lymphoproliferative disease. *Nat Rev Clin Oncol* 9: 510-519.

Bray F, Ferlay J, Laversanne M, et al. (2015) Cancer Incidence in Five Continents: Inclusion criteria, highlights from Volume X and the global status of cancer registration. *Int J Cancer* 137: 2060-2071.

Bristol JA, Djavadian R, Albright ER, et al. (2018) A cancer-associated Epstein-Barr virus BZLF1 promoter variant enhances lytic infection. *PLoS Pathog* 14: e1007179.

Brooks L, Yao QY, Rickinson AB, et al. (1992) Epstein-Barr virus latent gene transcription in nasopharyngeal carcinoma cells: coexpression of EBNA1, LMP1, and LMP2 transcripts. *J Virol* 66: 2689-2697.

Bryant H and Farrell PJ. (2002) Signal Transduction and Transcription Factor Modification during Reactivation of Epstein-Barr Virus from Latency. *J Virol* 76: 10290-10298.

Bu W, Joyce MG, Nguyen H, et al. (2019) Immunization with Components of the Viral Fusion Apparatus Elicits Antibodies That Neutralize Epstein-Barr Virus in B Cells and Epithelial Cells. *Immunity* 50: 1305-+.

Burch AD and Weller SK. (2004) Nuclear sequestration of cellular chaperone and proteasomal machinery during herpes simplex virus type 1 infection. *J Virol* 78: 7175-7185.

Burke AP, Yen TS, Shekitka KM, et al. (1990) Lymphoepithelial carcinoma of the stomach with Epstein-Barr virus demonstrated by polymerase chain reaction. *Mod Pathol* 3: 377-380.

Burkitt D and O'Conor GT. (1961) Malignant lymphoma in African children. I. A clinical syndrome. *Cancer* 14: 258-269.

Cai M, Liao Z, Chen T, et al. (2017) Characterization of the subcellular localization of Epstein-Barr virus encoded proteins in live cells. *Oncotarget* 8: 70006-70034.

Cai X, Schafer A, Lu S, et al. (2006) Epstein-Barr virus microRNAs are evolutionarily conserved and differentially expressed. *PLoS Pathog* 2: e23.

Caldwell RG, Wilson JB, Anderson SJ, et al. (1998) Epstein-Barr virus LMP2A drives B cell development and survival in the absence of normal B cell receptor signals. *Immunity* 9: 405-411.

Calender A, Cordier M, Billaud M, et al. (1990) Modulation of cellular gene expression in B lymphoma cells following in vitro infection by Epstein-Barr virus (EBV). *Int J Cancer* 46: 658-663.

Callan MF, Tan L, Annels N, et al. (1998) Direct visualization of antigen-specific CD8+ T cells during the primary immune response to Epstein-Barr virus In vivo. *J Exp Med* 187: 1395-1402.

Camargo MC, Murphy G, Koriyama C, et al. (2011) Determinants of Epstein-Barr virus-positive gastric cancer: an international pooled analysis. *Br J Cancer* 105: 38-43.

Cancer Genome Atlas Research N. (2014) Comprehensive molecular characterization of gastric adenocarcinoma. *Nature* 513: 202-209.

Cardone G, Winkler DC, Trus BL, et al. (2007) Visualization of the herpes simplex virus portal in situ by cryo-electron tomography. *Virology* 361: 426-434.

Carvalho LDS, Teixeira LK, Carrossini N, et al. (2007) The NFAT1 transcription factor is a repressor of cyclin A2 gene expression. *Cell Cycle* 6: 1789-1795.

Cavanaugh A, Juengst B, Sheridan K, et al. (2015) Combined inhibition of heat shock proteins 90 and 70 leads to simultaneous degradation of the oncogenic signaling proteins involved in muscle invasive bladder cancer. *Oncotarget* 6: 39821-39838.

Cayrol C and Flemington EK. (1995) Identification of cellular target genes of the Epstein-Barr virus transactivator Zta: activation of transforming growth factor beta igh3 (TGF-beta igh3) and TGF-beta 1. *J Virol* 69: 4206-4212.

Chang CW, Lee CP, Su MT, et al. (2015) BGLF4 kinase modulates the structure and transport preference of the nuclear pore complex to facilitate nuclear import of Epstein-Barr virus lytic proteins. *J Virol* 89: 1703-1718.

Chang ET and Adami HO. (2006) The enigmatic epidemiology of nasopharyngeal carcinoma. *Cancer Epidemiol Biomarkers Prev* 15: 1765-1777.

Chang KL, Albujar PF, Chen YY, et al. (1993) High Prevalence of Epstein-Barr-Virus in the Reed-Sternberg Cells of Hodgkins-Disease Occurring in Peru. *Blood* 81: 496-501.

Chang LK, Chuang JY, Nakao M, et al. (2010) MCAF1 and synergistic activation of the transcription of Epstein-Barr virus lytic genes by Rta and Zta. *Nucleic Acids Res* 38: 4687-4700.

Chang LK and Liu ST. (2000) Activation of the BRLF1 promoter and lytic cycle of Epstein-Barr virus by histone acetylation. *Nucleic Acids Res* 28: 3918-3925.

Chang YN, Dong DL, Hayward GS, et al. (1990) The Epstein-Barr virus Zta transactivator: a member of the bZIP family with unique DNA-binding specificity and a dimerization domain that lacks the characteristic heptad leucine zipper motif. *J Virol* 64: 3358-3369.

Chatila T, Ho N, Liu P, et al. (1997) The Epstein-Barr virus-induced Ca2+/calmodulin-dependent kinase type IV/Gr promotes a Ca(2+)-dependent switch from latency to viral replication. *J Virol* 71: 6560-6567.

Chen CC, Yang YC, Wang WH, et al. (2011) Enhancement of Zta-activated lytic transcription of Epstein-Barr virus by Ku80. *J Gen Virol* 92: 661-668.

Chen CJ, Deng Z, Kim AY, et al. (2001) Stimulation of CREB binding protein nucleosomal histone acetyltransferase activity by a class of transcriptional activators. *Mol Cell Biol* 21: 476-487.

Chen H, Huang J, Wu FY, et al. (2005) Regulation of expression of the Epstein-Barr virus BamHI-A rightward transcripts. *J Virol* 79: 1724-1733.

Chen H, Hutt-Fletcher L, Cao L, et al. (2003) A positive autoregulatory loop of LMP1 expression and STAT activation in epithelial cells latently infected with Epstein-Barr virus. *J Virol* 77: 4139-4148.

Chen J, Sathiyamoorthy K, Zhang XM, et al. (2018) Ephrin receptor A2 is a functional entry receptor for Epstein-Barr virus. *Nature Microbiology* 3: 172-180.

Chen L, Glover JN, Hogan PG, et al. (1998) Structure of the DNA-binding domains from NFAT, Fos and Jun bound specifically to DNA. *Nature* 392: 42-48.

Chen MR, Chang SJ, Huang H, et al. (2000) A protein kinase activity associated with Epstein-Barr virus BGLF4 phosphorylates the viral early antigen EA-D in vitro. *J Virol* 74: 3093-3104.

Chesnokova LS and Hutt-Fletcher LM. (2011) Fusion of Epstein-Barr Virus with Epithelial Cells Can Be Triggered by alpha v beta 5 in Addition to alpha v beta 6 and alpha v beta 8, and Integrin Binding Triggers a Conformational Change in Glycoproteins gHgL. *J Virol* 85: 13214-13223.

Chiu W and Rixon FJ. (2002) High resolution structural studies of complex icosahedral viruses: a brief overview. *Virus Res* 82: 9-17.

Choudhuri T, Verma SC, Lan K, et al. (2007) The ATM/ATR signaling effector Chk2 is targeted by Epstein-Barr virus nuclear antigen 3C to release the G(2)/M cell cycle block. *J Virol* 81: 6718-6730.

Chuma M, Sakamoto M, Hige SH, et al. (2003) Expression profiling in multistage hepatocarcinogenesis: Identification of HSP70 as a molecular marker of early hepatocellular carcinoma. *Hepatology* 38: 402a-402a.

Chung WC, Park JH, Kang HR, et al. (2015) Downregulation of Poly(ADP-Ribose) Polymerase 1 by a Viral Processivity Factor Facilitates Lytic Replication of Gammaherpesvirus. *J Virol* 89: 9676-9682.

Clipstone NA and Crabtree GR. (1992) Identification of Calcineurin as a Key Signaling Enzyme in Lymphocyte-T Activation. *Nature* 357: 695-697.

Cohen JI. (2000) Epstein-Barr virus infection. *N Engl J Med* 343: 481-492.

Cohen JI and Lekstrom K. (1999) Epstein-Barr virus BARF1 protein is dispensable for B-cell transformation and inhibits alpha interferon secretion from mononuclear cells. *J Virol* 73: 7627-7632.

Cohen JI, Wang F, Mannick J, et al. (1989) Epstein-Barr Virus Nuclear Protein-2 Is a Key Determinant of Lymphocyte-Transformation. *Proceedings of the National Academy of Sciences of the United States of America* 86: 9558-9562.

Connolly SA, Jackson JO, Jardetzky TS, et al. (2011) Fusing structure and function: a structural view of the herpesvirus entry machinery. *Nat Rev Microbiol* 9: 369-381.

Cooper A, Johannsen E, Maruo S, et al. (2003) EBNA3A association with RBP-Jkappa down-regulates c-myc and Epstein-Barr virus-transformed lymphoblast growth. *J Virol* 77: 999-1010.

Correia S, Bridges R, Wegner F, et al. (2018) Sequence Variation of Epstein-Barr Virus: Viral Types, Geography, Codon Usage, and Diseases. *J Virol* 92.

Correia S, Palser A, Elgueta Karstegl C, et al. (2017) Natural Variation of Epstein-Barr Virus Genes, Proteins, and Primary MicroRNA. *J Virol* 91.

Countryman J and Miller G. (1985) Activation of Expression of Latent Epstein-Barr Herpesvirus after Gene-Transfer with a Small Cloned Subfragment of Heterogeneous Viral-DNA. *Proceedings of the National Academy of Sciences of the United States of America* 82: 4085-4089.

Cox J, Hein MY, Luber CA, et al. (2014) Accurate proteome-wide label-free quantification by delayed normalization and maximal peptide ratio extraction, termed MaxLFQ. *Mol Cell Proteomics* 13: 2513-2526.

Cox J and Mann M. (2008) MaxQuant enables high peptide identification rates, individualized p.p.b.-range mass accuracies and proteome-wide protein quantification. *Nat Biotechnol* 26: 1367-1372.

Crawford DH, Swerdlow AJ, Higgins C, et al. (2002) Sexual history and Epstein-Barr virus infection. *Journal of Infectious Diseases* 186: 731-736.

Dambaugh T, Hennessy K, Chamnankit L, et al. (1984) U2 Region of Epstein-Barr Virus-DNA May Encode Epstein-Barr Nuclear Antigen-2. *Proceedings of the National Academy of Sciences of the United States of America-Biological Sciences* 81: 7632-7636.

Davison AJ. (2007) Comparative analysis of the genomes. In: Arvin A, Campadelli-Fiume G, Mocarski E, et al. (eds) *Human Herpesviruses: Biology, Therapy, and Immunoprophylaxis.* Cambridge.

Dawson CW, Dawson J, Jones R, et al. (1998) Functional differences between BHRF1, the Epstein-Barr virus-encoded Bcl-2 homologue, and Bcl-2 in human epithelial cells. *J Virol* 72: 9016-9024.

de Gorter DJJ, Vos JCM, Pals ST, et al. (2007) The B cell antigen receptor controls AP-1 and NFAT activity through Ras-mediated activation of Ral. *Journal of Immunology* 178: 1405-1414.

de Jesus O, Smith PR, Spender LC, et al. (2003) Updated Epstein-Barr virus (EBV) DNA sequence and analysis of a promoter for the BART (CST, BARF0) RNAs of EBV. *J Gen Virol* 84: 1443-1450.

Deacon EM, Pallesen G, Niedobitek G, et al. (1993) Epstein-Barr virus and Hodgkin's disease: transcriptional analysis of virus latency in the malignant cells. *J Exp Med* 177: 339-349.

Decaussin G, Sbih-Lammali F, de Turenne-Tessier M, et al. (2000) Expression of BARF1 gene encoded by Epstein-Barr virus in nasopharyngeal carcinoma biopsies. *Cancer Res* 60: 5584-5588.

Deng Z, Wang Z and Lieberman PM. (2012) Telomeres and viruses: common themes of genome maintenance. *Front Oncol* 2: 201.

Dennis G, Jr., Sherman BT, Hosack DA, et al. (2003) DAVID: Database for Annotation, Visualization, and Integrated Discovery. *Genome Biol* 4: P3.

Dethe G, Geser A, Day NE, et al. (1978) Epidemiological Evidence for Causal Relationship between Epstein-Barr Virus and Burkitts-Lymphoma from Ugandan Prospective-Study. *Nature* 274: 756-761.

Dolan A, Addison C, Gatherer D, et al. (2006) The genome of Epstein-Barr virus type 2 strain AG876. *Virology* 350: 164-170.

Dreyfus DH, Liu Y, Ghoda LY, et al. (2011) Analysis of an ankyrin-like region in Epstein Barr Virus encoded (EBV) BZLF-1 (ZEBRA) protein: implications for interactions with NF-kappaB and p53. *Virol J* 8: 422.

Dunmire SK, Hogquist KA and Balfour HH. (2015) Infectious Mononucleosis. *Curr Top Microbiol Immunol* 390: 211-240.

Dutton A, Reynolds GM, Dawson CW, et al. (2005) Constitutive activation of phosphatidyl-inositide 3 kinase contributes to the survival of Hodgkin's lymphoma cells through a mechanism involving Akt kinase and mTOR. *Journal of Pathology* 205: 498-506.

El-Guindy A, Ghiassi-Nejad M, Golden S, et al. (2013) Essential role of Rta in lytic DNA replication of Epstein-Barr virus. *J Virol* 87: 208-223.

El-Guindy A, Heston L and Miller G. (2010) A subset of replication proteins enhances origin recognition and lytic replication by the Epstein-Barr virus ZEBRA protein. *PLoS Pathog* 6: e1001054.

El-Guindy A, Lopez-Giraldez F, Delecluse HJ, et al. (2014) A locus encompassing the Epstein-Barr virus bglf4 kinase regulates expression of genes encoding viral structural proteins. *PLoS Pathog* 10: e1004307.

Ellis-Connell AL, Iempridee T, Xu I, et al. (2010) Cellular microRNAs 200b and 429 regulate the Epstein-Barr virus switch between latency and lytic replication. *J Virol* 84: 10329-10343.

Engelen E, Brandsma JH, Moen MJ, et al. (2015) Proteins that bind regulatory regions identified by histone modification chromatin immunoprecipitations and mass spectrometry. *Nat Commun* 6.

Epstein MA, Achong BG and Barr YM. (1964) Virus Particles in Cultured Lymphoblasts from Burkitt's Lymphoma. *Lancet* 1: 702-703.

Erikson J, ar-Rushdi A, Drwinga HL, et al. (1983) Transcriptional activation of the translocated c-myc oncogene in burkitt lymphoma. *Proc Natl Acad Sci U S A* 80: 820-824.

Ersing I, Nobre L, Wang LW, et al. (2017) A Temporal Proteomic Map of Epstein-Barr Virus Lytic Replication in B Cells. *Cell Reports* 19: 1479-1493.

Faggioni A, Zompetta C, Grimaldi S, et al. (1986) Calcium Modulation Activates Epstein-Barr-Virus Genome in Latently Infected-Cells. *Science* 232: 1554-1556.

Farrell PJ, Rowe DT, Rooney CM, et al. (1989) Epstein-Barr virus BZLF1 trans-activator specifically binds to a consensus AP-1 site and is related to c-fos. *Embo Journal* 8: 127-132.

Feederle R, Kost M, Baumann M, et al. (2000) The Epstein-Barr virus lytic program is controlled by the co-operative functions of two transactivators. *Embo Journal* 19: 3080-3089.

Feederle R, Linnstaedt SD, Bannert H, et al. (2011) A viral microRNA cluster strongly potentiates the transforming properties of a human herpesvirus. *PLoS Pathog* 7: e1001294.

Feng WH, Israel B, Raab-Traub N, et al. (2002) Chemotherapy induces lytic EBV replication and confers ganciclovir susceptibility to EBV-positive epithelial cell tumors. *Cancer Res* 62: 1920-1926.

Feng WH, Kraus RJ, Dickerson SJ, et al. (2007) ZEB1 and c-Jun levels contribute to the establishment of highly lytic Epstein-Barr virus infection in gastric AGS cells. *J Virol* 81: 10113-10122.

Ferlay J, Soerjomataram I, Dikshit R, et al. (2015) Cancer incidence and mortality worldwide: sources, methods and major patterns in GLOBOCAN 2012. *Int J Cancer* 136: E359-386.

Fernandez-Fernandez MR, Gragera M, Ochoa-Ibarrola L, et al. (2017) Hsp70 - a master regulator in protein degradation. *FEBS Lett* 591: 2648-2660.

Fior R, Vita N, Raphael M, et al. (1994) Interleukin-13 gene expression by malignant and EBV-transformed human B lymphocytes. *Eur Cytokine Netw* 5: 593-600.

Flaherty KM, DeLuca-Flaherty C and McKay DB. (1990) Three-dimensional structure of the ATPase fragment of a 70K heat-shock cognate protein. *Nature* 346: 623-628.

Flemington E and Speck SH. (1990a) Autoregulation of Epstein-Barr virus putative lytic switch gene BZLF1. *J Virol* 64: 1227-1232.

Flemington E and Speck SH. (1990b) Identification of phorbol ester response elements in the promoter of Epstein-Barr virus putative lytic switch gene BZLF1. *J Virol* 64: 1217-1226.

Flower K, Thomas D, Heather J, et al. (2011) Epigenetic control of viral life-cycle by a DNA-methylation dependent transcription factor. *Plos One* 6: e25922.

Fok V, Mitton-Fry RM, Grech A, et al. (2006) Multiple domains of EBER 1, an Epstein-Barr virus noncoding RNA, recruit human ribosomal protein L22. *RNA* 12: 872-882.

Fujii K, Yokoyama N, Kiyono T, et al. (2000) The Epstein-Barr virus pol catalytic subunit physically interacts with the BBLF4-BSLF1-BBLF2/3 complex. *J Virol* 74: 2550-2557.

Gao M, Matusick-Kumar L, Hurlburt W, et al. (1994) The protease of herpes simplex virus type 1 is essential for functional capsid formation and viral growth. *J Virol* 68: 3702-3712.

Gao Z, Krithivas A, Finan JE, et al. (1998) The Epstein-Barr virus lytic transactivator Zta interacts with the helicase-primase replication proteins. *J Virol* 72: 8559-8567.

Gibson W. (1996) Structure and assembly of the virion. *Intervirology* 39: 389-400.

Glaser SL, Canchola AJ, Keegan TH, et al. (2017) Variation in risk and outcomes of Epstein-Barr virus-associated breast cancer by epidemiologic characteristics and virus detection strategies: an exploratory study. *Cancer Causes Control* 28: 273-287.

Glaser SL, Lin RJ, Stewart SL, et al. (1997) Epstein-Barr virus-associated Hodgkin's disease: epidemiologic characteristics in international data. *Int J Cancer* 70: 375-382.

Goldfeld AE, Liu P, Liu S, et al. (1995) Cyclosporin A and FK506 block induction of the Epstein-Barr virus lytic cycle by anti-immunoglobulin. *Virology* 209: 225-229.

Gratama JW and Ernberg I. (1995) Molecular epidemiology of Epstein-Barr virus infection. *Adv Cancer Res* 67: 197-255.

Gregorovic G, Bosshard R, Karstegl CE, et al. (2011) Cellular Gene Expression That Correlates with EBER Expression in Epstein-Barr Virus-Infected Lymphoblastoid Cell Lines. *J Virol* 85: 3535-3545.

Grimm KE and O'Malley DP. (2018) Aggressive B cell lymphomas in the 2017 revised WHO classification of tumors of hematopoietic and lymphoid tissues. *Ann Diagn Pathol* 38: 6-10.

Gruffat H, Batisse J, Pich D, et al. (2002a) Epstein-Barr virus mRNA export factor EB2 is essential for production of infectious virus. *J Virol* 76: 9635-9644.

Gruffat H, Manet E and Sergeant A. (2002b) MEF2-mediated recruitment of class II HDAC at the EBV immediate early gene BZLF1 links latency and chromatin remodeling. *EMBO Rep* 3: 141-146.

Grundhoff A, Sullivan CS and Ganem D. (2006) A combined computational and microarray-based approach identifies novel microRNAs encoded by human gamma-herpesviruses. *RNA* 12: 733-750.

Gulley ML. (2015) Genomic assays for Epstein-Barr virus-positive gastric adenocarcinoma. *Experimental and Molecular Medicine* 47.

Gutsch DE, Holley-Guthrie EA, Zhang Q, et al. (1994) The bZIP transactivator of Epstein-Barr virus, BZLF1, functionally and physically interacts with the p65 subunit of NF-kappa B. *Mol Cell Biol* 14: 1939-1948.

Hadinoto V, Shapiro M, Greenough TC, et al. (2008) On the dynamics of acute EBV infection and the pathogenesis of infectious mononucleosis. *Blood* 111: 1420-1427.

Hahn AS, Kaufmann JK, Wies E, et al. (2012) The ephrin receptor tyrosine kinase A2 is a cellular receptor for Kaposi's sarcoma-associated herpesvirus. *Nature Medicine* 18: 961-+.

Hahne M, Renno T, Schroeter M, et al. (1996) Activated B cells express functional Fas ligand. *Eur J Immunol* 26: 721-724.

Hammerschmidt W and Sugden B. (1988) Identification and characterization of oriLyt, a lytic origin of DNA replication of Epstein-Barr virus. *Cell* 55: 427-433.

Hammerschmidt W and Sugden B. (1989) Genetic analysis of immortalizing functions of Epstein-Barr virus in human B lymphocytes. *Nature* 340: 393-397.

Hammerschmidt W and Sugden B. (2013) Replication of Epstein-Barr viral DNA. *Cold Spring Harb Perspect Biol* 5: a013029.

Handel AE, Williamson AJ, Disanto G, et al. (2010) An updated meta-analysis of risk of multiple sclerosis following infectious mononucleosis. *Plos One* 5.

Harris A, Young BD and Griffin BE. (1985) Random association of Epstein-Barr virus genomes with host cell metaphase chromosomes in Burkitt's lymphoma-derived cell lines. *J Virol* 56: 328-332.

Harth-Hertle ML, Scholz BA, Erhard F, et al. (2013) Inactivation of intergenic enhancers by EBNA3A initiates and maintains polycomb signatures across a chromatin domain encoding CXCL10 and CXCL9. *PLoS Pathog* 9: e1003638.

Heath E, Begue-Pastor N, Chaganti S, et al. (2012) Epstein-Barr virus infection of naive B cells in vitro frequently selects clones with mutated immunoglobulin genotypes: implications for virus biology. *PLoS Pathog* 8: e1002697.

Heilmann AM, Calderwood MA, Portal D, et al. (2012) Genome-wide analysis of Epstein-Barr virus Rta DNA binding. *J Virol* 86: 5151-5164.

Heming JD, Conway JF and Homa FL. (2017) Herpesvirus Capsid Assembly and DNA Packaging. *Adv Anat Embryol Cell Biol* 223: 119-142.

Henle W, Henle G, Ho HC, et al. (1970) Antibodies to Epstein-Barr virus in nasopharyngeal carcinoma, other head and neck neoplasms, and control groups. *J Natl Cancer Inst* 44: 225-231.

Henson BW, Perkins EM, Cothran JE, et al. (2009) Self-assembly of Epstein-Barr virus capsids. *J Virol* 83: 3877-3890.

Heslop HE. (2005) Biology and treatment of Epstein-Barr virus-associated non-Hodgkin lymphomas. *Hematology Am Soc Hematol Educ Program*: 260-266.

Hesse J, Ibsen KK, Krabbe S, et al. (1983) Prevalence of antibodies to Epstein-Barr virus (EBV) in childhood and adolescence in Denmark. *Scand J Infect Dis* 15: 335-338.

Hipp MS, Park SH and Hartl FU. (2014) Proteostasis impairment in protein-misfolding and -aggregation diseases. *Trends Cell Biol* 24: 506-514.

Hjalgrim H, Friborg J and Melbye M. (2007) The epidemiology of EBV and its association with malignant disease. In: Arvin A, Campadelli-Fiume G, Mocarski E, et al. (eds) *Human Herpesviruses: Biology, Therapy, and Immunoprophylaxis.* Cambridge.

Hoagland RJ. (1955) The transmission of infectious mononucleosis. *Am J Med Sci* 229: 262-272.

Hochberg D, Souza T, Catalina M, et al. (2004) Acute infection with Epstein-Barr virus targets and overwhelms the peripheral memory B-cell compartment with resting, latently infected cells. *J Virol* 78: 5194-5204.

Hofscheier A, Ponciano A, Bonzheim I, et al. (2011) Geographic variation in the prevalence of Epstein-Barr virus-positive diffuse large B-cell lymphoma of the elderly: a comparative analysis of a Mexican and a German population. *Mod Pathol* 24: 1046-1054.

Hogan PG, Chen L, Nardone J, et al. (2003) Transcriptional regulation by calcium, calcineurin, and NFAT. *Genes Dev* 17: 2205-2232.

Hong GK, Kumar P, Wang L, et al. (2005) Epstein-Barr virus lytic infection is required for efficient production of the angiogenesis factor vascular endothelial growth factor in lymphoblastoid cell lines. *J Virol* 79: 13984-13992.

Hong S, Wang D, Horton JR, et al. (2017) Methyl-dependent and spatial-specific DNA recognition by the orthologous transcription factors human AP-1 and Epstein-Barr virus Zta. *Nucleic Acids Res* 45: 2503-2515.

Horst D, Burrows SR, Gatherer D, et al. (2012) Epstein-Barr Virus Isolates Retain Their Capacity To Evade T Cell Immunity through BNLF2a despite Extensive Sequence Variation. *J Virol* 86: 572-577.

Hsieh JJ and Hayward SD. (1995) Masking of the CBF1/RBPJ kappa transcriptional repression domain by Epstein-Barr virus EBNA2. *Science* 268: 560-563.

Hsu CL, Kuo YC, Huang Y, et al. (2015) Application of a patient-derived xenograft model in cytolytic viral activation therapy for nasopharyngeal carcinoma. *Oncotarget* 6: 31323-31334.

Hsu M, Wu SY, Chang SS, et al. (2008) Epstein-Barr virus lytic transactivator Zta enhances chemotactic activity through induction of interleukin-8 in nasopharyngeal carcinoma cells. *J Virol* 82: 3679-3688.

Hudnall SD, Ge YM, Wei LX, et al. (2005) Distribution and phenotype of Epstein-Barr virus-infected cells in human pharyngeal tonsils. *Modern Pathology* 18: 519-527.

Hwang TS, Han HS, Choi HK, et al. (2003) Differential, stage-dependent expression of Hsp70, Hsp110 and Bcl-2 in colorectal cancer. *J Gastroenterol Hepatol* 18: 690-700.

Iempridee T, Das S, Xu I, et al. (2011) Transforming growth factor beta-induced reactivation of Epstein-Barr virus involves multiple Smad-binding elements cooperatively activating expression of the latent-lytic switch BZLF1 gene. *J Virol* 85: 7836-7848.

Ikuta K, Satoh Y, Hoshikawa Y, et al. (2000) Detection of Epstein-Barr virus in salivas and throat washings in healthy adults and children. *Microbes Infect* 2: 115-120.

Imai S, Koizumi S, Sugiura M, et al. (1994) Gastric carcinoma: monoclonal epithelial malignant cells expressing Epstein-Barr virus latent infection protein. *Proc Natl Acad Sci U S A* 91: 9131-9135.

Israele V, Shirley P and Sixbey JW. (1991) Excretion of the Epstein-Barr-Virus from the Genital-Tract of Men. *Journal of Infectious Diseases* 163: 1341-1343.

Jarrett RF, Gallagher A, Jones DB, et al. (1991) Detection of Epstein-Barr virus genomes in Hodgkin's disease: relation to age. *J Clin Pathol* 44: 844-848.

Jenkins PJ, Binne UK and Farrell PJ. (2000) Histone acetylation and reactivation of Epstein-Barr virus from latency. *J Virol* 74: 710-720.

Jiang S, Willox B, Zhou H, et al. (2014) Epstein-Barr virus nuclear antigen 3C binds to BATF/IRF4 or SPI1/IRF4 composite sites and recruits Sin3A to repress CDKN2A. *Proc Natl Acad Sci U S A* 111: 421-426.

Jin Y, Xie Z, Lu G, et al. (2010) Characterization of variants in the promoter of BZLF1 gene of EBV in nonmalignant EBV-associated diseases in Chinese children. *Virol J* 7: 92.

Jing YZ, Wang Y, Jia YP, et al. (2010) Polymorphisms of Epstein-Barr virus BHRF1 gene, a homologue of bcl-2. *Chin J Cancer* 29: 1000-1005.

Johannsen E, Koh E, Mosialos G, et al. (1995) Epstein-Barr-Virus Nuclear-Protein 2 Transactivation of the Latent Membrane-Protein-1 Promoter Is Mediated by J-Kappa and Pu1. *J Virol* 69: 253-262.

Johannsen E, Luftig M, Chase MR, et al. (2004) Proteins of purified Epstein-Barr virus. *Proc Natl Acad Sci U S A* 101: 16286-16291.

Johnson BV, Bert AG, Ryan GR, et al. (2004) Granulocyte-macrophage colony-stimulating factor enhancer activation requires cooperation between NFAT and AP-1 elements and is associated with extensive nucleosome reorganization. *Mol Cell Biol* 24: 7914-7930.

Jones RJ, Seaman WT, Feng WH, et al. (2007) Roles of lytic viral infection and IL-6 in early versus late passage lymphoblastoid cell lines and EBV-associated lymphoproliferative disease. *Int J Cancer* 121: 1274-1281.

Kampinga HH, Hageman J, Vos MJ, et al. (2009) Guidelines for the nomenclature of the human heat shock proteins. *Cell Stress Chaperones* 14: 105-111.

Kanda T, Otter M and Wahl GM. (2001) Coupling of mitotic chromosome tethering and replication competence in Epstein-Barr virus-based plasmids. *Mol Cell Biol* 21: 3576-3588.

Kataoka K, Miyoshi H, Sakata S, et al. (2019) Frequent structural variations involving programmed death ligands in Epstein-Barr virus-associated lymphomas. *Leukemia* 33: 1687-1699.

Kato H, Karube K, Yamamoto K, et al. (2014) Gene expression profiling of Epstein-Barr virus-positive diffuse large B-cell lymphoma of the elderly reveals alterations of characteristic oncogenetic pathways. *Cancer Sci* 105: 537-544.

Katsumura KR, Maruo S and Takada K. (2012) EBV lytic infection enhances transformation of B-lymphocytes infected with EBV in the presence of T-lymphocytes. *J Med Virol* 84: 504-510.

Katsumura KR, Maruo S, Wu Y, et al. (2009) Quantitative evaluation of the role of Epstein-Barr virus immediate-early protein BZLF1 in B-cell transformation. *J Gen Virol* 90: 2331-2341.

Kawaguchi A, Kanai K, Satoh Y, et al. (2009) The evolution of Epstein-Barr virus inferred from the conservation and mutation of the virus glycoprotein gp350/220 gene. *Virus Genes* 38: 215-223.

Kaye KM, Izumi KM and Kieff E. (1993) Epstein-Barr-Virus Latent Membrane Protein-1 Is Essential for B-Lymphocyte Growth Transformation. *Proceedings of the National Academy of Sciences of the United States of America* 90: 9150-9154.

Kempkes B and Ling PD. (2015) EBNA2 and Its Coactivator EBNA-LP. *Curr Top Microbiol Immunol* 391: 35-59.

Kenney S, Kamine J, Holley-Guthrie E, et al. (1989) The Epstein-Barr virus (EBV) BZLF1 immediate-early gene product differentially affects latent versus productive EBV promoters. *J Virol* 63: 1729-1736.

Kiehl A and Dorsky DI. (1995) Bipartite DNA-Binding Region of the Epstein-Barr-Virus Bmrf1 Product Essential for DNA-Polymerase Accessory Function. *J Virol* 69: 1669-1677.

Kimura H and Fujiwara S. (2018) Overview of EBV-Associated T/NK-Cell Lymphoproliferative Diseases. *Front Pediatr* 6: 417.

Kindler V, Matthes T, Jeannin P, et al. (1995) Interleukin-2 secretion by human B lymphocytes occurs as a late event and requires additional stimulation after CD40 cross-linking. *Eur J Immunol* 25: 1239-1243.

Knight JS and Robertson ES. (2004) Epstein-Barr virus nuclear antigen 3C regulates cyclin A/p27 complexes and enhances cyclin A-dependent kinase activity. *J Virol* 78: 1981-1991.

Koenig A, Linhart T, Schlengemann K, et al. (2010) NFAT-induced histone acetylation relay switch promotes c-Myc-dependent growth in pancreatic cancer cells. *Gastroenterology* 138: 1189-1199 e1181-1182.

Kondo E, Harashima A, Takabatake T, et al. (2003) NF-ATc2 induces apoptosis in Burkitt's lymphoma cells through signaling via the B cell antigen receptor. *Eur J Immunol* 33: 1-11.

Kuppers R. (2009) The biology of Hodgkin's lymphoma. *Nature Reviews Cancer* 9: 15-27.

Kwok H, Tong AH, Lin CH, et al. (2012) Genomic sequencing and comparative analysis of Epstein-Barr virus genome isolated from primary nasopharyngeal carcinoma biopsy. *Plos One* 7: e36939.

Kwok H, Wu CW, Palser AL, et al. (2014) Genomic Diversity of Epstein-Barr Virus Genomes Isolated from Primary Nasopharyngeal Carcinoma Biopsy Samples. *J Virol* 88: 10662-10672.

Lai PK, Mackay-Scollay EM and Alpers MP. (1975) Epidemiological studies of Epstein-Barr herpesvirus infection in Western Australia. *J Hyg (Lond)* 74: 329-337.

Lan YY, Yeh TH, Lin WH, et al. (2013) Epstein-Barr Virus Zta Upregulates Matrix Metalloproteinases 3 and 9 That Synergistically Promote Cell Invasion In Vitro. *Plos One* 8.

Laux G, Freese UK, Fischer R, et al. (1988a) TPA-inducible Epstein-Barr virus genes in Raji cells and their regulation. *Virology* 162: 503-507.

Laux G, Perricaudet M and Farrell PJ. (1988b) A Spliced Epstein-Barr Virus Gene Expressed in Immortalized Lymphocytes Is Created by Circularization of the Linear Viral Genome. *Embo Journal* 7: 769-774.

Lee CP, Huang YH, Lin SF, et al. (2008) Epstein-Barr virus BGLF4 kinase induces disassembly of the nuclear lamina to facilitate virion production. *J Virol* 82: 11913-11926.

Lee N, Moss WN, Yario TA, et al. (2015) EBV noncoding RNA binds nascent RNA to drive host PAX5 to viral DNA. *Cell* 160: 607-618.

Lerner MR, Andrews NC, Miller G, et al. (1981) Two small RNAs encoded by Epstein-Barr virus and complexed with protein are precipitated by antibodies from patients with systemic lupus erythematosus. *Proc Natl Acad Sci U S A* 78: 805-809.

Levine PH, Ablashi DV, Berard CW, et al. (1971) Elevated antibody titers to Epstein-Barr virus in Hodgkin's disease. *Cancer* 27: 416-421.

Li R, Liao G, Nirujogi RS, et al. (2015) Phosphoproteomic Profiling Reveals Epstein-Barr Virus Protein Kinase Integration of DNA Damage Response and Mitotic Signaling. *PLoS Pathog* 11: e1005346.

Liang CL, Chen JL, Hsu YPP, et al. (2002) Epstein-Barr virus BZLF1 gene is activated by transforming growth factor-beta through cooperativity of Smads and c-Jun/c-Fos proteins. *Journal of Biological Chemistry* 277: 23345-23357.

Liao G, Wu FY and Hayward SD. (2001) Interaction with the Epstein-Barr virus helicase targets Zta to DNA replication compartments. *J Virol* 75: 8792-8802.

Liao GL, Huang J, Fixman ED, et al. (2005) The Epstein-Barr virus replication protein BBLF2/3 provides an origin-tethering function through interaction with the zinc finger DNA binding protein ZBRK1 and the KAP-1 corepressor. *J Virol* 79: 245-256.

Liashkovich I, Hafezi W, Kuhn JM, et al. (2011) Nuclear delivery mechanism of herpes simplex virus type 1 genome. *J Mol Recognit* 24: 414-421.

Lieberman PM. (2013) Keeping it quiet: chromatin control of gammaherpesvirus latency. *Nat Rev Microbiol* 11: 863-875.

Lieberman PM and Berk AJ. (1990) In vitro transcriptional activation, dimerization, and DNA-binding specificity of the Epstein-Barr virus Zta protein. *J Virol* 64: 2560-2568.

Lieberman PM and Berk AJ. (1991) The Zta trans-activator protein stabilizes TFIID association with promoter DNA by direct protein-protein interaction. *Genes Dev* 5: 2441-2454.

Lieberman PM, Hu J and Renne R. (2007) Maintenance and replication during latency. In: Arvin A, Campadelli-Fiume G, Mocarski E, et al. (eds) *Human Herpesviruses: Biology, Therapy, and Immunoprophylaxis.* Cambridge.

Lieberman PM, Ozer J and Gursel DB. (1997) Requirement for transcription factor IIA (TFIIA)-TFIID recruitment by an activator depends on promoter structure and template competition. *Mol Cell Biol* 17: 6624-6632.

Lin Z, Wang X, Strong MJ, et al. (2013) Whole-genome sequencing of the Akata and Mutu Epstein-Barr virus strains. *J Virol* 87: 1172-1182.

Lindahl T, Klein G, Reedman BM, et al. (1974) Relationship between Epstein-Barr Virus (Ebv) DNA and Ebv-Determined Nuclear Antigen (Ebna) in Burkitt-Lymphoma Biopsies and Other Lymphoma Biopsies and Other Lymphoproliferative Malignancies. *Int J Cancer* 13: 764-772.

Liu F and Zhou ZH. (2007) Comparative virion structures of human herpesviruses. In: Arvin A, Campadelli-Fiume G, Mocarski E, et al. (eds) *Human Herpesviruses: Biology, Therapy, and Immunoprophylaxis.* Cambridge.

Liu J, Farmer JD, Lane WS, et al. (1991) Calcineurin Is a Common Target of Cyclophilin-Cyclosporine-a and Fkbp-Fk506 Complexes. *Cell* 66: 807-815.

Liu PF, Liu SF and Speck SH. (1998) Identification of a negative cis element within the ZII domain of the Epstein-Barr virus lytic switch BZLF1 gene promoter. *J Virol* 72: 8230-8239.

Liu SF, Liu PF, Borras A, et al. (1997) Cyclosporin A-sensitive induction of the Epstein-Barr virus lytic switch is mediated via a novel pathway involving a MEF2 family member. *Embo Journal* 16: 143-153.

Liu Y, Yang W, Pan Y, et al. (2016a) Genome-wide analysis of Epstein-Barr virus (EBV) isolated from EBV-associated gastric carcinoma (EBVaGC). *Oncotarget* 7: 4903-4914.

Liu Y, Zhang Y, Zhao Y, et al. (2016b) High PARP-1 expression is associated with tumor invasion and poor prognosis in gastric cancer. *Oncology Letters* 12: 3825-3835.

Lo AK, Liu Y, Wang X, et al. (2001) Identification of downstream target genes of latent membrane protein 1 in nasopharyngeal carcinoma cells by suppression subtractive hybridization. *Biochim Biophys Acta* 1520: 131-140.

Longnecker R and Neipel F. (2007) Introduction to the human gamma-herpesviruses. In: Arvin A, Campadelli-Fiume G, Mocarski E, et al. (eds) *Human Herpesviruses: Biology, Therapy, and Immunoprophylaxis.* Cambridge.

Lopez-Rodriguez C, Aramburu J, Rakeman AS, et al. (1999) NFAT5, a constitutively nuclear NFAT protein that does not cooperate with Fos and Jun. *Proc Natl Acad Sci U S A* 96: 7214-7219.

Lorenzetti MA, Gantuz M, Altcheh J, et al. (2012) Distinctive Epstein-Barr Virus Variants Associated with Benign and Malignant Pediatric Pathologies: LMP1 Sequence Characterization and Linkage with Other Viral Gene Polymorphisms (vol 50, pg 609, 2012). *Journal of Clinical Microbiology* 50: 2543-2543.

Lorenzetti MA, Gantuz M, Altcheh J, et al. (2014) Epstein-Barr virus BZLF1 gene polymorphisms: malignancy related or geographically distributed variants? *Clin Microbiol Infect* 20: O861-869.

Lu J, Chen SY, Chua HH, et al. (2000) Upregulation of tyrosine kinase TKT by the Epstein-Barr virus transactivator Zta. *J Virol* 74: 7391-7399.

Lucchesi W, Brady G, Dittrich-Breiholz O, et al. (2008) Differential gene regulation by Epstein-Barr virus type 1 and type 2 EBNA2. *J Virol* 82: 7456-7466.

Lupey-Green LN, Moquin SA, Martin KA, et al. (2017) PARP1 restricts Epstein Barr Virus lytic reactivation by binding the BZLF1 promoter. *Virology* 507: 220-230.

Ma SD, Hegde S, Young KH, et al. (2011) A new model of Epstein-Barr virus infection reveals an important role for early lytic viral protein expression in the development of lymphomas. *J Virol* 85: 165-177.

Macian F, Garcia-Rodriguez C and Rao A. (2000) Gene expression elicited by NFAT in the presence or absence of cooperative recruitment of Fos and Jun. *Embo Journal* 19: 4783-4795.

Mackey D and Sugden B. (1999) The linking regions of EBNA1 are essential for its support of replication and transcription. *Mol Cell Biol* 19: 3349-3359.

Mahot S, Sergeant A, Drouet E, et al. (2003) A novel function for the Epstein-Barr virus transcription factor EB1/Zta: induction of transcription of the hIL-10 gene. *J Gen Virol* 84: 965-974.

Manet E, Allera C, Gruffat H, et al. (1993) The acidic activation domain of the Epstein-Barr virus transcription factor R interacts in vitro with both TBP and TFIIB and is cell-specifically potentiated by a proline-rich region. *Gene Expr* 3: 49-59.

Manet E, Rigolet A, Gruffat H, et al. (1991) Domains of the Epstein-Barr virus (EBV) transcription factor R required for dimerization, DNA binding and activation. *Nucleic Acids Res* 19: 2661-2667.

Marchini A, Tomkinson B, Cohen JI, et al. (1991) Bhrf1, the Epstein-Barr-Virus Gene with Homology to Bc12, Is Dispensable for Lymphocyte-B Transformation and Virus-Replication. *J Virol* 65: 5991-6000.

Marquitz AR, Mathur A, Nam CS, et al. (2011) The Epstein-Barr Virus BART microRNAs target the pro-apoptotic protein Bim. *Virology* 412: 392-400.

Marquitz AR and Raab-Traub N. (2012) The role of miRNAs and EBV BARTs in NPC. *Semin Cancer Biol* 22: 166-172.

Martin KA, Lupey LN and Tempera I. (2016) Epstein-Barr Virus Oncoprotein LMP1 Mediates Epigenetic Changes in Host Gene Expression through PARP1. *J Virol* 90: 8520-8530.

Martinez-Lopez JL, Torres J, Camorlinga-Ponce M, et al. (2014) Evidence of Epstein-Barr virus association with gastric cancer and non-atrophic gastritis. *Viruses* 6: 301-318.

Martini M, Capello D, Serraino D, et al. (2007) Characterization of variants in the promoter of EBV gene BZLF1 in normal donors, HIV-positive patients and in AIDS-related lymphomas. *J Infect* 54: 298-306.

Maruo S, Wu Y, Ishikawa S, et al. (2006) Epstein-Barr virus nuclear protein EBNA3C is required for cell cycle progression and growth maintenance of lymphoblastoid cells. *Proceedings of the National Academy of Sciences of the United States of America* 103: 19500-19505.

Massey AJ, Williamson DS, Browne H, et al. (2010) A novel, small molecule inhibitor of Hsc70/Hsp70 potentiates Hsp90 inhibitor induced apoptosis in HCT116 colon carcinoma cells. *Cancer Chemother Pharmacol* 66: 535-545.

Mattila PS, Ullman KS, Fiering S, et al. (1990) The actions of cyclosporin A and FK506 suggest a novel step in the activation of T lymphocytes. *Embo Journal* 9: 4425-4433.

Mattiussi S, Tempera I, Matusali G, et al. (2007) Inhibition of Poly(ADP-ribose)polymerase impairs Epstein Barr Virus lytic cycle progression. *Infect Agent Cancer* 2: 18.

Mauser A, Holley-Guthrie E, Simpson D, et al. (2002) The Epstein-Barr virus immediate-early protein BZLF1 induces both a G(2) and a mitotic block. *J Virol* 76: 10030-10037.

Mayer MP. (2013) Hsp70 chaperone dynamics and molecular mechanism. *Trends Biochem Sci* 38: 507-514.

McClellan MJ, Wood CD, Ojeniyi O, et al. (2013) Modulation of enhancer looping and differential gene targeting by Epstein-Barr virus transcription factors directs cellular reprogramming. *PLoS Pathog* 9: e1003636.

McGeoch DJ, Dolan A and Ralph AC. (2000) Toward a comprehensive phylogeny for mammalian and avian herpesviruses. *J Virol* 74: 10401-10406.

McLean CY, Bristor D, Hiller M, et al. (2010) GREAT improves functional interpretation of cis-regulatory regions. *Nat Biotechnol* 28: 495-501.

Mellacheruvu D, Wright Z, Couzens AL, et al. (2013) The CRAPome: a contaminant repository for affinity purification-mass spectrometry data. *Nature Methods* 10: 730-736.

Meng Q, Hagemeier SR, Fingeroth JD, et al. (2010) The Epstein-Barr Virus (EBV)-Encoded Protein Kinase, EBV-PK, but Not the Thymidine Kinase (EBV-TK), Is Required for Ganciclovir and Acyclovir Inhibition of Lytic Viral Production. *J Virol* 84: 4534-4542.

Miller CL, Burkhardt AL, Lee JH, et al. (1995) Integral Membrane-Protein 2 of Epstein-Barr-Virus Regulates Reactivation from Latency through Dominant-Negative Effects on Protein-Tyrosine Kinases. *Immunity* 2: 155-166.

Miller G, El-Guindy A, Countryman J, et al. (2007) Lytic cycle switches of oncogenic human gammaherpesviruses. *Adv Cancer Res* 97: 81-109.

Moffat LE. (2001) Infectious mononucleosis. *Prim Care Update Ob Gyns* 8: 73-77.

Mohammed H, Taylor C, Brown GD, et al. (2016) Rapid immunoprecipitation mass spectrometry of endogenous proteins (RIME) for analysis of chromatin complexes. *Nat Protoc* 11: 316-326.

Morris MA, Dawson CW, Wei W, et al. (2008) Epstein-Barr virus-encoded LMP1 induces a hyperproliferative and inflammatory gene expression programme in cultured keratinocytes. *J Gen Virol* 89: 2806-2820.

Muhammad K, Rudolf R, Pham DAT, et al. (2018) Induction of Short NFATc1/alphaA Isoform Interferes with Peripheral B Cell Differentiation. *Front Immunol* 9: 32.

Mullen MM, Haan KM, Longnecker R, et al. (2002) Structure of the Epstein-Barr virus gp42 protein bound to the MHC class II receptor HLA-DR1. *Mol Cell* 9: 375-385.

Murata T, Narita Y, Sugimoto A, et al. (2013) Contribution of myocyte enhancer factor 2 family transcription factors to BZLF1 expression in Epstein-Barr virus reactivation from latency. *J Virol* 87: 10148-10162.

Murata T, Sato Y, Nakayama S, et al. (2009) TORC2, a Coactivator of cAMP-response Element-binding Protein, Promotes Epstein-Barr Virus Reactivation from Latency through Interaction with Viral BZLF1 Protein. *Journal of Biological Chemistry* 284: 8033-8041.

Murayama K, Nakayama S, Kato-Murayama M, et al. (2009) Crystal structure of epstein-barr virus DNA polymerase processivity factor BMRF1. *J Biol Chem* 284: 35896-35905.

Murphy ME. (2013) The HSP70 family and cancer. *Carcinogenesis* 34: 1181-1188.

Naher H, Gissmann L, Freese UK, et al. (1992) Subclinical Epstein-Barr-Virus Infection of Both the Male and Female Genital-Tract - Indication for Sexual Transmission. *Journal of Investigative Dermatology* 98: 791-793.

Neri A, Barriga F, Inghirami G, et al. (1991) Epstein-Barr virus infection precedes clonal expansion in Burkitt's and acquired immunodeficiency syndrome-associated lymphoma. *Blood* 77: 1092-1095.

Newcomb WW, Juhas RM, Thomsen DR, et al. (2001) The UL6 gene product forms the portal for entry of DNA into the herpes simplex virus capsid. *J Virol* 75: 10923-10932.

Nguyen-Van D, Keane C, Han E, et al. (2011) Epstein-Barr virus-positive diffuse large B-cell lymphoma of the elderly expresses EBNA3A with conserved CD8 T-cell epitopes. *Am J Blood Res* 1: 146-159.

Nguyen TN, Kim LJ, Walters RD, et al. (2010) The C-terminal region of human NFATc2 binds cJun to synergistically activate interleukin-2 transcription. *Mol Immunol* 47: 2314-2322.

Oh HM, Oh JM, Choi SC, et al. (2003) An efficient method for the rapid establishment of Epstein-Barr virus immortalization of human B lymphocytes. *Cell Prolif* 36: 191-197.

Onozawa E, Shibayama H, Imadome KI, et al. (2017) Stat3 Is Constitutively Activated and Can Be a Therapeutic Target of Jak Inhibitors in Chronic Active Epstein-Barr Virus Infection. *Haematologica* 102: 94-94.

Ossovskaya V, Koo IC, Kaldjian EP, et al. (2010) Upregulation of Poly (ADP-Ribose) Polymerase-1 (PARP1) in Triple-Negative Breast Cancer and Other Primary Human Tumor Types. *Genes Cancer* 1: 812-821.

Oyama T, Ichimura K, Suzuki R, et al. (2003) Senile EBV+ B-cell lymphoproliferative disorders: a clinicopathologic study of 22 patients. *Am J Surg Pathol* 27: 16-26.

Oyama T, Yamamoto K, Asano N, et al. (2007) Age-related EBV-associated B-cell lymphoproliferative disorders constitute a distinct clinicopathologic group: a study of 96 patients. *Clinical Cancer Research* 13: 5124-5132.

Ozkan A, Kilic SS, Kalkan A, et al. (2003) Seropositivity of Epstein-Barr virus in Eastern Anatolian Region of Turkey. *Asian Pac J Allergy Immunol* 21: 49-53.

Pallesen G, Hamilton-Dutoit SJ, Rowe M, et al. (1991) Expression of Epstein-Barr virus latent gene products in tumour cells of Hodgkin's disease. *Lancet* 337: 320-322.

Park S, Lee J, Ko YH, et al. (2007) The impact of Epstein-Barr virus status on clinical outcome in diffuse large B-cell lymphoma. *Blood* 110: 972-978.

Parra LA, Baust TB, Smith AD, et al. (2016) The Molecular Chaperone Hsc70 Interacts with Tyrosine Hydroxylase to Regulate Enzyme Activity and Synaptic Vesicle Localization. *J Biol Chem* 291: 17510-17522.

Pavlova S, Feederle R, Gartner K, et al. (2013) An Epstein-Barr virus mutant produces immunogenic defective particles devoid of viral DNA. *J Virol* 87: 2011-2022.

Pearson G, Dewey F, Klein G, et al. (1970) Relation between Neutralization of Epstein-Barr Virus and Antibodies to Cell-Membrane Antigens Induced by Virus. *Journal of the National Cancer Institute* 45: 989-&.

Perkins DN, Pappin DJC, Creasy DM, et al. (1999) Probability-based protein identification by searching sequence databases using mass spectrometry data. *Electrophoresis* 20: 3551-3567.

Peterson BR, Sun LJ and Verdine GL. (1996) A critical arginine residue mediates cooperativity in the contact interface between transcription factors NFAT and AP-1. *Proceedings of the National Academy of Sciences of the United States of America* 93: 13671-13676.

Petosa C, Morand P, Baudin F, et al. (2006) Structural basis of lytic cycle activation by the Epstein-Barr virus ZEBRA protein. *Mol Cell* 21: 565-572.

Pham LV, Tamayo AT, Yoshimura LC, et al. (2005) Constitutive NF-kappaB and NFAT activation in aggressive B-cell lymphomas synergistically activates the CD154 gene and maintains lymphoma cell survival. *Blood* 106: 3940-3947.

Piriou E, Kimmel R, Chelimo K, et al. (2009) Serological evidence for long-term Epstein-Barr virus reactivation in children living in a holoendemic malaria region of Kenya. *J Med Virol* 81: 1088-1093.

Portis T, Dyck P and Longnecker R. (2003) Epstein-Barr Virus (EBV) LMP2A induces alterations in gene transcription similar to those observed in Reed-Sternberg cells of Hodgkin lymphoma. *Blood* 102: 4166-4178.

Pournazari P, Padmore RF, Kosari F, et al. (2014) B-lymphoblastic leukemia/lymphoma: overexpression of nuclear DNA repair protein PARP-1 correlates with antiapoptotic protein Bcl-2 and complex chromosomal abnormalities. *Hum Pathol* 45: 1582-1587.

Price AM and Luftig MA. (2014) Dynamic Epstein-Barr virus gene expression on the path to B-cell transformation. *Adv Virus Res* 88: 279-313.

Raab-Traub N, Flynn K, Pearson G, et al. (1987) The differentiated form of nasopharyngeal carcinoma contains Epstein-Barr virus DNA. *Int J Cancer* 39: 25-29.

Raabtraub N, Dambaugh T and Kieff E. (1980) DNA of Epstein-Barr Virus-Viii - B95-8, the Previous Prototype, Is an Unusual Deletion Derivative. *Cell* 22: 257-267.

Ragoczy T, Heston L and Miller G. (1998) The Epstein-Barr virus Rta protein activates lytic cycle genes and can disrupt latency in B lymphocytes. *J Virol* 72: 7978-7984.

Ragoczy T and Miller G. (1999) Role of the epstein-barr virus RTA protein in activation of distinct classes of viral lytic cycle genes. *J Virol* 73: 9858-9866.

Ramasubramanyan S, Kanhere A, Osborn K, et al. (2012) Genome-wide analyses of Zta binding to the Epstein-Barr virus genome reveals interactions in both early and late lytic cycles and an epigenetic switch leading to an altered binding profile. *J Virol* 86: 12494-12502.

Ramasubramanyan S, Osborn K, Al-Mohammad R, et al. (2015a) Epstein-Barr virus transcription factor Zta acts through distal regulatory elements to directly control cellular gene expression. *Nucleic Acids Res* 43: 3563-3577.

Ramasubramanyan S, Osborn K, Al-Mohammad R, et al. (2015b) Epstein-Barr virus transcription factor Zta acts through distal regulatory elements to directly control cellular gene expression. *Nucleic Acids Res* 43: 3563-3577.

Rao A, Luo C and Hogan PG. (1997) Transcription factors of the NFAT family: regulation and function. *Annu Rev Immunol* 15: 707-747.

Rausch L, Koenecke C, Koch HF, et al. (2016) Matched-pair analysis: identification of factors with independent influence on the development of PTLD after kidney or liver transplantation. *Transplant Res* 5: 6.

Raver RM, Panfil AR, Hagemeier SR, et al. (2013) The B-cell-specific transcription factor and master regulator Pax5 promotes Epstein-Barr virus latency by negatively regulating the viral immediate early protein BZLF1. *J Virol* 87: 8053-8063.

Ray Chaudhuri A and Nussenzweig A. (2017) The multifaceted roles of PARP1 in DNA repair and chromatin remodelling. *Nat Rev Mol Cell Biol* 18: 610-621.

Reedman BM and Klein G. (1973) Cellular localization of an Epstein-Barr virus (EBV)-associated complement-fixing antigen in producer and non-producer lymphoblastoid cell lines. *Int J Cancer* 11: 499-520.

Rennekamp AJ and Lieberman PM. (2011) Initiation of Epstein-Barr Virus Lytic Replication Requires Transcription and the Formation of a Stable RNA-DNA Hybrid Molecule at OriLyt. *J Virol* 85: 2837-2850.

Rickinson AB, Young LS and Rowe M. (1987) Influence of the Epstein-Barr virus nuclear antigen EBNA 2 on the growth phenotype of virus-transformed B cells. *J Virol* 61: 1310-1317.

Riley KJ, Rabinowitz GS, Yario TA, et al. (2012) EBV and human microRNAs co-target oncogenic and apoptotic viral and human genes during latency. *Embo Journal* 31: 2207-2221.

Robertson ES, Lin J and Kieff E. (1996) The amino-terminal domains of Epstein-Barr virus nuclear proteins 3A, 3B, and 3C interact with RBPJ kappa. *J Virol* 70: 3068-3074.

Robertson ES, Tomkinson B and Kieff E. (1994) An Epstein-Barr-Virus with a 58-Kilobase-Pair Deletion That Includes Barf0 Transforms B-Lymphocytes in-Vitro. *J Virol* 68: 1449-1458.

Robinson AR, Kwek SS and Kenney SC. (2012) The B-cell specific transcription factor, Oct-2, promotes Epstein-Barr virus latency by inhibiting the viral immediate-early protein, BZLF1. *PLoS Pathog* 8: e1002516.

Rovedo M and Longnecker R. (2007) Epstein-barr virus latent membrane protein 2B (LMP2B) modulates LMP2A activity. *J Virol* 81: 84-94.

Rowe M, Glaunsinger B, van Leeuwen D, et al. (2007) Host shutoff during productive Epstein-Barr virus infection is mediated by BGLF5 and may contribute to immune evasion. *Proc Natl Acad Sci U S A* 104: 3366-3371.

Rowe M, Young LS, Cadwallader K, et al. (1989) Distinction between Epstein-Barr Virus Type-a (Ebna-2a) and Type-B (Ebna-2b) Isolates Extends to the Ebna-3 Family of Nuclear Proteins. *J Virol* 63: 1031-1039.

Ruiss R, Jochum S, Wanner G, et al. (2011) A virus-like particle-based Epstein-Barr virus vaccine. *J Virol* 85: 13105-13113.

Ryan JL, Morgan DR, Dominguez RL, et al. (2009) High levels of Epstein-Barr virus DNA in latently infected gastric adenocarcinoma. *Lab Invest* 89: 80-90.

Sabattini E, Bacci F, Sagramoso C, et al. (2010) WHO classification of tumours of haematopoietic and lymphoid tissues in 2008: an overview. *Pathologica* 102: 83-87.

Saha A, Halder S, Upadhyay SK, et al. (2011) Epstein-Barr virus nuclear antigen 3C facilitates G1-S transition by stabilizing and enhancing the function of cyclin D1. *PLoS Pathog* 7: e1001275.

Saha A, Murakami M, Kumar P, et al. (2009) Epstein-Barr virus nuclear antigen 3C augments Mdm2-mediated p53 ubiquitination and degradation by deubiquitinating Mdm2. *J Virol* 83: 4652-4669.

Salinas E, Byrum SD, Moreland LE, et al. (2016) Identification of Viral and Host Proteins That Interact with Murine Gammaherpesvirus 68 Latency-Associated Nuclear Antigen during Lytic Replication: a Role for Hsc70 in Viral Replication. *J Virol* 90: 1397-1413.

Samant H and Kothadia JP. (2018) Transplantation Posttransplantation Lymphoproliferative Disorders. *StatPearls.* Treasure Island (FL).

Sato Y, Shirata N, Kudoh A, et al. (2009) Expression of Epstein-Barr virus BZLF1 immediate-early protein induces p53 degradation independent of MDM2, leading to repression of p53-mediated transcription. *Virology* 388: 204-211.

Satoh MS and Lindahl T. (1992) Role of poly(ADP-ribose) formation in DNA repair. *Nature* 356: 356-358.

Scheenstra R, Verschuuren EA, de Haan A, et al. (2004) The value of prospective monitoring of Epstein-Barr virus DNA in blood samples of pediatric liver transplant recipients. *Transpl Infect Dis* 6: 15-22.

Schepers A, Pich D and Hammerschmidt W. (1996) Activation of oriLyt, the lytic origin of DNA replication of Epstein-Barr virus, by BZLF1. *Virology* 220: 367-376.

Schepers A, Pich D, Mankertz J, et al. (1993) cis-acting elements in the lytic origin of DNA replication of Epstein-Barr virus. *J Virol* 67: 4237-4245.

Schepers A, Ritzi M, Bousset K, et al. (2001) Human origin recognition complex binds to the region of the latent origin of DNA replication of Epstein-Barr virus. *Embo Journal* 20: 4588-4602.

Schlecht R, Scholz SR, Dahmen H, et al. (2013) Functional analysis of Hsp70 inhibitors. *Plos One* 8: e78443.

Schober T, Framke T, Kreipe H, et al. (2013) Characteristics of early and late PTLD development in pediatric solid organ transplant recipients. *Transplantation* 95: 240-246.

Semmes OJ, Chen L, Sarisky RT, et al. (1998) Mta has properties of an RNA export protein and increases cytoplasmic accumulation of Epstein-Barr virus replication gene mRNA. *J Virol* 72: 9526-9534.

Seo JS, Park YM, Kim JI, et al. (1996) T cell lymphoma in transgenic mice expressing the human Hsp70 gene. *Biochem Biophys Res Commun* 218: 582-587.

Sergeant A, Gruffat H and Manet E. (2008) The Epstein-Barr virus (EBV) protein EB is an mRNA export factor essential for virus production. *Front Biosci* 13: 3798-3813.

Shaknovich R, Basso K, Bhagat G, et al. (2006) Identification of rare Epstein-Barr virus infected memory B cells and plasma cells in non-monomorphic post-transplant lymphoproliferative disorders and the signature of viral signaling. *Haematologica* 91: 1313-1320.

Shaulian E. (2010) AP-1-The Jun proteins: Oncogenes or tumor suppressors in disguise? *Cellular Signalling* 22: 894-899.

Sinclair AJ. (2003) bZIP proteins of human gammaherpesviruses. *J Gen Virol* 84: 1941-1949.

Sinclair AJ. (2006) Unexpected structure of Epstein-Barr virus lytic cycle activator Zta. *Trends Microbiol* 14: 289-291.

Sinclair AJ. (2013) Epigenetic control of Epstein-Barr virus transcription - relevance to viral life cycle? *Front Genet* 4: 161.

Sinclair AJ, Palmero I, Peters G, et al. (1994) EBNA-2 and EBNA-LP cooperate to cause G0 to G1 transition during immortalization of resting human B lymphocytes by Epstein-Barr virus. *Embo Journal* 13: 3321-3328.

Sista ND, Pagano JS, Liao W, et al. (1993) Retinoic Acid Is a Negative Regulator of the Epstein-Barr-Virus Protein (Bzlf1) That Mediates Disruption of Latent Infection. *Proceedings of the National Academy of Sciences of the United States of America* 90: 3894-3898.

Skalsky RL, Kang D, Linnstaedt SD, et al. (2014) Evolutionary conservation of primate lymphocryptovirus microRNA targets. *J Virol* 88: 1617-1635.

Smith AL, Dohn MR, Brown MV, et al. (2012) Association of Rho-associated protein kinase 1 with E-cadherin complexes is mediated by p120-catenin. *Molecular Biology of the Cell* 23: 99-110.

Sokal EM, Antunes H, Beguin C, et al. (1997) Early signs and risk factors for the increased incidence of Epstein-Barr virus-related posttransplant lymphoproliferative diseases in pediatric liver transplant recipients treated with tacrolimus. *Transplantation* 64: 1438-1442.

Sokal EM, Hoppenbrouwers K, Vandermeulen C, et al. (2007) Recombinant gp350 vaccine for infectious mononucleosis: a phase 2, randomized, double-blind, placebo-controlled trial to evaluate the safety, immunogenicity, and efficacy of an Epstein-Barr virus vaccine in healthy young adults. *Journal of Infectious Diseases* 196: 1749-1753.

Speck SH and Ganem D. (2010) Viral latency and its regulation: lessons from the gamma-herpesviruses. *Cell Host Microbe* 8: 100-115.

Spender LC, Cornish GH, Sullivan A, et al. (2002) Expression of transcription factor AML-2 (RUNX3, CBF alpha-3) is induced by Epstein-Barr virus EBNA-2 and correlates with the B-cell activation phenotype. *J Virol* 76: 4919-4927.

Strockbine LD, Cohen JI, Farrah T, et al. (1998) The Epstein-Barr virus BARF1 gene encodes a novel, soluble colony-stimulating factor-1 receptor. *J Virol* 72: 4015-4021.

Sugden B and Warren N. (1989) A Promoter of Epstein-Barr Virus That Can Function during Latent Infection Can Be Transactivated by Ebna-1, a Viral Protein Required for Viral-DNA Replication during Latent Infection. *J Virol* 63: 2644-2649.

Swaminathan S, Tomkinson B and Kieff E. (1991) Recombinant Epstein-Barr virus with small RNA (EBER) genes deleted transforms lymphocytes and replicates in vitro. *Proc Natl Acad Sci U S A* 88: 1546-1550.

Swerdlow SH CE, Harris NL, Jaffe ES, Pileri SA, Stein H, Thiele J. (2016) WHO Classification: Tumours of the Haematopoietic and Lymphoid Tissues (2008). *Postgraduate Haematology, 7th Edition*: 885-887.

Szklarczyk D, Franceschini A, Wyder S, et al. (2015) STRING v10: protein-protein interaction networks, integrated over the tree of life. *Nucleic Acids Res* 43: D447-452.

Tagawa T, Albanese M, Bouvet M, et al. (2016) Epstein-Barr viral miRNAs inhibit antiviral CD4(+) T cell responses targeting IL-12 and peptide processing. *Journal of Experimental Medicine* 213: 2065-2080.

Takada H, Imadome KI, Shibayama H, et al. (2017) EBV induces persistent NF-kappaB activation and contributes to survival of EBV-positive neoplastic T- or NK-cells. *Plos One* 12: e0174136.

Takada K. (1984) Cross-linking of cell surface immunoglobulins induces Epstein-Barr virus in Burkitt lymphoma lines. *Int J Cancer* 33: 27-32.

Tao Q, Robertson KD, Manns A, et al. (1998) Epstein-Barr virus (EBV) in endemic Burkitt's lymphoma: molecular analysis of primary tumor tissue. *Blood* 91: 1373-1381.

Tardif M, Savard M, Flamand L, et al. (2002) Impaired protein kinase C activation/translocation in Epstein-Barr virus-infected monocytes. *J Biol Chem* 277: 24148-24154.

Teixeira LK, Carrossini N, Secca C, et al. (2016) NFAT1 transcription factor regulates cell cycle progression and cyclin E expression in B lymphocytes. *Cell Cycle* 15: 2346-2359.

Thacker EL, Mirzaei F and Ascherio A. (2006) Infectious mononucleosis and risk for multiple sclerosis: a meta-analysis. *Ann Neurol* 59: 499-503.

Thompson A, Schafer J, Kuhn K, et al. (2003) Tandem mass tags: a novel quantification strategy for comparative analysis of complex protein mixtures by MS/MS. *Anal Chem* 75: 1895-1904.

Thompson MP and Kurzrock R. (2004) Epstein-Barr virus and cancer. *Clinical Cancer Research* 10: 803-821.

Thorley-Lawson DA. (2015) EBV Persistence--Introducing the Virus. *Curr Top Microbiol Immunol* 390: 151-209.

Tierney RJ, Shannon-Lowe CD, Fitzsimmons L, et al. (2015) Unexpected patterns of Epstein-Barr virus transcription revealed by a high throughput PCR array for absolute quantification of viral mRNA. *Virology* 474: 117-130.

Tikhmyanova N, Schultz DC, Lee T, et al. (2014) Identification of a new class of small molecules that efficiently reactivate latent Epstein-Barr Virus. *ACS Chem Biol* 9: 785-795.

Tomkinson B, Robertson E and Kieff E. (1993) Epstein-Barr virus nuclear proteins EBNA-3A and EBNA-3C are essential for B-lymphocyte growth transformation. *J Virol* 67: 2014-2025.

Traylen C, Ramasubramanyan S, Zuo J, et al. (2015) Identification of Epstein-Barr Virus Replication Proteins in Burkitt's Lymphoma Cells. *Pathogens* 4: 739-751.

Tsai CL, Li HP, Lu YJ, et al. (2006) Activation of DNA methyltransferase 1 by EBV LMP1 Involves c-Jun NH(2)-terminal kinase signaling. *Cancer Res* 66: 11668-11676.

Tsai MH, Raykova A, Klinke O, et al. (2013) Spontaneous lytic replication and epitheliotropism define an Epstein-Barr virus strain found in carcinomas. *Cell Reports* 5: 458-470.

Tsai PF, Lin SJ, Weng PL, et al. (2011) Interplay between PKC delta and Sp1 on Histone Deacetylase Inhibitor-Mediated Epstein-Barr Virus Reactivation. *J Virol* 85: 2373-2385.

Tsai SC, Lin SJ, Chen PW, et al. (2009) EBV Zta protein induces the expression of interleukin-13, promoting the proliferation of EBV-infected B cells and lymphoblastoid cell lines. *Blood* 114: 109-118.

Tsurumi T, Daikoku T, Kurachi R, et al. (1993) Functional Interaction between Epstein-Barr-Virus DNA-Polymerase Catalytic Subunit and Its Accessory Subunit in-Vitro. *J Virol* 67: 7648-7653.

Tsurumi T, Kishore J, Yokoyama N, et al. (1998) Overexpression, purification and helix-destabilizing properties of Epstein-Barr virus ssDNA-binding protein. *J Gen Virol* 79 (Pt 5): 1257-1264.

Tugizov SM, Herrera R and Palefsky JM. (2013) Epstein-Barr Virus Transcytosis through Polarized Oral Epithelial Cells. *J Virol* 87: 8179-8194.

Turrini R, Merlo A, Martorelli D, et al. (2017) A BARF1-specific mAb as a new immunotherapeutic tool for the management of EBV-related tumors. *Oncoimmunology* 6.

Tyanova S, Temu T, Sinitcyn P, et al. (2016) The Perseus computational platform for comprehensive analysis of (prote)omics data. *Nature Methods* 13: 731-740.

Upadhyay AS, Stehling O, Panayiotou C, et al. (2017) Cellular requirements for iron-sulfur cluster insertion into the antiviral radical SAM protein viperin. *Journal of Biological Chemistry* 292: 13879-13889.

Venerito M, Nardone G, Selgrad M, et al. (2014) Gastric cancer--epidemiologic and clinical aspects. *Helicobacter* 19 Suppl 1: 32-37.

Visalli RJ, Schwartz AM, Patel S, et al. (2019) Identification of the Epstein Barr Virus portal. *Virology* 529: 152-159.

Vockerodt M, Yap LF, Shannon-Lowe C, et al. (2015) The Epstein-Barr virus and the pathogenesis of lymphoma. *J Pathol* 235: 312-322.

Wahl A, Linnstaedt SD, Esoda C, et al. (2013) A Cluster of Virus-Encoded MicroRNAs Accelerates Acute Systemic Epstein-Barr Virus Infection but Does Not Significantly Enhance Virus-Induced Oncogenesis In Vivo. *J Virol* 87: 5437-5446.

Wang A, Welch R, Zhao B, et al. (2015) Epstein-Barr Virus Nuclear Antigen 3 (EBNA3) Proteins Regulate EBNA2 Binding to Distinct RBPJ Genomic Sites. *J Virol* 90: 2906-2919.

Wang H, Bu L, Wang C, et al. (2018) The Hsp70 inhibitor 2-phenylethynesulfonamide inhibits replication and carcinogenicity of Epstein-Barr virus by inhibiting the molecular chaperone function of Hsp70. *Cell Death Dis* 9: 734.

Wang X, Kenyon WJ, Li Q, et al. (1998) Epstein-Barr virus uses different complexes of glycoproteins gH and gL to infect B lymphocytes and epithelial cells. *J Virol* 72: 5552-5558.

Weinreb M, Day PJR, Niggli F, et al. (1996) The role of Epstein-Barr virus in Hodgkin's disease from different geographical areas. *Archives of Disease in Childhood* 74: 27-31.

Weiss LM, Chen YY, Liu XF, et al. (1991) Epstein-Barr virus and Hodgkin's disease. A correlative in situ hybridization and polymerase chain reaction study. *American Journal of Pathology* 139: 1259-1265.

Wemel AC, Mayet A, Bellier S, et al. (2017) Severe infectious mononucleosis in immunocompetent adults. *Med Mal Infect* 47: 540-545.

White RE, Ramer PC, Naresh KN, et al. (2012) EBNA3B-deficient EBV promotes B cell lymphomagenesis in humanized mice and is found in human tumors. *Journal of Clinical Investigation* 122: 1487-1502.

Wiese S, Reidegeld KA, Meyer HE, et al. (2007) Protein labeling by iTRAQ: a new tool for quantitative mass spectrometry in proteome research. *Proteomics* 7: 340-350.

Williamson DS, Borgognoni J, Clay A, et al. (2009) Novel Adenosine-Derived Inhibitors of 70 kDa Heat Shock Protein, Discovered Through Structure-Based Design. *Journal of Medicinal Chemistry* 52: 1510-1513.

Wilmore JR, Asito AS, Wei CW, et al. (2015) AID expression in peripheral blood of children living in a malaria holoendemic region is associated with changes in B cell subsets and Epstein-Barr virus. *Int J Cancer* 136: 1371-1380.

Wilson JB, Bell JL and Levine AJ. (1996) Expression of Epstein-Barr virus nuclear antigen-1 induces B cell neoplasia in transgenic mice. *Embo Journal* 15: 3117-3126.

Winslow MM, Gallo EM, Neilson JR, et al. (2006) The calcineurin phosphatase complex modulates immunogenic B cell responses. *Immunity* 24: 141-152.

Wolf H, Werner J and Zurhausen H. (1974) Ebv DNA in Nonlymphoid Cells of Nasopharyngeal Carcinomas and in a Malignant Lymphoma Obtained after Inoculation of Ebv into Cottontop Marmosets. *Cold Spring Harbor Symposia on Quantitative Biology* 39: 791-796.

Wood CD, Veenstra H, Khasnis S, et al. (2016) MYC activation and BCL2L11 silencing by a tumour virus through the large-scale reconfiguration of enhancer-promoter hubs. *Elife* 5.

Wu FY, Chen H, Wang SE, et al. (2003) CCAAT/enhancer binding protein alpha interacts with ZTA and mediates ZTA-induced p21(CIP-1) accumulation and G(1) cell cycle arrest during the Epstein-Barr virus lytic cycle. *J Virol* 77: 1481-1500.

Wu FY, Wang SE, Chen H, et al. (2004) CCAAT/enhancer binding protein alpha binds to the Epstein-Barr virus (EBV) ZTA protein through oligomeric interactions and contributes to cooperative transcriptional activation of the ZTA promoter through direct binding to the ZII and ZIIIB motifs during induction of the EBV lytic cycle. *J Virol* 78: 4847-4865.

Xia T, O'Hara A, Araujo I, et al. (2008) EBV microRNAs in primary lymphomas and targeting of CXCL-11 by ebv-mir-BHRF1-3. *Cancer Res* 68: 1436-1442.

Xue L, Blythe EE, Freiberger EC, et al. (2016) Valosin-containing protein (VCP)-Adaptor Interactions are Exceptionally Dynamic and Subject to Differential Modulation by a VCP Inhibitor. *Mol Cell Proteomics* 15: 2970-2986.

Xue SA, Labrecque LG, Lu QL, et al. (2002) Promiscuous expression of Epstein-Barr virus genes in Burkitt's lymphoma from the central African country Malawi. *Int J Cancer* 99: 635-643.

Yang YC, Feng TH, Chen TY, et al. (2015) RanBPM regulates Zta-mediated transcriptional activity in Epstein-Barr virus. *J Gen Virol* 96: 2336-2348.

Yates J, Warren N, Reisman D, et al. (1984) A Cis-Acting Element from the Epstein-Barr Viral Genome That Permits Stable Replication of Recombinant Plasmids in Latently Infected-Cells. *Proceedings of the National Academy of Sciences of the United States of America-Biological Sciences* 81: 3806-3810.

Yates JL, Warren N and Sugden B. (1985) Stable Replication of Plasmids Derived from Epstein-Barr Virus in Various Mammalian-Cells. *Nature* 313: 812-815.

Yiu GK and Toker A. (2006) NFAT induces breast cancer cell invasion by promoting the induction of cyclooxygenase-2. *J Biol Chem* 281: 12210-12217.

Young LS, Arrand JR and Murray PG. (2007) EBV gene expression and regulation. In: Arvin A, Campadelli-Fiume G, Mocarski E, et al. (eds) *Human Herpesviruses: Biology, Therapy, and Immunoprophylaxis.* Cambridge.

Young LS, Lau R, Rowe M, et al. (1991) Differentiation-associated expression of the Epstein-Barr virus BZLF1 transactivator protein in oral hairy leukoplakia. *J Virol* 65: 2868-2874.

Young LS and Rickinson AB. (2004) Epstein-Barr virus: 40 years on. *Nature Reviews Cancer* 4: 757-768.

Yu MC, Ho JHC, Lai SH, et al. (1986) Cantonese-Style Salted Fish as a Cause of Nasopharyngeal Carcinoma - Report of a Case-Control Study in Hong-Kong. *Cancer Res* 46: 956-961.

Yu X, Wang Z and Mertz JE. (2007) ZEB1 regulates the latent-lytic switch in infection by Epstein-Barr virus. *PLoS Pathog* 3: e194.

Yuan J, Cahir-McFarland E, Zhao B, et al. (2006) Virus and cell RNAs expressed during Epstein-Barr virus replication. *J Virol* 80: 2548-2565.

Zeng MS, Li DJ, Liu QL, et al. (2005) Genomic sequence analysis of Epstein-Barr virus strain GD1 from a nasopharyngeal carcinoma patient. *J Virol* 79: 15323-15330.

Zerby D, Chen CJ, Poon E, et al. (1999) The amino-terminal C/H1 domain of CREB binding protein mediates zta transcriptional activation of latent Epstein-Barr virus. *Mol Cell Biol* 19: 1617-1626.

Zhang Q, Gutsch D and Kenney S. (1994) Functional and Physical Interaction between P53 and Bzlf1 - Implications for Epstein-Barr-Virus Latency. *Mol Cell Biol* 14: 1929-1938.

Zhang Q, Hong Y, Dorsky D, et al. (1996) Functional and physical interactions between the Epstein-Barr virus (EBV) proteins BZLF1 and BMRF1: Effects on EBV transcription and lytic replication. *J Virol* 70: 5131-5142.

Zhao B, Zou J, Wang H, et al. (2011) Epstein-Barr virus exploits intrinsic B-lymphocyte transcription programs to achieve immortal cell growth. *Proc Natl Acad Sci U S A* 108: 14902-14907.

Zheng XH, Lu LX, Li XZ, et al. (2015) Quantification of Epstein-Barr virus DNA load in nasopharyngeal brushing samples in the diagnosis of nasopharyngeal carcinoma in southern China. *Cancer Sci* 106: 1196-1201.

Zhu JY, Pfuhl T, Motsch N, et al. (2009) Identification of novel Epstein-Barr virus microRNA genes from nasopharyngeal carcinomas. *J Virol* 83: 3333-3341.

Zhu XT, Zhao X, Burkholder WF, et al. (1996) Structural analysis of substrate binding by the molecular chaperone DnaK. *Science* 272: 1606-1614.

Zimmermann J and Hammerschmidt W. (1995) Structure and role of the terminal repeats of Epstein-Barr virus in processing and packaging of virion DNA. *J Virol* 69: 3147-3155.

Zuo JM, Thomas WA, Haigh TA, et al. (2011) Epstein-Barr Virus Evades CD4(+) T Cell Responses in Lytic Cycle through BZLF1-mediated Downregulation of CD74 and the Cooperation of vBcl-2. *PLoS Pathog* 7.

zur Hausen A, Brink AATP, Craanen ME, et al. (2000) Unique transcription pattern of Epstein-Barr virus (EBV) in EBV-carrying gastric adenocarcinomas: Expression of the transforming BARF1 gene. *Cancer Res* 60: 2745-2748.

zur Hausen H, Schulte-Holthausen H, Klein G, et al. (1970) EBV DNA in biopsies of Burkitt tumours and anaplastic carcinomas of the nasopharynx. *Nature* 228: 1056-1058.